Identification of predictive biomarkers of treatment free remission in patients with chronic myeloid leukaemia

Isla Nosratzadeh

BSc (Hons), MRes

Thesis submitted in fulfilment of the requirements for the Degree of Doctor of Philosophy

School of Cancer Sciences

College of Medical, Veterinary and Life Sciences

University of Glasgow

March 2026

This thesis is dedicated entirely to my incredible mum, who gave up everything so her children could have a good life. I couldn't have done a single day of this without you. Thank you for everything. This is for you.

In loving memory of my dad, who was so excited to see me finish this PhD.
I love you. I miss you. I hope you're proud.

Abstract

Chronic myeloid leukaemia (CML) is a haematological malignancy that occurs because of a translocation between chromosomes 9 and 22 to produce the *BCR::AB1* fusion oncogene on the so-called Philadelphia (Ph) chromosome. The subsequent BCR::ABL1 protein is a constitutively active tyrosine kinase which results in overactive downstream signalling pathways resulting in uncontrolled proliferation and expansion of myeloid cells, which if left untreated can be fatal.

Targeted tyrosine kinase inhibitors (TKIs) for patients with CML elicit an excellent response and patients can have close to normal life expectancy. However, patients will remain on treatment for the rest of their lives risking side effects which will dramatically effect their quality of life. To avert this many patients who achieve a deep molecular response (DMR)/MR4 (*BCR::ABL1 to ABL*<0.01% on international scale) are able to stop taking their TKI but remain in remission, this gives them all the benefits of being in remission without any negative side effects, this is called treatment free remission (TFR). While this is an excellent and attractive option for many patients, only about 50% of patients that attempt TFR are able to maintain it. In order to examine the difference between patients that maintain TFR and those that relapse the De- Escalation and Stopping Treatment of Imatinib, Nilotinib or sprYcel in Chronic Myeloid Leukaemia (DESTINY) clinical trial was carried out (NCT01804985). During this trial bone marrow (BM) samples were taken from 160 patients looking to achieve TFR. Patients in MMR response (MR3; *BCR::ABL1*<0.1%) and DMR were recruited, these patients had an initial de-escalation period where they reduced their TKI dose to half for 12 months, if TFR was maintained they then went on to total TKI cessation for a further 24 months. At the trial endpoint 72% of MR4 and 36% of MR3 patients maintained TFR. BM samples from both relapse (R_E) and TFR (TFR_E) patients at trial entry, point of relapse (R_X) and end point of trial (TFR_X) were obtained. These were used to characterise the bone marrow microenvironment (BMM) between the two outcome groups and importantly identify predictive biomarkers of TFR.

The BMM is a complex, multi-cellular niche in the BM with its primary purpose being to maintain and protect haematopoietic stem cells (HSCs) and allow for

haematopoiesis to occur in response to the body's needs. The intricate network of cells and proteins within the BMM are dependent on a delicate balance of these parts working together to prevent haematological disease. In patients with CML there are several changes that occur to the BMM which allow for the survival and protection of leukaemic stem cells (LSCs) and disease progression.

To better understand the changes to the BMM and LSCs in CML patients that maintain TFR a three-pronged approach was taken.

The supportive stroma of the BMM comprising mesenchymal stem cells (MSCs) is essential to the BMM; MSCs are responsible for tissue repair, immunomodulation, HSC maintenance and produce several cell types of the BMM (multipotency). MSCs extracted from DESTINY samples were found to have increased senescence in R_E compared to TFR_E. Using RNAseq the same comparison found increased CXCL12 expression, known for maintaining quiescence in LSCs and HSCs. Additionally, RNAseq analysis of MSCs found increased expression of *PTK7*, known to be part of senescence associated secretory phenotype (SASP), in R_E patients vs TFR_E. The *HLA-B* gene, which is a part of the MHC and is involved in presenting to cytotoxic $CD8^+$ T lymphocytes, was found to be downregulated within the same comparison. This indicates MSCs of patients at the start of trial who go on to relapse have an increased senescent profile which is producing a pro-inflammatory response within the BMM, additionally these MSCs have increased immunosuppressive activity. These factors could contribute to producing BMM that is unable to support remission after TKI cessation.

The stem and progenitor populations of CML are essential in the treatment and understanding of the disease, CML begins and is maintained by LSCs, and this results in the aberrant expansion of the progenitor cells. To first distinguish between TFR and relapse patients, cell surface markers that had previously been established as potential markers of LSCs were used to generate LSC panels. While none of the markers selected were viable predictive biomarkers of TFR, CD44 marker was found to be increased in all DESTINY samples compared to CML patients at diagnosis, apparently indicating an increased expression in LSCs after TKI use, but this could be due to increased quiescence of LSCs in patients. Additionally, colony forming assays of these samples also showed increased number of colonies produced by progenitors at end point of trial compared to

start of trial within TFR patients indicating increased cell proliferation is occurring in TFR patients after TKI cessation however this is part of normal haematopoiesis as this is not leading to relapse.

Finally, to gain a high-throughput, detailed, unbiased examination of the changes within the BMM proteomic analysis was used, in the form of liquid chromatography mass spectrometry (LC-MS). This provided a comprehensive examination of the proteomic profile of patients that relapse and those that maintain TFR. From this, gene set enrichment analysis (GSEA) was carried out which found negative enrichment of 'humoral immune response', 'complement activation', 'complement activation, classical pathway' and 'humoral immune response mediated by circulating immunoglobulin' pathways in R_E compared to TFR_E. This suggests a decreased immune function in CML patients that go on to relapse.

Overall, we can say the supportive stroma of relapse patients is more senescent and appears to have increased pro-inflammatory markers than patients that are able to maintain TFR. Additionally, patients who relapse have a dysregulated immune response which could be contributing to relapse. The changes seen identify significant differences between the two outcomes and provide potential predictive markers for the prediction of TFR that would need to be further elucidated.

Table of Contents

List of Tables

List of Figures

Conference abstracts

ESH-iCMLf 26th Annual John Goldman Conference. Prague, Czech Republic. 26th – 29th September 2024. Poster presentation.

British Society of Haematology conference. Glasgow, UK. 27th – 29th April 2025. Oral presentation.

ESH-iCMLf 27th Annual John Goldman Conference. Estoril, Portugal. 10th – 12th October 2025. Poster presentation.

American Society of Haematology Conference. Orlando, Florida. 5th - 9th December 2025. Poster presentation.

Acknowledgement

Firstly, I must start by thanking my supervisors Dr Heather Jorgensen, Professor Helen Wheadon and Professor Mhairi Copland. Thank you Heather for taking me on as a master's student all those years ago and showing me how rewarding research can be, I appreciate your help and support over the years and during this PhD. Helen, I can't thank you enough for being a constant source of support, and guidance, thank you for always making time for me and for answering all my questions. Mhairi, thank you for all of your guidance over the years and for always making time for me despite your busy schedule. To Shaun, the only person that knows this project as well as I do. I can't thank you enough for being such a constant throughout this project, for answer my 1 million questions and for being such a wonderful friend. Our chats and laughter made all of the long hours bearable. Thank you Alex for all the proteomics help.

Amy, thank you for your constant encouragement, for reminding me that I am capable and smart and for being you, I feel so lucky to have met you. Lucy, you have the kindest heart, and I truly couldn't have done these last couple of years without you, thank you. Jodie you convinced me to keep going when I truly didn't think I could, thank you I'll never forget it. Alan, for everything you do in the lab to support us, I will forever be grateful. Thank you Jen for your expertise and help in guiding me through the flow cytometry data. To Rachel, Frank, Shumaya, Valdemar, Nam, and Xenia and to everyone in the Michie, Copland, Jorgensen and Wheadon group, a massive thank you to you all. The POG is such a special place and the people that work there are a big part of this.

Thank you to my wonderful family in Iran, who somehow manage to be the most loving, supportive and involved family despite being thousands of miles away, thank you for always encouraging me and taking care of me. To my aunty Sima, who I lost the week before I submitted this thesis, the kindest human I have ever met. To my amazing aunty Nasrin and Mojgan, for always checking in, you're the best.

Shahad, being your best friend since we were 5 years old has been my favourite thing, thank you for the years of support, even from miles away. Shannon, thank

you for forcing me to leave the house when I needed it and reminding me to look after myself.

Zarah, thank you for being the best big sister in the world. Life would be extremely dull without you, I know we are sisters in every lifetime. I am so grateful I get to go through life knowing I have your support, thank you for keeping me sane these last few years and ensuring I'm having fun, my first and forever best friend. John, you're the best brother-in-law I could ever ask for, thank you for all the encouragement over the years and for being such a constant in all our lives, I'm so lucky to know you. Teddy my sweet, perfect dog who has never done anything wrong in his life. You deserve this PhD as much as me. I'm so sorry for all the late nights and lack of attention this PhD has left you with. You sat beside me for this entire write up and were my constant source of love and joy throughout my PhD. I love you my sweet boy.

My dad always encouraged me to try my best in education and reminded me what a privilege it was to have the opportunities I had. Losing him in the third year of my PhD was by far the hardest thing I have ever been through, but I'm glad I continued on, just like he taught me. Dad, I have missed you endlessly since you passed but I promise to keep going and live the life you always wanted for me. I'll tell you all about it when we meet again.

My wonderful mum, Maryam, to say thank you would never be enough for all you have done for me in my life. Despite everything you have been through you still manage to be the kindest, warmest, sweetest person I have ever met. You are the definition of strong and hard-working and seeing your determination every day is the only reason I have been able to complete this work. I love you mum, and I couldn't have done any of this without you. Thank you so much.

Finally, to myself, you did it, well done! The next time you think you can't do something, that you're not smart enough or not capable, come back and read this. Remember you did it all and you did it well.

Author's Declaration

I declare that, except where explicit reference is made to the contribution of others, that this thesis is the result of my own work and has not been submitted for any other degree at the University of Glasgow or any other institution.

Isla Nosratzadeh

March 2026

Abbreviations

ABL1	Abelson murine leukaemia viral oncogene homolog 1
ACA	Additional chromosomal abnormalities
AGM	Aorta-gonad-mesonephros
ALL	Acute lymphoblastic leukaemia
AML	Acute myeloid leukaemia
ANAXA1	Annexin A1
Ang1	Angiopoietin 1
AP	Accelerated phase
ARCH	Age related clonal haematopoiesis
ASC	Adipose derived mesenchymal stem cells
AUC	Area under the curve
BCR	Breakpoint cluster region
BFU-E	Burst-forming unit-erythroid
BM	Bone marrow
BMM	Bone marrow microenvironment
BMP	Bone morphogenic protein
BP	Blast phase
CAR	CXCL12-abundant reticular
CC	Coiled-coil domain
CCL	C-C motif chemokine ligand
CCyr	Complete cytogenic response
CFU-G	Colony forming unit - granulocyte
CFU-GEMM	Colony forming unit – granulocyte erythrocyte macrophage megakaryocyte
CFU-GM	Colony forming unit – granulocyte macrophage
CFU-M	Colony forming unit - macrophage
CHR	Complete haematological response
CLL	Chronic lymphocytic leukaemia
CLP	Common lymphoid progenitor
CML	Chronic myeloid leukaemia
CMP	Common myeloid progenitor
CNL	Chronic neutrophilic leukaemia
CP	Chronic phase
CTL	CD8+ cytotoxic T cell
CXCL	C-X-C motif chemokine ligand
CXCR	C-X-C motif chemokine receptor
DC	Dendritic cell
DDA	Data dependent acquisition
DEG	Differentially expressed genes
DEP	Differentially expressed proteins
DESTINY	DeEscalation and Stopping Treatment of Imatinib, Nilotinib or sprYcel in chronic myeloid leukaemia
Dhh	Desert hedgehog
DIA	Data independent acquisition
DMEM	Dulbecco’s Modified Eagle Medium
DMR	Deep molecular response
DMSO	Dimethyl sulfoxide
dPBS	Dulbecco’s phosphate buffered saline
DPP4	Dipeptidyl peptidase-4

ECM	Extracellular matrix
EFEMP2	EGF-containing fibulin-like extracellular matrix protein 2
EGF	Epidermal growth factor
EGFR	Epidermal growth factor receptor
ELTS	EUTOS Long Term Survival
EMM	Extramedullary multiple myeloma
ENOA	Enolase 1
ER	Endoplasmic reticulum
FACS	Fluorescence-activated cell sorting
FMO	Fluorescence minus one
FBS	Foetal bovine serum
FGF	Fibroblast growth factor
FGG	Fibrinogen Gamma Chain
FLT3	FMS-like tyrosine kinase 3
G-CSF	Granulocyte colony-stimulating factor
G-MDSC	Granulocyte-like myeloid-derived suppressor cells
GAP	GTPase-activating protein
Glrx1	Glutaredoxin-1
GMP	Granulocyte-monocyte progenitor
GO	Gene ontology
GSEA	Gene set enrichment analysis
GVHD	Graft versus host disease
HAS	Human albumin serum
HGF	Hepatocyte growth factor
HGFA	Hepatocyte growth factor activator
Hh	Hedgehog
HIF1-α	Hypoxia-inducible factor-1α
HSC	Haematopoietic stem cell
HSP60	Heat Shock Protein 60
HSPC	Haematopoietic stem and progenitor cell
HSPD1	Heat Shock Protein Family D Member 1
IFN-α	Interferon – α
IFN-γ	Interferon - γ
Ihh	Indian hedgehog
IL	Interleukin
IMDM	Iscove's Modified Dulbecco's Medium
IRIS	International Randomized Study of Interferon and STI571
IS	International scale
IT-HSC	Intermediate – haematopoietic stem cell
IκBα	Inhibitor of κBα
JAK/STAT	Janus Kinase/Signal Transducer and Activator of Transcription
LAA	Leukaemia-associated antigens
LC	Liquid chromatography
Lepr+	Leptin-receptor-positive
LIC	Leukaemia initiating cells
LMPP	Lymphoid-primed multipotent progenitor
LSC	Leukaemic stem cell
LT-HSC	Long term – haematopoietic stem cell
LTC-IC	Long term colony-initiating cell
MCP-1	Monocyte chemoattractant protein-1
MDS	Myelodysplastic syndrome
MDSC	Myeloid derived suppressor cells
MegE	Megakaryocyte/erythroid

MEP	Megakaryocytic-erythroid progenitors
MHC	Major histocompatibility complex class
MM	Multiple myeloma
MMP	Mitochondrial membrane potential
MMR	Major molecular remission
MNC	Mononuclear cell
MO-MDSC	Monocytic myeloid derived suppressor cells
MPFC	Multi-parameter flow cytometry
MPP	Multipotent progenitor
MRS	Molecular recurrence-free survival
MS	Mass spectrometry
MS-LC	Mass spectrometry liquid chromatography
MSC	Mesenchymal stem cell
NCCN	National Comprehensive Cancer Network
NFκβ	Nuclear Factor Kappa-light-chain-enhancer of activated B cells
NK	Natural killer
NLS	Nuclear localisation signal
OPN	Osteopontin
ORA	Over-representation analysis
PB	Peripheral blood
PBS	Phosphate-buffered saline
PCA	Principal component analysis
PD-1	Programmed death - 1
pDC	Plasmacytoid dendritic cells
PDGF	Platelet-derived growth factor
PDGFR	Platelet-derived growth factor receptor
PDGFRA	Platelet-derived growth factor receptor alpha
PEDF	Pigment epithelium-derived factor
Pen-Strep	Penicillin - Streptomycin
PGE2	Prostaglandin E2
Ph	Philadelphia
PI3K/AKT	Phosphatidylinositol 3-Kinase/Protein Kinase B
Ptch	Patched
QC	Quality control
R_E	Relapse at trial entry
R_X	Relapse patient at point of relapse
RAS/MAPK	Ras/Mitogen-Activated Protein Kinase
RBC	Red blood cell
Relapse_E	Relapse at trial entry
Relapse_X	Relapse patient at point of relapse
RFS	Recurrence free survival
RNAseq	RNA sequencing
ROC	Receiver operating characteristic
ROS	Reactive oxygen species
RPMI	Roswell Park Memorial Institute
SASP	Senescence-associated secretory phenotype
SCF	Stem cell factor
Shh	Sonic hedgehog
Smo	Smoothened
SPTA1	Spectrin alpha 1
ST-CFC	Short term colony forming cell
ST-HSC	Short-term HSC
T-ALL	T cell acute lymphocytic leukaemia

TFR	Treatment free remission
TFR_E	TFR at trial entry
TFR_X	TFR at trial endpoint
TGF-β	Transforming growth factor β
TGM2	Transglutaminase 2
TK	Tyrosine kinase
TKI	Tyrosine kinase inhibitor
TNF-α	Tumour necrosis factor - α
TNT	Tunnelling nanotubules
TPO	Thrombopoietin
UMRD	Undetectable minimal residual disease
VCAM1	Vascular adhesion molecule 1
VEGF	Vascular endothelial growth factor
β2-GP1	beta-2-glycoprotein 1

1 Introduction

1.1 Haematopoiesis

The process of blood cell production is called haematopoiesis. Human haematopoiesis takes place in the yolk sac and aorta-gonad-mesonephros (AGM) region of an embryo *in utero* and during development. In the foetus haematopoiesis takes place in the placenta, the foetal liver and spleen, then after birth it takes place in the bone marrow (BM) (Morrison and Scadden 2014).

1.1.1 Hierarchy of haematopoiesis

Haematopoiesis is a hierarchal system which begins when haematopoietic stem cells (HSCs), that are the most primitive cells at the top of the hierarchy, proliferate and differentiate into mature blood cells. These mature blood cells include immune cells, red blood cells (RBCs) and platelets. The process by which haematopoiesis occurs has been extensively studied over the years. HSCs are multipotent cells that self-renew and can produce all blood cell types. HSCs are a very rare population of cells that can be found in the adult in peripheral blood (PB), however most reside in the BM. HSCs have two main states in which they are found: when they are actively in the process of haematopoiesis, or when they are quiescent when they leave the cell cycle and are dormant within the BM (Wilson et al. 2008). Traditional understanding of the process of haematopoiesis begins with HSCs; these can be further classified into long-term HSCs (LT-HSC) which are the most primitive form of the HSC that when they lose some potency become functionally short-term HSCs (ST-HSC). The LT-HSC is the rare, quiescent population within the BM that has a full reconstitution capacity (Cheng et al. 2020), while the ST-HSC has a short-term reconstitution capacity (Cheng et al. 2020). The ST-HSC then differentiates into multipotent progenitors (MPP), these are less primitive and have no self-renewal capability (L. Yang et al. 2005). The MPPs then go on to produce lineage committed cells either common lymphoid progenitors (CLP) or common myeloid progenitors (CMP). The CLPs are responsible for the lymphoid lineage production branch which includes B cells, T cells and natural killer (NK) cells, these cells are responsible for the adaptive immune system. CMPs differentiate to produce megakaryocytic-erythroid progenitors (MEP) and granulocyte-monocyte progenitor (GMP); MEPs

differentiate into megakaryocytes/platelets (involved in clotting) and erythrocytes (also called red blood cells (RBCs) which are involved in oxygen transport) while GMPs produce basophils, eosinophils, neutrophils, monocytes, macrophages, and dendritic cells (DC) that are responsible for innate immune system (NK cells are also part of innate immune response). This strict hierarchical system was initially thought to be how haematopoiesis took place.

Research by Beneveniste et al., and Yamamoto et al., identified the presence of intermediate HSC (IT-HSC) which is a cell population found between LT-HSC and ST-HSC (Benveniste et al. 2010; Yamamoto et al. 2013). Additionally, it was found that the MPP population could be further defined into MPP1 (Pietras et al. 2015), which is similar to ST-HSC, that then differentiates into MPP2, MPP3 and MPP4 (Pietras et al. 2015; Wilson et al. 2008). The MPP2 and MPP3 populations are myeloid biased and constitute the traditional CMPs, with MPP2 found to be upstream of pre-megakaryocyte/erythroid (MegE) which makes up the MEPs that produce erythrocytes and platelets (Pietras et al. 2015). MPP3 is also myeloid biased however this was found to be upstream of pre-GM which differentiates to GMPs to produce basophils, eosinophils, neutrophils, monocytes, macrophages and DCs (Pietras et al. 2015). The MPP4 population appears to be more lymphoid biased differentiating to a lymphoid-primed MPP (LMPP), which goes on to produce the CLPs. As well as this MPP4 does also have some low myeloid potential associated with MegE (Pietras et al. 2015).

While these were the previously understood models of haematopoiesis, thought to occur in a stepwise manner, through the utilisation of new methodology like single-cell omics, it is now understood that haematopoiesis is a more continuous process with less rigid hierarchical categories (Velten et al. 2017; Yifan Zhang et al. 2018; Qin et al. 2021; Yokota 2019; Shaban et al. 2025; Laurenti and Göttgens 2018; Liggett and Sankaran 2020). Instead of different cell types being produced as a result of differentiation of the primitive cells, it is thought that HSCs fate, i.e., which lineage is going to be produced, is decided based on external signals from the body according to what is required and this provides a continuum of production of haematopoietic cells.

A

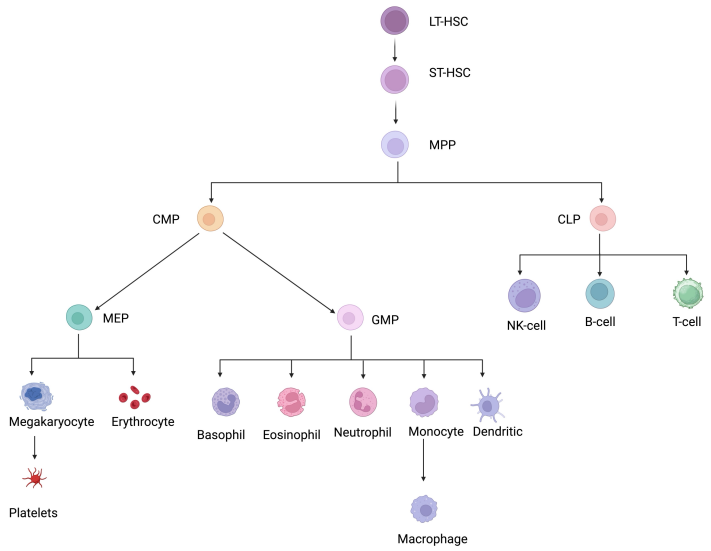
LT-HSC
ST-HSC
MPP
CMP
CLP
MEP
GMP
NK-cell
B-cell
T-cell
Megakaryocyte
Erythrocyte
Basophil
Eosinophil
Neutrophil
Monocyte
Dendritic
Platelets
Macrophage

B

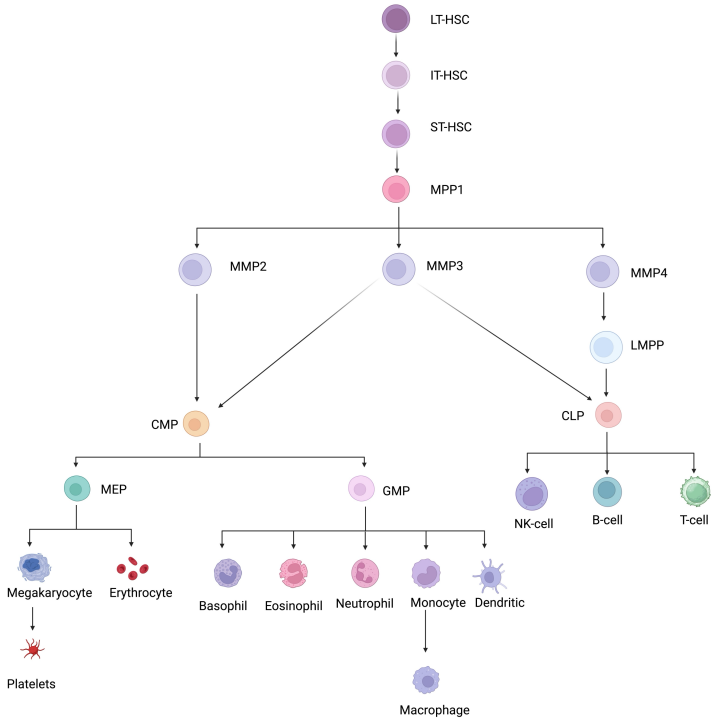
LT-HSC
IT-HSC
ST-HSC
MPP1
MMP2
MMP3
MMP4
LMPP
CMP
CLP
MEP
GMP
NK-cell
B-cell
T-cell
Megakaryocyte
Erythrocyte
Basophil
Eosinophil
Neutrophil
Monocyte
Dendritic
Platelets
Macrophage

C

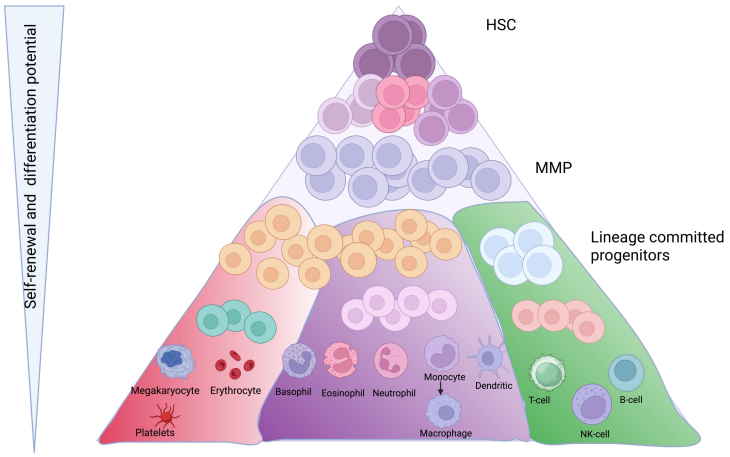
Self-renewal and differentiation potential
HSC
MMP
Lineage committed progenitors
Megakaryocyte
Erythrocyte
Basophil
Eosinophil
Neutrophil
Monocyte
Dendritic
T-cell
B-cell
Platelets
Macrophage
NK-cell

Figure 1-1 Hierarchy of haematopoesis (A) Classical system of haematopoesis: This begins with long term HSC (LT-HSC) which differentiates into short-term HSC (ST-HSC) and produces multipotent progenitors (MPP) these produce lineage committed cells called common lymphoid progenitors (CLPs) which produce B cells, T cells and natural killer (NK) cells. The MPP also produce common myeloid progenitors (CMP) that differentiate into megakaryocytic-erythroid progenitors (MEP) and granulocyte-monocyte progenitor (GMP). MEPs further differentiate into megakaryocytes/platelets and erythrocytes. While the GMPs produce basophils, eosinophils, neutrophils, monocytes, macrophages, and dendritic cells (DC). **(B)** Revised classical system of haematopoesis: This begins with long term HSC (LT-HSC) which differentiates into intermediate HSC (IT-HSC) into short-term HSC (ST-HSC) and produces multipotent progenitors (MPP) 1. From MPP1 there is the production of MPP2 and MPP3 which produce common myeloid progenitors (CMP) and differentiate into megakaryocytic-erythroid progenitors (MEP) and granulocyte-monocyte progenitor (GMP). MEPs further differentiate into megakaryocytes/platelets and erythrocytes. While the GMPs produce basophils, eosinophils, neutrophils, monocytes, macrophages, and DCs. MPP1 also produces MPP4 which produces lymphoid-primed MPP (LMPP). The LMPP along with MPP3 then goes on to produce lineage committed cells called common lymphoid progenitors (CLPs) which produce B cells, T cells and natural killer (NK) cells. **(C)** Updated haematopoesis hierarchy: This depicts a more continuous process of haematopoesis with less rigid stepwise progression. Image adapted from: (Yifan Zhang et al. 2018; Laurenti and Göttgens 2018; Yokota 2019; Liggett and Sankaran 2020; Qin et al. 2021; Shaban et al. 2025).

1.2 Bone marrow microenvironment (BMM)

Within the BM there are microenvironments that can be separated into specific ‘niches’, these are specialised sections of the BM that are responsible for a particular role in maintaining HSCs and controlling haematopoiesis. There are two main niches in the bone marrow: the endosteal and vascular niche, HSCs inhabit both of these, and different processes of haematopoiesis take place in different parts of the BM niches. Each niche is tightly controlled and provides the appropriate signals and interactions for regulating HSCs and progenitor populations, which is necessary for all blood cells to be produced based on what is required by the body (Galán-Díez et al. 2018; Mukaida et al. 2017). Within these niches there are a wide range of cells including mesenchymal stem cells (MSCs), sinusoidal endothelium and perivascular stromal cells, immune cells, soluble factors and several others that play important roles in HSC regulation (Nwajei and Konopleva 2013). Many HSCs are quiescent and are maintained this way in the endosteal niche, when these HSCs receive a signal to differentiate they move to the vascular niche, which is closer to sinusoidal blood vessels, and provides an environment where HSCs are stimulated to proliferate, mobilise, differentiate and mature (Lee et al. 2020).

As previously mentioned the vascular niche is associated with proliferation and differentiation of HSCs as well as their maintenance. One feature of the vascular niche is the blood vessels, the arterioles which are close to the bone and

endosteum, are covered by smooth muscle and extend into the vascular niche into sinusoids, the network of sinusoids then merge into the central venous sinus. It is through the sinusoidal network that blood cells are able to enter PB allowing for transport of oxygen, nutrients and waste. Within this niche there are also endothelial cells that line the blood vessel, several types of specialised MSCs, and smooth muscle cells that are surrounded by an extracellular matrix (ECM). Furthermore, Leptin-receptor-positive (LepR+) cells, C-X-C motif chemokine ligand 12 (CXCL12)-abundant reticular (CAR) and Nestin+ cells are specialised types of MSCs, which are found within this niche in the bone marrow microenvironment (BMM) particularly around the blood vessel and sinusoids (Kwon et al. 2024). These cells found in the vascular niche are responsible for secreting growth factors that regulate HSCs and haematopoiesis. Two important growth factors secreted by these cells are CXCL12 (also called SDF-1) and stem cell factor (SCF) which are involved in the regulation of HSCs. One of the most important pathways within the BMM and haematopoiesis is the interaction between CXCL12 and C-X-C motif chemokine receptor 4 (CXCR4). CXCL12 is a chemokine that binds to CXCR4 receptors, found on HSCs, the interaction results in the increased quiescence of HSCs and homing of HSCs to their niche (Sugiyama et al. 2006). The expression of CXCR4 is decreased on $CD34^+$ cells after exposure to CXCL12, but the expression of CXCR4 is increased with stimulation from SCF and interleukin 6 (IL-6), indicating these cytokines are also involved in regulating the HSCs (Peled et al. 1999). SCF is a cytokine that binds to c-Kit receptor (CD117) found on all HSCs, maintaining HSC survival (Hassan and Zander 1996) and self-renewal (Bowie et al. 2007). Previous research found matrix metalloproteinase 9 caused an increased release of soluble SCF from endothelial cells into the BMM which resulted in the HSCs moving to the vascular niche and becoming proliferative (Heissig et al. 2002), indicating SCF is involved in both the maintenance and survival of HSCs as well as their proliferation. Furthermore, the HSCs in the vascular niche are found adhered to the endothelial cells (Sugiyama et al. 2006), these endothelial cells express adhesion molecules like P-selectin (CD62P), E-selectin (CD62E) and vascular cell adhesion molecule-1 (VCAM-1/CD106), their receptor molecules, CD162, CD44 and VLA-4 (CD49d), are expressed by haematopoietic stem and progenitor cells (HSPCs) which drives the cell-cell interaction (Kwon et al. 2024).

The endosteal niche, also called the osteoblastic niche, is closest to the bone of the BM and as its name suggests this niche is mostly composed of osteoblast cells. The endosteal niche is known for the maintenance of quiescent HSCs, it is also known for having very low oxygen and the most quiescent HSCs are positioned in areas of low oxygen (Jang and Sharkis 2007). This is due to the transcription factor hypoxia-inducible factor-1α (HIF-1α), in low oxygen conditions HIF-1α stabilises and causes transcription of many pathways including inducing quiescence in HSCs (Takubo et al. 2010). The osteoclasts found in this niche produce Ca^{2+} ions (Silver et al. 1988) and HSCs have Ca^{2+} receptors, causing them to home to this niche (Lévesque et al. 2010). The osteoclasts are also essential to this niche, while it was found that removal of osteoclasts did not affect mobilisation of HSPCs (Miyamoto et al. 2011) the presence of osteoclast is essential for the formation of the niche as the removal of osteoclasts significantly reduces HSC homing within the niche and MSCs have a reduced expression of genes involved in HSC homing and quiescence (Mansour et al. 2012). CXCL12 and SCF are also produced by osteoblasts, here their role is to maintain the homing of HSCs to this niche and cause quiescence of HSCs. This is usually in response to oxidative stress, external stimulus and to protect HSCs for long term use and prevent their exhaustion. In addition, osteoblasts found here are also thought to be involved with lymphopoiesis, the production of IL-7 by osteoblasts was found to be crucial for the production of CLPs, inhibition of IL-7 caused a significant decrease to the production of T and B cells within the mouse femur (Terashima et al. 2016).

There are several other factors found within the BMM including granulocyte colony-stimulating factor (G-CSF) which is known for its essential role in activation and proliferation of HSCs to produce granulocytes as well as the mobilisation of HSCs into the bloodstream. G-CSF does this by decreasing the CXCL12 levels secreted by osteoblasts, this leads to increased mobilisation of the stem cells out of the BM (Petit et al. 2002).

In recent years the essential involvement of megakaryocytes in haematopoiesis has been researched. It was previously shown (Figure 1-1) that megakaryocytes are produced from MPPs, however, new research has found a specific subpopulation of HSCs that can also directly produce megakaryocytes (P. Zhang et al. 2022). As well as being involved in platelet production, megakaryocytes

are responsible for maintaining the quiescence of HSCs, through their production of CXCL4, transforming growth factor β1 (TGF-β1) and TPO. Bruns et al., found that CXCL4 was being released directly from megakaryocytes, as the removal of megakaryocytes caused a significant reduction in the production of CXCL4. Furthermore, the removal of CXCL4 in mice increases the number and proliferation of HSCs, however when CXCL4 was administered the quiescence of HSCs returned (Bruns et al., 2014). Additionally, it was found that megakaryocytes had the highest production of TGF-β1 than other stromal cells in the BM, and the activation of the TGF-β1 protein maintained HSC quiescence through the phosphorylation of SMAD2/3 (Zhao et al., 2014). Finally, megakaryocytes also had the highest production of TPO, compared to other niche cells, the addition of TPO in the absence of megakaryocytes restored HSC quiescence (Nakamura-Ishizu et al. 2014). Overall, megakaryocytes appear to be responsible for maintaining the quiescence of HSCs.

The signalling pathways within the BMM area another crucial aspect of maintenance of haematopoietic homeostasis. Namely, the Notch, Wnt, Hedgehog (Hh) and TGF-β signalling pathway. The Notch signalling pathway is essential within the BMM for regulation of haematopoiesis. NOTCH1 receptor is found on HSCs (Varnum-Finney et al. 1998), the NOTCH1 ligand (JAG1) that interacts with this receptor is produced by MSCs (Varnum-Finney et al. 1998), osteoblasts (Calvi et al. 2003) and endothelial cells (Poulos et al. 2013). The activation of the NOTCH signalling pathway via JAG1 secretion from endothelial cells was found to maintain HSC quiescence and self-renewal capacity while maintaining the HSC pool (Poulos et al. 2013). The Wnt signalling pathway can be separated into two categories: canonical and non-canonical Wnt signalling. The activation of this pathway from Wnt ligand binding to its receptor, stabilises β-catenin. The β-catenin is able to translocate to the nucleus where it binds to transcription factors which increases expression of target genes. The activation of the Wnt signalling pathway has been found to be essential for the self-renewal and proliferation of HSCs (Reya et al. 2003). The Hh pathway can be activated by a Hh protein (Sonic Hh (Shh), Indian Hh (Ihh), Desert Hh (Dhh)), these bind to the Patched (Ptch) receptor, preventing its inhibition of smoothened (Smo) receptor. The activation of Smo allows the Gli transcription factors to move to the nucleus and promotes the expression of target genes (J.

Gao et al. 2009). This pathway was not found to have a significant effect on the function of normal HSCs (J. Gao et al. 2009) however Hh signalling pathway has been found to be dysregulated in CML. Finally, the TGF-β signalling pathway has a wide range of ligands involved in its regulation. With regards to HSCs there are several factors involved in activating the TGF-β signalling pathway, activation of TGF-β signalling has been found to maintain HSC quiescence (Yamazaki et al. 2009).

The understanding of haematopoiesis hierarchy is ongoing and constantly evolving as novel techniques and approaches are used to understand this complex process. There are several factors outwith the BMM that can affect the tightly regulated process of haematopoiesis and the structured regulation that occurs within the BMM.

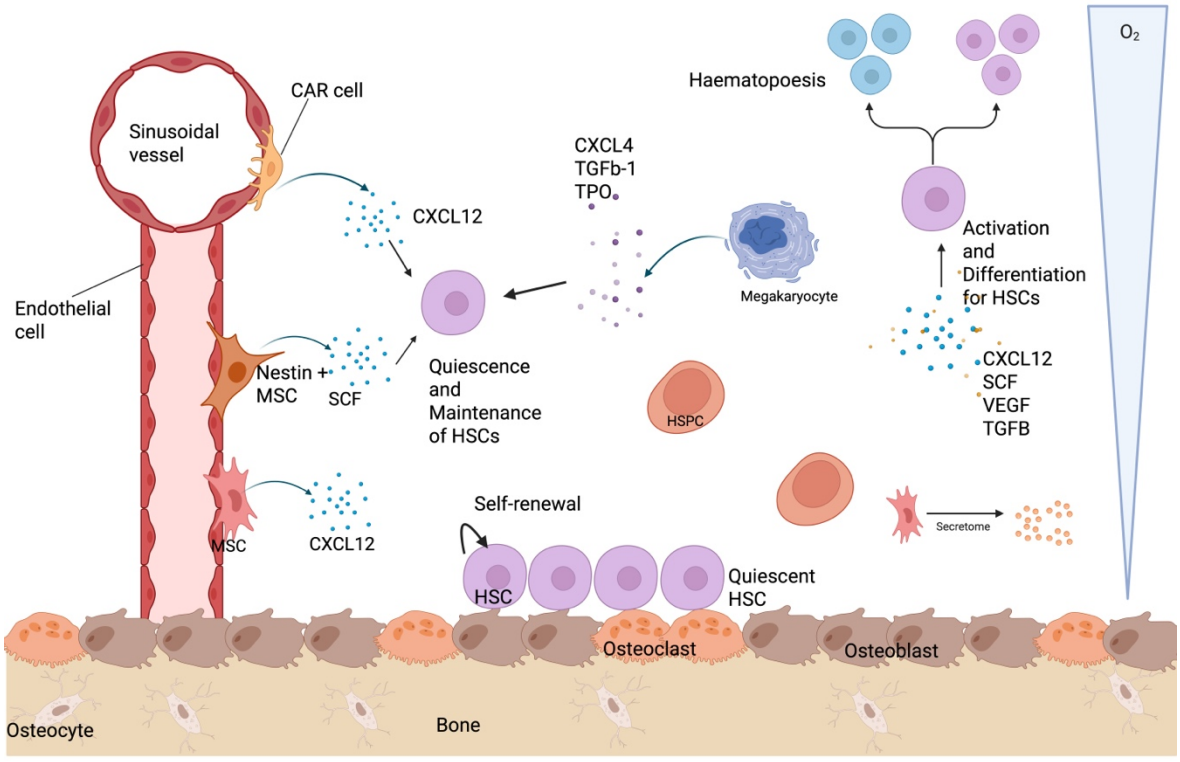

Figure 1-2 Representative image of a healthy BMM Within the BMM there are osteoblasts and osteoclasts, mesenchymal stem cells (MSCs), Nestin+ MSCs, sinusoidal vessel, CXCL12-abundant reticular (CAR) cells, immune cells, cytokines, growth factors, and several others that play important roles in HSC regulation. Many HSCs are quiescent and are maintained this way and when these HSCs receive a signal to differentiate, they move closer to sinusoidal vessels (higher O_2 levels), which provides an environment where HSCs are activated to proliferate, mobilise, differentiate and mature. The BMM is tightly controlled and provides the appropriate signals and interactions for regulating HSCs and progenitor populations, which is necessary for all blood cells to be produced based on what is required by the body.

Various signals are involved in the regulation of haematopoiesis, among these inflammatory signals within the BMM have emerged as playing a significant role, many factors including infections and chronic diseases can induce inflammation which in turn can affect HSC development and maintenance. Inflammation can promote HSCs into differentiating by altering the balance within the BM niche, through changes in pro-inflammatory cytokines/chemokines, alterations in cell populations and changes to the ECM. Inflammation can result in HSC skewing their differentiation to myeloid lineage, if this inflammatory exposure persists it can lead to the exhaustion of HSCs (Bousounis et al. 2021). Additionally, a person's age is also an important factor in the changes seen to haematopoiesis within the BMM. Age related clonal haematopoiesis (ARCH) is a common phenomenon with a high incidence in the over 70 age group, this results in the selection of HSCs with a somatic mutation many of which are DNA epigenetic modifiers or genes involved in response to DNA damage (Bolton et al. 2020; Bowman et al. 2018; Lundberg et al. 2014). ARCH has been linked to myeloproliferative disorders and secondary leukaemia following cancer treatment (Bolton et al. 2020; Bowman et al. 2018; Lundberg et al. 2014).

1.2.1 Mesenchymal stem cells (MSCs)

The MSCs are the supportive stroma of the BMM and play a fundamental role in the formation of the niches as well as the support and maintenance of HSCs and haematopoiesis. As well as having specialised forms of MSCs in the vascular niche, MSCs can also be found in the endosteal niche. They are multipotent cells which can differentiate to produce adipocytes, osteoblasts and chondrocytes which are all essential cell types found in the BMM. The MSCs are involved in supporting HSCs, immunomodulation, and ECM secretion to control mechanobiology aspects of the BMM. Additionally, MSCs release soluble molecules such as cytokines, chemokines and growth factors into the BMM which is called the secretome.

The differentiation potential of MSCs is dependent on stimulus from the microenvironment based on what is required. The differentiation capacity of MSCs was examined using single-cell sequencing, this found two main branches of the MSCs: adipocyte progenitors and osteoblast-chondrocyte progenitors (Wolock et al. 2019). The adipocyte progenitors then further differentiate into

pre-adipocyte progenitors, while the osteoblast-chondrocyte progenitors differentiate into pre osteoblast-chondrocyte and then again into pro-osteoblast and pro-chondrocyte. Gene set enrichment analysis (GSEA) by Wolock et al., of these groupings found TNFα signalling via NFKβ and adipogenesis pathway enrichment of pre-adipocyte and adipocyte progenitors. The osteoblast-chondrocyte progenitors and pre osteoblast-chondrocyte were found to have enrichment of ECM, epithelial-mesenchymal transition, extracellular space and tissue development. Enrichment within the pre-osteoblast cluster found endoplasmic reticula, Golgi apparatus, skeletal system development, and ossification while pro-chondrocyte had tissue development, extracellular space, and biomineral tissue development. For the formation of chondrocytes, the transcription factors SOX9 (Bi et al. 1999) and Scleraxis (Cserjesi et al. 1995) have been identified. For osteoblast differentiation of MSCs Runx2 and Osterix are two transcription factors that are involved in this, they also inhibit adipocyte differentiation (Gao et al. 2022). However, adipocyte differentiation is controlled by the transcription factors PPARγ and CEBPα (S.-S. Liu et al. 2024). Additionally, there are several bone morphogenic proteins (BMPs) which are part of the TGF-β family, that have been implicated in production of osteoblasts (Lee et al. 2025) and chondrocytes (Zhou et al. 2011) as well as regulation of HSCs (Crisan et al. 2015).

MSCs also have immunomodulatory effects within the BM either by cell-cell contact or through secretory molecules. They have mostly been found to exhibit anti-inflammatory and immunosuppressive effects. One example of these immunomodulatory effects is the MSCs regulation of B cell activity, BM MSCs from interleukin - 1 receptor antagonist (*IL-1RA)* knockout mice were unable to inhibit the differentiation of B cells, unlike the wild-type MSCs (Luz-Crawford et al. 2016) indicating IL-1RA produced from BM MSCs is required for the differentiation of B cells. Additionally, MSCs inhibit T cell proliferation, the presence of MSCs with activated T cells led to T cell apoptosis (Plumas et al. 2005). MSCs induce macrophages with a pro-inflammatory phenotype, M1, to differentiate into an anti-inflammatory phenotype (M2) (J. Liu et al. 2022), this is through the secretion of TGF-β (F. Liu et al. 2019) and C-C motif chemokine ligand 2 (CCL2) (Papa et al. 2018). While MSCs are mostly known for their immunoinhibitory effects, under certain conditions they also rarely induce

inflammation within the BM. MSCs can secrete pro-inflammatory factors such as IL-6, IL-8 and CCL2 (Hoogduijn et al. 2010), however this is seen much less and is thought to occur in response to stress, to activate the immune response and is seen in disease and aging. With aging MSCs become senescent which causes the secretome they produce to become more pro-inflammatory.

One of the most important roles of MSCs within the BMM is their role in supporting HSCs, this is particularly through the secretion of CXCL12 and SCF which as previously described are involved in maintaining the quiescence of HSCs. Additionally, the differentiation of MSCs directly affects the HSC population. Many HSCs reside in the endosteal niche on the osteoblasts, a reduction of osteoblast lineage in the BMM also leads to a reduction in the number of HSCs and haematopoiesis (Visnjic et al. 2004), osteoblasts are essential for the maintenance of HSCs (Taichman et al. 1996). Additionally, the osteoblasts produce thrombopoietin (TPO) (Qian et al. 2007), angiopoietin 1 (Ang1) (Arai et al. 2004), osteopontin (OPN) (Nilsson et al. 2005) and WNT5A (Nemeth et al. 2007; Maeda et al. 2012) which maintain HSC quiescence. The increased production of adipocytes within the BM is also associated with having a negative effect by impairing the haematopoietic process (Naveiras et al. 2009).

The ECM in the BMM is a structural network composed of proteins such as fibronectin, proteoglycans and collagens, and contains growth factors, cytokines and metalloproteinases (Krause et al. 2013). The ECM is an essential part of the BMM and provides structural support, cell adhesion and migration as well as cell-cell interactions. A major source of production for ECM is MSCs which produce fibronectin, collagens, laminin and osteopontin which are all involved in the regulation of HSCs (Suresh et al. 2025). MSCs are very adaptive to the needs of the BMM and one way in which they have been seen to adapt to their environment is through tissue repair, it has been demonstrated that administration of MSCs to lung tissue after injury reduced inflammation and collagen deposition (Ortiz et al. 2003). Additionally, patients experiencing graft vs host disease (GVHD), which is an inflammatory state in patients who have received a BM transplant where graft immune cells attack the host, were given an infusion of MSCs after which 6 out of 8 patients had reversal of their GVHD (Ringdén et al. 2006).

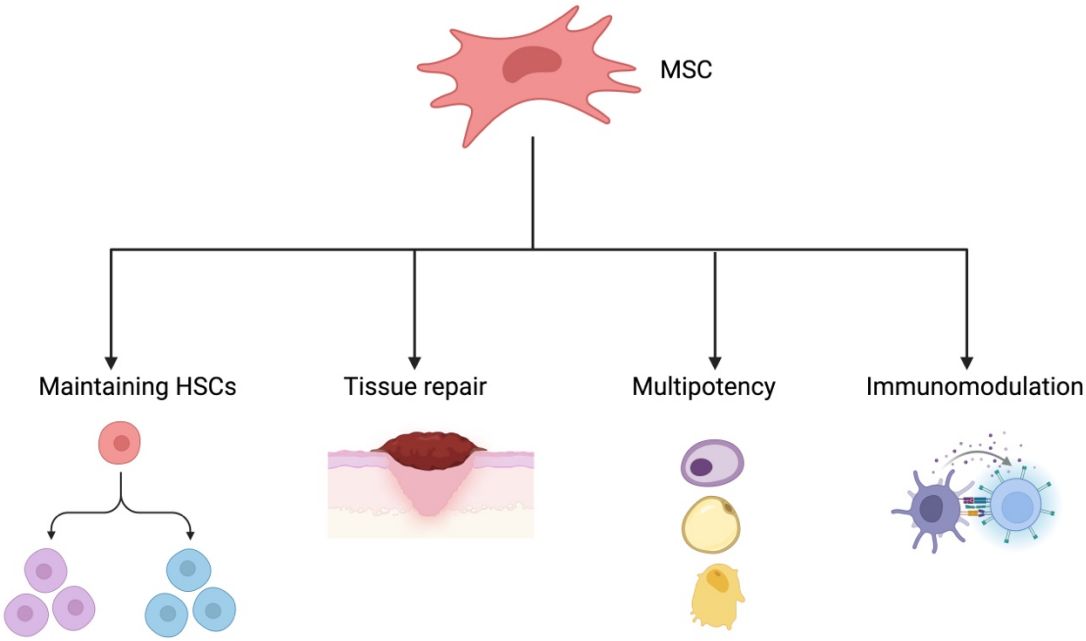

Figure 1-3 Role of MSCs within the BMM

Due to the essential role MSCs play not only in maintaining the BMM but also in supporting HSCs and haematopoiesis, changes to MSCs can be detrimental to BM health and normal blood production.

The BMM is composed of a delicate balance and any changes to the equilibrium of the interactions within the BMM are detrimental to HSCs and haematopoiesis. If the closely regulated, highly sensitive process of haematopoiesis is compromised this can in some instances cause leukaemia.

1.3 Chronic myeloid leukaemia (CML)

Chronic myeloid leukaemia (CML) occurs in around 1 per 100,000 of the population, with the median age of diagnosis being 56 (Eden and Coviello 2025). Up to 15% of new cases of adult leukaemia are CML (Shammas et al. 2025). CML is a myeloproliferative neoplasm that occurs when HSCs gain a *BCR::ABL1* mutation and transform into leukaemic stem cells (LSCs).

This mutation arises from the reciprocal translocation between chromosomes 9 and 22 which produces: t(9;22)(q34;q11), also known as the Philadelphia (Ph) chromosome. This was first identified by Peter Nowell and David Hungerford who reported on an abnormal chromosome 22 in CML patients (Nowell and

Hungerford 1960). Following this, in 1973 Janet Rowley discovered that the Ph chromosome was the result of a reciprocal translocation between chromosomes 9 and 22 (Rowley 1973). While there are no known risk factors including hereditary risk factors that increase the chances of a CML diagnosis, the incidence does increase with age. It is unknown how exactly this mutation occurs, often thought to be due to random chance however this mutation is mostly seen in older patients. The translocation includes the breakpoint cluster region (*BCR*) gene which is found on chromosome 22 and the Abelson murine leukaemia viral oncogene homolog 1 (*ABL1)* gene which is found on chromosome 9. This translocation results in the *BCR::ABL1* oncogene which produces the BCR::ABL1 oncoprotein, a constitutively active tyrosine kinase (TK) (Hamad 2021).

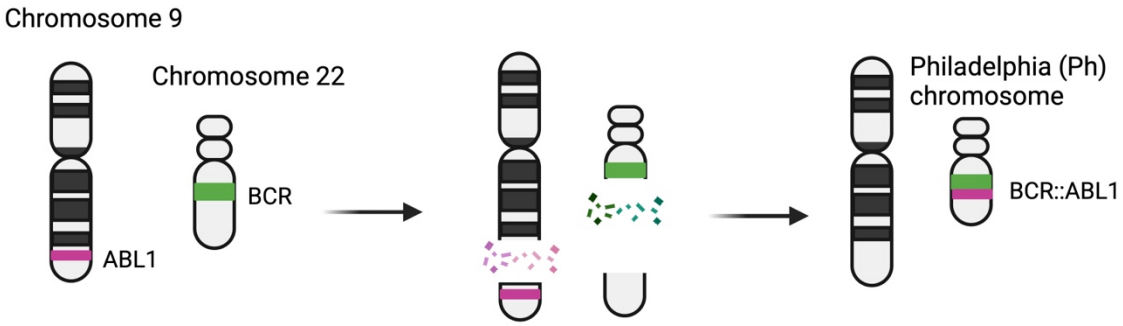

Figure 1-4 Representative image of BCR::ABL1 translocation Image adapted from (Irgit et al. 2025).

The break can cause three possible variants to arise as a result of the translocation: p190, p210 and p230, these are named after the size of protein they produce in kilodaltons. The most common variant found in CML patients is p210, which is the result of fusion of major breakpoint cluster region (M-BCR) (breaking between exons 12 and 14) and ABL. Together this produces two main isoforms e13a2 and e14a2, both of these isoforms give rise to the p210 protein (J. Lee et al. 2017). This p210 variant is found in 95% of CML patients and is also found in acute lymphoblastic leukaemia (ALL) patients. The p190 variant is the result of breakpoint in the minor breakpoint cluster region, this variant produces e1a2 which is more aggressive than p210 (Li et al. 1999) and mostly occurs in Ph+ ALL (Chan et al. 1987). Finally, the p230 produces e19a2 and is mostly found in cases of chronic neutrophilic leukaemia (CNL). This is the result of a break in

the micro breakpoint cluster region. This is the largest form and was reported that patients present with more mild clinical symptoms as it has the lowest tyrosine kinase activity of all three (Li et al. 1999).

BCR is a GTPase-activating protein (GAP). ABL1 is a non-receptor tyrosine kinase and has active and inactive states. ABL1, in its active form, phosphorylates proteins through its SH1/tyrosine kinase (TK) domain leading to downstream signalling pathways being activated (Hamad 2021). Through the fusion with BCR, the regulatory SH2 and SH3 domain is lost so TK/SH1 domain is constitutively active, resulting in deregulation of downstream signalling pathways and ultimately inhibition of apoptosis and unrestricted proliferation.

The TK/SH1 domain consists of two subdomains: a N-terminal lobe and a C-terminal lobe. There is a phosphate binding loop within the N-terminal and a substrate binding site in the C-terminal. Between these two terminals there is an ATP-binding site and activation loop (A-loop) (Rossari et al. 2018). If the A-loop is unphosphorylated the ABL1 kinase is inactive as the A-loop folds into the binding site which blocks the binding of ATP and substrate (A. Wu et al. 2024). In the active state the A-loop is phosphorylated and takes on an open form which allows binding within the binding site (A. Wu et al. 2024).

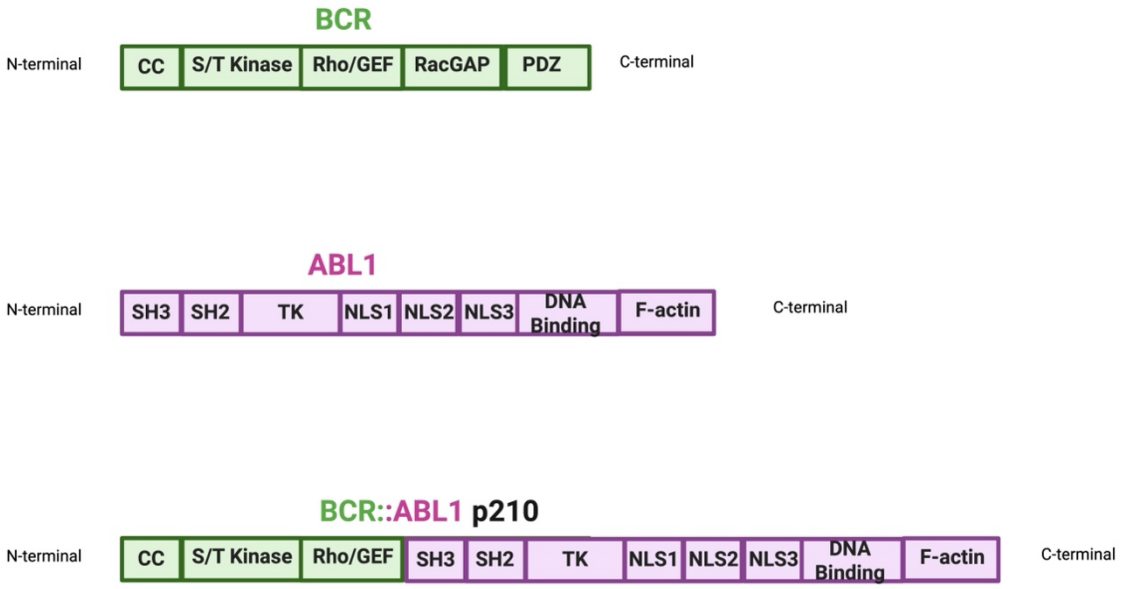

Figure 1-5 Representative image of BCR and ABL1 BCR gene encodes a coiled-coil domain (CC), a serine/threonine kinase domain (S/T kinase), a Rho/GEF domain, a RacGAP domain and a PDZ domain. The ABL gene encodes a SH3 domain, a SH2 domain, a tyrosine kinase (TK)/(SH1) domain, nuclear localisation signal 1 (NLS1), nuclear localisation signal 2 (NLS2), nuclear localisation signal 3 (NLS3), and DNA-binding domain and F-actin domain.

The c-terminal of the BCR fuses with the N-terminal of the ABL1, the loss of the N-terminal of ABL1 includes the loss of the myristoylation group, and loss of the autoinhibitory effect on the activity of ABL1. The autoinhibitory effect occurs when the myristoylation group binds to the kinase domain, this in turn stabilises the SH2 and SH3 domains of ABL1 which have inhibitory effects, they restrict the TK domain to ensure it remains inactive (A. Wu et al. 2024; Irgit et al. 2025). Additionally, the coiled-coil (CC) region of BCR causes dimerization and oligomerization of the BCR::ABL1 making it constitutively active (Irgit et al. 2025; A. Wu et al. 2024). Furthermore, the fusion causes a disruption of the normal movement of ABL from the nucleus to the cytoplasm, keeping it in the cytoplasm and therefore increasing the proliferation signalling pathways that ABL1 is responsible for activating (Cilloni and Saglio 2012). This is due to the disruption of nuclear localisation signal (NLS) and DNA-binding domains on ABL1.

The presence of BCR::ABL1 leads to the dysregulation of several signalling pathways that result in a range of downstream effects. These include Ras/Mitogen-Activated Protein Kinase (RAS/MAPK) pathway, Phosphatidylinositol 3-Kinase/Protein Kinase B (PI3K/AKT), Janus Kinase/Signal Transducer and Activator of Transcription (JAK/STAT) pathway and Nuclear Factor Kappa-light-chain-enhancer of activated B cells (NFκß) pathway.

Presence of *BCR::ABL1* causes the transformation of HSCs to LSCs (Hamad 2021). LSCs share many of the same attributes of HSCs including self-renewal and quiescence (Toofan et al. 2018). The quiescence of LSCs (and HSCs) is in part to be due to HIF-1α, as it has been reported the loss of HIF-1α causes loss of quiescence in LSCs (H. Zhang et al. 2012). This transformation hijacks the normal process of haematopoiesis causing the aberrant haematopoiesis resulting in leukaemogenesis. The persistence of LSCs is also linked to the signalling environment within the BM. As previously mentioned, the microenvironment is organised by many signalling proteins including chemokines, cytokines, and morphogens, when *BCR::ABL1* gives rise to LSCs in CML these signals are distorted to maintain the LSCs and encourage disease progression. Initially, CML was described as a triphasic disease that initially presents with the chronic phase (CP) which is when there is an increase in myeloid cells, if there is no

therapeutic intervention the disease will progress due to additional genetic mutations to accelerated phase (AP) and eventually blast phase (BP), at this point there is a huge expansion of myeloid precursors that are found throughout the circulatory system. More recent classification has removed AP, recognising only CP and BP in CML. BP is an aggressive form of the disease with limited treatment options. Most people with CML initially present in the CP. While an incurable disease due to LSC persistence, if diagnosed in CP, CML is highly treatable due to the use of tyrosine kinase inhibitors (TKIs), which target BCR::ABL1 and prevent proliferation and survival of leukaemic cells.

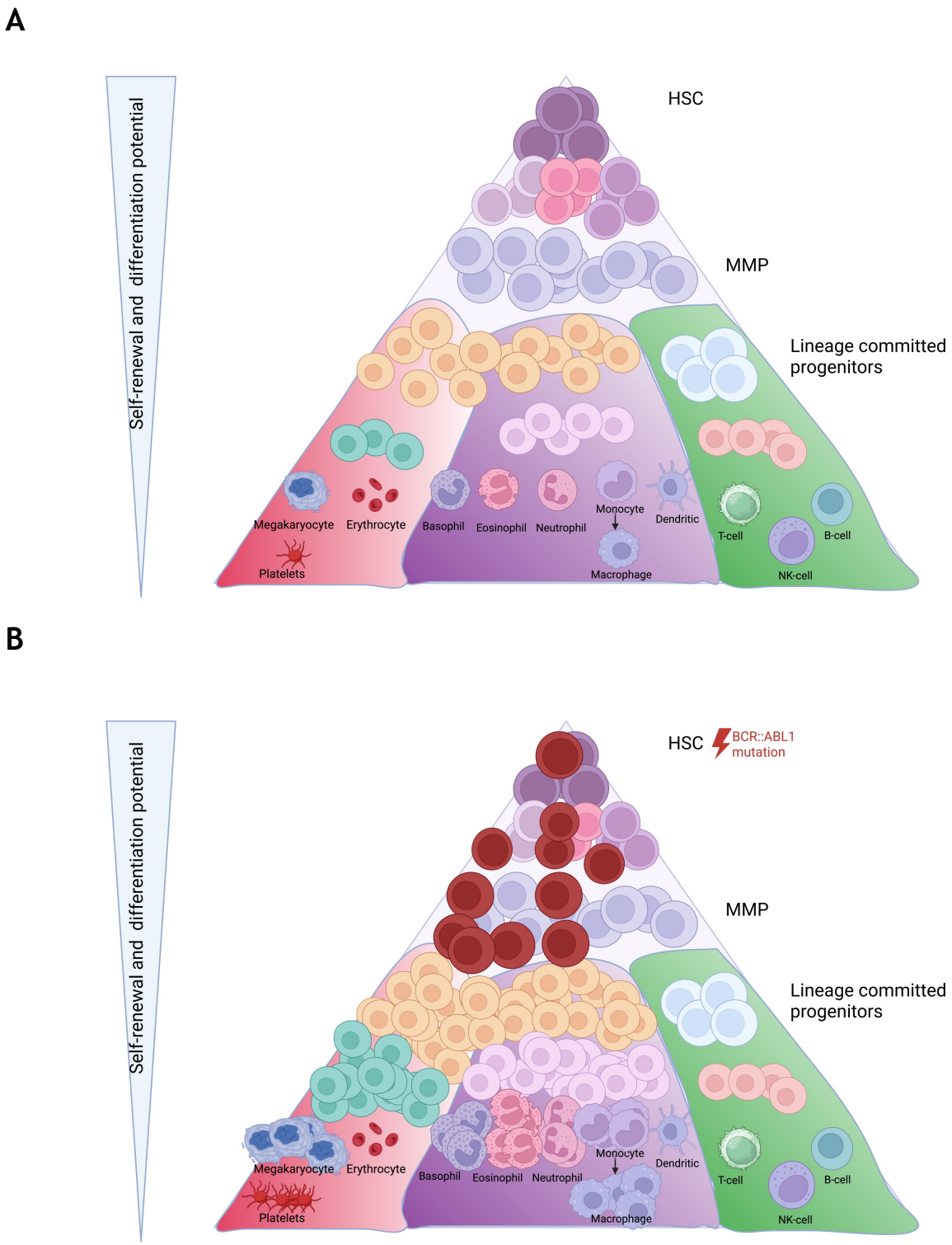

Figure 1-6 Hierarchy of haematopoesis under normal conditions and in CML (A) Represents normal haematopoesis **(B)** Represents hameatopoesis in CML when HSCs gain a *BCR::ABL1* mutation.

1.4 Tyrosine kinase inhibitors (TKI)

The treatment options for patients with CML are excellent, and this comes from the revolutionary development of TKIs. TKIs are small molecule inhibitors that block the ATP-binding site on the BCR::ABL1 kinase and therefore stop the phosphorylation of downstream effector proteins (Hughes and Yong 2017). As well as targeting and inhibiting the oncokinase, the TKIs other mode of action is to restore the immune system back to normal, as it is found to be dysfunctional in CML patients (Hughes and Yong 2017). The use of TKIs in CML has revolutionised prognosis of patients, most patients respond well to TKIs and because of this have a close to normal life expectancy (Bower et al. 2016).

Before the discovery of TKIs the first line treatment option for CML patients was interferon-alpha (IFN-α). Clinical trials using IFN-α found in 20-60% of patients cytogenetic response ("*reduced Ph+ metaphases in BM*") was observed with 5-30% having a complete cytogenetic response ("*by conventional karyotyping, that is analysing mitotic BM cells, when zero out of 20 are found to have Ph chromosome 0% Ph+, the patient is said to have a complete cytogenetic response*") (Kujawski and Talpaz 2007). While this provided a level of control /delay to CML progression the toxicities and side effects of using IFN-α were often intolerable.

The first TKI developed was imatinib mesylate (Glivec™, formerly STI571) in the year 2000, this was a groundbreaking therapy that changed the trajectory of CML patients' lives and was found to be a therapy that was able to directly target BCR::ABL1 and inhibit its actions. Imatinib works by competitively binding with ATP for the binding site in the enzymatic pocket of Abl1 kinase resulting in inactivating the substrate tyrosine residues preventing their phosphorylation which stops downstream signalling pathways that are usually upregulated in CML (Iqbal and Iqbal 2014). Imatinib also targets platelet-derived growth factor receptor alpha (PDGFRA) and c-KIT (Iqbal and Iqbal 2014). As imatinib is a more specific treatment that is able to inhibit the root cause of CML this has an exceptional ability to prevent disease progression. There was a trial carried out called International Randomized Study of Interferon and STI571 (IRIS) where a direct comparison of CML patients taking imatinib compared to patients taking IFN-α plus cytarabine. This found 87% of patients on imatinib were in complete

cytogenic response (CCyr) after 60 months, only 7% of patients did progress to AP-CML or BP-CML (Druker et al. 2006). However, in an 8-year follow-up of the same trial only 55% of patients were still taking imatinib, the rest had stopped for a range of reasons including adverse effects and unsatisfactory therapeutic outcome (Deininger et al. 2009). It is known that TKIs like imatinib can cause various side effects including rashes, fatigue, muscle aches and more (Bourne et al. 2024). As well as incompatibility due to side effects, around 30% of patients will develop resistance to imatinib due to the development of point mutations on the kinase domain of BCR::ABL1 (Martínez-Castillo et al. 2023).

Due to these limitations of imatinib and the identification of mutant versions of BCR::ABL1 that were preventing effective disease control from imatinib, this incited further advances in the production of new TKIs to make them more effective for patients that cannot use imatinib, these are called second-generation TKIs. These second generation TKIs are more potent and targeted than imatinib. These include dasatinib (Sprycel™), nilotinib (Tasigna™) and bosutinib (Bosulif™), which are all found to have a greater potency than imatinib, they do also come with different side effects and toxicities.

TKIs can be separated into two categories: type 1 and type 2, both types are ATP-competitive inhibitors however type 1 inhibitors bind to an active state of BCR::ABL1 while type 2 inhibitors bind to the inactive state (Patel et al. 2017).

Dasatinib can target both active and inactive forms of BCR::ABL1 (Shammas et al. 2025), patients that were given dasatinib were more likely to achieve major molecular response (MMR) and achieved it faster than those given imatinib (H. Kantarjian et al. 2010). Dasatinib binds to the ATP binding site and also binds to other kinases including the Src family kinases. Compared to imatinib, dasatinib has a 2-log higher potency, and was effective in 14 out of 15 imatinib resistant BCR::ABL1 mutants (Shah et al. 2004) making it a good choice for patients that develop point mutations and become resistant to imatinib.

Nilotinib is structurally very similar to imatinib and works in the same way by binding near the ATP binding site and inactivating the tyrosine kinase. While nilotinib has no effect on Src tyrosine kinases (Manley et al. 2007) like imatinib it does inhibit c-kit and platelet-derived growth factor receptor (PDGFR) activity

(Weisberg et al. 2005). This was also able to target imatinib resistant BCR::ABL1 variants, except for T315I (Kantarjian et al. 2007).

Finally, there is also bosutinib which targets both BCR::ABL1 and Src kinases. Like the other second-generation TKIs this is effective against imatinib resistant BCR::ABL1, with the exception of the T315I mutation (Steinbach et al. 2013).

While second-generation TKIs were an excellent next step for overcoming imatinib resistance, the T315I mutation of the TK domain is an issue as it was found most first and second generation TKIs were unable to target the mutant. This mutation alters the ATP-binding site and reduces TKI binding affinity (Pierro et al. 2025). To overcome these mutations within *BCR::ABL1,* third-generation TKI ponatinib was produced. Ponatinib is able to bind to several BCR::ABL1 mutants including T315I, with a high affinity and successfully inhibit its activity (Tanneeru and Guruprasad 2013).

Once patients begin treatment, to monitor their treatment response, they have regular blood tests taken to measure the *BCR::ABL1* mRNA levels. This is measured using quantitative (q)RT-PCR to measure the expression of *BCR::ABL1* in PB samples of patients compared to a housekeeping gene (*ABL1, BCR, or GUSB*). The levels are measured in reference to the International Scale (IS) (BCR::ABL1^{IS}), this was created to standardise testing and results for all CML patients. This is shown as a percentage with baseline set at 100%. From the IRIS study, alongside testing of imatinib, this study looked at the level of BCR::ABL1 reduction in patients and how that related to their risk of disease progression. It was here that they defined MMR as patients with 0.1% BCR::ABL1 levels and these patients had a 100% chance of staying progression free after 12 months (Hughes et al. 2003). In patients with a 4-log reduction or higher of *BCR::ABL1* transcripts from the baseline, this is also called deep molecular response (DMR). This is the best possible response a patient can have to TKI and indicates and almost completely eradicated CML, although patients will have remaining quiescent LSCs. Due to the exceptional response to treatment, it was initially proposed for patients in DMR to attempt stopping TKIs to see if they could maintain remission.

Response	Definition
Complete haematological response (CHR)	Completely normal peripheral blood cell counts
Minimal cytogenetic response	36% to 95% Ph+ metaphases in BM
Partial cytogenetic response	1% to 35% Ph+ metaphases in BM
Major cytogenetic response (MCyR),	0% to 35% Ph+ metaphases in BM
Complete cytogenetic response (CCyR)	0% Ph+ metaphases in BM
Equivalent to CCyR	≤1% *BCR::ABL1* transcript levels
Major molecular response (MMR)/MR3	≤0.1% *BCR::ABL1* transcript levels
4 log reduction from the IS standardized baseline (MR4)	≤0.01% *BCR::ABL1* transcript levels
4.5 log reduction from the IS standardized baseline (MR4.5)	≤0.0032% *BCR::ABL1* transcript levels
5 log reduction from the IS standardized baseline (MR5)	≤0.001% *BCR::ABL1* transcript levels

Table 1-1 Demonstration of the patient response to CML Information from CHR to CCyR was taken from (Cortes et al. 2011). From equivalent to CCyR to MR5 table taken from EuropeanLeukaemia Net 2025 recommendations (Apperley et al. 2025).

After diagnosis, for testing, PB samples are taken every 2 weeks until patient achieves CHR, unless patient is determined not compatible and they have haematological toxicity to the TKI. After reaching CHR, measurements of PB are taken every 3 months until the patient achieves MMR at which point testing every 4-6 months takes place.

The time frame in which patients achieve a certain response is monitored closely as this can be indicative of a patients overall health. The 2025 European LeukemiaNet reported the current milestones that are monitored in CML patients:

	Favourable Low risk of developing resistance: treatment switch unnecessary	Warning Possible risk of developing resistance: treatment switch may become necessary	Unfavourable High risk of developing resistance: treatment switch preferred
Baseline	NA	High-risk additional chromosomal abnormalities (ACA), high-risk EUTOS Long Term Survival (ELTS) score	NA
3 months	≤10%	>10%	>10% if confirmed within 1–3 months
6 months	≤1%	>1–10%	>10%-established resistance
12 months	≤0.1%	>0.1–1%	>1% (1–10%)
At any time	≤0.1%	>0.1–1% loss of ≤0.1% (MMR)	Loss of a previous response, resistant *BCR::ABL1* mutations, high-risk ACA

Table 1-2 Response milestones for TKIs Table taken from: 2025 European LeukemiaNet (Apperley et al. 2025).

These timelines are used as guidelines for patients taking TKIs to help decide if the patient is taking the optimal TKI. However, a change of TKI would be carefully considered along with other factors for a patient, although it does appear that those first 12 months are essential in forecasting how a patient will react long term to treatment. A recent study found patients that achieve MR3 within the first 3 months of taking TKIs was predictive of achieving DMR (Breccia et al. 2025).

Patients who achieve DMR (defined as *BCR::ABL1* to *ABL1* ratio of ≤0.01% IS (MR4) or lower) are potential candidates to trial treatment free remission (TFR). TFR is the process by which some CP-CML patients stop taking TKIs and can maintain remission, this is an excellent way to combat the negative impact associated with prolonged TKI use, however not all patients can successfully maintain TFR.

While the outcomes for most patients with CML has vastly improved there are several implications for those on life-long treatment of TKIs. This can result in physiological, economic and psychological side effects associated with long term treatment and disease monitoring.

According to 2025 European LeukemiaNet there are 6 TKIs for first-line therapy in CML: imatinib, dasatinib, nilotinib, bosutinib and in some countries asciminib and in South Korea they also use radotinib (Kwak et al. 2017) (Apperley et al. 2025).

1.5 Treatment free remission (TFR)

A major obstacle for treatment of CML is the persistence of LSCs through treatment owing to their quiescence and self-renewal properties within the BMM. These LSCs can then be activated when treatment is stopped thereby driving relapse (Hsieh et al. 2021). Several factors play a role in this; there is particular interest in the role immunological changes within the BMM has in protecting LSCs and causing relapse when attempting TFR.

While the success of TKIs has meant CML patients now have a close to normal life expectancy (Bower et al. 2016; Maas et al. 2022), patients will need to be on treatment for the rest of their lives. For many patients their quality of life is affected from the use of these TKIs and one way to help with this is with TFR. TFR was first reported by Mauro et al., who reported two patients on TKIs who had achieved molecular remission then attempted TFR, with one patient maintaining their remission after one year, while the other relapsed (Mauro et al. 2004). This trial was done to understand if the remaining LSCs in patients with undetectable disease was able to cause patients to relapse, TFR is not a new concept and in fact something that has been considered for over 20 years.

TFR is the process by which patients that have been in deep remission for a period of time are able to stop taking their TKIs and maintain remission. The criteria to be eligible for TFR is provided by two societies. The first is the American National Comprehensive Cancer Network (NCCN) (Shah et al. 2024) who have recommended patients should be: “*an age >18 years, chronic-phase CML (CP-CML) with no prior history of AP-CML or BP-CML, being on approved TKI*

therapy for at least 3 years with prior evidence of a quantifiable BCR-ABL1 transcript and MR4 (BCR-ABL PCR ≤ 0.01% IS) for ≥2 years with reliable access to qPCR testing with a sensitivity of detection of at least MR4.5 (BCR-ABL PCR ≤ 0.0032% IS) that provides results within 2 weeks" (Bourne et al. 2024). The second society is European LeukemiaNet (Hochhaus et al. 2020) who recommend "*Minimally required criteria include the following: the patient must be on first-line therapy (or second-line therapy if intolerance was only reason for changing TKI), typical e13a2 or e14a2 BCR-ABL1 transcripts, a duration of TKI therapy >5 years (>4 years for second generation (2GTKI)), a stable molecular response (MR4 or better) for >2 years and no prior treatment failure. Optimal criteria for TKI cessation include the following: a duration of TKI therapy >5 years and a duration of DMR >3 years if MR4 or >2 years if MR4.5*" (Bourne et al. 2024). The ability to maintain TFR is often seen as the goal for many patients, as they would have all the benefits of being in remission without any of the physical and psychological side effects of life long TKI treatment. The first study of TFR was from Rousselot et al., where 12 patients taking imatinib with undetectable residual disease for more than 2 years attempted TKI discontinuation (Rousselot et al. 2006), after this there have been several TFR trials over the years.

Trial	Criteria	Reference
Pilot study	12 patients that had been taking imatinib for more than 2 years were in CCyR attempted TFR. After 18 months 50% of patients maintained molecular remission.	(Rousselot et al. 2006)
Argentina stop trial	46 patients that had been taking imatinib, dasatinib or nilotinib for 4 or more years and were in DMR for 2 or more years attempted TFR. From the patients 33% relapsed and had to resume TKI use.	(Pavlovsky et al. 2020)
DASFREE	84 patients that had been taking dasatinib and were in DMR for 2 years or longer attempted TFR. After 5 years 44% of patients had maintained TFR	(Shah et al. 2023)
DESTINY	174 patients that had been taking imatinib, nilotinib and dasatinib for 3 or more years and were in MMR or DMR. Patients had initial de-escalation phase (half of drug dosage) if they maintained TFR they stopped TKIs altogether. At trial end point (24 months after TKI cessation) 72% for DMR patients and 36% for MMR patients maintained TFR.	(Clark et al. 2019)

ENEST	190 patients that had been taking nilotinib for 2 or more years and were in MR4.5. After 5 years, 42.6% of patients were still in TFR.	(Radich et al. 2021)
EURO-SKI	728 patients in DMR attempted TFR. After 36 months 309 patients of 678 (46%) of patients were in MMR.	(Mahon et al. 2024)
LAST	173 patients that had been taking imatinib, dasatinib, nilotinib, or bosutinib for 3 or more years and were in DMR for at least 2 years attempted TFR. 60.8% achieved TFR.	(Atallah et al. 2021)
STIM1	100 patients that had been taking Imatinib for at least 2 years and had undetectable minimal residual disease (UMRD) attempted TFR. After 60 months 38% patients achieved molecular recurrence-free survival (MRS)	(Etienne et al. 2017)
STIM2	200 patients that had been taking imatinib for at least 2 years and had been in DMR (MR4.5) for at least 2 consecutive years. After 24 months 54% of patients relapsed.	(Dulucq et al. 2022)
STOP 2G-TKI	60 patients that had been taking dasatinib or nilotinib for at least 3 years and were in MR4.5 attempted TFR. After 48 months 53.57% of patients maintained TFR.	(Rea et al. 2017)
TWISTER	40 patients that had undetectable minimal residual disease (UMRD) attempted TFR. After 27 months 47.1% maintained TFR.	(Ross et al. 2013)

Table 1-3 List of previous TFR clinical trials

The success rates for patients that attempt TFR to maintain remission is 38-54% (Bourne et al. 2024). It is currently not well understood why some patients are able to maintain remission while others relapse. There have been several factors previously found to be potential predictors of TFR: duration of TKI use, duration of maintained DMR, *BCR::ABL1* isoform type, sokal score (a scoring system that ranked patients risk group, no longer used) and the immune response (Saifullah and Lucas 2021). Increasing evidence suggests that changes to the immune repertoire within the BMM plays a part in the relapse of TFR patients (Rea et al. 2013; Saifullah and Lucas 2021; Castagnetti et al. 2021). Although it is known that at diagnosis patients with CML have a reduced immune response, after TKI use this has been seen to improve, with a study reporting patients who maintained TFR had a higher expression of NK cells compared to patients who relapsed, suggesting the NK cells play a role in maintaining remission in patients (Vigón et al. 2020).

While there has been increasing numbers of clinical trials carried out to help the understanding of TFR (Giles et al. 2019; Mahon et al. 2010; Ross et al. 2013; Saussele et al. 2018; Shah et al. 2020; Atallah et al. 2018) it is still not understood why only some patients can maintain TFR and how they differ from those that relapse. There have been many factors indicated to having an effect on the ability of patients to maintain TFR however none of these markers have been identified as useful markers of predicting TFR that could be used in a clinical setting. The ability to predict candidates for TFR is an extremely attractive and sought after question as this would prevent patients from going through relapse and having to go back on medication. It would also provide a deeper understanding between the changes that occur in CML patients and how these are beneficial to the patients.

1.6 DESTINY trial

One clinical trial that looked at TFR is DESTINY (Pilot of De-Escalation followed by Stopping Treatment with Imatinib, Nilotinib or sprYcel; NCT01804985) (Clark et al. 2019). This was a non-randomised, phase 2 trial, this means patients were manually assigned a group prior to the trial, either MMR or MR4. The trial recruited patients from 20 hospitals all around the UK. The criteria for patients in the trial were: "*patients were 18 years or older, were in CP-CML, had any of the known transcripts of BCR::ABL1 (e13a2, e14a2, or e19a2), had been using imatinib, nilotinib or dasatinib for 3 years or longer and had three or more PCR measurements taken over the previous 12 months at a ratio of 0.1% or less. In this trial, patients were required to have been stable DMR (ratio of less than 0.01%) or MMR (ratio between 0.01% and 0.1%)*". If in the previous 12 months to the trial the patient had all their PCR results at 0.01% or less they were assigned to the DMR group. Patients were assigned to the MMR group if some or all their measurements were higher than 0.01% but 0.1% or less. This trial was unique in that it included MMR and DMR patients in attempting TFR, this was unusual as most trials looking at TFR recruit patients in DMR. As well as this, this trial was the first that had de-escalation before cessation of TKI therapy. Usually, patients that attempt TFR go straight to stopping TKIs without a de-escalation phase. In the DESTINY trial, initially the normal dose of TKI that patients were already taking was reduced to 50% for 12 months, during which the molecular response of patients was monitored. For imatinib the daily dose of 400mg was

reduced to 200mg, dasatinib changed from 100mg daily to 50mg daily and nilotinib changed from 300mg twice a day to 150mg twice a day.

If patients did not have a rise in *BCR::ABL1* transcripts the treatment was stopped and they were monitored for another 24 months. Patients that had two consecutive PCR results of >0.1% ratio (i.e. loss of MMR) were considered to have 'relapsed' and were put back onto treatment, patients that made it to the trial endpoint had maintained MMR throughout the trial.

Any adverse effects that occurred for patients during the trial were found to not be related to CML or TKIs (Clark et al. 2017). During the trial patients were asked to take notes of new symptoms and changed symptoms. All patients reported improved symptoms after de-escalation or stopping TKIs.

This trial also looked at the financial benefit of TFR. The ability to stop lifelong treatment in a group of patients would be extremely cost effective, this was examined in the DESTINY clinical trial who found there were savings in the drug costs during this trial that attempted TFR (Clark et al. 2017).

The trial set up was as follows:

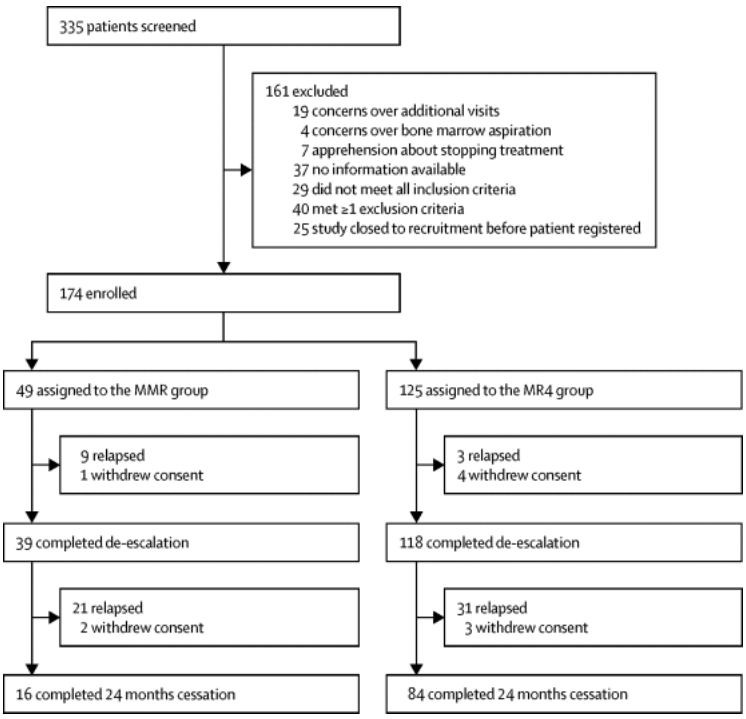

Figure 1-7 Recruitment procedure of patients to the DESTINY trial This flow chart shows the process of selecting patients to the DESTINY clinical trial and how these patients did in the trial. Image taken from (Clark et al. 2019).

After 36 months, at trial endpoint, molecular recurrence free survival (RFS) was 72% for DMR patients and 36% for MMR patients.

From this trial 160 BM samples were collected at study entry, at molecular recurrence and at trial end point and stored in the University of Glasgow POGLRC haematological cell research bank. This project used BM mononuclear cells (MNCs) and BM plasma samples from patients who took part in the DESTINY clinical trial in order to identify changes in the BMM, with the aim of predicting which patients are good candidates for TFR.

1.7 Dysregulation of LSCs and BMM found in CML patients for LSC survival

The current inability to completely eradicate LSCs, even in patients with deep remission, is a plausible reason relapse occurs in some patients who attempt TFR from DMR. Persistent LSCs in DMR comprise a small fraction of the total stem cell population; marked as $Lin^{-}CD34^{+}38^{-}$, these stem cells are often found to be quiescent so not actively in the cell cycle. While TKIs do an excellent job of removal of leukaemic cells they mostly target less primitive cells and cannot fully eradicate LSCs. There are several features of LSCs that prevent them from being targeted by TKIs. For example, they do not rely only on BCR::ABL1 signalling to maintain their survival; this was demonstrated when BCR::ABL1 signalling was inhibited by imatinib yet LSCs were able to survive (Corbin et al. 2011). Additionally, knockdown of BCR::ABL1 did not eliminate the CML LSC population (Hamilton et al. 2012). CML LSCs also exhibit increased expression of ABCB1 (MDR) and ABCG2 compared to normal HSCs (Jiang et al. 2007), these are drug efflux transporters which may underpin another mechanism of LSC TKI insensitivity through increased cellular elimination of the drugs. While the primitive LSCs were found to have increased *BCR::ABL1* mRNA expression this did not translate to the protein level. Furthermore, as well as LSCs having cell intrinsic methods of survival, the BMM can also be altered to maintain the LSCs.

LSCs are predominantly located in the BM, where they interact with and subvert the BMM in order to promote their survival and persistence (Figure 1-8). There

are changes to the BMM that provide optimal environment for these LSCs (Houshmand et al. 2019) that are commonly found in CML patients. This includes an increased secretion of pro-inflammatory cytokines and chemokines which produce a more pro-inflammatory BMM. These proteins were found to directly target progenitors and were responsible for the increase in myeloid differentiation and the progression of CML (Aguayo et al. 2000; Järås et al. 2010; Reynaud et al. 2011; B. Zhang et al. 2012; Baba et al. 2013; Hoermann et al. 2015; Guo et al. 2016; Peled et al. 2018; Staversky et al. 2018). There is increasing evidence the MSCs in patients of CML have an altered secretome and produce a more pro-inflammatory immunosuppressive environment. MSCs from CML patients were found to have increased gene expression of pro-inflammatory cytokines: IL-6, TGF-ß and IL-10, these are all factors involved in activating granulocyte-like myeloid-derived suppressor cells (G-MDSC) which are known to supress T cells (Giallongo et al. 2016). Additionally, the secretion of CXCL12 from MSCs is essential for maintaining the quiescence of LSCs (Agarwal et al. 2019).

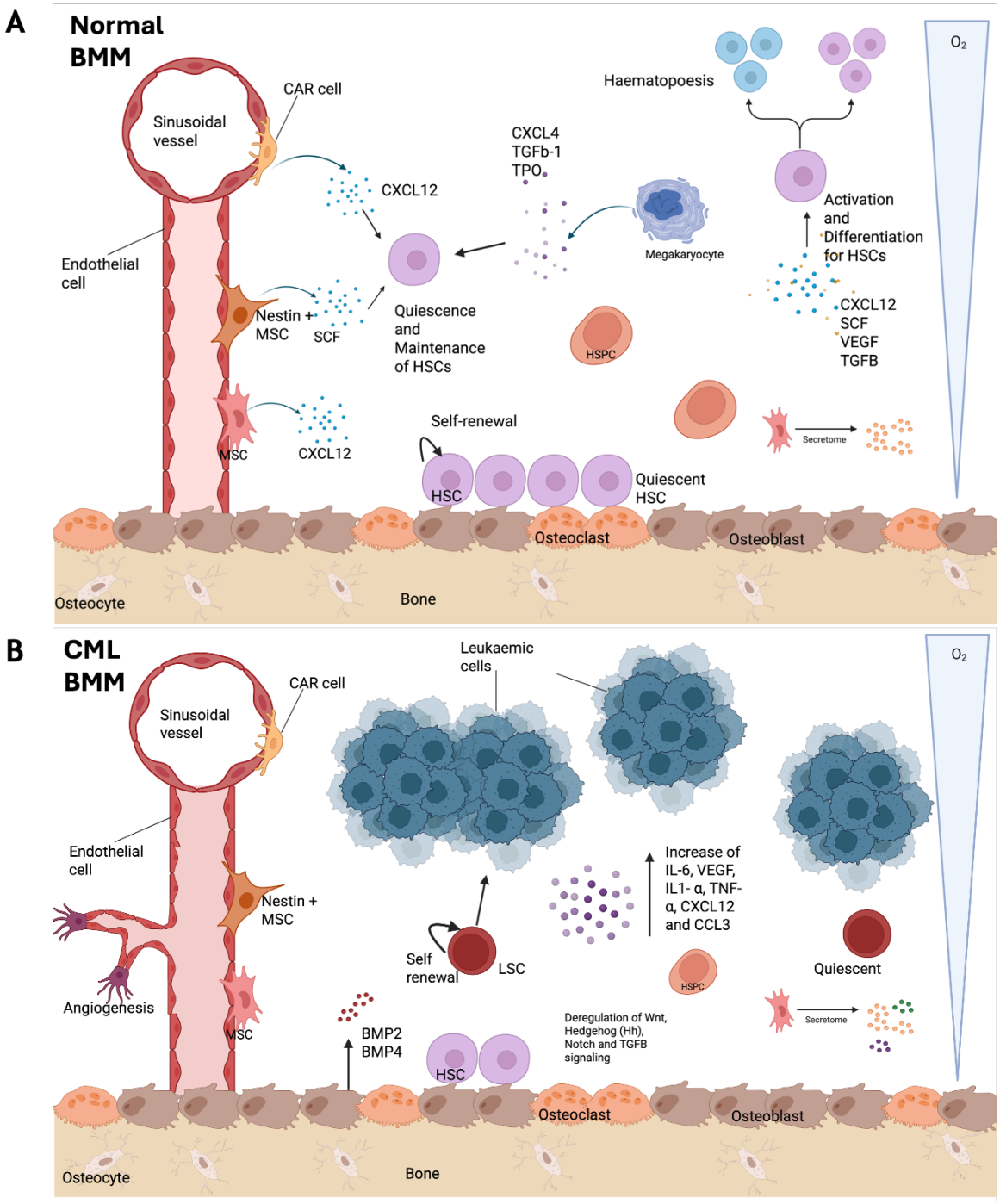

Figure 1-8 Representative image of a healthy BMM and changes in CML (A) Figure 1-2 (B) The BMM changes in patients with CML with an increase in pro-inflammatory cytokines, chemokines, and morphogens as well as changes to signaling pathways, this results in angiogenesis and HSC skewing their differentiation to myeloid lineage and an increase in leukaemic cells.

1.7.1 Changes to mesenchymal stem cells (MSCs)

Due to the integral role MSCs play within the BMM and supporting HSCs, it is perhaps unsurprising that within CML the dysregulation of MSCs disrupts the BMM and allows for protection of LSCs.

The co-culture of BM MSCs with CML stem and progenitor cells was found to significantly decrease the apoptosis of the CML cells when treated with imatinib (Zhang et al. 2013). The treatment of CML cells with TKIs reduced their proliferation, however with the addition of MSCs to the co-culture found the proliferation of the cells did not change (Zhang et al. 2013). This demonstrates the protective effect MSCs have on primitive CML cells and prevent their apoptosis from TKIs (Zhang et al. 2013). The treatment of TKIs caused an increased expression of N-cadherin in the CML cells which resulted in increased adhesion of the cells to MSCs (Zhang et al. 2013). The increased N-cadherin is thought to increase Wnt-β-catenin signalling pathways which provides protection and survival to LSCs (Zhang et al. 2013).

The differentiation capacity of MSCs is an essential aspect of their function and produces essential cells that comprise the niches and protect HSCs, this factor is also affected in patients with CML. Additionally, a CP-CML mouse model demonstrated CML cells cause MSCs to increase production of osteolineage cells, this was through direct contact with the MSCs and increased production of C-C motif chemokine ligand 3 (CCL3) and TPO (Schepers et al. 2013). This change to the BMM prevented maintenance of HSCs however did not affect LSCs (Schepers et al. 2013). When compared osteoblastic cells from normal mice to the osteoblastic cells from CML mice, they had an increased TGF-β signalling (increased expression Smad7, Timp1, and Serpine) and increased inflammatory signalling (increased expression of IL-1R, IL-1 receptor antagonist (IL-1RN), TNF-α and inhibitor of κBα (IκBα)) (Schepers et al. 2013). Similar to HSCs, LSCs maintain their quiescence through interactions with the endosteal niche and osteoblasts, the increased production of osteoblasts would favour the protection of LSCs (Busch and Wheadon 2019). This indicates MSCs are a potential cell of interest in CML due to their ability to bring about changes within the BMM.

MSCs also exert immunomodulatory effects which can enable survival of LSCs through alterations in immune surveillance (Huang et al. 2022). They have been found to have effects on/interact with T cells, B cells, NK cells, macrophages, monocytes, DCs and neutrophils through secreted factors from the MSCs and cell-cell contact (Song et al. 2020). BM-MSCs inhibit the activity of $CD4^+$ and $CD8^+$ T cells (Najar et al. 2010; Gieseke et al. 2010). It is thought that these effects are caused by both cell-cell interactions and soluble factors (Duffy et al.

2011). MSCs have also been found to have inhibitory effects on the proliferation and differentiation of B cells (Tabera et al. 2008). Manferdini *et al.*, reported that in adipose tissue, MSCs can change M1-like macrophages to M2 like macrophages, using prostaglandin E2 (PGE2), reducing the inflammatory effect of the macrophages (Manferdini et al. 2017). Additionally, it was found that PGE2 released by MSCs inhibits the maturation of monocytes to DCs. DCs induced by CML-MSCs inhibited T cell proliferation and instead induced the production of Tregs from T cells through increased TGFβ1 production (Z.-G. Zhao et al. 2012). Due to the immunosuppressive role Tregs play it is suggested CML-MSCs are part of producing an immunosuppressive BMM. The effect MSCs have on the immune system is well researched and continues to develop, this provides an interesting basis for the role the MSCs could be playing within the BM and how this could change patient response to TKIs in CML.

The secretory molecules produced by MSCs are an integral part of their function. The production of CXCL12 from stromal cells was found to be decreased in BCR::ABL1 mice, which could cause defective homing and quiescence of HSCs within the BMM (B. Zhang et al. 2012). GSEA from RNA sequencing (RNAseq) analysis of normal MSCs compared to CML-MSCs found increased enrichment of TNF-α and inflammation signalling (Agarwal et al. 2021). The TNF-α signalling caused increased gene expression of *CXCL1* and *CXCL5,* these inflammatory chemokines were upregulated in CML-MSCs compared to normal MSCs (Agarwal et al. 2021). The CXCL1 and CXCL5 chemokines act on the CXCR2 receptor and this interaction was demonstrated as being essential for the maintenance of LSCs, suggesting CML-MSCs demonstrated increased support of LSCs compared to HSCs (Agarwal et al. 2021).

1.7.2 Decreased immune cell activity in CML patients

Another significant aspect of changes that occur within CML BM is in the immune cells. As previously mentioned, it is considered that TKI treatment may aid restoration of normal immunological function. Patients who achieve DMR with TKIs have best recovery of immune system (Hughes and Yong 2017). The innate and adaptive cells within the immune system are known to play an essential role to protect the host from many diseases including cancer. In CML patients there has been a reduction in cell count, cytotoxicity, and antigen-presenting function

within DCs, plasmacytoid DCs (pDCs), and NK cell populations (Dong et al. 2003; Schütz et al. 2017; Nakajima et al. 2002). Changes can also be seen within the adaptive immune system including the presence of dysfunctional $CD8^+$ cytotoxic T cells (CTL) and expression /overexpression of leukaemia-associated antigens (LAAs) (Hughes and Yong 2017). Therefore, immune cells and immune proteins offer an interesting area of investigation for identifying an immunological biomarker signature that may be used to predict if CML patients are good candidates for TFR.

1.7.3 Changes to cytokines

Disease progression of CML is highly influenced by the BMM, many pro-inflammatory cytokines have been identified linked to CML (Hoermann et al. 2015). One of these cytokines is vascular endothelial growth factor (VEGF), which was increased in the BM of CML patients compared to normal (Aguayo et al. 2000), CML patients also had an increase in BM vascularity compared to healthy controls that is associated with poorer prognosis (Aguayo et al. 2000). Furthermore, overexpression of the pro-inflammatory cytokine IL-6 has also been identified in the BMM of CML patients, Reynaud et al., reported that IL-6 is produced by leukaemic cells and leukaemic MPPs and increases their myeloid lineage production (Reynaud et al. 2011). The increase of IL-6 creates a paracrine feedback loop that leads to increase in myeloid production and CML progression (Reynaud et al. 2011). As well as this, Zhang et al., found that in the BM of *BCR::ABL1*$^+$ mice, IL-1α and ß and tumour necrosis factor-α (TNF-α) expression is increased and these cytokines are involved in the decreased proliferation of normal LT-HSC over *BCR::ABL1*$^+$ LT-HSC (Zhang et al. 2012). In addition to this there are also reports of primitive CML cells producing inflammatory signatures and producing cytokines within the BMM. Holyoake et al., reported that quiescent primitive CML cells express IL-3 and expression is increased as the cells become activated and enter the cell cycle (Holyoake et al. 2001). Additionally, increased expression of TNF-α was seen in LSC stem cells of mice, its inhibition using a TNF-α antibody in combination with TKI (nilotinib) reduced the number of LSCs (Herrmann et al. 2019). There is clearly an interplay with the LSCs and their effect on the BMM and vice versa.

1.7.4 Changes in chemokines

There are also several chemokines which are involved in the maintenance and regulation of the local BMM and HSCs and LSCs. The interaction of CXCL12 with its receptor CXCR4 plays an important role in HSC homing and maintenance in the BM niche. This interaction can also play a role in encouraging tumour growth and metastasis, and they are often found to be overexpressed in several cancers (Guo et al. 2016); the overexpression of CXCR4 was found to help leukaemic cells (in acute myeloid leukaemia (AML), ALL and chronic lymphocytic leukaemia (CLL)) avoid apoptosis from chemotherapy (Peled et al. 2018). Another chemokine that is known to disrupt the BMM within various leukaemia's, including CML, is CCL3 (Staversky et al. 2018). This chemokine is responsible for recruiting lymphocytes to sites of infection as well as regulating myeloid differentiation and HSC numbers (Staversky et al. 2018). This was demonstrated when CCL3-deficient BCR::ABL-expressing leukaemia initiating cells (LICs) were injected into the BM of nude mice and were unable to cause CML-like leucocytosis and splenomegaly (Baba et al. 2013) suggesting CCL3 plays an essential role in the development of CML.

1.7.5 Changes in morphogens

While the chemokines and cytokines drive the expansion of the progenitors, morphogenic signalling is thought to be responsible for the protection of the LSCs (Toofan et al. 2014). One example of this is bone morphogenic proteins (BMPs) which are part of the TGF-β superfamily, they play a crucial role in haematopoiesis, BM homeostasis and are key players in the maintenance of LSCs and the leukaemic BMM (Laperrousaz et al. 2013). Expression of bone morphogenic protein 2 (BMP2) and bone morphogenic protein 4 (BMP4) is increased in CML patients as well as BMP type 1 receptors (BMPR1) that causes further expansion of leukaemic myeloid progenitors (Laperrousaz et al. 2013). The study also indicates that the LSCs in the BM have an increased sensitivity to BMP ligands and demonstrate higher survival rates in the presence of these ligands (Laperrousaz et al. 2013). Evidence shows the morphogenic pathways crosstalk with each other and together these are important for sustaining LSCs and is a driver for disease progression (Sands et al. 2013).

1.7.6 Changes to signalling pathways

Reports also show deregulation in Wnt, Hedgehog (Hh), Notch and TGF-ß superfamily signalling in CML (Sengupta et al. 2007; Gerber et al. 2013), crucial pathways involved in stem cell maintenance and homeostasis of the haematopoietic system within the BM niche (Toofan and Wheadon 2016).

The increased ß-catenin produced from increased Wnt signalling pathway activity seen in CML patients, has been shown to increase the self-renewal capacity of GMPs (Jamieson et al. 2004). This was found in leukaemia cells from blast crisis in CML, imatinib resistant patients who had elevated levels of ß-catenin compared to normal cells (Jamieson et al. 2004). The increased ß-catenin therefore leads to increased production of myeloid cells. Additionally, it has been identified that ß-catenin gene expression was increased in LSCs of mice with CML by 2.5-fold compared to normal HSCs (Hu et al. 2009). The same study also found ß-catenin gene knockout of mice did not develop CML and therefore the LSCs of CML require ß-catenin for survival and leukaemogenesis (Hu et al. 2009).

The Hh signalling pathway is another interesting pathway as it has been reported that LSCs in patients with CML require Hh signalling for LSC maintenance. It was found that by inhibiting Hh signalling, normal HSCs were not affected while there was an increase in apoptosis of *BCR::ABL1*$^{+}$ cells (Dierks et al. 2008). Another example of the Hh pathway in CML is when it was found that knockout of the *Smo* gene, an activator of the Hh pathway, in BCR::ABL1^{+} mice, this caused a decrease of CML stem cells (Zhao et al. 2009).

It is well understood and reported that the Notch signalling pathway plays a very important role in HSC quiescence and self-renewal. In the context of CML it has been found that Notch signalling is low in CML cells while Wnt signalling was found to be high, this combination caused an increase in myeloid activation pathways, encouraging disease progression (Kang et al. 2019). In patients with CP-CML it has been identified that Notch signalling is downregulated, as shown by the downregulation of Notch target genes in CML patients (Horne et al. 2016). Additionally, activation of the Notch signalling pathway significantly decreased the self-renewal capacity of the LSCs (Horne et al. 2016).

Finally, as has been mentioned the TGF-β signalling pathway maintains the quiescence of LSCs in the BM of patients with CML. The ability of TGF-β signalling to increase self-renewal and quiescence of LSCs was further demonstrated as the inhibition of TGF-β-Foxo3a (via a combination of Foxo3 knockout mice administered with pharmacological inhibitor of TGF-β (Ly364947)) decreased the number of colonies from LICs, equally treatment with TGF-β1 caused an increase of Foxo3a which results in an increased colony formation of LICs (Naka et al. 2010).

1.7.7 Changes to metabolism

It is well known in cancer cells the glucose uptake and lactate production is increased, this is called the Warburg effect (Liberti and Locasale 2016). This is no different in CML where there have been extensive reports looking into the metabolism of CML cells which have shown an increase in metabolic activity due to increased cell activity and energy demands. An investigation of the metabolic changes of CML LSCs found an increase of lipolysis and fatty acid oxidation when compared to CML progenitor cells, they also found increased mitochondrial oxidative function in CML LSCs compared to HSCs (Kuntz et al. 2017). Additionally, Giustacchini et al., found positive enrichment of oxidative phosphorylation and glycolysis pathways in CML LSCs compared (from patients on TKIs for 3 months and in haematological remission) to normal HSCs, using GSEA of single-cell analysis (Giustacchini et al. 2017). An examination of CML cell line, K562, which were made TKI resistant, found these cells had changed metabolic processes and relied more on glycolysis and had mitochondrial dysfunction (Noel et al. 2019).

1.8 Proteomic approach to understanding the BMM

The BMM is a complex, fluctuating area which relies heavily on the homeostasis of each intricate part to ensure haematopoiesis can proceed and disease does not occur. In patients with CML this becomes even more complex as there are several dysregulated factors that account for the protection and persistence of LSCs. While great strides have been taken to expand the comprehension of this multi-faceted area there are still major questions about the exact mechanisms that take place within the BMM in patients with CML. In order to understand and

analyse this in-depth and without bias a sensitive method is required which would still allow for broad coverage. As many of the changes described above that are currently known and understood about the BMM are based on the proteins found here, a deeper understanding of the proteome could be the key.

The proteome is a blanket statement referring to all proteins within an organism. Due to the nature of the BMM, the fluctuation based on biological/physiological changes, stimulus, infection, trauma and more the protein expression can be extremely varied between people at any one time for a variety of reasons and is difficult to assess. If you combine that with the increased dysregulation that occurs with CML patients, this becomes even more complex. A comprehensive examination of these proteins would provide a detailed and informative insight into the biological systems within the BMM of patients with CML and could provide more context of how they differ between patients that respond differently to treatment.

A large-scale examination of the proteome is called proteomics, this is an evolving and exciting methodology that is quantitative and is able to provide an in-depth analysis of proteins and the changes to biological processes. While the changes to genetic variations can also provide very enlightening information within biological context, this can sometimes be different than the translation at a protein level. Understanding changes of proteins provides evidence of the genuine changes to biological functions within a system, whereas genetic alterations provide suggestions. Proteins are much more targetable in the context of treatment and biomarkers. Understanding this is essential for characterising the proteome and advancing knowledge of disease. Due to its descriptive nature, proteomics has become a promising tool within cancer biology and biomarker identification.

There are many different methods to examine protein expression through proteomics but the introduction of mass spectrometry (MS) into proteomics has been advantageous as a high throughput method of analysis. An MS machine is able to measure the mass of molecules by separating their ions using their mass-to-charge ratios (m/z) (Sinha and Mann 2020). Alongside this many mass spectrometers use liquid chromatography (LC) to help with the separation of mixtures before being measured by the MS. Together this produced LC-MS, which

is considered the method of choice for identification and quantification of proteins (Gillet et al. 2012).

There are different mass spectrum methods for protein identification depending on what is being looked at, for example data dependent acquisition (DDA), however this does not look at low-abundance proteins. The data independent acquisition (DIA) measurement method for proteomics was created to allow for unbiased protein identification and quantification of all proteins using MS-based technology. LC-MS based proteomics begins with the degradation of proteins, usually using enzymes like trypsin which breaks down the protein into smaller peptides, making it easier to be identified, and allows identification of the peptides using the LC-MS. The peptides are then separated by liquid chromatography, they are then ionised, which produces charged ions which can be measured by the MS for the first time (MS1). This measures the mass to charge ratio for the ions (m/z) and allows the peptides to be separated. With DIA all the precursor ions (ionised peptide) of MS1 are taken and fragmented and a secondary MS measurement is taken (MS2), these fragments are used for the identification of the protein by comparing to a database. The first MS1 detection provides information on the initial peptide and its quantity, which the MS2 provides detailed information of the peptide which can be used to identify which protein it came from. These peptides are protein specific and therefore identification of these peptides is equal to identification of the protein. This is called a bottom-up approach as it begins with a simpler peptide that can be traced back to the corresponding protein.

Using proteomics allows for an unbiased analysis of samples where the examination is more exploratory and does not have a specific target. This high-throughput method allows for the analysis of thousands of proteins at one time, some of which might have otherwise been missed with a more targeted approach. This approach is also very translational and could provide markers of interest that could be further validated and potentially used within clinical settings.

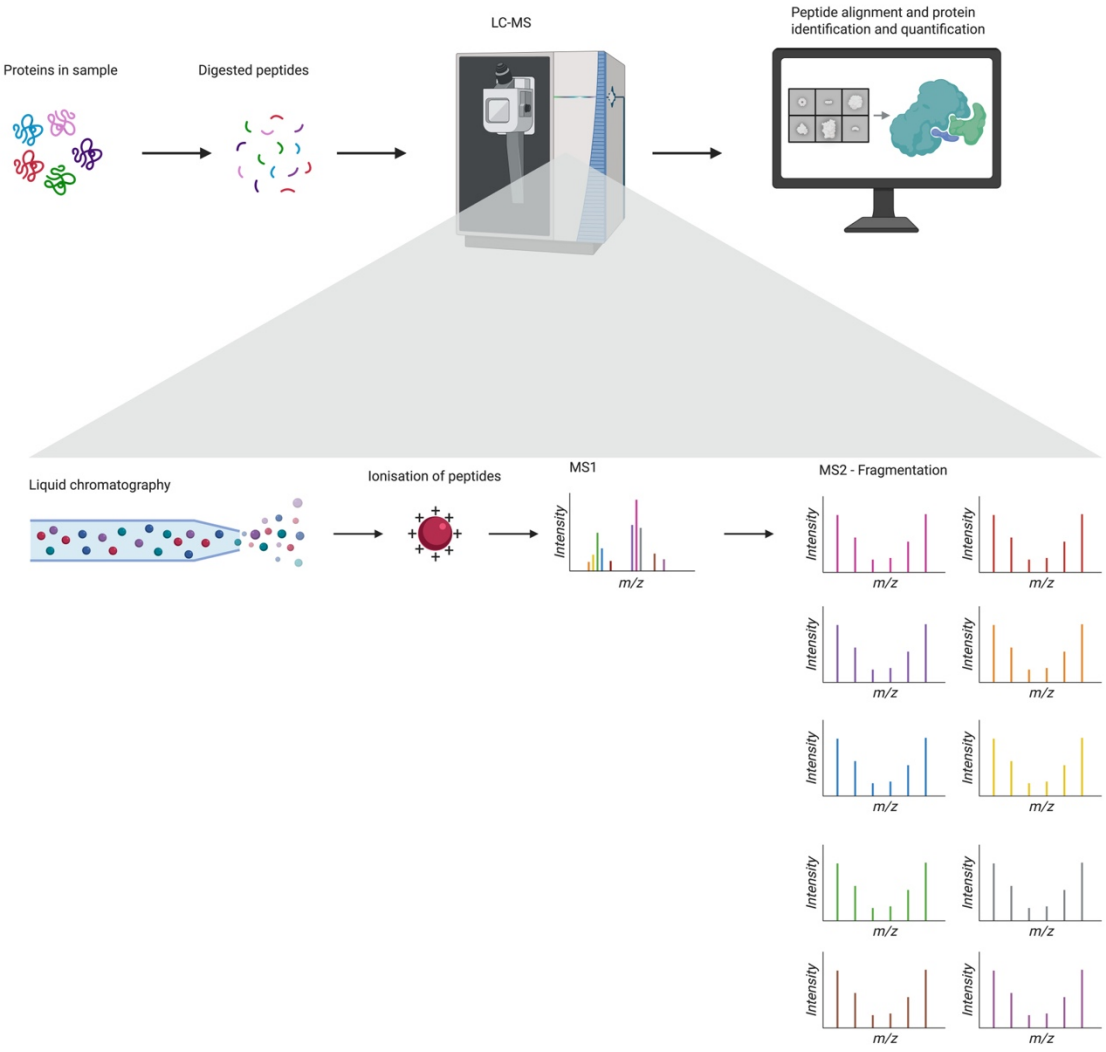

Figure 1-9 Visual representation of LC-MS process with DIA Image adapted from (Karpievitch et al. 2010; Anjo et al. 2017; Ludwig et al. 2018; Sinha and Mann 2020; Krasny and H. Huang 2021).

One of the best, most cutting-edge machines that uses this technology is Thermo Scientific™ Orbitrap™ Astral™ MS. Considered to be the gold-standard for DIA MS, when compared to Thermo Scientific Orbital MS, it was found the Astral produced results faster, at a better quality and produce more in-depth analysis and identification of the samples (Heil et al. 2023). This allows for a much deeper analysis of the proteome and a broad range of identification and quantification of the proteins within samples. Proteomics can be used for protein identification and quantification which could be used for more in-depth understanding of signalling pathways, targeted treatment options, identification of dysregulation of protein interactions and biomarker discovery.

As this technique becomes more accessible, increasingly researchers have turned to proteomics to ask their biological questions. This has been used in several haematological malignancies and disorders with BM samples. Moura et al., used LS-MS and found changes to the TLN1 and CEP55 proteins in high and low risk Myelodysplastic syndrome (MDS) patients and could potentially be looked at as markers of the disease (Moura et al. 2022). Additionally, proteomic analysis of BM plasma from AML patients compared to normal patients found increased expression of IL-8 cytokine in AML patients compared to healthy patients (Çelik et al. 2020), considering IL-8 has been found to encourage chemoresistance in AML cells (Vijay et al. 2019) this shows the importance of this cytokine in AML and this could be exploited as a potential therapeutic target for AML. Through LC-MS, it was discovered that in the BM plasma of extramedullary multiple myeloma (EMM) patients, which is a rare and more aggressive type of multiple myeloma (MM), they had an increase of vascular adhesion molecule 1 (VCAM1), hepatocyte growth factor activator (HGFA), pigment epithelium-derived factor (PEDF) proteins in their BM plasma (Dunphy et al. 2023). This was validated alongside metabolomics and found that these proteins could be used as potential markers of EMM. Interestingly, research has also been done to find protein biomarkers in T cell acute lymphoblastic leukaemia (T-ALL) (Singh et al. 2024). Whole blood samples were taken from T-ALL patients and healthy donors, these were compared using LC-MS, from this they found 9 upregulated proteins and 35 downregulated proteins in T-ALL patients compared to the normal samples. These findings were then validated by RT-PCR and ELISA and have shown reasonable suggestions that these proteins could be used as predictive biomarkers of T-ALL. Similar analysis was carried out on AML patients, where LC-MS was used to compare PB and BM samples from both AML patients and healthy individuals (Jajula et al. 2024). In the BM samples there was 203 differentially expressed proteins (DEPs) and in the PB samples there were 123 DEPs all found in the AML patients when compared to normal samples. A crossover of these results found there was 28 proteins that were common to both BM and PB samples, 18 of these were upregulated. Verification data of these proteins found there was significant changes to pro-platelet basic protein (CXCL7), enolase 1 (ENOA), and beta-2-glycoprotein 1 (β2-GP1) proteins, which was then validated using ELISA on a new batch of samples. The validation data found these proteins

had high predictive potential and could therefore be used as prognostic/ diagnostic biomarkers.

Overall, it is clear to see the valuable role proteomics plays in disease understanding and how this approach allows for analysis of a wide range of proteins, that otherwise may have been missed if a more targeted panel was examined. The research provides unbiased analysis of complex samples that can ultimately give an extensive exploration of protein changes and their biological consequences as well as novel treatment targets and predictive markers.

1.9 Hypothesis

There are distinct changes to the cellular components and secretome of BMM in patients with CML, these differences in patients could be related to their ability to maintain TFR through for example immune modulation.

We hypothesised that given these anticipated changes in the BMM of a patient that maintains TFR, a predictive signature could be elucidated to distinguish those that can safely stop treatment.

1.10 Overall Project Aims

1. To characterise the MSCs of the BMM to understand their changes in patients who maintain TFR vs those who relapse and identify if any of these changes can be predictive of TFR success.

2. To enumerate and characterise the stem and progenitor population of patients to identify predictive cellular signature of TFR.

3. To identify a predictive protein signature within BMM of TFR patients.

2 Materials and Methods

2.1 Materials

2.1.1 Tissue Culture

2.1.1.1 Tissue culture plastics

Plastics	Supplier
BD Microlance 19G Needles	BD Biosciences, Oxford, UK
Cell culture dish with lid	Thermo Fisher Scientific, Paisley, UK
Cell culture dish with lid NUNC (35 mm)	Thermo Fisher Scientific, Paisley, UK
Collagen I 6-Well Clear Flat Bottom TC Plates	BioCoat, BD Labware
Cryovial	Fisher Scientific, Loughborough, UK
Eppendorf tubes (0.5/1.5 mL)	Thermo Fisher Scientific, Paisley, UK
Falcon tubes (15/50 mL)	Fred Baker Scientific, Cheshire, UK
Freezing container, Nalgene® Mr. Frosty	Sigma-Aldrich, Dorset, UK
Haemocytometer	SLS, LTD
Nunc cell culture 6-well plate	Thermo Fisher Scientific, Paisley, UK
Nunc cell culture flask (T75)	Thermo Fisher Scientific, Paisley, UK
Pasteur Pipette (3 mL)	Greiner BioOne, Gloucestershire, UK
Pipette tips (p10/20/100/200/1000)	Greiner BioOne, Gloucestershire, UK
Single-Use Filter Unit (0.2 µM, 0.45 µM)	Sartorius Stedim Biotech, Epsom, UK
Stripettes (5/10/25 mL)	Greiner BioOne, Gloucestershire, UK
Syringe (1/3/5/10/20/50 mL)	Greiner BioOne, Gloucestershire, UK
Tissue culture flask (T25, T75)	Thermo Fisher Scientific, Paisley, UK
Vacuum filter with storage bottle (500mL, 0.22 µM)	Fisher Scientific, Loughborough, UK

Table 2-1 Tissue culture plastics used

2.1.1.2 Tissue culture reagents and media

Reagent	Supplier	Catalogue number
2-Mercaptoethanol	Sigma-Aldrich, Dorset, UK	M6250
Accutase	Stemcell Technologies, Grenoble, France	07920
Dimethyl sulfoxide (DMSO)	Sigma-Aldrich, Dorset, UK	D8418
DNase I (2500 U/mL)	Sigma-Aldrich, Dorset, UK	-
Dulbecco's Modified Eagle Medium (DMEM)	Thermo Fisher Scientific, Paisley, UK	21969035
Dulbecco's PBS (dPBS) (magnesium/calcium free)	Thermo Fisher Scientific, Paisley, UK	14190144
EDTA	Sigma-Aldrich, Dorset, UK	324503
Foetal Bovine Serum (FBS)	Sigma-Aldrich, Dorset, UK	F9665
H2DCFDA (reactive oxygen species (ROS) stain)	Thermo Fisher Scientific, Paisley, UK	D399
HBSS (magnesium/calcium free)	Gibco, Paisley, UK	14170112
Human Albumin Serum (HAS)	University of Glasgow	-
Human FMS-like tyrosine kinase 3 (FLT3) cytokine	Stemcell Technologies, Grenoble, France	-
Human G-CSF cytokine	Stemcell Technologies, Grenoble, France	-
Human IL-3 cytokine	Stemcell Technologies, Grenoble, France	-
Human IL-6 cytokine	Stemcell Technologies, Grenoble, France	-
Human SCF cytokine	Stemcell Technologies, Grenoble, France	-
Hydrocortisone	Stemcell Technologies	-
Iscove's Modified Dulbecco's Medium (IMDM)	Life Technologies, Paisley, UK	12440053
JC-1 Dye (Mitochondrial Membrane Potential Probe)	Thermo Fisher/Invitrogen	T3168
L-Glutamine (200 mM)	Gibco, Paisley, UK	25030024
Magnesium chloride (1 M)	Sigma-Aldrich, Dorset, UK	M1028
Mesenchymal Stem Cell Growth Medium 2	Promocell, Heidelberg, Germany	C-28009
MethoCult H4034	Stemcell Technologies, Grenoble, France	04034
Mitomycin C	Tocris Bioscience, Abingdon, UK	3258
MyeloCult H5100	Stemcell Technologies, Grenoble, France	05150

Penicillin-Streptomycin (Pen-Strep) (10,000 U/mL) (100g/mL)	Thermo Fisher Scientific (Gibco), Paisley, UK	15140122
Phosphate-buffered saline (PBS)	Thermo Fisher Scientific, Paisley, UK GIBCO?	18912014
Roswell Park Memorial Institute (RPMI) 1640 medium	Thermo Fisher Scientific, Paisley, UK	31870025
Tri-sodium Citrate (0.155 M)	Sigma-Aldrich, Dorset, UK	-
Trypan Blue (0.4%) (w/v)	Merck (Sigma Aldrich), UK	T8154
Trypsin-EDTA (0.25%) (w/v)	Thermo Fisher Scientific, Paisley, UK	25200072
Valinomycin	Thermo Fisher/Invitrogen	V1644

Table 2-2 Tissue culture reagents and media

2.1.1.3 Tissue culture cell line origins and media

Cell type	Cell origin	Supplier	Media preparation
M210B4	Stromal cell line from BM of (C57BL/6J x C3H/HeJ) F1 mouse genetically modified to express IL-3 and G-CSF	Stem Cell Technologies	RPMI, 10% (v/v) FBS, 1% (v/v) Pen-Strep, 1 mM L-glutamine
SL/SL	Stromal cell line BM of SL/SL mouse. Genetically modified to express IL-3 and SCF	Stem Cell Technologies	DMEM, 10% (v/v) FBS, 1% (v/v) PEN/STREP, 1 mM L-glutamine
Promocell MSC	Human bone marrow	Promocell, Heidelberg, Germany	Mesenchymal stem cell growth medium 2 + supplement mix, 1% (v/v) Pen/Strep

Table 2-3 Tissue culture cell line origins and media

2.1.2 Tissue culture solutions

2.1.2.1 DAMP (thawing media)

Component	Volume	Final concentration
DNase I (2500 U/mL)	2 mL	10 U/mL
Magnesium chloride (1 M)	1.25 mL	2.5 mM
Tris-Sodium Citrate (0.155 M)	53 mL	16.34 mM
Human Serum Albumin (20%) (w/v)	25 mL	1% (v/v)
Dulbecco's PBS (magnesium/calcium free)	418.75 mL	-

Table 2-4 DAMP (thawing media)

2.1.2.2 Fluorescence-activated cell sorting (FACS) wash

Component	Volume	Final concentration
PBS	48.8 mL	-
FBS	1 mL	2%
EDTA (2 mM)	200 µL	0.4%

Table 2-5 FACS wash

2.1.2.3 Cell freezing solution

Reagent	Volume
FBS	9 mL
DMSO	1 mL

Table 2-6 Cell freezing solution

2.1.2.4 MSC cell culture media

Cells	Media preparation
Primary MSCs	Mesenchymal stem cell growth medium 2 + supplement mix, 1% (v/v) Pen/Strep

Table 2-7 MSC cell culture media

2.1.3 Fluidigm

2.1.3.1 Fluidigm plastics

Product	Supplier	Catalogue number
96.96 Dynamic Array™ IFC for Gene Expression	Fluidigm Biomark, United States	BMK-M-96.96
Control Line Fluid 150	Fluidigm Biomark, United States	101-7602
48.48 Dynamic Array™ IFC for Gene Expression	Fluidigm Biomark, United States	BMK-M-48.48
Control Line Fluid 300 (300 µL x 4)	Fluidigm Biomark, United States	101-6335
Nucleotide-Free Pipette Tips	Applied Biosystems, Warrington, UK	-
20X DNA Binding Dye— 5 Tubes	Fluidigm Biomark, United States	100-7609

Table 2-8 Fluidigm plastics

2.1.4 Molecular biology

2.1.4.1 Kits

Product	Supplier	Catalogue Number
Arcturus PicoPure RNA Isolation Kit	Thermo Fisher Scientific	12204-01
High-Capacity cDNA Reverse Transcription Kit with RNase inhibitor	Thermo Fisher Scientific	4374966
Illumina TruSeq Stranded RNA Core LP	Illumina	-
Micro BCA Protein Assay Kit	Thermo Fisher Scientific	23235
RNeasy Micro Kit	Qiagen	74004
Senescence ß-Galactosidase staining kit	Cell Signalling Technology, Hitchin, UK	9860

Table 2-9 Molecular biology kits

2.1.5 Flow cytometry

2.1.5.1 Antibodies and reagents

Antibody	Supplier	Catalogue number
Mouse anti-human CXCR4-PE	BioLegend	306506
Mouse anti-human Lineage cocktail (CD3, CD14, CD16, CD19, CD20, and CD56)-FITC	BioLegend	348801
Mouse anti-human IL-1RAP -PE	R&D Systems	FAB676P
Mouse anti-human VIABILITY- 7 amino actinomycin (7AAD)	BioLegend	420404
Mouse anti-human CD25-BV605	BD Biosciences, Oxford, UK	567571/562660
Mouse anti-human CD26-APC	BD Biosciences, Oxford, UK	563670
Mouse anti-human CD34 APC	BD Biosciences, Oxford, UK	555824
Mouse anti-human CD34-BV421	BioLegend	343610
Mouse anti-human CD35-PE	BioLegend	332403
Mouse anti-human CD36-BV711	BD Biosciences, Oxford, UK	745470
Mouse anti-human CD38-BV786	BioLegend	303530
Mouse anti-human CD44-APC-H7	BD Biosciences, Oxford, UK	560532
Mouse anti-human CD45 APC-CY7	BD Biosciences, Oxford, UK	561863
Mouse anti-human CD45RA-BV510	BD Biosciences, Oxford, UK	563031
Mouse anti-human CD47-Alexa Fl647	BD Biosciences, Oxford, UK	561249
Mouse anti-human CD49d-BV711	BD Biosciences, Oxford, UK	563177
Mouse anti-human CD73 PE	BD Biosciences, Oxford, UK	550257
Mouse anti-human CD90-PE-Cy7	BD Biosciences, Oxford, UK	561558
Mouse anti-human CD93-PerCP	BD Biosciences, Oxford, UK	745982
Mouse anti-human CD105 PerCp-Cy 5.5	BD Biosciences, Oxford, UK	560819
Mouse anti-human CD117 – Dazzle 594	BioLegend	313226

Table 2-10 Flow cytometry antibodies and reagents

2.1.6 Fluidigm primers

2.1.6.1 MSC genes and associated primers

Gene	Sequence	Ref Seq
CDC25B F'	AGCCGGATCATTCGAAACGAG	NM_021873.4
CDC25B R'	GCCTGGGAGTTGGTGATGTT	
MELK F'	TCCGCCCCTCAGGTTCTTT	NM_014791.4
MELK R'	AGCCACCTGTCCCAATAGTTTC	
PRKACA F'	CGAGCAGGAGAGCGTGAAA	NM_002730.4
PRKACA R'	GCCGAGGGTCTTGATTCGTT	
TMEM200A F'	ACATCTGGCTCTGGAGAGTAAAAG	NM_001258277.2
TMEM200A R'	TGACATGCTGCTGTGATCTGG	
POU3F3 F'	GGACCAAGGAGGCATTTTTGC	NM_006236.3
POU3F3 R'	ATCGCCCCCTTTTTCTCTTCC	
TOX2 F'	CACGGCGGCAAGTTTGATG	NM_001098797.2
TOX2 R'	TCTCGCTCTGGCCGTTGTA	
LNPK F'	CCCCAGAAAGGACTGTTACTCC	NM_030650.3
LNPK R'	ACCTGGAGGATGAAGACCCAT	
LIMS1 F'	GGGATGACCCACAGCAACAT	NM_001193483.3
LIMS1 R'	CTGCTCATGGTACAGCTCCC	
DLG1 F'	AAACGGCACTGCTGAGTGAG	NM_001366207.1
DLG1 R'	TGCTCTCTGGGTATCTTGCTTC	
DLGAP5 F'	AGAAGGTGGCTCAGGATGTCT	NM_014750.5
DLGAP5 R'	CTGAGACAGTGATTTCCTATGAGCA	
PTK7 F'	CCTCTATGTCGTGGACAAGCC	NM_002821.5
PTK7 R'	AATGATGTAGGCCACAGCGG	
MMP14 F'	ACCCAAAAACCCCACCTATGG	NM_004995.4
MMP14 R'	CAGAACCAGCGCTCCTTGAA	
CDC42BPA F'	GCTCGCCATGTCCGAGATAA	NM_001394014.1
CDC42BPA R'	GCTTCTGTATGAACTTCCAGCTCT	
FAM89B F'	TGCGCAAGGAGATGGTGG	NM_001098785.2
FAM89B R'	TGGCAGAAGCTCAGGTCTTG	
SSC5D F'	GGGGTACCTGGACACACTCT	NM_001144950.2
SSC5D R'	AACCATCTTTGCTGCCTGTGT	
APCDD1 F'	CTGCAGAATGCCAAGAACCAC	NM_153000.5
APCDD1 R'	ATGGTCAGGTCTGCCTTTGG	
APCDD1L F'	GCTTTTGGGAGCCCACACT	NM_153360.3
APCDD1L R'	GGGCACTCTATCTGGCAAGG	
AQP1 F'	CATCTTCCGTGCCCTCATGT	NM_198098.4
AQP1 R'	CACACCATCAGCCAGGTCAT	
MINDY4 F'	GAGAGGCTGGAAAGAGCGTT	NM_032222.3
MINDY4 R'	ATCCTCCACATCCTCGAGCC	
KLF1 F'	ATGACTTCCTCAAGTGGTGGC	NM_006563.5
KLF1 R'	TCTCATCGTCCTCTTCCTCCC	
MOK F'	TTGTCCCCACAATGCCTCTC	NM_014226.3
MOK R'	CCCGCTTCTCTGTTTTCCTCT	
CYP27C1 F'	TGATTCCGAAAGGCACCCAG	NM_001367502.1
CYP27C1 R'	AAGTCTCCTTTCCGCAGCC	

AMZ1 F'	CCCGAGGACTTCCAGACCTT	NM_001384743.1
AMZ1 R'	GGCTCCTCGCTCAGGTCTAT	
HLA-B F'	CATCGTGGGCATTGTTGCTG	NM_005514.8
HLA-B R'	TCCCTCCTTTTCCACCTGAAC	
LILRB1 F'	GAGCTCCAAACCCTACCTGC	NM_001081637.3
LILRB1 R'	CTCAGGGCCTGCAGATGT	
LILRB4 F'	GCACTGGGAGGTACTGATCG	NM_001278426.4
LILRB4 R'	CCTGTCTCTGGGCCAATGTC	
FRG1 F'	CAGAGCTTCCAAGACCACAAAC	NM_004477.3
FRG1 R'	GCTTTCAATTTGGCTCTCCTGTC	
DHX16 F'	GAGTTCGTGCAGCGCCTA	NM_003587.5
DHX16 R'	CTGCCTTTCGTGGTACCTTGT	
FMO3 F'	CGCACAGCAGAACAGGTCAT	NM_001002294.3
FMO3 R'	AAATCGAGTGACGAGCAGCA	
ZIC1 F'	GCAAACACATGAAGGTCCACG	NM_003412.4
ZIC1 R'	CTTGTGGTCGGGTTGTCTGT	
MDFIC F'	CCACAGCCCAGGGAAAATGT	NM_001166345.3
MDFIC R'	TCCCCAAATGGACTGGTCTTG	
CXCL12 F'	GCCCTTCAGATTGTAGCCCG	NM_199168.4
CXCL12 R'	AGTCCTTTTTGGCTGTTGTGC	
USP14 F'	GGAGGAACGCTAAAGGATGATGA	NM_005151.4
USP14 R'	TGGCTGAGGGTTCTTCTGGA	
GRK6 F'	TCTTCAGTCGCCAAGATTGCT	NM_001004106.3
GRK6 R'	TAAACGGCGCTCGGAGTAG	
RGS1 F'	AGGAGGCCAAAGACTTTTGGAA	NM_002922.4
RGS1 R'	CCATTGCATTACTTCAGCAGCA	
HAPLN1 F'	AAGAGTCTACTTCTTCTGGTGCTG	NM_001884.4
HAPLN1 R'	GGGGCCATTTTCTGCTTGGA	
PRDM5 F'	TCAGTGCACAGCGAAAAGCA	NM_018699.4
PRDM5 R'	TGGTGCTGCTCAAAACTCGAT	
CPXM2 F'	CCGCCTCCACCAGGTAAAC	NM_198148.3
CPXM2 R'	GGTGGGCAACTCTCTCTGAC	
TNF F'	CCTGCTGCACTTTGGAGTGA	NM_000594.4
TNF R'	TTCGAGAAGATGATCTGACTGCC	
MAPKAPK2 F'	ATGACTACAAGGTCACCAGCC	NM_032960.4
MAPKAPK2 F'	GGCAGTCCTGAAGCATTTTGAG	
EPB41 F'	AACCACGGCCTAGTGAATGG	NM_001376013.1
EPB41 R'	CTTCACCAGGGGAGGTCCTT	
LAPTM5 F'	TGATCGGCGTAGTCAAGAACC	NM_006762.3
LAPTM5 R'	GCAGCTCAATGTAGGAGCCC	

Table 2-11 MSC genes and associated primers for Fluidigm

2.1.6.2 BCR::ABL1 signalling genes

Gene	Sequence	Ensemble ID
AAMDC F'	GAGACAGTGCGGTGGACTT	
AAMDC R'	TGGCCATACTTTGCAGTCCT	
ANXA2 F'	GCACGGCCCAGCTTCCT	

ANXA2 R'	GCTTTGACAGACCCATATGCACT	
ANXA2P2 F'	AACTTTGATGCTGAGCGGGA	
ANXA2P2 R'	CTGTCTCTGTGCATTGTCGC	
AREG F'	GCAGTAACATGCAAATGTCAGC	
AREG R'	CAGCTATGGCTGCTAATGCAA	
ARRDC3 F'	TGGGCACGAAAGAGATGATG	
ARRDC3 R'	GAGGTAGCGAGTGGTGTCTG	
C16orf54 F'	GACTGACCCAAGATGCCGTT	
C16orf54 R'	GACCAGCATGATGGGGATGC	
CALR F'	AGCAGAACATCGACTGTGGG	
CALR R'	CCACAGATGTCGGGACCAAA	
CD164 F'	ACAAGAACACGACCCAGCAC	
CD164 R'	CGACCTTCACAGGTTTCTGG	
CLEC4GP1 F'	TCTAGCGTAGACCCAGGCAA	
CLEC4GP1 R'	GTGGCTGCAGTGGTTGAATG	
CRHBP F'	CAGAGGCAAGGCCAGCAT	
CRHBP R'	CGCTTCCCTCAGCTCTAGGT	
CTNNB1 F'	CCTGTTCCCCTGAGGGTATTT	
CTNNB1 R'	AGCCGCTTTTCTGTCTGGTT	
CTSG F'	GGCTGAGGCAGGGGAGAT	
CTSG R'	CACCAGGAACCCTCCACATC	
CYP51A1 F'	CTCTTGTCCATGCTGCTGATCG	
CYP51A1 R'	ATGTATGGAGGACTTTTCACCCCTG	
DNTT F'	AACACCAGCTTGTTGTGAGA	
DNTT R'	TGGTTCTTCTCTGACACGCAT	
DUSP1 F'	CACTCTACGATCAGGGTGGC	
DUSP1 R'	ATCAAGGCAGTGATGCCCAA	
EIF5A F'	AGAACATTCCAGAGGTCGCC	
EIF5A R'	CGAAGCGCAGCGAGGAG	
EIF5AL1 F'	TGTCCCCACCCTAAAGGAGTT	
EIF5AL1 R'	CTTCCCTCCAGACTCAGGTT	
ERAP2 F'	TGACAAGTAACATGCTCGCCT	
ERAP2 R'	GGAGTGAACACCCGTCTTGT	
FTH1 F'	CCTACGTTTACCTGTCCATGTCTT	
FTH1 R'	CTCAGCATGTTCCCTCTCCTC	
FTH1P3 F'	GGGCTGAATGCGATGGATTAC	
FTH1P3 R'	GGGGTCATTTTTGTCAGTGGC	
FTL F'	TGAGCTCCCAGATTCGTCAG	
FTL R'	GGTCGAAATAGAAGCCCAGAG	
GAS2 F'	GCTGCTGCAGGACCTGTG	
GAS2 R'	CACTTGTAATACCCCCGCGT	
GAS5 F'	TATGGTGCTGGGTGCAGATG	
GAS5 R'	TGGCTTGAGTTAGGCTTGCT	
GMNN F'	GGTACGCAGGGGCGCAA	
GMNN R'	ATGGTGAAGCACAGAAGACCAGG	
HLA-E F'	AGGACTCAGAGGCTGGGATCA	
HLA-E R'	GGGACACGGAAGTGTGGAAAT	
HNRNPH1 F'	AGTTCAGCGACCACGTTTGT	
HNRNPH1 R'	CGAGCAAGACCAGGGCAA	
HNRNPL F'	CACCCCGCAGAATATGGAGG	

HNRNPL R'	CACTGGTGGACCCATCCTTC	
HOPX F'	CCTTTGCCTCTTCCACACTA	
HOPX R'	GCCCAGGAAAATGAGCATAGG	
IFITM1 F'	TAGTAGCCGCCCATAGCCT	
IFITM1 R'	GCTGTATCTAGGGGCAGGAC	
KIAA0125 F'	CAGTTCTGACAGGGCCTCAG	
KIAA0125 R'	TTCCTCCGTCCATCCTCCAT	
LGALS1 F'	CCTGACGCTAAGAGCTTCGT	
LGALS1 R'	CTTGCTGTTGCACACGATGG	
LINC00987 F'	AGGGACTCTGGCGATAAAGC	
LINC00987 R'	AACATTGTCCTGCCCCACTG	
MRPL16 F'	AGGAGACAGCCGGAGTCG	
MRPL16 R'	GGAGTGCCCAGGAATCTGAC	
NFKBIA F'	CCCTACACCTTGCCTGTGAG	
NFKBIA R'	TAGACACGTGTGGCCATTGT	
NOG F'	CCTGGTGGACCTCATCGAAC	
NOG R'	CCATGAAGCCTGGGTCGTAG	
PF4 F'	TGCCCAACTGATAGCCACG	
PF4 R'	AGCAAATGCACACACGTAGG	
RAB31 F'	CTTTCAAGGAATCAGCCGCC	
RAB31 R'	GCCCTTGGGTCAACAGCA	
RPL18A F'	CGGGTGAAGAACTTCGGGAT	
RPL18A R'	CCCATGTCTCGGTAGCACTG	
RSL1D1 F'	AGATGGAGGATTCGGCCTCG	
RSL1D1 R'	CCACTGCCTTTCTAACCTGTTC	
SELL F'	GCCCCAGTGTCAGTTTGTGAT	
SELL R'	AAGGCACACTGTGAGCTGAA	
SOCS2 F'	CTCGGTCAGACAGGATGGTA	
SOCS2 R'	GTCTGAATGCGAGCTATCTCTA	
SPINK2 F'	GGGTTTGGGAGTCAGACCG	
SPINK2 R'	TTGAGGGATCAGAGAGGCTGG	
STON2 F'	ACCAGCAGTCCTAGCTTTGG	
STON2 R'	CACTCCGTCCTCTTGTCAGT	
TSC22D3 F'	CTCTTCTTCCACAGTGCCTCCG	
TSC22D3 R'	CACCTCCTCTCTCACAGCATAC	
ADGRG7 F'	TGTGATCAGGATCCAAAGAGGAAAA	NM_032787.3
ADGRG7 R'	ACAAATACATCTGCCATTTTCCCAG	
TRA2A F'	TCCTGCTCGTGTAAAATCGGAG	NM_013293.5
TRA2A R'	TCTCCTTGACCTCGACCTGG	
TMSB10 F'	CAGACAAACCAGACATGGGGG	NM_021103.4
TMSB10 R'	CTTCTCCTGCTCAATGGTCTCTTT	
CD69 F'	TCTCATTGCCTTATCAGTGGGC	NM_001781.2
CD69 R'	TTCCTCTGGTAGCCAACCCA	
GOLGA8A F'	GACTTGGAGGAGCTGAAGCA	NM_181077.5
GOLGA8A R'	GAGGTGAGCGTCTCCATCAC	
ANXA1 F'	TCCACAACTTCGCAGAGTGTT	NM_000700.3
ANXA1 R'	TTGTGGCGCACTTCACGATA	
IFITM2 F'	GCGTACTCCGTGAAGTCTAGG	NM_006435.3
IFITM2 R'	CATGAAGATGCCCAAAATCAGGG	
CXCL11 F'	ACAGTTGTTCAAGGCTTCCCC	NM_005409.5

CXCL11 R'	TGGAGGCTTTCTCAATATCTGCC	
RTN4 F'	TCGGGCTCAGTGGATGAGA	NM_020532.5
RTN4 R'	GAAATCCTCTTGACCAGCCGA	
RPL37A F'	GTGCCTGGACGTACAATACCA	NM_000998.5
RPL37A R'	AGGCCAGTGATGTCTCAAAGAG	
GOLGA8B F'	GCTCTCAAGGAGCTCAGCC	NM_001023567.5
GOLGA8B R'	TTCTTCATCTCAGTAGAGCTGGC	
CD74 F'	GCTCCACCGAAAGTACTGACC	NM_001025159.3
CD74 R'	ATAGTTGCCGTTCTCGTCGC	
GNAS F'	TACTCCTGAGGATGCTACTCCC	NM_016592.5
GNAS R'	AGTAGTGACGCCCATCTCCA	
PIP4K2A F'	GAAGCACTTCGTAGCGCAGA	NM_005028.5
PIP4K2A R'	GCTCAGTTCATTGATCGAGTGGT	
LRRC75A F'	CTCACCACACTGGCACTCAA	NM_001113567.3
LRRC75A R'	TCCACGTGACATTGGGGAAC	
YBX1 F'	AAAAGCAGCCGATCCACCAG	NM_004559.5
YBX1 R'	TTCTTGTTGGATGACTAAACCGGA	
NCF4 F'	AGGTGAACTCAGCCTGGGA	NM_000631.5
NCF4 R'	GAAGCTGTTCAAAGTCACTCTCG	
TSC22D1 F'	TGAAGGTGCTACCGCTGAC	NM_183422.4
TSC22D1 R'	TGGCTTTTCACTAGATCCATAGCTT	
CDC42 F'	CGGTGGAGAAGCTGAGGTCAT	NM_001791.4
CDC42 R'	CATCGCCCACAACAACACAC	
RPL10A F'	GTTCCCTTCCCTGCTCACAC	NM_007104.5
RPL10A R'	AGCCAGACATAACACCTTCTTCA	
EIF2S3 F'	GTTAGTGCTGTCAAGGCCGA	NM_001415.4
EIF2S3 R'	CCCCAACCAATTAAACGCCAG	
RSPO1 F'	GGCAAGGACTGGGTTGGTT	NM_001242908.2
RSPO1 R'	CTCCATCAGCTCAAAGGGAGG	
DAZAP2 F'	GGAAGTAGCTCCGAACAGGAAG	NM_014764.4
DAZAP2 R'	CTGTGTTGGATATTGACCTTTGCTG	
AVP F'	GAGGAGAACTACCTGCCGTC	NM_000490.5
AVP R'	ACGCAGCTCTCGTCGTTG	
MPIG6B F'	CGACCACTCCCTAGATTTGCTC	NM_138272.3
MPIG6B R'	ATAGAGCAGGCTCGGTTCCT	
RPS15 F'	CTGAGGATCCGGCAAGATGG	NM_001018.5
RPS15 R'	GCATCAGCTGCTCGTAGGAC	
PROM1 F'	AATTCAGTGCTAGGAGGCGG	NM_006017.3
PROM1 R'	TGGTCTCCTTGATCGCTGTTG	
PRSS1 F'	ACTGCTACAAGTCCCGCATC	NM_002769.5
PRSS1 R'	GTCTTCCTGTCGTATTGGGGG	
PCDH9 F'	TGCTGCTTCTGATTTCTCCCC	NM_203487.3
PCDH9 R'	CAGCCGGTTAGTTGCCTCAA	
HLA-DRB1 F'	CTGGACTTCAGCCAACAGGATT	NM_002124.4
HLA-DRB1 R'	TTGTGGAAGAATAACTGCCAAGC	
CD53 F'	GACAGCATCCACCGTTACCA	NM_000560.4
CD53 R'	GGTCCAATCACTCGTGCCAT	
WTAP F'	CCTCTTCCCAAGAAGGTTCGATT	NM_001270531.2
WTAP R'	GATCTGTGTACTTGCCCTCCAA	
CKS2 F'	TGGACGTGGTTTTGTCTGCT	NM_001827.3

CKS2 R'	GCCGGTACTCGTAGTGTTCG	
ALG11 F'	GGGGAATCAGACTGCTGCTAC	NM_001004127.3
ALG11 R'	TCTCCTCCTCCACCAGCATT	

Table 2-12 BCR::ABL1 genes and associated primers for Fluidigm First half of these primers for BCR::ABL1 were created by Dr Shaun Patterson, the Ensemble ID is unknown.

2.1.6.3 Housekeeping genes for BCR::ABL1 and MSC gene list

Gene	Sequence	Ensemble ID	BCR::ABL1 or MSC
ACTB	-	-	Both
ATP5B	-	-	Both
B2M	-	-	Both
ENOX2	-	-	BCR::ABL1
GAPDH	-	-	Both
RNF20	-	-	Both
TYW1	-	-	BCR::ABL1
UBE2D2	-	-	Both

Table 2-13 Housekeeping genes for BCR::ABL1 and MSC gene list

2.1.7 Equipment

Equipment	Supplier
BD FACS Aria™ IIu (sorter)	BD Biosciences, Oxford, UK
BD FACS Canto™ II	BD Biosciences, Oxford, UK
Biomark™ HD	Standard Biotools, Fluidigm
Biomark™ IFC Controller MX	Standard Biotools, FLuidigm
IKA Vortex 3 Mixer	Fisher Scientific
MiniGalaxy E - (Model 050-600) CO_2 Incubators (dry incubator – no CO_2)	-
Nanodrop spectrophotometer Nd-1000	Labtech International
PHCbi CO_2 Incubator	Fisher Scientific
Scientific Herasafe Biological Safety Cabinet	Thermo
Sigma 1-15K refrigerated benchtop centrifuge	SciQuip
Sigma 3-16pk centrifuge	SciQuip

Table 2-14 Equipment used

2.1.8 Webtools and software platforms

Software	Version
STRING	Version 12.0
Galaxy	Version 24.2
RStudio	Version 2025.09.2+418
GraphPad Prism	Version 10.6.1
Spectronaut	Version 20.1.250624.92449
FlowJo	Version 10
ImageJ/Fiji	Version 2.16.0/1.54p
FACS Diva	Version 6.1.3

Table 2-15 Webtools and software platforms

All images were created with BioRender

2.1.9 RStudio code

The code that was used for proteomics and RNAseq analysis was taken from University of Glasgow Bioinformatics and R course (Dr John Cole).

2.2 Methods

2.2.1 Culturing BM MNCs

2.2.1.1 Ethics

All patient samples were taken with informed consent. All samples were pseudonymised to maintain patient confidentiality however all patient and trial information was available. The samples were in accordance with the declaration of Helsinki and the Greater Glasgow and Clyde National Health Service Ethics agreement. The REC reference number of this cell bank is: 25/WS/0056, the expiry date is: 23rd June 2030.

2.2.1.2 Patients

Patient samples used in this study were BM MNCs and BM plasma of patients at the point of entry into the clinical trial, point of relapse or end point of trial. There was also BM MNCs and BM plasma from patients who were at the point of

diagnosis of their CML before they had received any treatment and patients who did not have CML ('normal' non-CML).

Samples were abbreviated as follows:

Abbreviation	Sample type
R_E/Relapse_E	Patients who went on to relapse at some point during the trial (de-escalation or stopping TKI). Sample taken at point of entry into trial, before TKI de-escalation.
TFR_E	Patients who maintained TFR until end point of trial. Sample taken at point of entry into trial, before TKI de-escalation
R_X/Relapse_X	Patients who when on to relapse during the trial, either during TKI de-escalation or stopping. Taken at point of relapse.
TFR_X	Patients who had maintained TFR throughout the trial. Taken at trial exit (72 months).
N/Normal	Non-CML donors, normal
CML/CML at diagnosis	Patients at diagnosis, before treatment.

Table 2-16 Abbreviations of sample type

2.2.1.3 Cell recovery

Primary patient MNC DESTINY samples were thawed in 37°C water bath and mixed with pre-warmed DAMP by adding 10 mL dropwise over 10 minutes. Cells were then centrifuged at 200g for 10 minutes and the supernatant was removed from the pellet which was then once again resuspended in 10mL DAMP by dropwise addition of 10 mL over 10 minutes. At this point cells were again centrifuged and once supernatant was removed samples were resuspended with 5 mL FACS wash. Cell viability was checked with trypan blue dye exclusion.

2.2.1.4 Cell viability using trypan blue

Cell viability was determined using trypan blue exclusion assay. Cells were mixed with trypan blue in a 1:1 dilution and cells were counted using a haemocytometer. Live cells were determined by cells that maintained round shape and were not blue in the centre as this would mean the cells were dead and had absorbed the trypan blue. The cells on the 4 outer corners of the haemocytometer were counted. To calculate the number of cells/mL the total

number of viable cells was multiplied by 2 (the dilution factor) and also multiplied by 10,000 this was then divided by 4 (the total number of squares counted).

$$Total\ cells/mL\ = \frac{total\ number\ of\ cells\ counted\ in\ squares\ x\ 2\ x\ 10{,}000}{4}$$

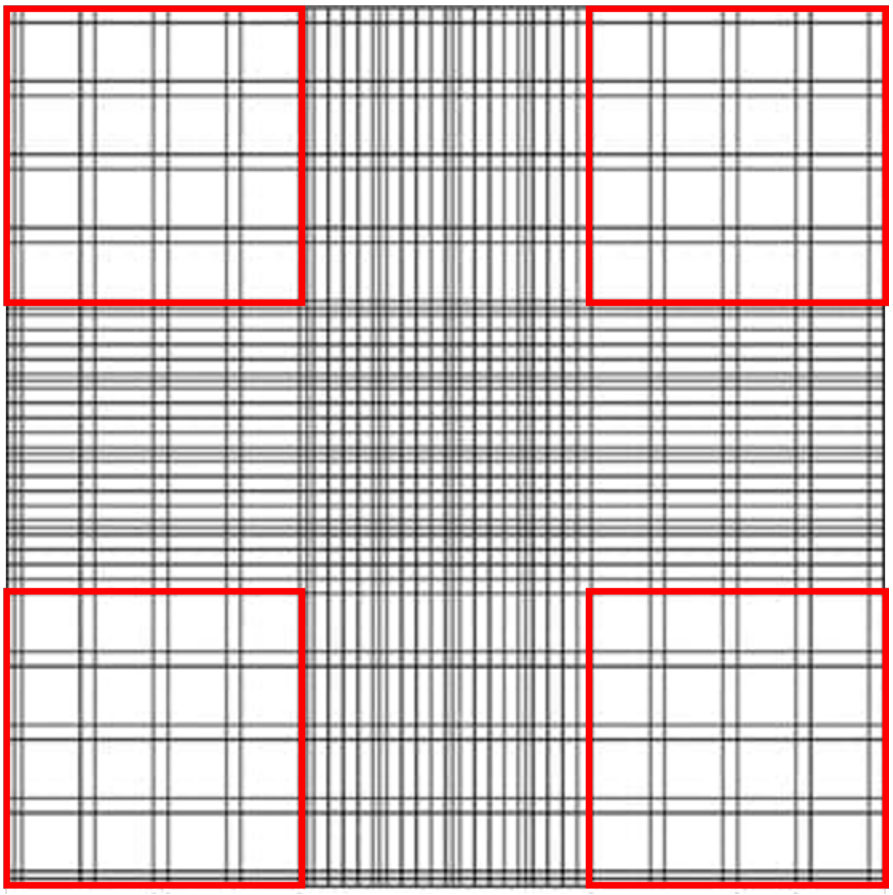

Figure 2-1 Example of hemacytometer grid Haemocytometer grid (image taken from SigmaAldrich.com). Red squares represent squares that were counted for analysis.

2.2.2 Flow cytometry

Once cells had been thawed and counted they were assessed using multi-parameter flow cytometry (MPFC). Samples were spun down at 200g for 10 minutes and resuspended in 100 µL (antibody cocktail made up to 100 µL with FACS wash) of each HSC/LSC marker (Table 2-17, Table 2-18 and Table 2-19) per sample. These samples were incubated at room temperature in the dark until they were ready to be used. For compensation, 1 drop of flow cytometry beads

were run with 1 µL of each antibody stain. Each sample with each HSC/LSC panel was analysed on the BD FACS Aria using Diva software.

Additionally, where possible for samples they were sorted and $Lin^{-}CD34^{+}$ cells were taken for used for long term colony-initiating cell (LTC-IC) (section 2.2.5).

Three HSC/LSC panels were used for MPFC analysis, each sample was stained with each panel separately, sometimes due to variability and limitations of samples, some markers or some samples could not be run. Additionally, when certain samples were thawed more than once, sometimes if there were additional cells the sample would be run with the same panels more than once.

Due to the large MPFC panels used, these were analysed using the BD FACS Aria which can run all samples and markers at the same time. Once the cells had been stained they were given to Miss Jennifer Cassels to carry out to run on the machine and sort the samples under the guidance of what was being analysed.

An example of an HSC/LSC panel 1 run with a sample is shown below:

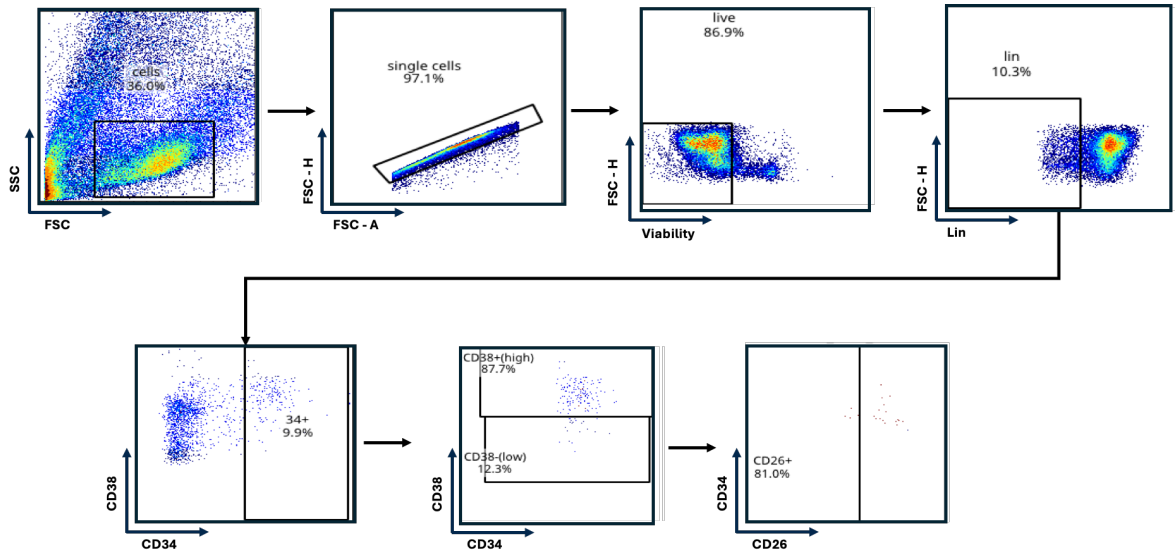

Figure 2-2 Representative image of the gating of analysis of flow cytometry done using with FACS Using HSC/LSC 1 panel to identify to CD26 marker.

Target	Fluorochrome	Antibody volume (µL)
Lineage (Lin)	FITC	8
CD34	BV421	2.5
CD38	BV786	2
CD90	PE-Cy7	3
CD25	BV605	2
CD26	APC	2
CD93	BB700	2
IL1-RAP	PE	4
CD36	BV711	2
VIABILITY	7-AAD	2

Table 2-17 HSC/LSC panel 1

Target	Fluorochrome	Antibody volume (µL)
Lineage (Lin)	FITC	8
CD34	BV421	2.5
CD38	BV786	2
CD45RA	BV510	3
CD49d	BV711	2
CD44	APC-H7	3
CD47	Alexa Fl 647	2.5
CXCR4	PE	2
CD117	PE/Dazzle 594	2
VIABILITY	7-AAD	2

Table 2-18 HSC/LSC panel 2

Target	Fluorochrome	Antibody volume (µL)
Lineage (Lin)	FITC	8
CD34	BV421	2.5
CD38	BV786	2
CD90	PE-Cy7	3
CD25	BV605	2
CD26	APC	2
CD93	BB700	2
CD35	PE	3
VIABILITY	7-AAD	2

Table 2-19 HSC/LSC panel 3

The markers were presented as percentage of $Lin^{-}CD34^{+}38^{-}$ parent population and raw counts of cell number for the marker. An additional limitation of presenting the data as percentage of population is that for some samples there was no stem/progenitor cell ($Lin^{-}CD34^{+}38^{-}$) population. As a result, there could be no data produced for the markers within these samples. While these samples

were still included in the analysis for counts they were removed for the percentage of population graphs which is why counts and percentage of population have different numbers of samples.

2.2.3 Cell sorting

All sorting was done by POGLRC flow cytometry specialist, Miss Jennifer Cassels. This was done to isolate $Lin^{-}CD34^{+}$ fraction from samples for LTC-IC and to run samples with antibody panels (Table 2-17, Table 2-18 and Table 2-19). Each time samples were thawed, when enough viable cells were present, that sample was sorted to get the $Lin^{-}CD34^{+}$ population, this would be done after staining a sample with one of the HSC/LSC panels. The maximum number of cells possible was always taken from each sample, this was kept as consistent as possible however sometimes due to sample variability it could change.

Figure 2-3 shows the gating strategy used to look at the CD markers within the $Lin^{-}CD34^{+}$ fraction of the samples.

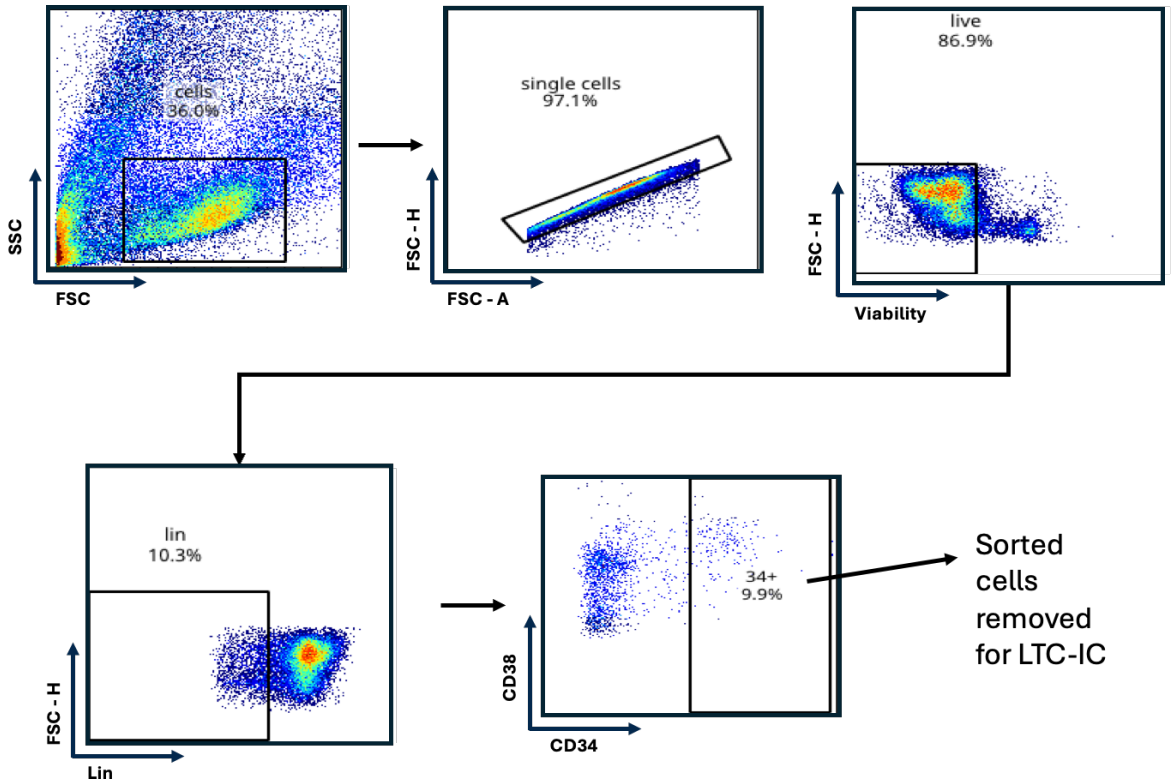

Figure 2-3 Representative image of cell sorting taken from HSC/LSC panel 1

2.2.4 Short-term colony forming cell (ST-CFC) assay

After thawing BM MNCs and sorting for $Lin^{-}CD34^{+}$ cells, 10,000 viable MNCs were resuspended in 100 µL RPMI base media and were added to 900 µL of Methocult H4034 supplemented with cytokines and mixed gently using a 19G needle and 1 mL syringe. Once fully resuspended 1 mL of this mixture was plated into 35 mm tissue culture dishes (avoiding bubbles) and incubated at 37°C and 5% CO_2 for 14 days. After the 14 days, counts were performed under phase contrast with EVOS microscope on colonies formed. Additionally, the colonies were characterised into either: burst-forming unit - erythroid (BFU-E), colony forming unit – macrophage (CFU-M), colony forming unit - granulocyte (CFU-G), colony forming unit - granulocyte macrophage (CFU-GM), and colony forming unit – granulocyte erythrocyte macrophage megakaryocyte (CFU-GEMM).

2.2.4.1 ST-CFC mixture

Reagent	Supplement
Methocult H4034	IL-3, IL-6, G-CSF, FLT3, SCF (final concentration of all at 50 µg/mL)

Table 2-20 ST-CFC mixture

Samples from LTC-IC were also set up in ST-CFC assay, the method was the same although instead of seeding 10,000 BM MNCs into Methocult, all remaining cells from each LTC-IC sample was used.

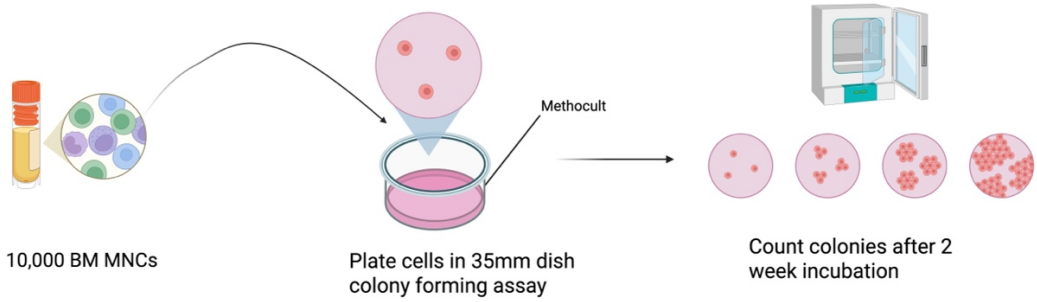

Figure 2-4 ST-CFC assay Schematic representation of ST-CFC assay.

2.2.5 Long term colony-initiating cell (LTC-IC) assay

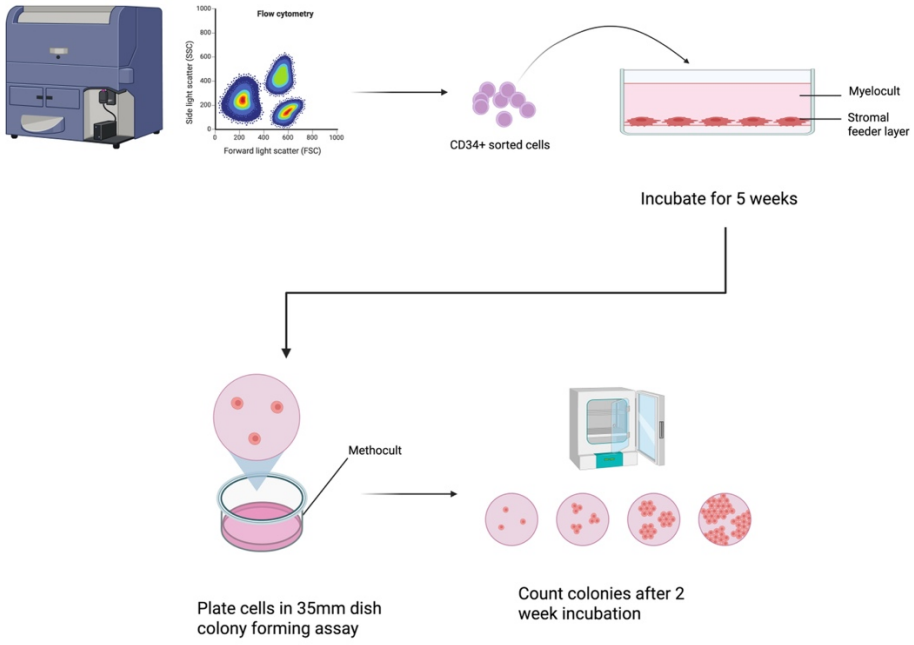

Figure 2-5 LTC-IC assay Schematic representation of LTC-IC assay.

The LTC-IC assay uses two murine fibroblast cell lines: M210B4 cells and SL/SL, these have been genetically modified to express human IL-3 and G-CSF, and IL-3 and SCF, respectively. These cells make up the supportive stromal layer to allow primitive haematopoietic cells to grow. A viable cell count was performed on these cell lines where $1.5x10^5$ of each cell line was added per well onto a collagen I coated 6 well plate in 2 mL of Myelocult. These were incubated overnight at 37°C and 5% CO_2 for the cells to adhere to the plate after which time cell growth was arrested by adding a final concentration 20 µg/mL mitomycin c per well and incubating for 3 hours; the media was then removed and the plate was then washed 5 times with PBS and replaced with Myelocult supplemented with hydrocortisone (10 mM) (made up in DMSO, stored at -20°C freezer) (Table 2-21).

2.2.5.1 LTC-IC mixture

Reagent	Volume	Concentration
Myelocult	9.9 mL	-
Hydrocortisone (10 mM)	0.1 mL	0.1 mM

Table 2-21 LTC-IC mixture

Next, on the same day, the $Lin^{-}CD34^{+}$ sorted cells (described in section 2.2.3) were added to the well and maintained in culture for 5 weeks with weekly half media changes, 1 mL of media was removed and disposed of, and this was replaced with 1 mL Myelocult supplemented with hydrocortisone.

After 5 weeks the cells were harvested by first removing the supernatant of each well and placing it into a flacon tube. The adherent cells in the wells were then washed with 2 mL HBSS, plates were swirled gently, and the liquid removed and put into the falcon tube of that well which has the corresponding supernatant. To remove the adherent layer, 2 mL of trypsin was added to each well for 5 minutes to allow the cells to detach, this was facilitated by gently pipetting the trypsin solution repeatedly over the cells; the supernatant was then removed and added into the same falcon tube, separate one for each well. Each well then had 2 mL IMDM/2% (v/v) FBS added, to remove any remaining cells and stop the activity of the trypsin, that was gently swirled around and then transferred to the corresponding flacon tube.

2.2.5.2 IMDM mixture

Reagent	Volume
IMDM	9.8 mL
FBS	200 µL

Table 2-22 IMDM and FBS mixture used in LTC-IC

The falcon tubes were then centrifuged at 300g for 10 minutes after which the supernatant was removed and discarded. The remaining pellet was used to set up ST-CFC (as described above, section 2.2.4).

2.2.6 RNA extraction of CFUs

Once colonies have been produced from ST-CFC (or LTC-IC) RNA was extracted by adding 10 mL of PBS to each well, 1 mL at a time, pipetting up and down repeatedly to remove all Methocult from the wells and placed into a 15 mL falcon tube. Once a suspension was achieved this was spun down at 300g for 10 minutes at which point another 10 mL of PBS was added and the cells were once again washed at 300g for 10 minutes. Once the supernatant was removed RNA extraction was done using the Arcturus® PicoPure® (ThermoFisher) kit according

to manufacturer's instructions. RNA quality and quantity was measured using nanodrop spectrophotometer Nd-1000 (Labtech International). Samples were stored in -80°C freezer until use for Fluidigm PCR analysis.

2.2.7 Fluidigm of colonies for BCR::ABL1 genes

In order to identify the leukaemic burden between the TFR and relapse patient cohorts and see how this correlated to their colony formation, a panel of the top ranked genes most related genes for *BCR::ABL1* (Giustacchini et al. 2017) were selected (Table 2-12). The Fluidigm system is a high throughput real-time PCR method that allows you to test up to 96 samples in one go using small volumes and concentrations. A Fluidigm chip was run on the RNA extracted from colony samples (see section 2.2.6) using a 96.96 Dynamic Array Gene Expression chip. To make the input cDNA, a maximum of 500ng of RNA was used with the High-Capacity cDNA Reverse Transcription Kit (Thermo Fisher Scientific) according to the manufacturer's instructions. This Fluidigm protocol was adapted from a protocol produced by Dr Xu Huang's lab.

First, specific target amplification (STA) was carried out on the samples, this increases the concentration of cDNA in the samples ensuring a high enough level of cDNA to allow detection.

A master mix was made up:

Component	Volume (µL)
Forward primer (100 µM)	1 (of each primer)
Reverse primer (100 µM)	1 (of each primer)
Water	Up to 200

Table 2-23 Pooled primer mix

Samples were mixed with this mastermix:

	Component	Volume/reaction (µL)
Pre-Mix	2X Multiplex PreAmp MasterMix (Qiagen)	2.50
	500 nM (10x) pooled primer mix	0.50
	Water	0.75

	cDNA	1.25
	Total volume	5.00

Table 2-24 Pre-mix and samples for STA

The sample and pre-mix mixture was put onto the thermal cycler:

Hold	95°C	15 minutes
14 cycles	94°C	30 seconds
	60°C	90 seconds
	72°C	90 seconds
Final Extension	72°C	10 minutes

Table 2-25 STA cycle parameters

Once the STA cycles had finished, samples were treated with Exonuclease I to remove the primers from the reaction leaving a clean cDNA sample.

Component	Volume (µL)
Water	1.4
Exonuclease I Rxn Buffer	0.2
Exonuclease I (20U/µL)	0.4
Final volume	2.0

Table 2-26 Exonuclease I treatment

From the exonuclease I treatment, 2 µL was added to each 5 µL sample from the STA, this was then vortexed and centrifuged and was once again placed into the thermo cycler (Table 2-27):

Role	Temperature	Time
Digest	37°C	30 minutes
Inactive	80°C	15 minutes
Hold	4°C	

Table 2-27 Exonuclease I cycle

Into each sample (7 µL), the final product was diluted by adding 18 µL TE buffer. Samples were then stored at -20°C until the next day.

Samples were then thawed and mixed with pre-mix:

	Component	Volume (µL)
Pre-Mix	2X SsoFast EvaGreen Supermix Low Rox	3.0
	20X DNA Binding Dye Sample Loading Reagent (green cap)	0.3
	ExoI + STA sample	2.7
	Total	6.0

Table 2-28 Sample mix

This was then briefly vortexed and spun down. The sample mix was stored on ice until ready to be loaded onto the chip.

While that was on ice the primer assay mix was made up:

Component	Volume (µL)
2X Assay Loading Reagent	3
10 µM mix of Forward and Reverse primers (500 nM final concentration of each primer in the final reaction)	3
Total volume	6

Table 2-29 Primer assay mix

Priming and Loading the chip:

The 96.96 chip appears as follows:

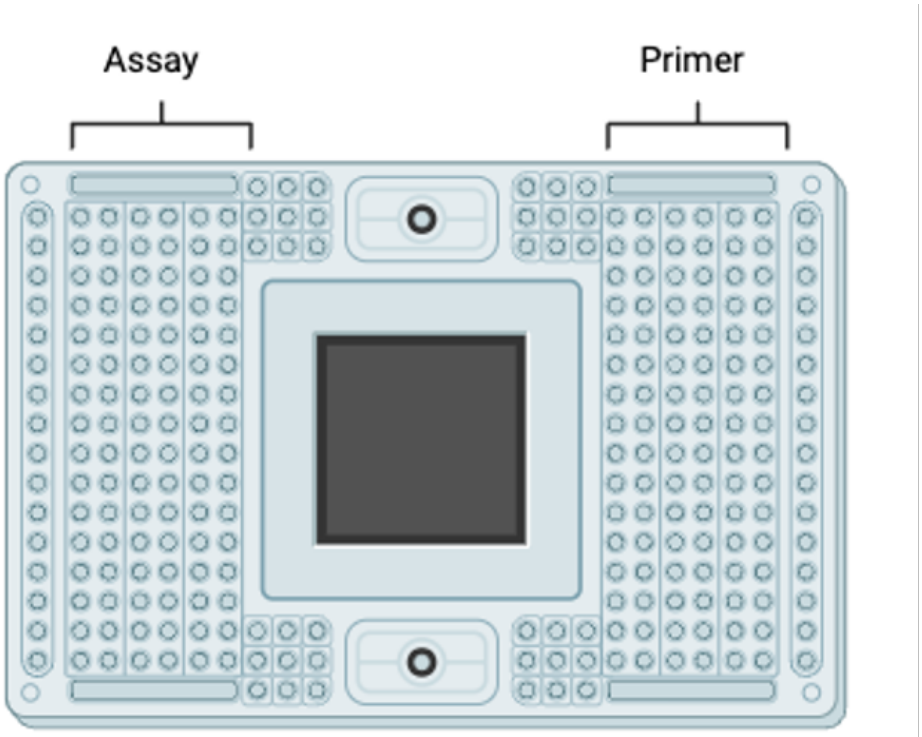

Figure 2-6 Example of fluidigm chip

The chip was firstly primed by adding control line fluid into the valves at the side and placed on the IFC machine with the 'Prime' script. Once this was completed the samples and primers are then added to the corresponding inlets (5 µL of each), and the plate was run on the IFC machine with the 'Load mix' script to allow the samples and primers to mix. When this finished the chip was placed in the Biomark™ HD and the reaction was recorded.

From the Fluidigm data, the average Ct value of the housekeeping genes was subtracted from each sample. This gave the ΔCt value for all of the samples, this was then flipped to -ΔCt to provide the accurate representation of the expression levels.

For MSC analysis (section 2.2.8), the outcome groups were compared. To compare the TFR and relapse samples both samples were normalised to the normal BM MSC. To do this the average ΔCt of the normal samples was subtracted from the ΔCt of each sample from TFR and relapse individually. This gave ΔΔCt, the -(ΔΔCt) gave the $\log_2$ fold change and the 2^-(ΔΔCt) was used to

find the fold change. For all comparisons, samples were normalised to normal and then compared.

Once the log_2 fold change and the fold change of these samples had been identified, the log_2 fold change was compared on Prism using a Two-Way ANOVA to get the q-value. This produced a q value for both the relapse and TFR samples and their corresponding log_2 fold change values.

2.2.8 Fluidigm of colonies for MSC genes

This was as described above, however a 48.48 Dynamic Array Gene Expression chip was used with MSC RNA samples (from section 2.2.12) and the gene list was from Table 2-11. Genes were selected from RNAseq DEGs and associated DEGs. The programme for the experiment was the same, the volumes used were all halved for the 48.48 chip.

2.2.9 Isolating MSCs

MSCs were extracted by taking cells from BM MNCs, before sorting for Lin^-CD34^+ after they had been thawed, cells were spun down at 200g for 5 minutes, the supernatant was then discarded, and cells were resuspended in MSC media and placed in T75 nunc flask. Media was removed from the flasks once every two to three days, cultures were incubated for 3-4 weeks until cell growth was seen. After visually noting growth had reached 80% confluency, cells were passaged/frozen, cells kept in culture till passage 3, for each passage vials were frozen down and characterisation was carried out.

2.2.10 MSC culturing and phenotyping

The MSC cells were cultured in MSC growth media. Frozen vials of MSCs were thawed in 37°C water bath and mixed with pre-warmed MSC media by adding 10 mL dropwise over 10 minutes. Cells were then centrifuged at 200g for 10 minutes and the supernatant was removed from the pellet which was then once again resuspended in 10 mL MSC media by dropwise addition of 10 mL over 10 minutes. At this point cells were once again centrifuged and once supernatant was removed samples were resuspended with 10 mL MSC media. Cell viability was checked with trypan blue dye exclusion. The cells were maintained in tissue

culture treated T75 flasks and incubated at 37°C and 5% CO_2. All experiments were set up in the laminar airflow tissue culture safety cabinet.

Once MSCs reached desired confluence (~80%), to remove cells for use or to passage cells, media was removed from flasks and cells were gently washed with PBS. After PBS was removed, 5 mL of accutase, which is gentler than trypsin and does not affect the cell surface markers, was added and the flask was incubated at 37°C for 5 minutes to detach cells. To stop the reaction 5 mL of MSC media, which dilutes the accutase, was added to the flask and cells could then be removed and pelleted at 300g for 5 minutes. The supernatant was then removed, and cells were resuspended in 2 to 5 mL of media (depending on confluency), the cells were then counted using trypan blue and used as required per experiment.

To phenotype the cells confirming they were MSCs, a predetermined panel of surface antibodies was used. Cells were detached and $1x10^5$ cells added to flow cytometry tubes; cells were washed twice with 2% (v/v) FBS in PBS then resuspended with 100 µL of antibody cocktail (Lineage-FITC, CD34-APC, CD73-PE, CD45-APCCy7, CD90-PE-Cy7, CD105-PerCP-Cy5.5 made up to 100 µL with 2% (v/v) FBS in PBS).

Target	Fluorochrome	Antibody volume (µL)
Lineage	FITC	3.0
CD34	APC	1.5
CD73	PE	3.0
CD45	APCCy7	1.5
CD90	PE-Cy7	3.0
CD105	PerCP-Cy5.5	3.0

Table 2-30 MSC characterisation antibody cocktail

These cells were incubated for 30 minutes to 1 hour in the dark on ice with occasional agitation, after this the cells were washed with 2% (v/v) FBS in PBS and resuspended in 200 µL 2% (v/v) FBS in PBS before analysis by flow cytometry.

2.2.11 MSC characterisation

To set up the plates for MSC characterisation experiments, cells were counted with trypan blue and $4.8x10^4$ cells/well were added to each well of two 6-well plates. The plates were incubated at 37°C 5% CO_2 for 96 hours after which assays were carried out.

2.2.11.1 MSC senescence stain

The senescence of levels of MSCs was measured using Senescence ß-galactosidase Staining Kit according to the manufacturer's instructions (Cell Signalling Technology®). This stain uses X-gal which in the presence of ß-galactosidase cleaves the X-gal and produces a blue precipitate that can be quantified and viewed under a microscope. Once cells were stained overnight wells were split into 5 squares where 1 image was taken per square using the EVOS XL Core Inverted Microscope.

Analysis for images was based on method created by Miss Lucy Clarke, POGLRC, who adapted a method from (Idelfonso-García et al. 2024). Images were uploaded to Image J (FIJI) software, the image was then deconvoluted using the 'Brilliant_Blue' vector, the image option 'Colour_3' was selected from the options and the threshold was set to 0 to 100 for this image. From this the '%Area' value was exported and used for each image as a representative for the level of senescence presence. For each sample 5 images were used and the average of these was taken to ensure an accurate representation of the plate was captured.

2.2.11.2 MSC ROS detection

For the ROS detection, a fluorescent probe, H2DCFDA, was used, this becomes oxidised when it comes into contact with ROS and produces a fluorescence which can be measured (Ameziane-El-Hassani and Dupuy 2013). To MSC cells growing in the 6-well plates, 20 mM H2DCFDA was added to test for changes to ROS levels. For the test well 10 µL/mL media volume was added to well 1. For the positive control 5 µL/mL of 30% (v/v) H_20_2 was added to well 2, well 3 was untouched and used for the unstained control. The plate was then incubated at 37°C for 45 minutes after which cells were harvested as a suspension by removing them from

the plate using accutase. At this point cells were washed with PBS twice and resuspended in PBS to use for flow cytometry analysis. DAPI was also added before cells were run through the flow cytometer to detect live cells. The 488-530/30 channel was used to detect for ROS and 405-450/50 for DAPI staining.

2.2.11.3 MSC JC1 stain

The ratio of green to red JC1 staining is used to evaluate mitochondrial health. In healthy cells JC1 forms aggregates which produce red/orange fluorescence. If the mitochondrial membrane potential decreases the JC1 becomes a monomer and produces green florescence. Hence increased red to green fluorescence indicates healthy mitochondria. A yellow colour is seen when the green and red colocalize.

Cells were harvested from 6-well plates with accutase as described. To one tube 1.3 µL of JC1 dye (1 mg/mL) (test) was added. To the second tube 1.3 µL of JC1 dye (1 mg/mL) and 5 µL valinomycin (10mM) (positive control) were added and to a third tube cells were left unstained. These cells were incubated at 37°C for 30 minutes. The cells were then removed, washed twice with PBS and resuspended in fresh PBS. The cells were analysed by flow cytometry using 488-530/30 channel for JC1 green fluorescence, 488-585/42 channel for JC1 red fluorescence and 405-450/50 for DAPI staining.

2.2.12 MSC RNA extraction

For extraction of RNA from MSCs, around 1 to $3x10^5$ cells were needed. Following removal of confluent cells from the flasks, the cells were spun down at 200g for 5 minutes after which the supernatant was removed and 350 µL of Buffer RLT was added (with ß-mercaptoethanol), and RNA extraction was carried out using the RNeasy® Micro (QIAGEN) kit according to manufacturer's instructions. The RNA quality and quantity was measured using nanodrop spectrophotometer Nd-1000. Samples were stored in -80°C freezer until use for Fluidigm PCR and RNAseq.

2.2.13 MSC bulk RNA sequencing

For the first RNAseq run: the extracted RNA (section 2.2.12) was used to make cDNA libraries that were prepared using Illumina TruSeq Stranded RNA Core Library Prep. Samples were then sent to Novogene to be sequenced using their NovaSeq 6000 platform, read depths of 6GB per sample. The raw data files were processed using Galaxy server, initially the quality of the files, uploaded as FastQ, were assessed using FastQC tool. The files were then trimmed with the Trimmomatic tool, with 'Paired End (two separate input files)' option. The files returned were aligned to hg38 human genome with the hisat2 tool and counts were generated using ht-seq count tool. These counts were exported and differential expression was then analysed using DESeq2 on RStudio (with the help of Mr John Cole). All analysis was done using RStudio.

For the second RNAseq run: the extracted RNA samples were sent to University of Glasgow – Shared Research Facilities. RNAseq was carried out using NextSeq2000 with read length of 1x100bp, 25M reads per sample. The data was trimmed, aligned and differential analysis was carried out by Shared Research Facilities. From the data returned all analysis was done using RStudio.

2.2.14 Freezing and storing cells

All cell lines and MSCs mentioned above were frozen and kept in liquid nitrogen (-185°C) for long term storage. DESTINY samples had been previously banked by Dr Alan Hair, in POGLRC. All cells (MSCs and cell lines) were stored at 3 to $5x10^6$ cells/mL per vial in freezing media. These vials were put into freezing container (Mr Frosty) and slowly frozen at a rate of 1°C/minute until reaching -80°C at this point vials were transferred to liquid nitrogen the next day where they were stored long term.

2.2.15 Protein quantification

Before proteomics analysis could proceed, protein concentration of each BM plasma sample was calculated. Each BM plasma sample was diluted by 1 in 100 in water and the Micro BCA™ Protein Assay Kit (Thermo Fisher Scientific) was used according to the manual instructions to calculate the protein concentration.

2.2.16 Mass Spectrometry for protein discovery (proteomics)

The sample processing and MS analysis was all carried out by the University of Dundee Proteomics facility, FingerPrints. All samples were run on the Orbitrap Astral MS (Thermo Scientific). Data analysis was performed using Spectronaut v19 with directDIA.

2.2.17 Bioinformatics

Differential expression analysis of proteomics data was carried out by University of Dundee Fingerprinting Proteomics department.

The RNAseq was carried out by Novogene and University of Glasgow Shared Research Facilities (analysis described above in section 2.2.13).

Data from both the RNAseq and proteomics data was analysed using RStudio.

2.2.18 Statistical analysis

All figures and statistical analysis were produced on GraphPad Prism and RStudio. For two outcome groups being tested a student's t-test was used. For comparing more than two outcome groups a one-way ANOVA or two-way ANOVA was applied. The specific statistical test for each comparison and specific cutoffs for identifying differentially expressed genes (DEGs) and DEPs are in the requisite figure legends. For all statistical tests including groups with samples less than 3 values, only comparisons that were statistically significant are shown.

3 Results I – MSCs

3.1 Introduction

MSCs are found within the BMM and are one of the main cell types that is involved in maintaining haematopoiesis and supporting HSCs. There is also strong evidence to suggest MSCs are involved in the alterations to the BMM that lead to the survival of LSCs in CML and helps protect LSC from TKIs (Hsieh et al. 2021).

While MSCs provide an interesting and important area of clinical research focus they have limited proliferation and differential capacity in culture, and over time they become senescent, a phenomenon that was first described by Hayflick and Moorhead in 1961 (Hayflick and Moorhead 1961). Senescence is a cell cycle arrest that inhibits cell differentiation to prevent the growth of old and damaged cells but still enables them to survive (Herranz and Gil 2018). The inhibition of cell growth in senescence is owing to activation of $p16^{INK4a}$/Rb and $p53/p21^{CIP1}$ tumour suppressor networks (McHugh and Gil 2018). There are several changes that occur in MSCs when they become senescent including changes to their size and shape, as well as differentiation and proliferation potential. Importantly, when cells become senescent they produce proinflammatory substances, this is called senescence-associated secretory phenotype (SASP), that is particularly interesting in the context of the diseased BMM. Senescence of MSCs can lead to effects on surrounding cells and microenvironment. There are many mechanisms that can lead to senescence including ROS production, mitochondrial dysfunction, DNA damage and telomere attrition (Weng et al. 2022). Within the BM there is normally a limited number of MSCs that become senescent over time with aging, this is a process that is thought to be amplified in disease. This increased senescent profile also indicates these patients have an increased pro-inflammatory profile as MSCs produce SASP factors when they become senescent which includes IL-1, IL-3, IL-4, IL-6, IL-8, IL-17, epidermal growth factor (EGF), VEGF, TGF-ß and more (Weng et al. 2022).

Within CML the median onset of age is 56 years old (Harutyunyan et al. 2021; Ernst et al. 2026), however patients younger than this can develop CML, although it is less common. The issue of patient age is widely discussed within

the topic of MSCs senescence. Research from Gnani et, al. found BM MSCs from healthy donors that were older (≥70 years old) have been found to have higher senescence than younger donors (<35 years old), this includes reduced proliferation, increased senescent morphology and increased ß-galactosidase staining (Gnani et al. 2019). This was further demonstrated in aged BM-MSCs that had amplified senescent features including an increased pro-inflammatory profile that caused clonogenic impairment of HSPCs (Gnani et al. 2019). A less talked about and researched driver of senescence in MSCs is gender. For example, it was found that the clonogenicity of BM MSCs was higher in female donors than in male donors (Siegel et al. 2013). Additionally, it has been identified that with female adipose derived MSCs (ASC) there was a reduced senescence and pro-inflammatory IL-6 cytokine expression compared to male (OCK et al. 2016). The changes that sex can cause in MSCs, and their senescence, is less well understood but this is a potential area to consider when dealing with clinical samples.

While ROS is a normal byproduct of the proliferation and differentiation of MSCs, in homeostasis MSCs maintain low intracellular ROS levels (Atashi et al. 2015), this is thought to help MSCs maintain the BMM and haematopoiesis (Atashi et al. 2015). It has been reported that increased levels of ROS in MSCs can cause stress-induced senescence (Denu and Hematti 2016) and overall cause cell damage to MSCs. Increased levels of ROS can alter the self-renewal, differentiation and proliferation capacity of MSCs (Atashi et al. 2015; Denu and Hematti 2016). As well as this, increased ROS levels in MSCs results in increased adipogenic differentiation and reduced osteogenic differentiation.

In addition to the senescence and ROS production, MMP is a good measurement of MSC activity and health. Mitochondrial dysfunction is another cause of senescence, therefore mitochondrial health is an indicator of differentiation ability, immunomodulatory capacity of MSCs and their senescence (Yan et al. 2021). In CML it has been reported that during treatment, mitochondria are transferred between CML cells and MSCs through tunnelling nanotubules (TNTs), potentially restoring the metabolism in CML cells and endorsing their survival (Miao et al. 2025). Furthermore, it has been found in AML that when mitochondria are transferred to AML cells, this provides these cells with more

energy which is then used as a mechanism of chemoprotection (Marlein et al. 2017) (Moschoi et al. 2016). Therefore, MSC function can be evaluated by cellular ROS levels and MMP with changes being associated with a pro-inflammatory phenotype and increased levels of senescence.

Another important feature of MSCs is their production of a range of molecules called the secretome including cytokines, chemokines and growth factors. There is evidence of changes in the growth factor secretome, released by MSCs, in patients with CML, with increase expression of several cytokines including fibroblast growth factor (FGF), hepatocyte growth factor (HGF), IL-1α, IL-6, IL-8, (platelet-derived growth factor) PDGF, TGF-β, TNF-α, VEGF, BMP2 and BMP4 (Busch and Wheadon 2019). This is particularly important in BM-MSCs as this helps to control haematopoiesis and the activity of HPSCs by secreting substances like CXCL12, Ang1 and TGF-β (Baberg et al. 2019). The secretome can change in CML with increase of IL-7 from MSCs, that can help the survival of leukaemic cells exposed to TKIs (Xiaoyan Zhang et al. 2016). MSCs also secrete immunomodulatory substances which could lead to CML immune evasion (Giallongo et al. 2016). Furthermore, the soluble protein profile within the BM of patients with CML has been shown to be vastly different to healthy scenario including c-Myc binding protein 1, 53BP1, Mdm4, OSBP-related protein 3 and Mortalin (Pizzatti et al. 2006).

While MSCs are known for having an anti-inflammatory effect in normal conditions, in patients with CML it appears the opposite is true. Exosomes produced by CML cells caused activation of EGF receptor (EGFR) increase production of IL-8 and matrix metalloproteinase 9 from MSCs, which are pro-inflammatory (Corrado et al. 2016). Additionally, treatment of BM MSCs with CML exosomes caused increased adhesion of CML cells to the MSC stromal layer via annexin A2 (Corrado et al. 2016), indicating not only are MSCs producing increased inflammatory cytokines in CML BMM but also are used to support LSCs.

It is clear to see why MSCs have become such a popular topic of research in many health issues including pathology that starts in the BM, like CML. Evidence suggests the MSCs are involved in the protection of LSCs within the BMM as well as changes to their secretion to increase inflammatory profile, changes to their immunomodulatory response and changes to their differentiation potential. This

further causes disruption to the delicate equilibrium of the BMM and allows for CML to occur and for difficulties to the goal of disease eradication.

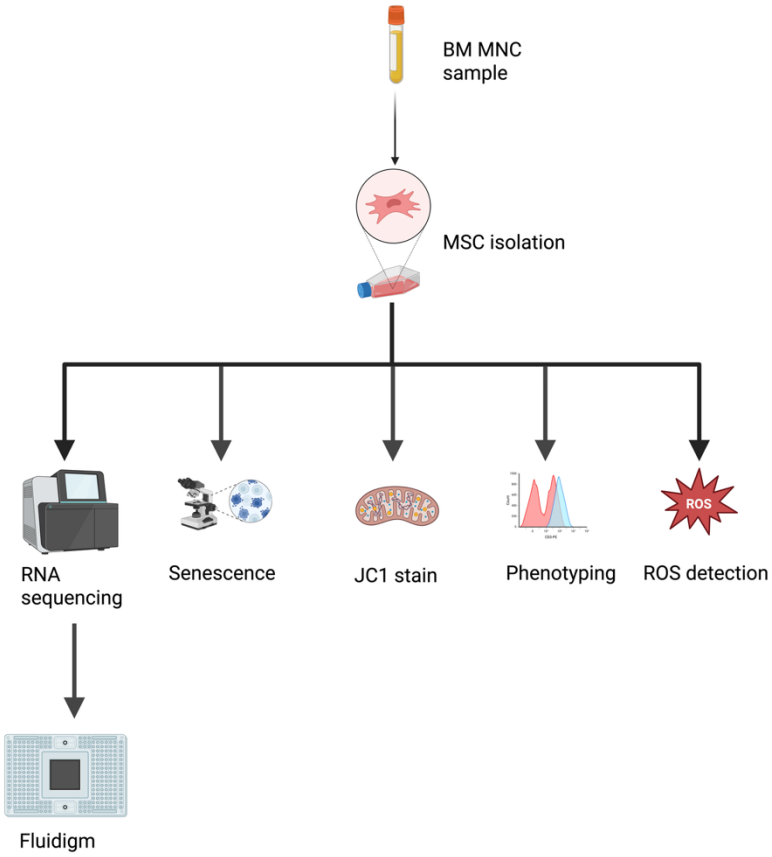

Figure 3-1 Schematic representation of experiments performed on MSCs The BM MSCs were isolated from BM MNC samples and cultured in blue cap Nunc flasks. Samples that were isolated were confirmed to be MSCs through phenotyping using flow cytometry, samples were tested using JC1 stain, ROS and senescence levels. Samples were also sent for RNA sequencing, where results were validated using Fluidigm.

3.2 Aims

1. To characterise the MSCs of the BMM to understand their changes in patients who maintain TFR vs those who relapse and identify if any of these changes can be predictive of TFR success.

3.3 Objectives/sub aims

1. To elucidate if characterising the metabolic and senescent changes in patient derived MSCs from DESTINY trial patients predicts which patients are candidates for successful TFR.

2. To profile the transcriptional changes using RNAseq of patient derived MSCs to understand whether changes in the supportive stroma in the BMM are predictive of TFR success.

3. To validate transcriptional changes using Fluidigm in DESTINY trial patient derived MSCs and establish if these changes are seen in a larger cohort of patient samples.

3.4 Results

3.4.1 Patient derived bone marrow MSC extraction and phenotyping

MSCs were isolated from the BM samples by placing the cells into nunc tissue culture flasks with Promocell® MSC media. Once cells started to grow they displayed the expected features of MSCs. The International Society for Cellular Therapy has produced minimal criteria for defining MSCs that is they should: 1) adhere to plastic in tissue culture; 2) '*must express CD105, CD73 and CD90, and lack expression of CD45, CD34, CD14 or CD11b, CD79a or CD19 and HLA-DR surface molecules*'; and 3) be able to differentiate into adipocytes, osteoblasts and chondroblasts (Dominici *et al*. 2006).

The cells appeared to have a classic spindle shape associated with MSCs and were adherent to nunc tissue culture flasks (Figure 3-2 B). To confirm the MSC phenotype, the expression of cell surface CD molecules by the cells was evaluated using a panel [expectation is $Lin^{-}CD34^{-}CD45^{-}CD73^{+}CD90^{+}CD105^{+}$]. The phenotype of all samples was tested at passage 1.

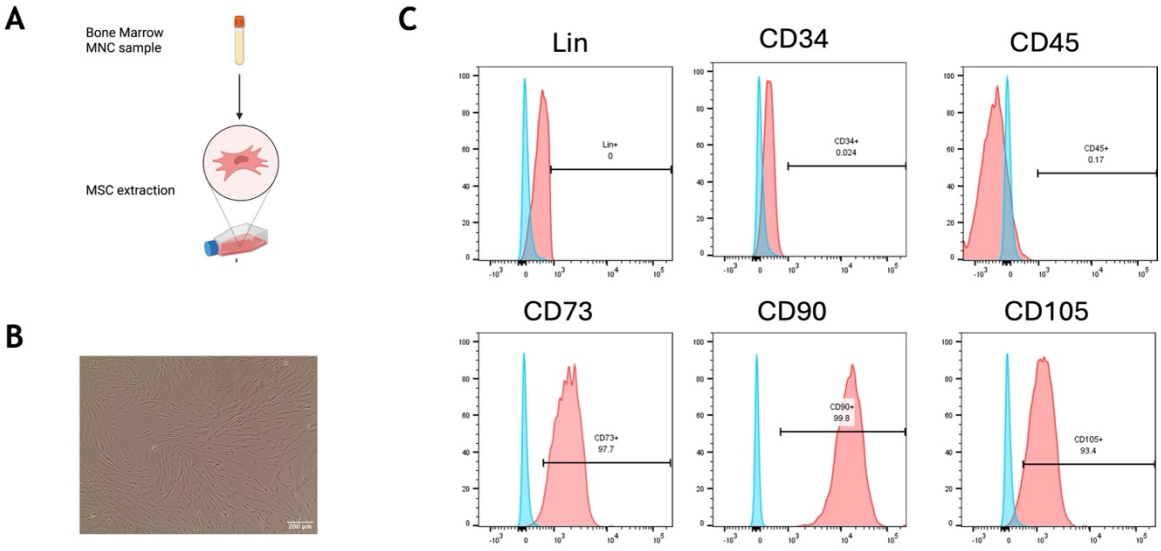

Figure 3-2 Isolation of MSCs and confirmation of phenotype (A) Schematic representation of how MSCs were isolated. **(B)** Image of MSC cells at 10X magnification. Scale bar - 200 µm. Images taken on EVOS Inverted microscope. **(C)** Example of MSC sample tested with CD markers to confirm phenotype by MPFC. The red histogram is the fully stained MSC sample and the blue histogram is the unstained control.

Sample number	Trial Response	Timepoint of sampling	Days to relapse	MMP	ROS	Senescence	Phenotype	RNAseq	Validation of RNAseq -Fluidigm
RB1120	-	-							
CML535	-	-							
NRML	-	-							
NRML 409									
RB1119	-	-							
RB810	-	-							
RB771	-	-							
RB768	-	-							
RB900	-	-							
3X	Relapse in stopping	Exit – relapse during trial	455						
9	Relapse in stopping	Entry – at start point of trial	449						
10	TFR	Entry – at start point of trial	-						
17	TFR	Entry – at start point of trial	-						
20	TFR	Entry – at start point of trial	-						
23	Relapse in de-escalation	Entry – at start point of trial	244						

23X	Relapse in de-escalation	Exit – relapse during trial	244						
28X	Relapse in de-escalation	Exit – relapse during trial	262						
44	Relapse in de-escalation	Entry – at start point of trial	124						
49X	Relapse in stopping	Exit – relapse during trial	475						
60	Relapse in stopping	Entry – at start point of trial	485						
62	Relapse in stopping	Entry – at start point of trial	828						
62X	Relapse in stopping	Exit – relapse during trial	828						
64	TFR	Entry – at start point of trial	-						
67	TFR	Entry – at start point of trial	-						
68	TFR	Entry – at start point of trial	-						
78	Relapse in de-escalation	Entry – at start point of trial	75						
82X	TFR	Exit – end point of trial	-						
84	TFR	Entry – at start point of trial	-						

84X	TFR	Exit – end point of trial	-						
115	TFR	Entry – at start point of trial	-						
116	TFR	Entry – at start point of trial	-						
118	TFR	Entry – at start point of trial	-						
141	Relapse in stopping	Entry – at start point of trial	472						

Table 3-1 BM MSC samples used for each experiment MSCs isolated from BM samples and the experiments they were used for. The information about each sample is also shown. Boxes highlighted in green indicate this sample was used with this technique.

3.4.2 MSC characterisation - Senescence in MSC cell samples is higher in relapse compared to TFR

To test the basal level activity of MSCs the cells were left to grow to confluency for 96 hours. The cells were presumed to be optimally active at this point when they are releasing their secretome allowing mirroring of how these cells might be acting within the BMM. From this the senescence, ROS, and MMP were assayed.

Initially the comparison between relapse vs TFR MSCs was examined at trial entry, this showed a significant decrease of senescence in TFR patients' cells compared to relapse ($p=0.0068$) (Figure 3-3 A). However, when the comparison of all potential outcomes groups was looked at together, this change was not noted as statistically significant. Interestingly, this comparison did find an increase in the senescence levels of normal donor MSCs compared to patients who maintained their remission ($p=0.02$) (Figure 3-3 B).

All samples examined were at passage 2 (P2), this was owing to the known increase in senescence that occurs in primary MSCs with higher passage number (Figure 3-3 C). As the passage number increased the blue stain (β-galactosidase activity) also increased as expected, a loss of proliferation of the cells is observed which is also typical of increased senescence. In addition, cells lost their typical small, spindle-like shape characteristic of healthy MSCs, instead, the cells become longer and flatter in shape with visible vacuoles. These are all typical signs of senescence. Hence, to avoid this variable all samples were subsequently tested at their most healthy and active (P2).

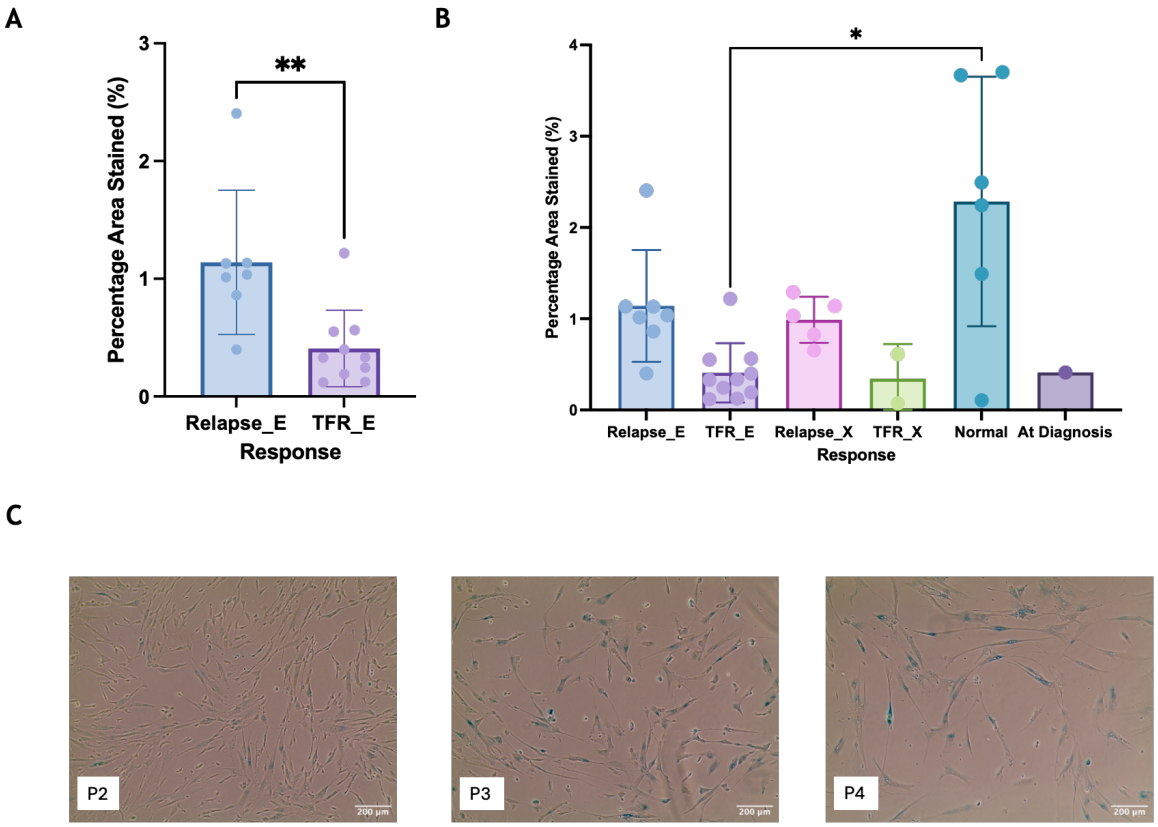

Figure 3-3 Change of senescence levels in MSCs (A) Quantification of percentage area stained for senescence using ß-galactosidase in MSC from relapse (R_E) and TFR (TFR_E) patients at trial entry. **(B)** Quantification of the percentage area stained for senescence in MSC from all patient outcome groups. Relapse at trial entry (R_E) (blue) (n=7), TFR at trial entry (TFR_E) (purple) (n=10), Relapse at trial exit (R_X) (pink) (n=5), TFR at trial exit (TFR_X) (green) (n=2), Normal (turquoise) (n=6), CML at diagnosis (dark purple) (n=1). All samples were tested at passage 2. **(C)** BM MSC sample 62 with ß-galactosidase staining in passage 2-4. Images were taken on an EVOS Inverted microscope at 10X magnification. Scale bar – 200 µm. Error bars show Mean ± SD. Mann-Whitney test was carried out on **(A)** and One way ANOVA, Kruskal-Walis test was carried out on **(B)**. P values: >0.05 (ns), <0.05 (*), <0.01 (**), <0.001 (***), <0.0001 (****). For all statistical tests including groups with samples less than 3 values, only comparisons that were statistically significant are shown.

3.4.3 MSC characterisation – MSCs from female patients in TFR have lower senescence levels than in relapse

Age, sex, molecular cohort, and the TKI prescribed were assessed for their influence on the MSC sample characteristics. Age and sex of patients have been identified as drivers of cellular senescence and so potential patient characteristics that could change the behaviour and activity of their MSCs. Interestingly patients in MR4 at trial entry had a higher TFR success rate than MMR (Clark et al. 2019), therefore it was of interest to study if molecular remission status altered the MSCs. Finally, while almost all patients of the DESTINY trial were on imatinib, the effect of long term use of different TKIs was of interest as it was known, for example, that TKI resistant CML patients' MSCs

secrete higher amounts of BMP4 compared to healthy cells (Grockowiak et al. 2017), increased BMP4 production would promote BM remodelling and bias osteoblastogenesis (Liu et al. 2022). MSCs are also thought to play an essential role in manifesting drug resistance by protecting leukaemic CML cells from TKIs (Y. Yang et al. 2013).

It was seen that MSC samples at trial entry from female patients who maintained their TFR had lower senescence staining compared to patients who went on to relapse ($p=0.0485$). Suggesting within the DESTINY cohort, female patients who went on to maintain TFR had lower senescence of their MSCs before TKI cessation.

This was the only statistically significant change seen within these comparisons. From the analysis of molecular cohort, TKI used and age, there was no significant changes to the senescence of the MSCs within the outcome groups tested.

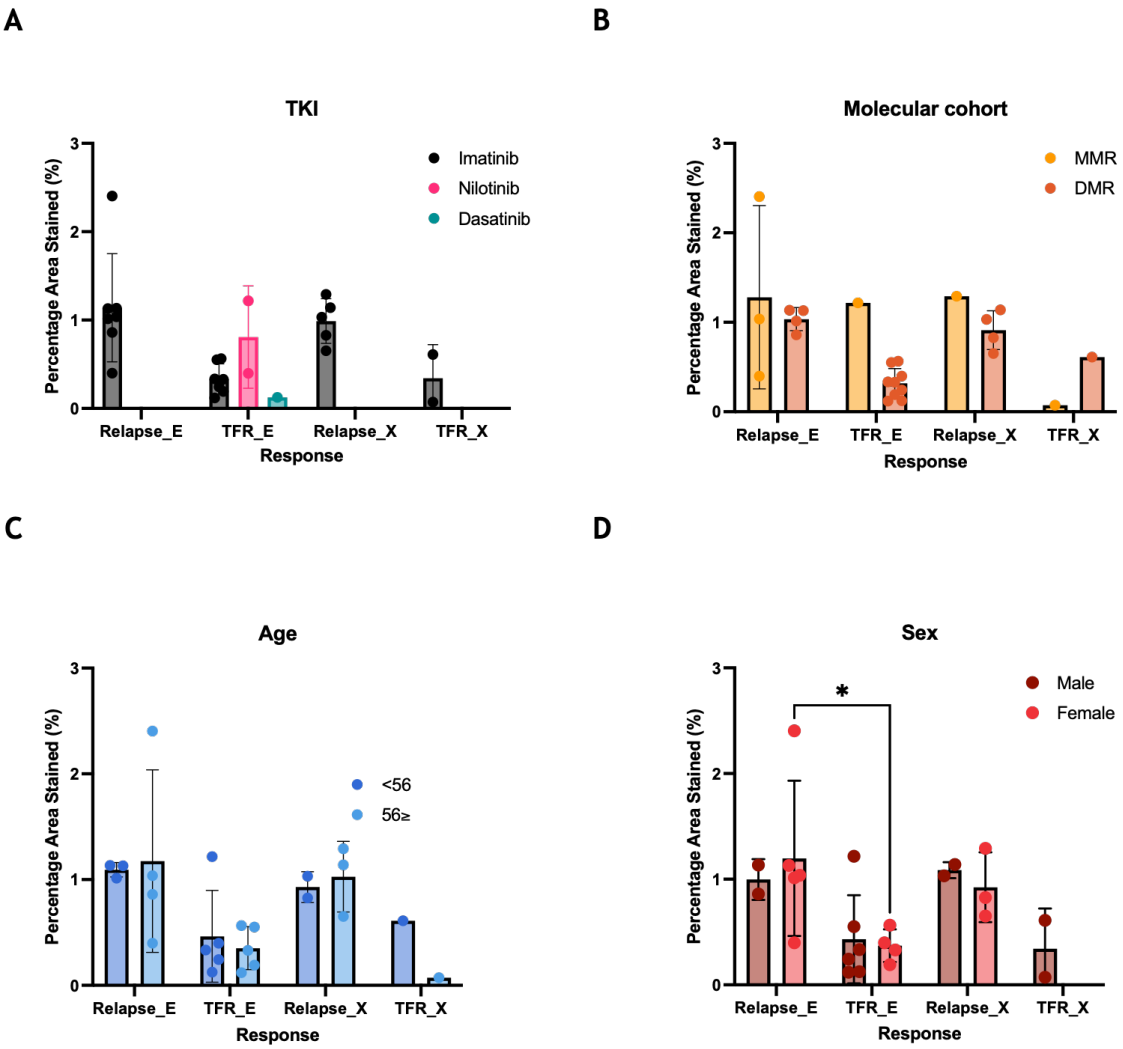

Figure 3-4 Changes to senescence levels in MSCs based on TKI, molecular cohort, age and sex **(A)** Changes to senescence levels comparing type of TKI used across all patient outcome groups. **(B)** Changes to senescence levels comparing molecular cohort across all patient outcome groups. MMR = major molecular response, DMR = deep molecular response. **(C)** Changes to senescence levels by age of patients in all patient outcome groups. **(D)** Changes to senescence levels by sex of patients in all patient outcome groups. All samples were tested at passage 2. Percentage area stained of ß-galactosidase staining from MSCs was analysed on EVOS microscope. Bars are represented as mean ± SD. Outcomes were compared to each other using Two-Way ANOVA using PRISM. P values: >0.05 (ns), <0.05 (*), <0.01 (**), <0.001 (***), <0.0001 (****). For all statistical tests including groups with samples less than 3 values, only comparisons that were statistically significant are shown.

3.4.4 MSC characterisation - MSCs have higher ROS levels at point of relapse and exit from the trial

After determining the senescence of the samples, the ROS levels were assessed for each outcome group to further characterize the MSCs and determine their overall health.

It was found that the ROS levels increased in patients' MSCs at time of relapse (Relapse_X) compared to relapse patients trial entry samples (Relapse_E)

(p=0.011) (Figure 3-5). An increase in ROS production was also found in patients MSCs at time of relapse (Relapse_X) with those who maintained TFR in samples taken at trial entry (TFR_E) (p=0.0212). It would have provided more context to the analysis if R_X and TFR_X could be compared, however due to the TFR_X being n=2, statistical analysis could not be done. Overall, the data suggest that there are increased levels of ROS in the MSCs of relapsing patients within the BMM.

The ROS levels within the MSCs also increased with each passage (Figure 3-5 A), this is consistent with previous research (Jeong and Cho 2015) and is expected as the cells also become more senescent as the passage number increases (Figure 3-3 C).

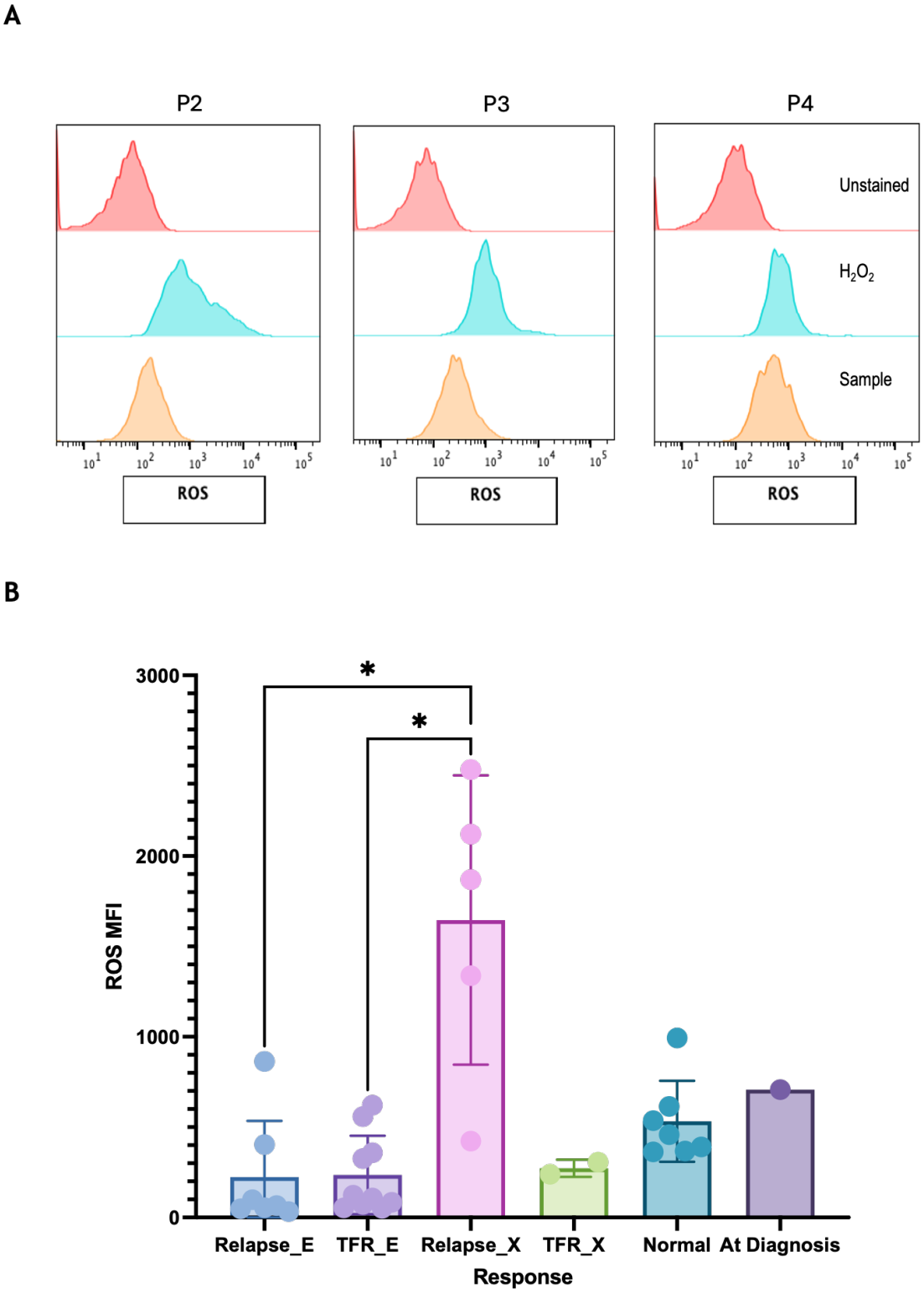

Figure 3-5 Changes of ROS levels in MSCs (A) Histograms representing ROS levels produced by positive control (H_2O_2) [in blue], unstained cells [in red], and sample tested [in orange]. Sample 141 over passages 2, 3 and 4. **(B)** Quantification of the mean fluorescence intensity (MFI) of ROS levels found in MSC from all patient outcome groups. Relapse at trial entry (R_E) (blue) (n=7), TFR at trial entry (TFR_E) (purple) (n=10), Relapse at trial exit (R_X) (pink) (n=5), TFR at trial exit (TFR_X) (green) (n=2), Normal (turquoise) (n=6), CML at diagnosis (dark purple) (n=1). All samples were tested at passage 2. Error bars show Mean with SD. One way ANOVA, Kruskal-Walis test was carried out on **(B)**. P values: >0.05 (ns), <0.05 (*), <0.01 (**), <0.001 (***), <0.0001 (****). For all statistical tests including groups with samples less than 3 values, only comparisons that were statistically significant are shown.

3.4.5 MSC characterisation – ROS secretion by MSCs is increased in DMR patients at point of relapse compared to relapse patients at start of trial

Older patients have been found to have increased ROS levels in MSCs (Stolzing et al. 2008). To determine if this and other factors were affecting the ROS production of the MSCs, correlation with the type of TKI, molecular cohort, age and sex of the patients was analysed.

For the analysis of TKI used there was a significant increase in ROS produced in patients taking imatinib when comparing R_E compared to R_X ($p=0.0004$). Additionally, patients who were in DMR at the start of the trial had a statistically significant increase in ROS production within R_E vs R_X ($p=<0.0001$), suggesting even in patients that were in deep remission there was an increase in ROS from MSCs at the point of relapse. The patients ≥56 years old had an increase of ROS production from MSCs within the comparison of R_E vs R_X ($p=0.0223$). For the analysis of sex, the female patients had an increase in ROS production in relapse patients at the point of trial entry compared to relapse patients at the point of relapse ($p=0.0004$). Overall, the data suggests sex, TKI use, molecular cohort and age all affect the ROS production of MSCs for patients who relapse.

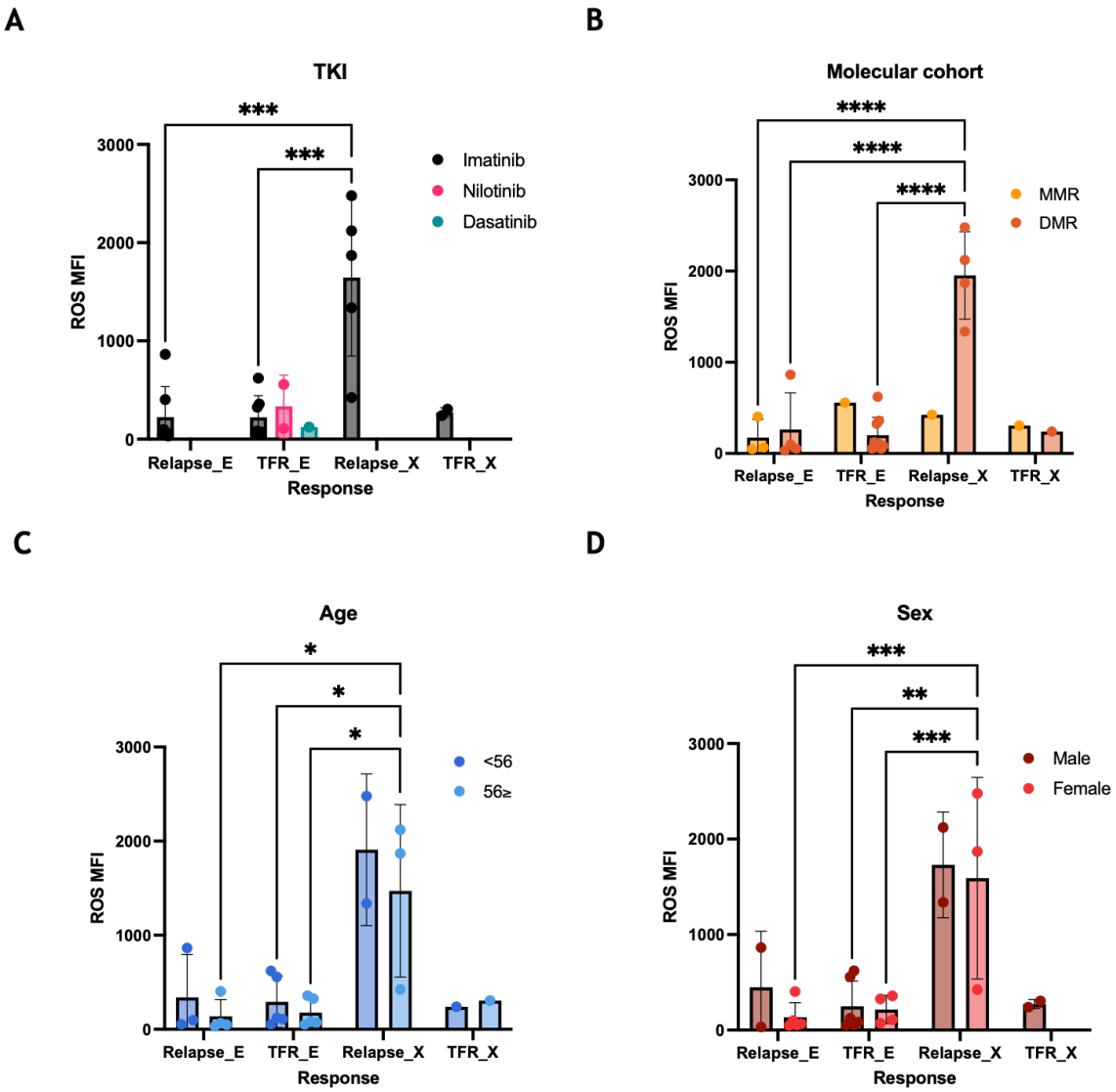

Figure 3-6 Changes of ROS levels in MSCs based on TKI, molecular cohort, age and sex (A) Changes to ROS levels comparing type of TKI used in all patient outcome groups using ROS MFI from MSCs analysed by flow cytometry. **(B)** Changes to ROS levels comparing molecular cohort used in all patient outcome groups using ROS MFI from MSCs analysed by flow cytometry. MMR = major molecular response, DMR = deep molecular response. **(C)** Changes to ROS levels comparing age of patients in all patient outcome groups using ROS MFI from MSCs analysed by flow cytometry. **(D)** Changes to ROS levels comparing sex of patients in all patient outcome groups using ROS MFI from MSCs analysed by flow cytometry. All samples were tested at passage 2. Bars are represented as mean with SD. Outcomes were compared to each other using Two-Way ANOVA using PRISM. P values: >0.05 (ns), <0.05 (*), <0.01 (**), <0.001 (***), <0.0001 (****). For all statistical tests including groups with samples less than 3 values, only comparisons that were statistically significant are shown.

3.4.6 MSC characterisation – MMP of MSCs is not changed across all outcomes groups

To evaluate the mitochondrial health the samples were tested with JC1 stain. In healthy cells JC1 forms aggregates which produce red/orange fluorescence. If the mitochondrial membrane potential decreases the JC1 becomes a monomer and produces green florescence. The ratio of green to red fluorescence is used

to evaluate mitochondrial health. Yellow is seen when green and red signals co-localize. Treatment with valinomycin can be used as a control as it causes a decrease to the MMP and therefore a decrease to the red/green ratio.

Although there was a slight increase in the MMP of MSCs from patients at point of relapse compared to all other patient outcomes these changes were not statistically significant.

A

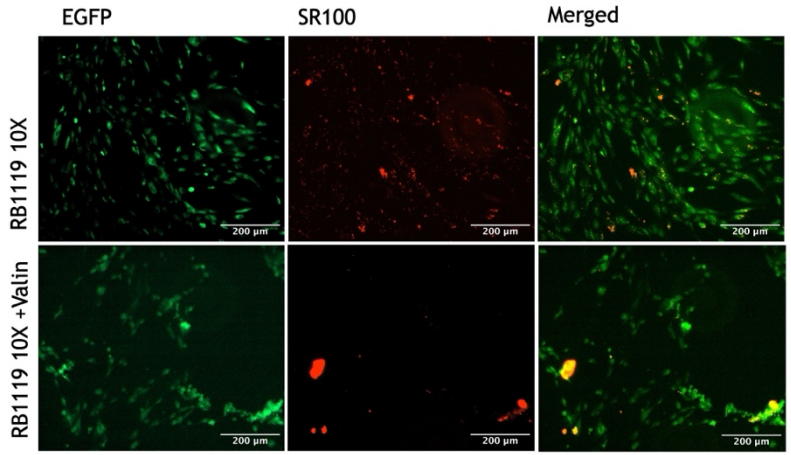
EGFP
SR100
Merged
RB1119 10X
RB1119 10X +Valin
200 µm

B

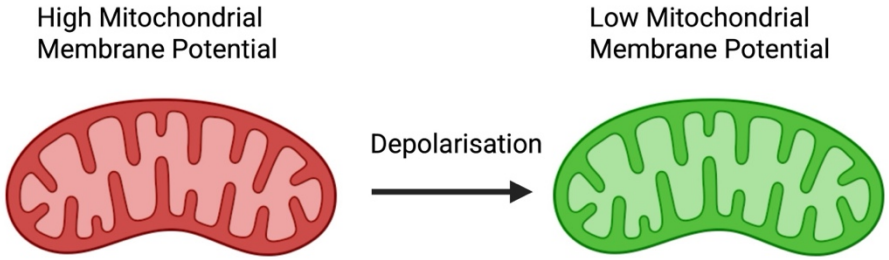
High Mitochondrial Membrane Potential
Depolarisation
Low Mitochondrial Membrane Potential

C

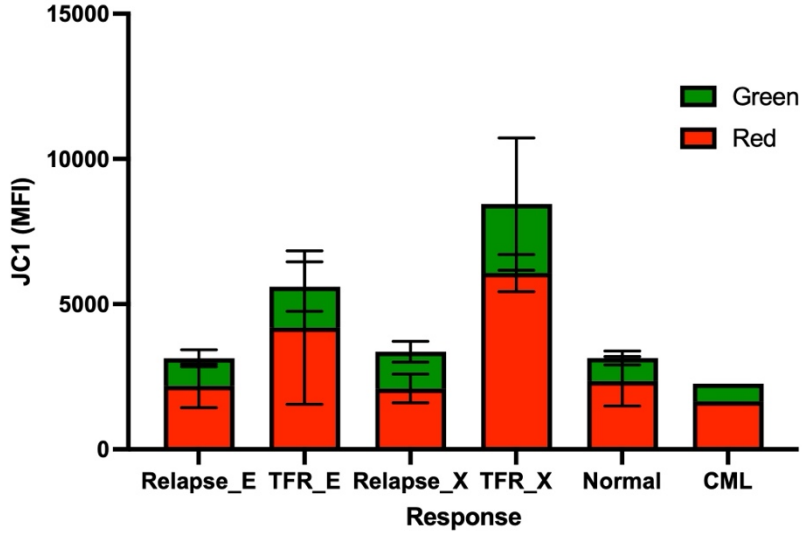
15000
10000
5000
0
JC1 (MFI)
Green
Red
Relapse_E
TFR_E
Relapse_X
TFR_X
Normal
CML
Response

D

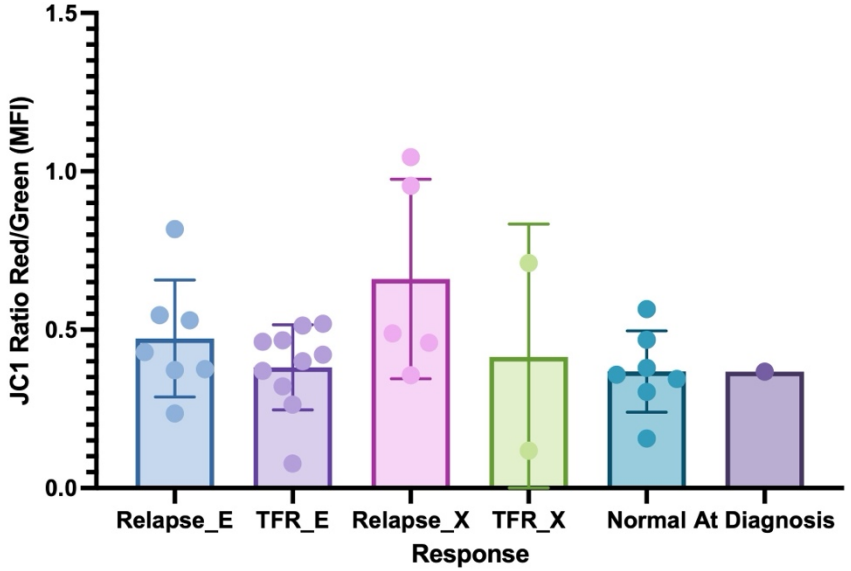
1.5
1.0
0.5
0.0
JC1 Ratio Red/Green (MFI)
Relapse_E
TFR_E
Relapse_X
TFR_X
Normal At Diagnosis
Response

Figure 3-7 Changes of MMP within MSCs (A) Normal BM MSC RB1119 with JC1 stain at 10X magnification with EGFP filter (for showing JC1 monomers which produces green fluorescence, this is a sign of low MMP), SR100 filter (for showing JC1 polymers which produce a red fluorescence and are a sign of high MMP) and the filters merged. Bottom row shows the same thing with the addition of Valinomycin as a positive control. Scale bar - 200 µm. **(B)** Schematic representation of JC1 within the mitochondria. This image readapted from an image taken from Dojindo.com (Yeasen - Lead. Innov. Mol. Enzym. Reag., n.d.). **(C)** Representative bar graphs of cells with green fluorescence (MFI) and red fluorescence (MFI). **(D)** Changes to MMP of all outcome groups using Red/Green ratio of MFI from MSCs analysed by flow cytometry. Relapse at trial entry (R_E) (blue) (n=7), TFR at trial entry (TFR_E) (purple) (n=10), Relapse at trial exit (R_X) (pink) (n=5), TFR at trial exit (TFR_X) (green) (n=2), Normal (turquoise) (n=6), CML at diagnosis (dark purple) (n=1). All samples were tested at passage 2. Error bars show Mean with SD. One way ANOVA, Kruskal-Wallis test was carried out on **(D)**. P values: >0.05 (ns), <0.05 (*), <0.01 (**), <0.001 (***), <0.0001 (****). For all statistical tests including groups with samples less than 3 values, only comparisons that were statistically significant are shown.

3.4.7MSC characterisation – MMP of MSCs is not affected by age, sex, TKI use or molecular cohort

It has previously been found that MMP is lower in aged MSCs (Barilani et al. 2022). The DESTINY trial recruited patients in MMR and MR4 and patients on three different TKIs (imatinib, nilotinib, and dasatinib). Currently not much is known about how molecular cohort and the use of different TKIs can affect MSCs. To understand this further and see if age, sex, TKI use and molecular cohort affected the MSCs the MMP was measured.

Interestingly the MMP in MSCs was not affected by age, sex, TKI use or molecular cohort, as there were no statistically significant changes between these factors within the outcome groups that were assessed (Figure 3-8).

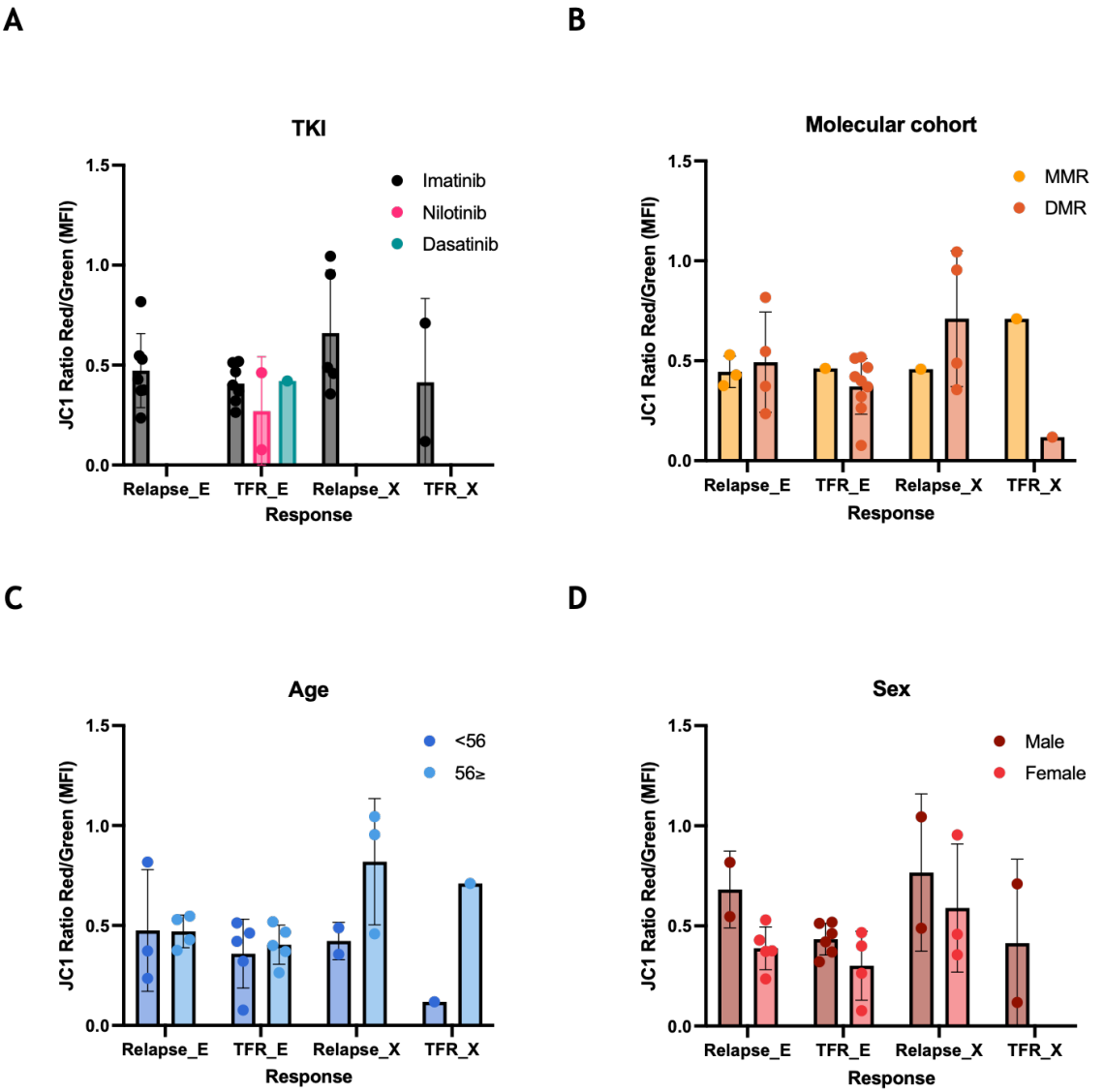

Figure 3-8 Changes to MMP levels in MSCs based on TKI, molecular cohort, age and sex (A) Changes to MMP comparing type of TKI used in all patient outcome groups using Red/Green ratio of MFI from MSCs analysed by flow cytometry. **(B)** Changes to MMP comparing molecular cohort in all patient outcome groups using Red/Green ratio of MFI from MSCs analysed by flow cytometry. MMR = major molecular response, DMR = deep molecular response. **(C)** Changes to MMP comparing age of patients in all outcome groups using Red/Green ratio of MFI from MSCs analysed by flow cytometry **(D)** Changes to MMP comparing sex of patients in all patient outcome groups using Red/Green ratio of MFI from MSCs analysed by flow cytometry. All samples were tested at passage 2. Bars are represented as mean with SD. Outcomes were compared to each other using Two-Way ANOVA using PRISM. P values: >0.05 (ns), <0.05 (*), <0.01 (**), <0.001 (***), <0.0001 (****). For all statistical tests including groups with samples less than 3 values, only comparisons that were statistically significant are shown.

3.4.8 Initial RNAseq analysis identified 10 DEGs in MSCs at relapse vs TFR at trial entry

RNA samples were sent away for bulk sequencing by Novogene (section 2.2.13) to determine the transcriptional changes between MSCs of TFR (TFR_E) (n=6) and relapse (R_E) (n=6) taken at entry into trial. The samples sent away were as follows:

Sample number	Outcome group	Pass/Fail quality control (QC)
9	Relapse (at trial entry)	Fail
23	Relapse (at trial entry)	Pass
44	Relapse (at trial entry)	Pass
60	Relapse (at trial entry)	Fail
62	Relapse (at trial entry)	Fail
141	Relapse (at trial entry)	Pass
10	TFR (at trial entry)	Pass
64	TFR (at trial entry)	Pass
84	TFR (at trial entry)	Fail
115	TFR (at trial entry)	Pass
118	TFR (at trial entry)	Fail
166	TFR (at trial entry)	Fail

Table 3-2 List of samples used in first RNAseq analysis at Novogene Table of their outcome group and if they passed/failed QC and therefore were used in analysis.

After data was aligned, the samples analysed were 3 TFR_E and 4 R_E samples. The samples that were not analysed failed QC and did not produce data when samples when aligned to the reference genome.

A principal component analysis (PCA) plot was used to visualise the similarities/differences between the samples and their outcome groups. Within a PCA plot samples (each point) that group close together have similar overall gene expression while the further apart samples are the more they differ (Dawadi et al. 2025). Based on these samples the PCA graph did not show clustering of the TFR and relapse outcome groups. From the relapse samples, sample 23, 62 and 44 appeared to produce a small cluster while sample 141 was further removed from these samples. Additionally, within the TFR samples there was no clustering as sample 10, 64 and 115 were all positioned far away from each other. There does not appear to be grouping between the TFR and relapse samples suggesting the samples being tested could not be separated by outcome group. The lack of clustering was unsurprising as samples being compared were from patients at start point of the trial, before patients stopped treatment and when they were all reacting well to treatment; any changes seen between the two outcome groups at the mRNA level are therefore presumed to be subtle. The lack of separation between the two groups indicates similarity between the conditions.

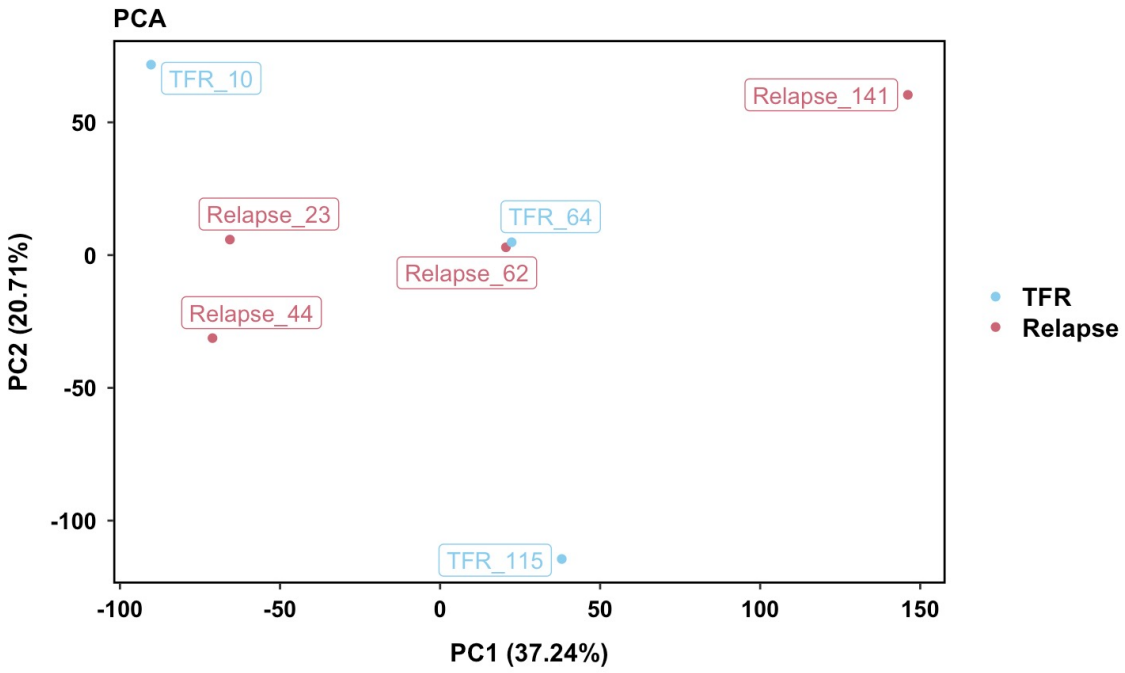

Figure 3-9 Clustering of relapse vs TFR samples from RNAseq PCA plot showing gene expression data between relapse (R_E) (n=4) (red) and TFR (TFR_E) (n=3) (blue). Showing PC1 (37.24%) vs PC2 (20.71%). Each sample is identified as an individual dot.

For the samples that passed QC and were able to be aligned, a cutoff of p.adj<0.1 and $\log_2$ fold>0.5 was used to determine the DEGs. This identified a total of 11 DEGs which are shown on the volcano plot (Figure 3-10). There were 8 upregulated DEGs: *FMO3*, *ZIC1*, *CXCL12*, *HAPLN1*, *2966*, *LINC01583*, *CPXM2*, and *ZIC4* and 3 downregulated: *HLA-B*, *FRG1* and *DHX16*.

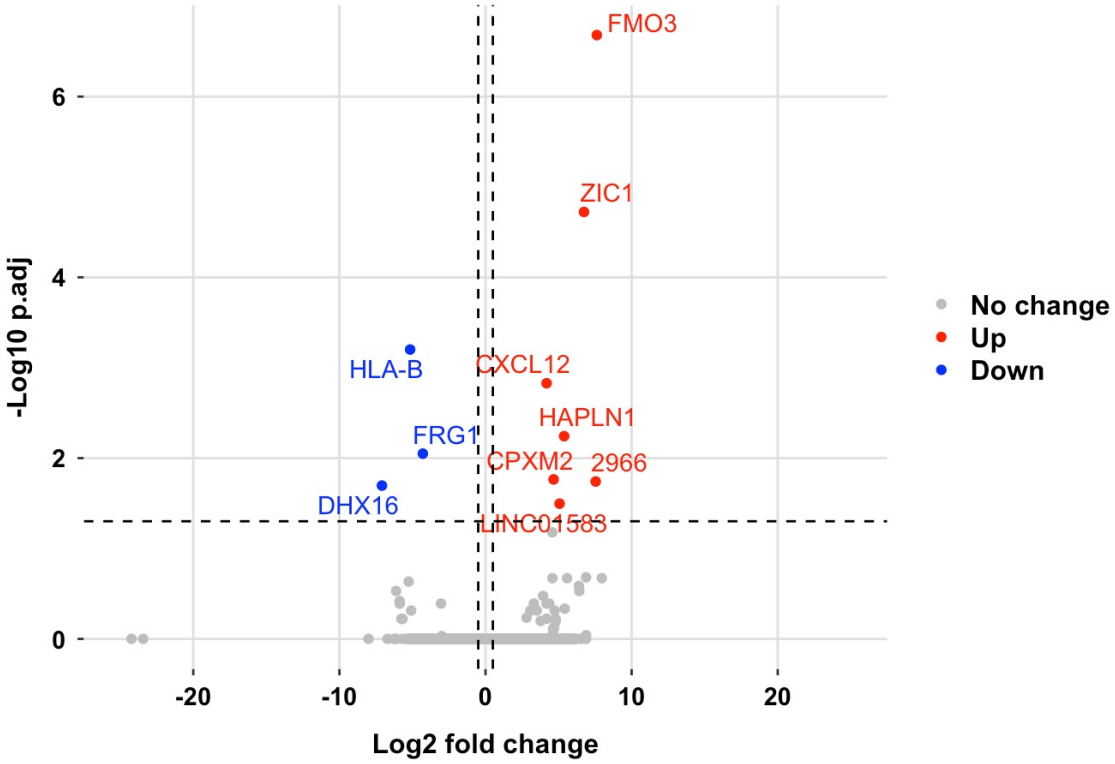

Figure 3-10 DEGs of BM MSCs comparison of relapse vs TFR Volcano plot of comparison of relapse (R_E) (n=4) vs TFR (TFR_E) (n=3) at trial entry. DEGs were established at p.adj<0.1 and log_2 fold>0.5. These are shown as upregulated (red), downregulated (blue) and no change (grey).

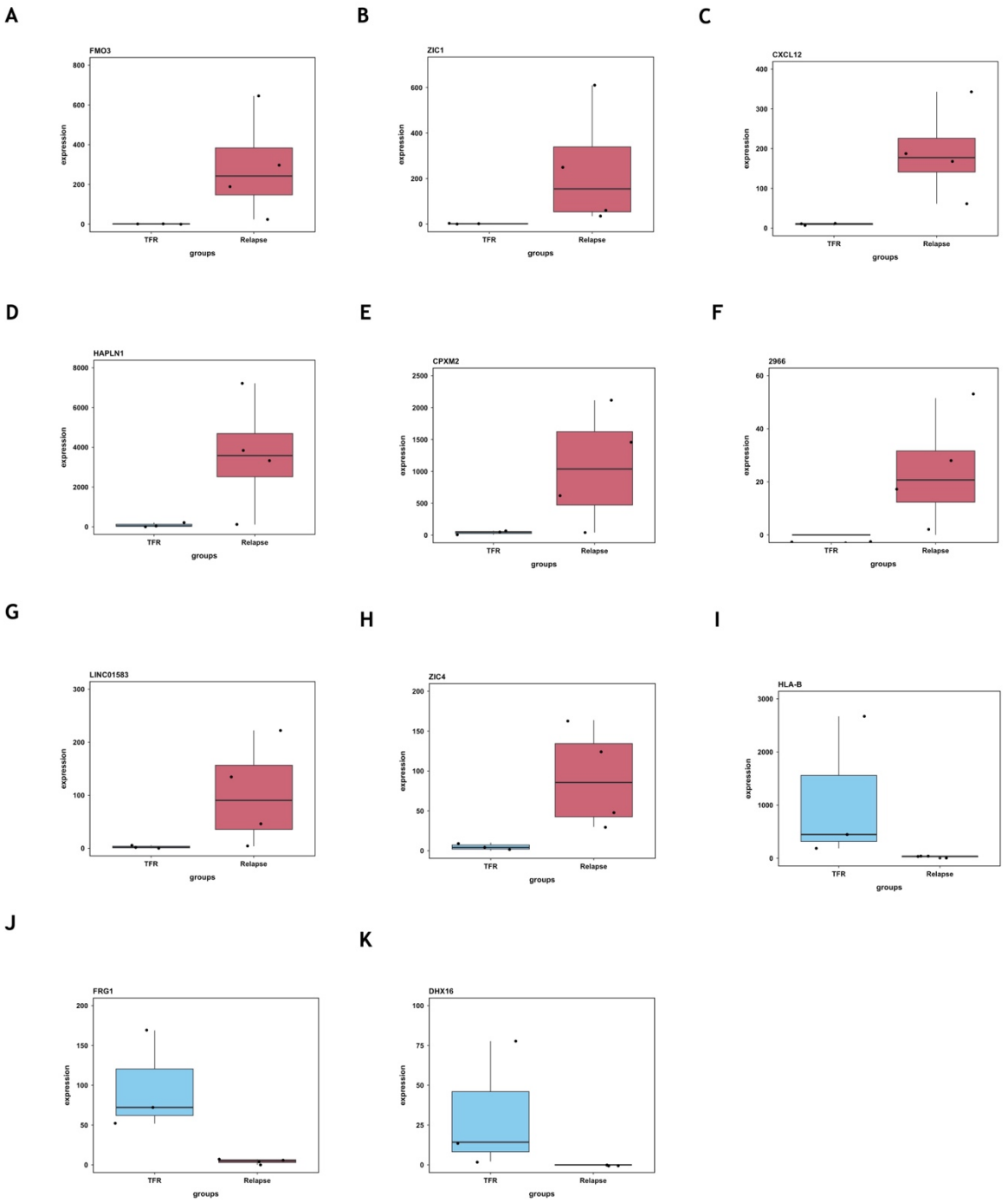

Figure 3-11 The 11 DEGs of BM MSCs (A-G) Upregulated DEGs. **(H-J)** Downregulated DEGs. Each graph shows one of the 10 DEGs identified in relapse vs TFR comparison by p-value and $\log_2$ fold change. The dots represent one sample. **(A)** Boxplot of *FMO3* gene; **(B)** Boxplot of *ZIC1* gene; **(C)** Boxplot of *CXCL12* gene; **(D)** Boxplot of *HAPLN1* gene; **(E)** Boxplot of *CPXM2* gene; **(F)** Boxplot of *2966* gene; **(G)** Boxplot of *LINC01583* gene; **(H)** Boxplot of ZIC4 **(I)** Boxplot of *HLA-B* gene; **(J)** Boxplot of *FRG1* gene; **(K)** Boxplot of *DHX16* gene.

Gene	Function	Change	Log_2 fold	Adjusted p value
FMO3	Hepatic enzyme	Upregulated	7.62	2.1e-07
ZIC1	Transcriptional activator	Upregulated	6.74	1.9e-05
CXCL12	Chemoattractant	Upregulated	4.18	1.5e-03
HAPLN1	Stabilises proteoglycan monomers	Upregulated	5.38	5.7e-03
CPXM2	In peptidase M14 family	Upregulated	4.66	1.7e-02
2966 (GTF2H2)	Component of the general transcription and DNA repair factor IIH (TFIIH) core complex	Upregulated	7.54	1.8e-02
LINC01583	-	Upregulated	5.07	3.2e-02
ZIC4	Paralog of ZIC1	Upregulated	4.57	6.6e-02
HLA-B	Antigen-presenting major histocompatibility complex class I (MHCI) molecule	Downregulated	-5.16	6.3e-04
FRG1	Binds to mRNA	Downregulated	-4.29	8.9e-03
DHX16	Pre-mRNA splicing factor	Downregulated	-7.09	2.0e-02

Table 3-3 DEGs from first RNAseq comparing relapse (R_E) vs TFR (TFR_E) at trial entry Table shows the function of the genes, the change within the comparison, the log_2 fold change and adjusted p value.

The gene expression of the 11 DEPs within the 7 samples was normalised in RStudio to get the z-score. The z-score scales the expression values based on their distance to the mean (Dawadi et al. 2025). This normalises the expression of the genes and makes it easier for the changes of the genes to be compared throughout the data. The data on the heatmap was then clustered by row for the difference to be seen within the samples and how the DEGs differ in expression.

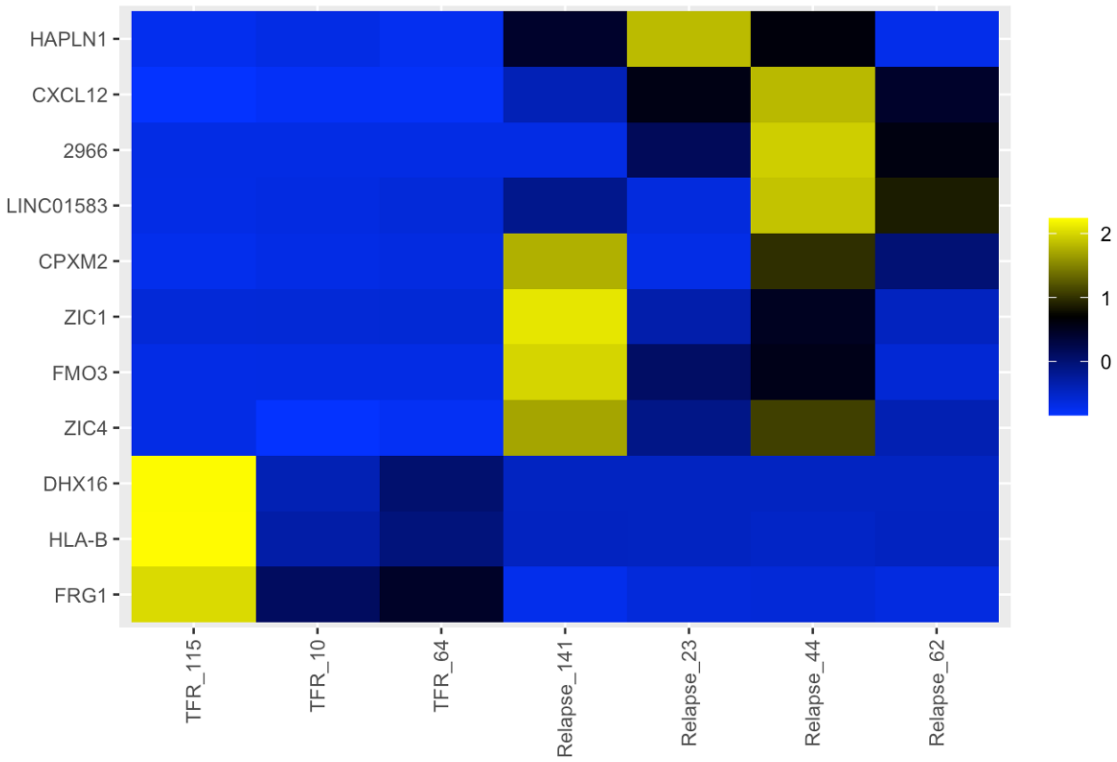

Figure 3-12 Expression level of 11 DEGs identified comparing relapse to TFR Heatmap showing the 11 DEGs found in the R_E (n=4) vs TFR_E (n=3) comparison. Samples are shown on the x axis, and genes are on the y axis. The scale at the side shows the colour intensity based on the expression level, yellow is the highest expression and blue is the lowest. The expression levels have been normalised into z-scores. The heatmap has clustering of the genes within these samples. DEGs were identified at p.adj<0.05 and $\log_2$ fold>0.5.

3.4.9 Second round of RNAseq analysis identified 10 DEGs in MSCs at relapse vs TFR at trial entry

Due to the first RNAseq having several samples that failed, samples were sent away again to gain a more robust dataset. From the first experiment, RNAseq was carried out at Novogene, and the library prep was done in the lab. To avoid QC failure, for the second experiment RNA was sent to University of Glasgow – Shared Research Facilities (section 2.2.13) and library prep was completed by them. Samples sent away were:

Sample number	Outcome group	Pass/Fail QC
9	Relapse (at trial entry)	Pass
60	Relapse (at trial entry)	Pass
141	Relapse (at trial entry)	Pass
78	Relapse (at trial entry)	Pass
44	Relapse (at trial entry)	Pass
28	Relapse (at point of relapse)	Pass
49	Relapse (at point of relapse)	Pass
3	Relapse (at point of relapse)	Pass
23	Relapse (at point of relapse)	Pass
62	Relapse (at point of relapse)	Pass
116	TFR (at trial entry)	Pass
10	TFR (at trial entry)	Pass
84	TFR (at trial entry)	Pass
20	TFR (at trial entry)	Pass
118	TFR (at trial entry)	Pass

Table 3-4 List of samples used in second RNAseq analysis at University of Glasgow – Shared Research Facilities Table of their outcome group and if they passed/failed QC and therefore were used in analysis.

Due to sample availability not all samples selected for the first RNAseq were able to be used for the second RNAseq experiment. Therefore, it is expected the two datasets might produce varying results.

Additionally, relapse samples at the point of relapse (R_X) were also sent away for analysis for the second RNAseq.

From the second round all samples passed QC and were successfully aligned to the reference genome. The comparison of relapse (R_E) (n=5) vs TFR (TFR_E) (n=5) at entry into trial was first compared. The PCA plot for this also did not identify clustering between the samples of the two outcome groups being measured. Relapse samples 9 and 60 and 44 and 78 were closely associated, while sample 141 is not close to these samples. For TFR samples, sample 116 and 20 and 84 and 10 were closely associated while sample 118 did not show associating within these samples. While there was clustering between certain samples, there was no clustering that separated out TFR and relapse.

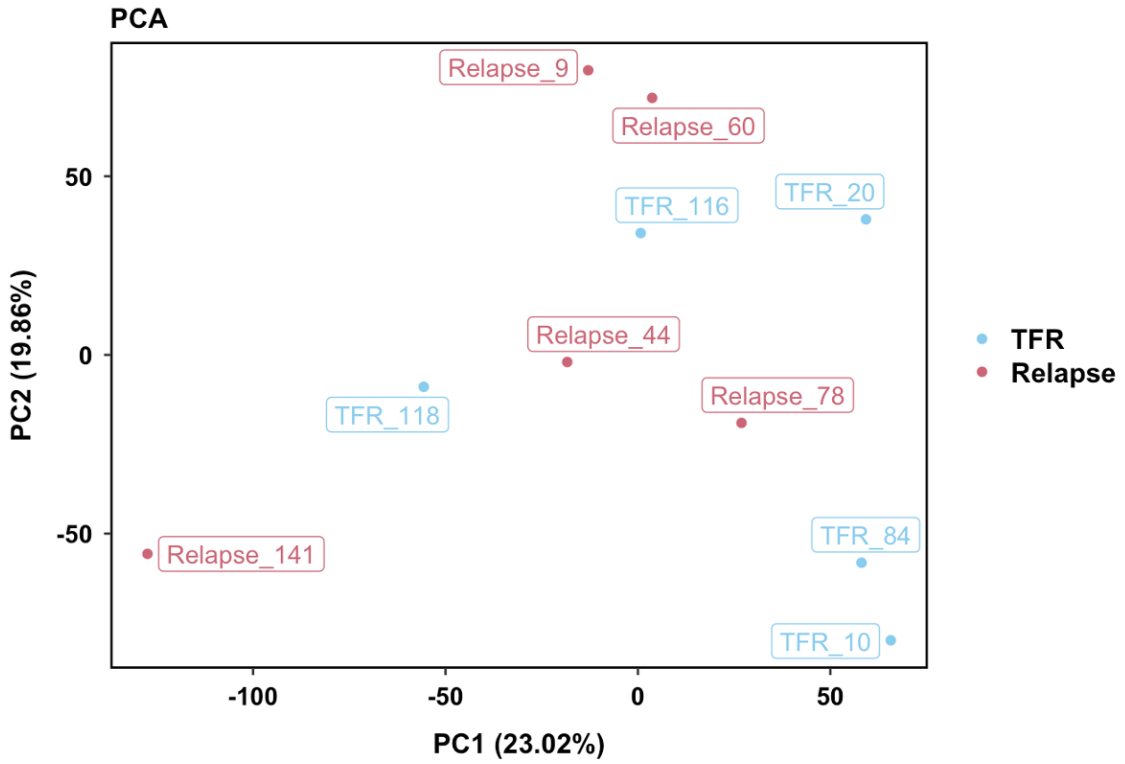

Figure 3-13 Clustering of relapse vs TFR from RNAseq PCA plot showing gene expression data between relapse (R_E) (n=5) (red) and TFR (TFR_E) (n=5) (blue). Showing PC1 (23.02%) vs PC2 (19.86%). Each sample is identified as an individual dot.

The second round of RNAseq with the samples produced different DEGs compared to the first. Both experiments provide valid information even though the number of usable samples was lower in the first RNAseq experiment. The differences seen could be due to a range of things most importantly and perhaps significantly, the samples used in each run are different (Table 3-2 and Table 3-4). Additionally, the first batch the library prep was done in-house while for the second batch, the library prep was done as part of the service, these are all factors that could cause variability. The second batch RNAseq was also carried out in a different service facility, which could affect how the samples ran and the results that were gained. All these factors were considered when the sequencing was analysed and as both batches use samples that passed QC the data from both runs are valid in their own right.

The changes to bone marrow supportive stroma were evaluated by the second RNAseq run on BM MSC samples from R_E vs TFR_E patients. There was a total of 10 DEGs identified (threshold was set to p.adj<0.1 and $\log_2$ fold>0.5). There were 9 upregulated DEGs: *TMEM200A, SSC5D, LNPK, CDC42BPA, PTK7, LIMS1,*

TOX2, *POU3F3*, and *DLG1* and 1 downregulated DEG: *CDC25B*. The distribution of values within the log_2 fold change for this round of samples was much narrower and more consistent, this suggests much less variability between the samples within this batch of RNAseq and potentially higher quality data.

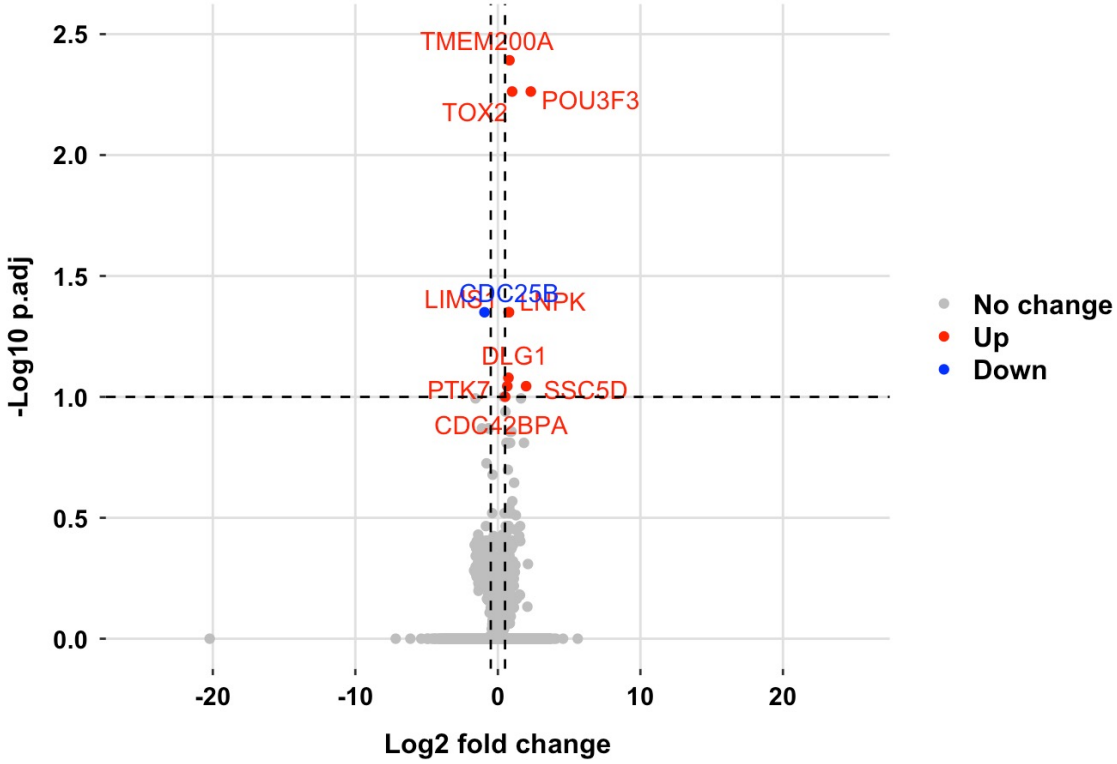

Figure 3-14 DEGs of BM MSCs comparison of relapse vs TFR Volcano plot of comparison of relapse (R_E) (n=5) vs TFR (TFR_E) (n=5) at trial entry. DEGs were established as p.adj < 0.1 and log_2 fold > 0.5. These are shown as upregulated (red), downregulated (blue) and no change (grey).

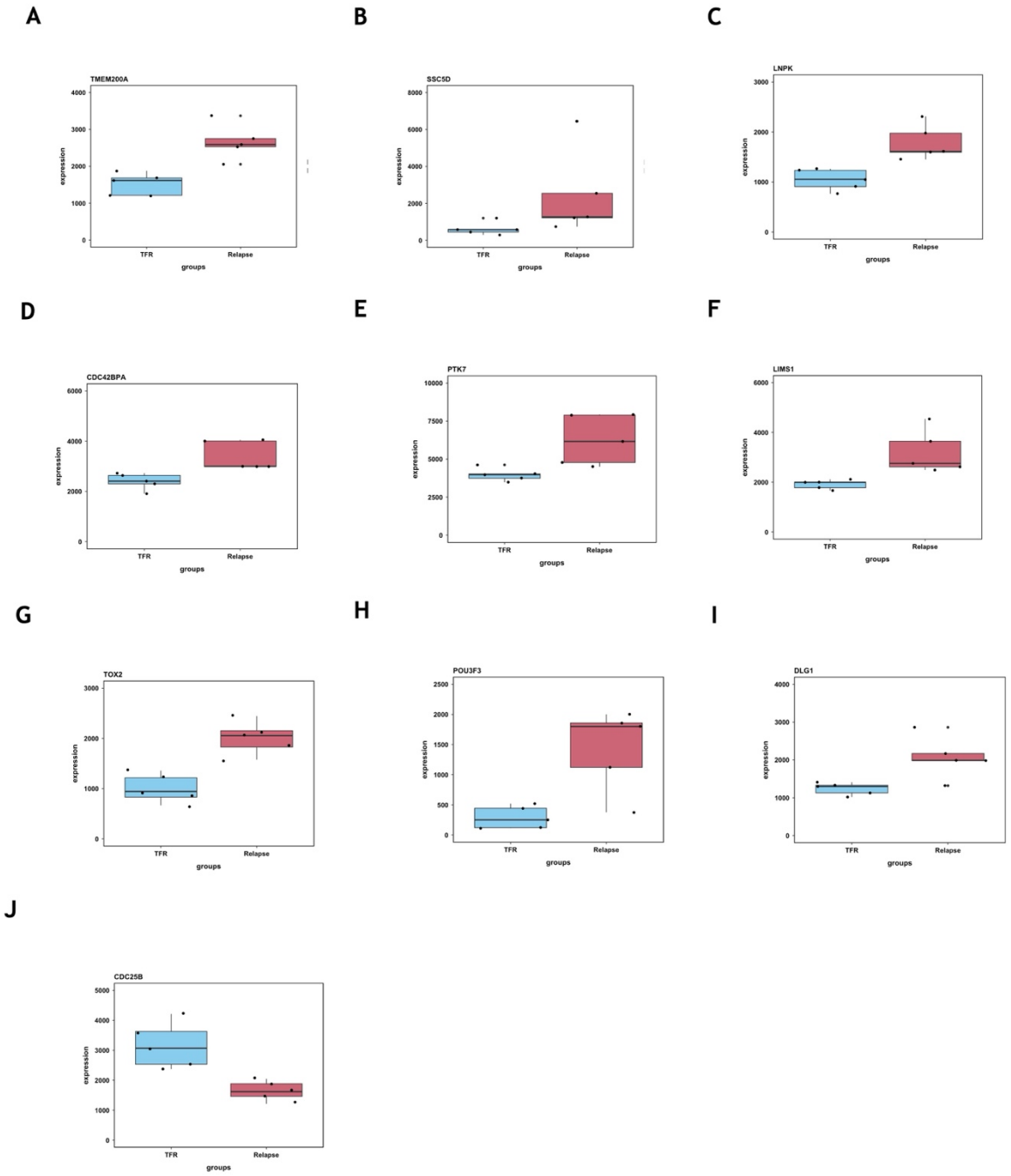

Figure 3-15 10 DEGs identified in MSCs of R_E vs TFR_E (A-I) Upregulated DEGs **(J)** Downregulated DEG. Each graph shows one of the 10 DEGs identified in relapse vs TFR comparison by p.adj < 0.1 and $\log_2$ fold > 0.5. The dots represent one sample. **(A)** Boxplot of *TMEM200A* gene; **(B)** Boxplot of *SSC5D* gene; **(C)** Boxplot of *LNPK* gene; **(D)** Boxplot *CDC42BPA* gene; **(E)** Boxplot of *PTK7* gene; **(F)** Boxplot of *LIMS1* gene; **(G)** Boxplot of *TOX2* gene; **(H)** Boxplot of *POU3F3* gene; **(I)** Boxplot of *DLG1* gene; **(J)** Boxplot of *CDC25B* gene.

Gene	Function	Change	Log_2fold	Adjusted p value
SSC5D	Soluble scavenger receptor	Upregulated	1.98	0.090308896
LNPK	Endoplasmic reticulum (ER)-shaping membrane protein	Upregulated	0.78	0.044674784
TMEM200A	Transmembrane protein	Upregulated	0.81	0.004055400
PTK7	Inactive tyrosine kinase involved in Wnt signalling pathway	Upregulated	0.66	0.090308896
LIMS1	Adapter protein in a cytoplasmic complex	Upregulated	0.75	0.044674784
TOX2	Putative transcriptional activator	Upregulated	1.00	0.005461428
POU3F3	Transcription factor	Upregulated	2.31	0.005461428
DLG1	Essential multidomain scaffolding protein	Upregulated	0.74	0.083382587
CDC42BPA	Serine/threonine protein kinase	Upregulated	0.51	0.099884726
CDC25B	Tyrosine protein phosphatase	Downregulated	-0.94	0.044674784

Table 3-5 DEGs from second RNAseq comparing relapse (R_E) vs TFR (TFR_E) at trial entry
Table shows the function of the genes, the change within the comparison, the log_2 fold change and adjusted p value.

The gene expression of the 10 DEGs was normalised to get the z-score using RStudio. The data on the heatmap was then clustered by row and the difference can be seen within the samples and how they differ in expression of the DEGs. The heatmap shows upregulation of *CDC25B* within the TFR samples at the bottom left corner of the plot. While the rest of the genes show upregulation with clustering from the relapse samples.

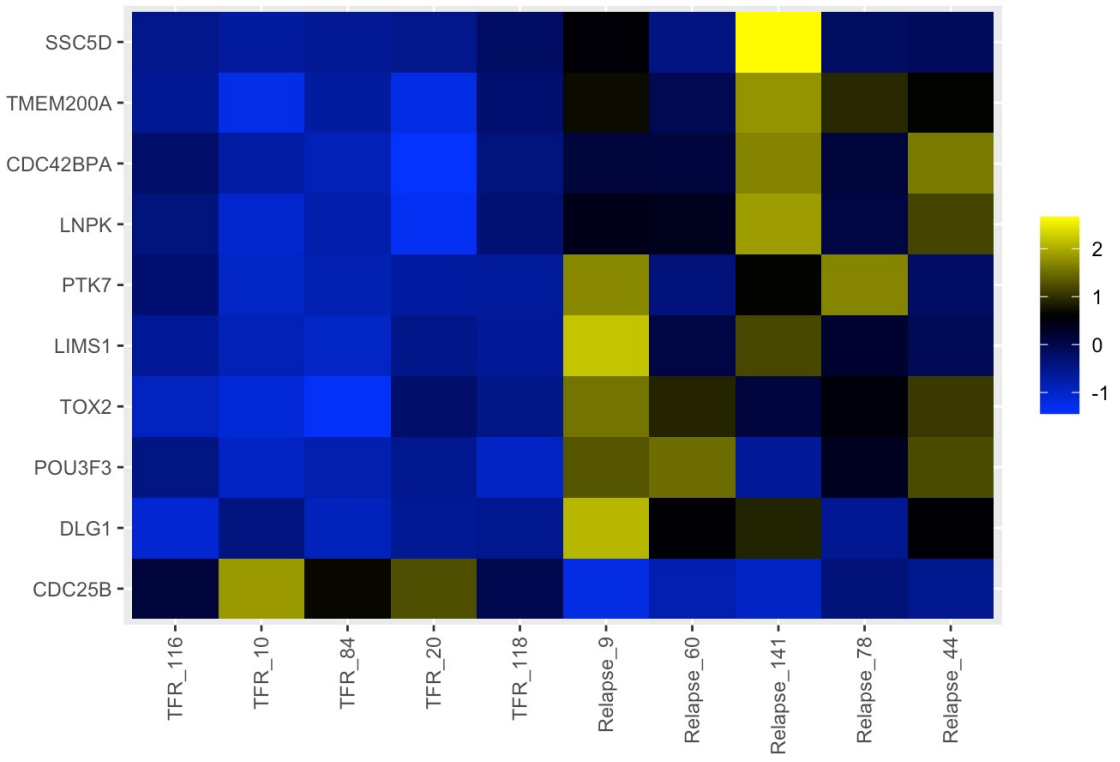

Figure 3-16 Expression level of 10 DEGs identified comparing relapse to TFR Heatmap showing 10 DEGs found in the relapse (R_E) (n=5) vs TFR (TFR_E) (n=5) comparison. Samples are shown on the x axis, and genes are on the y axis. The scale at the side shows the colour intensity based on the expression level, yellow is the highest expression and blue is the lowest. The expression levels have been normalised into z-scores. The heatmap has clustering of the genes within these samples. DEGs were identified at p.adj < 0.1 and $\log_2$ fold > 0.5.

3.4.10 Second RNAseq analysis identified 5 DEGs in MSCs from relapse patients at point of relapse vs at trial entry

With the second run of RNAseq 5 samples of MSCs from relapse group at point of relapse were analysed (Table 3-4). This was to examine the change between patients who relapsed and how they differed from the start of the trial compared to when they relapsed; the information could be used to further elucidate what happens in patients to cause the relapse.

To do this, a comparison between relapse at point of relapse (R_X) (n=5) and relapse from entry into trial (R_E) (n=5) was assessed. The PCA plot for this also did not identify clustering between the two outcome groups. The samples at point of relapse (R_X) had sample 49, 23 and 62 in a small cluster together, while sample 3 and 28 were further apart and not in any visible cluster.

Additionally, the samples from R_E were spread far apart with no clear clustering between the groups.

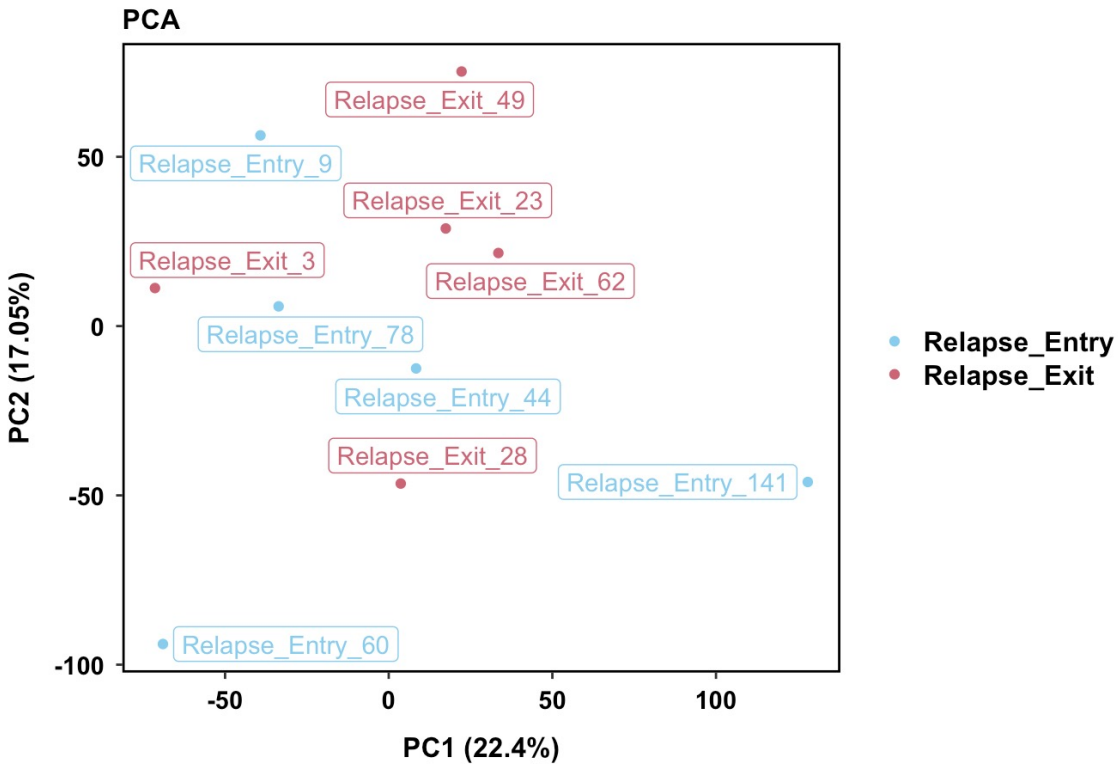

Figure 3-17 Clustering of Relapse_Exit vs Relapse_Entry from RNAseq PCA plot showing gene expression data between relapse at exit (R_X) (n=5) (red) and relapse at trial entry (R_E) (n=5) (blue). Showing PC1 (22.4%) vs PC2 (17.05%). Each sample is identified as an individual dot.

From the comparison of samples from R_X vs R_E, a total of 5 DEGs (Figure 1-18) were identified (threshold was set to p.adj<0.1 and $\log_2$ fold>0.5). All DEGs were upregulated: *APCDD1*, *AQP1*, *MOK*, *CYP27C1* and *AMZ1*.

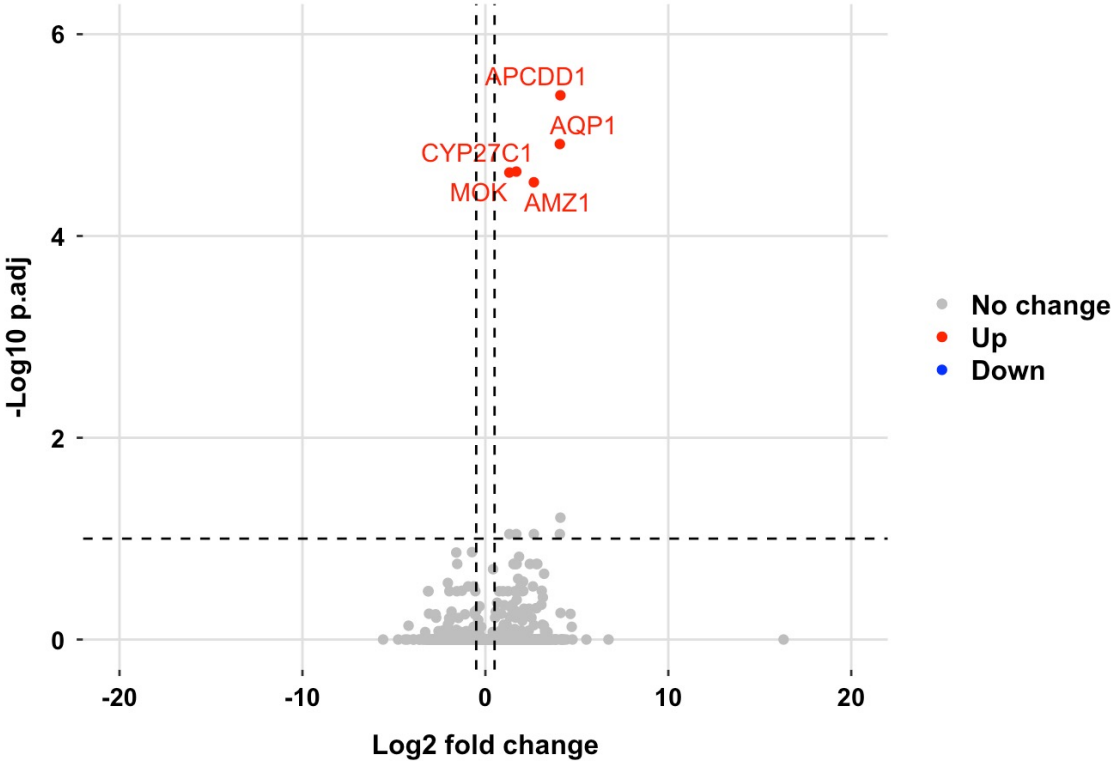

Figure 3-18 DEGs of BM MSCs comparison of Relapse_Exit vs Relapse_Entry Volcano plot of comparison of relapse patients at point of relapse (R_X) (n=5) vs samples taken from patients at entry into trial who later went on to relapse (R_E) (n=5). DEGs were established at p.adj < 0.1 and $\log_2$ fold > 0.5. These are shown as upregulated (red) and downregulated (blue).

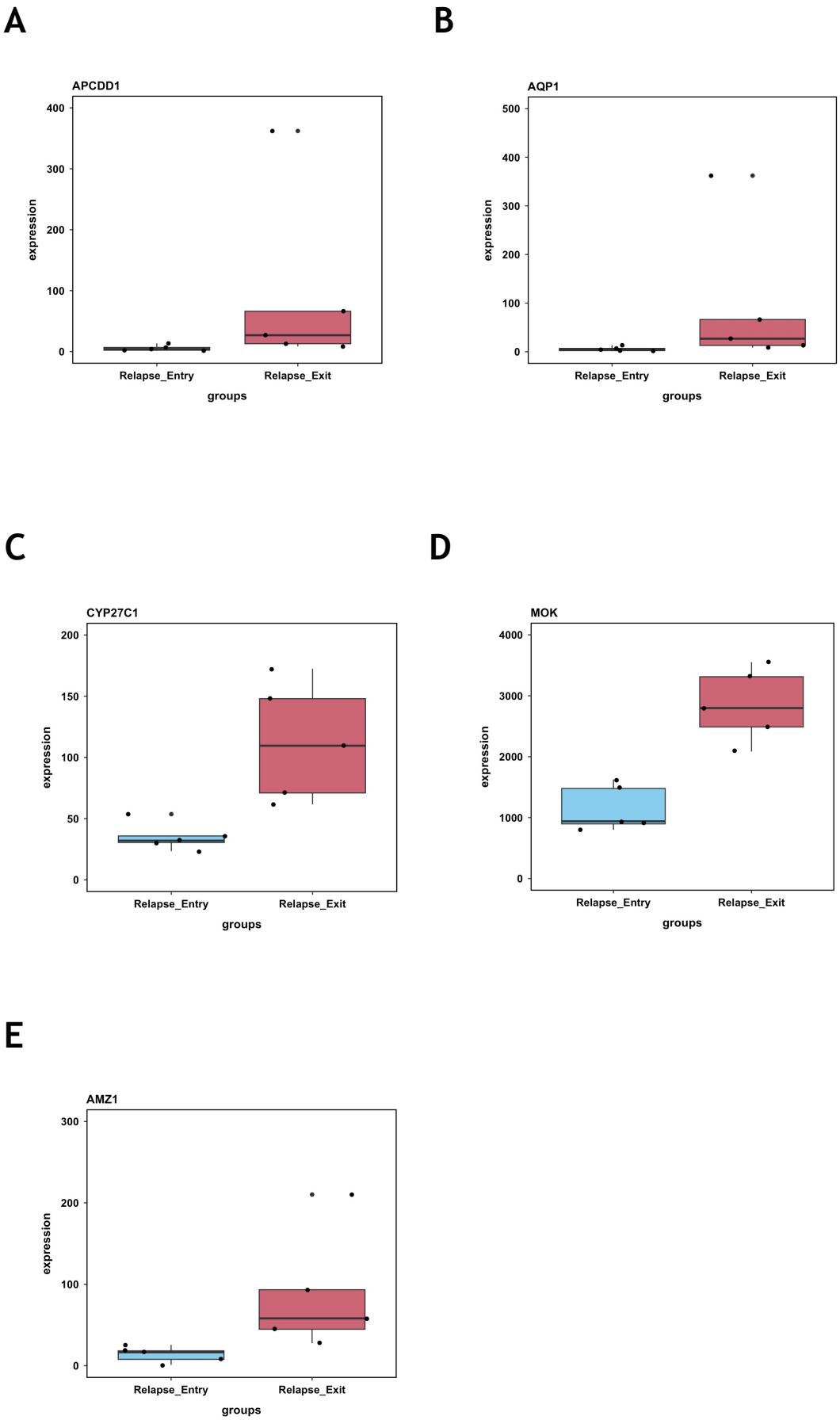

Figure 3-19 The 5 DEGs of BM MSCs (A-E) Upregulated DEGs. Each graph shows one of the 5 DEGs identified in R_X vs R_E comparison by p-value and $\log_2$ fold change. The dots represent one sample. **(A)** Boxplot of *APCDD1* gene; **(B)** Boxplot of *AQP1* gene; **(C)** Boxplot *CYP27C1* of gene; **(D)** Boxplot *MOK* gene; **(E)** Boxplot of *AMZ1* gene.

Gene	Function	Change	Log_2 fold	Adjusted p value
APCDD1	Negative regulator of the Wnt signalling pathway	Upregulated	4.10	0.06195816
AQP1	Forms a water-specific channel	Upregulated	4.07	0.09010276
CYP27C1	Catalyses the conversion of all-trans retinol	Upregulated	1.69	0.09010276
MOK	Able to phosphorylate several exogenous substrates and to undergo autophosphorylation	Upregulated	1.31	0.09010276
AMZ1	Exhibits aminopeptidase activity	Upregulated	2.65	0.09010276

Table 3-6 DEGs from second RNAseq comapring relapse at point of relapse (R_X) vs relapse at trial entry (R_E). Table shows the function of the genes, the change within the comparison, the log_2 fold change and adjusted p value.

The gene expression of the 5 DEGs was normalised to get the z-score using RStudio. The data on the heatmap was then clustered by row and the difference can be seen within the samples and how they differ in expression of the genes of interest. There is a clear increase in the DEGs from the relapse samples at exit from trial (R_X) as identified within the volcano plot.

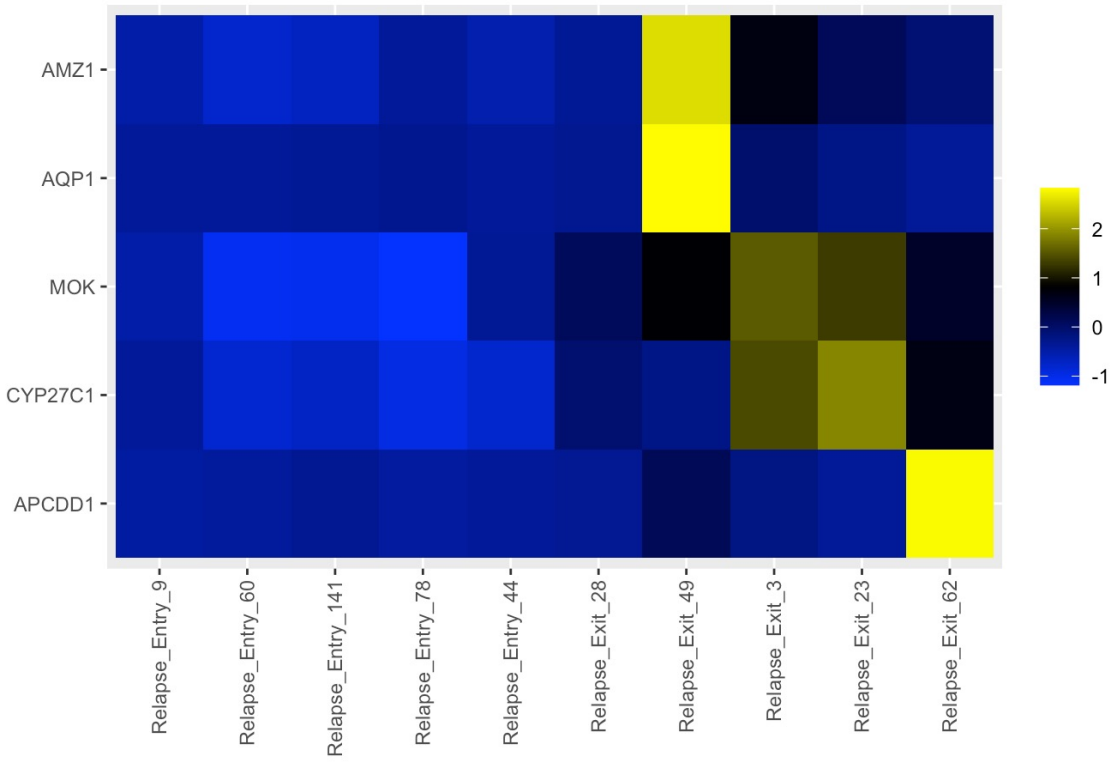

Figure 3-20 Expression level of 5 DEGs identified comparing relapse at point of relapse to relapse at trial entry Heatmap showing the 5 DEGs found in the relapse at point of relapse (R_X) (n=5) vs relapse at entry into trial (R_E) (n=5) comparison. Samples are shown on the x axis, and genes are on the y axis. The scale at the side shows the colour intensity based on the expression level, yellow is the highest expression and blue is the lowest. The expression levels have been normalised into z-scores. The heatmap has clustering of the genes within these samples. DEGS were identified at p.adj < 0.1 and $\log_2$ fold > 0.5.

For all RNAseq data GSEA was attempted to produce pathway analysis and highlight pathways of interest within the data. However, for all data this did not produce any pathways.

Once these DEGs had been identified within the comparison of the BM MSCs after RNAseq, the genes were looked at in a bigger patient cohort for validation.

3.4.11 Validation of RNAseq data by chip based real-time PCR (Fluidigm™)

To validate the DEGs identified within the RNAseq data as well as correlating genes, a 48x48 Fluidigm Biomark™ chip was used. For the validation the same samples used within both RNAseq experiments were used as well as additional

samples. The chip is able to hold 48 samples therefore a large cohort of patients samples was able to be tested for validation.

For the selection of genes to be analysed by Fluidigm, all the DEGs identified from the RNAseq data were put into the STRING database to identify protein-protein interactions and how the genes interact with each other. However, there were no interactions found within the gene list (Table 3-3, Table 3-5, Table 3-6). The Fluidigm chip used was 48x48, this means 48 genes can be tested against 48 samples. For the samples there is usually 6 housekeeping genes, this leaves 42 genes to be tested, for the Fluidigm there was 26 genes from the first and second RNAseq analysis, which left 18 genes to be selected. While no correlations were found using STRING, the software gives options of related genes and their functions underneath the genes listed. These were the genes used to make up the 42 genes and provides an additional investigation into related genes alongside the validation (Table 2-11).

There were 12 TFR_E and 9 R_E samples that were used within the Fluidigm chip, including some duplicates to fill spaces. Despite the concentration and the quality of the RNA used in the chip being optimal, data from only 8 TFR and 4 relapse were usable for the analysis of relapse vs TFR. The first comparison analysed was relapse (R_E) vs TFR (TFR_E) at trial entry, these samples were normalised to the normal BM MSC samples and comparison of these two patient cohorts to identify statistically significant genes was carried out on PRISM. The significantly changed genes that were identified within the RNAseq data that were validated by Fluidigm were *AQP1, AMZ1, CXCL12* (Figure 3-7). Genes that were not identified in RNAseq data but were found to be significant in the Fluidigm data were *EPB41, GRK6,* and *RGS1*. All genes identified were upregulated within this comparison.

Gene	Comparison	Q value
AMZ1	Relapse - TFR (normalised to normal)	0.0046
AQP1	Relapse - TFR (normalised to normal)	0.0014
CXCL12	Relapse - TFR (normalised to normal)	0.002
EPB41	Relapse - TFR (normalised to normal)	0.032
GRK6	Relapse - TFR (normalised to normal)	0.0001
RGS1	Relapse - TFR (normalised to normal)	0.0003

Table 3-7 Genes significantly changed in Fluidigm Relapse (R_E) vs TFR (TFR_E) at trial entry comparison of MSCs Samples were all normalised to normal BM MSC samples. Outcomes were compared to each other using Two-Way ANOVA with Šídák's multiple comparisons test, using PRISM. Q values: >0.05 (ns), <0.05 (*), <0.01 (**), <0.001 (***), <0.0001 (****).

The heatmap shows the individual expression values, normalised to normal, for each gene of interest that was examined. In the relapse samples it appeared that sample 44 and 9 have higher expression toward the top right quadrant, this increased expression was found within the genes found to be significantly changed within this comparison. Samples from the TFR_E cohort appear to have little change to the gene expression of the genes being tested. The relapse samples 44 (R_E) and 9 (R_E) have the most notable increases across the gene list. A heatmap was generated using heatmap.2 on RStudio with the $\log_2$ fold change for each sample with each gene (Figure 3-21).

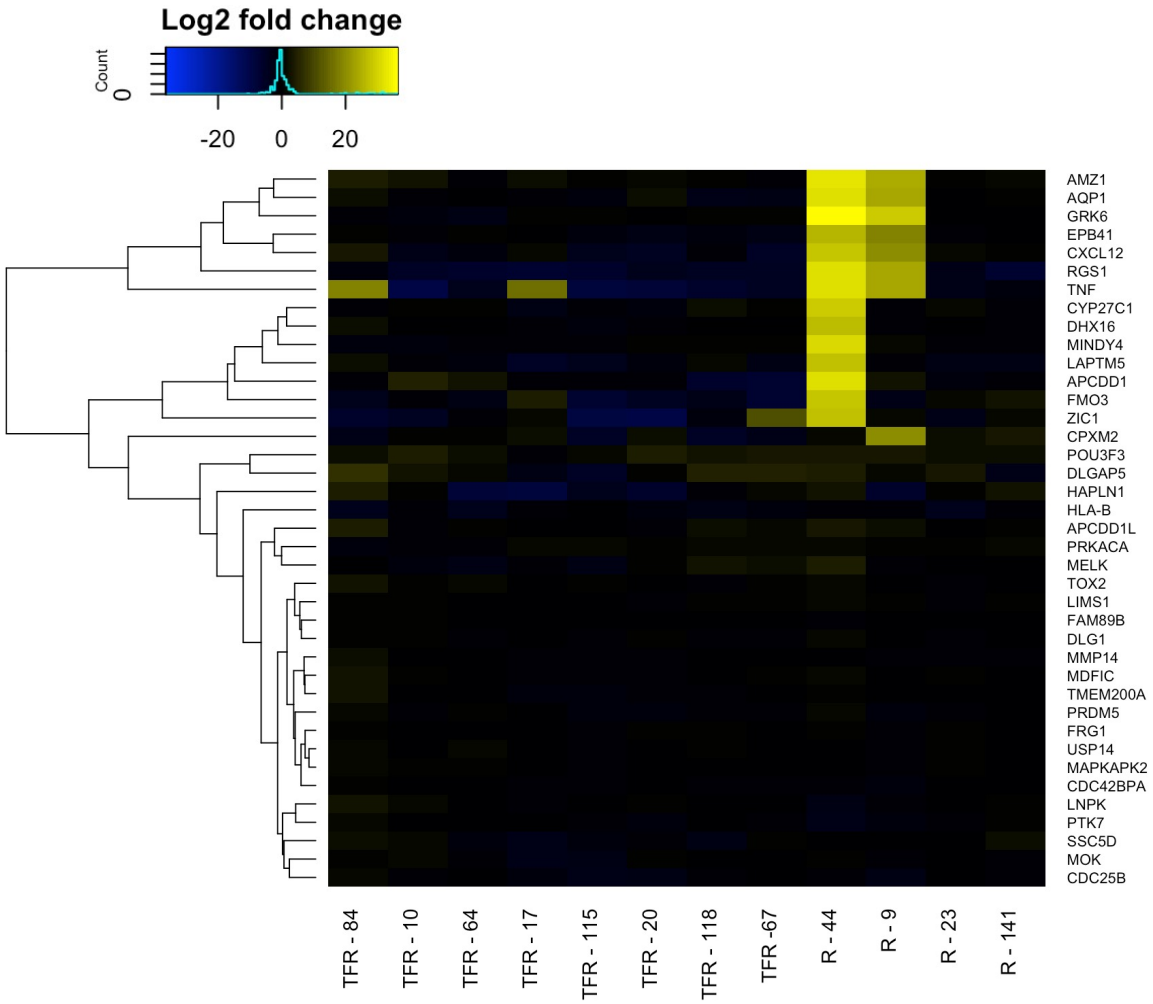

Figure 3-21 Expression level of MSC samples within R_E vs TFR_E Heatmap of log_2 fold expression values of TFR (TFR_E) (n=8) and relapse (R_E) (n=4) at trial entry samples. The scale at the side shows the colour intensity based on the expression level, yellow is the highest expression and blue is the lowest. The heatmap has row clustering of the genes within these samples. Heatmap made in Rstudio using heatmap.2.

From the genes that were significantly changed (Table 3-7), the fold change of these points between each outcome group was identified. There were two samples within the relapse entry (R_E) outcome group that appeared to be consistently higher in their expression values than the rest of the samples. While initial QC analysis did not identify anything irregular within these samples, in comparison to other samples they do appear to be potential outliers.

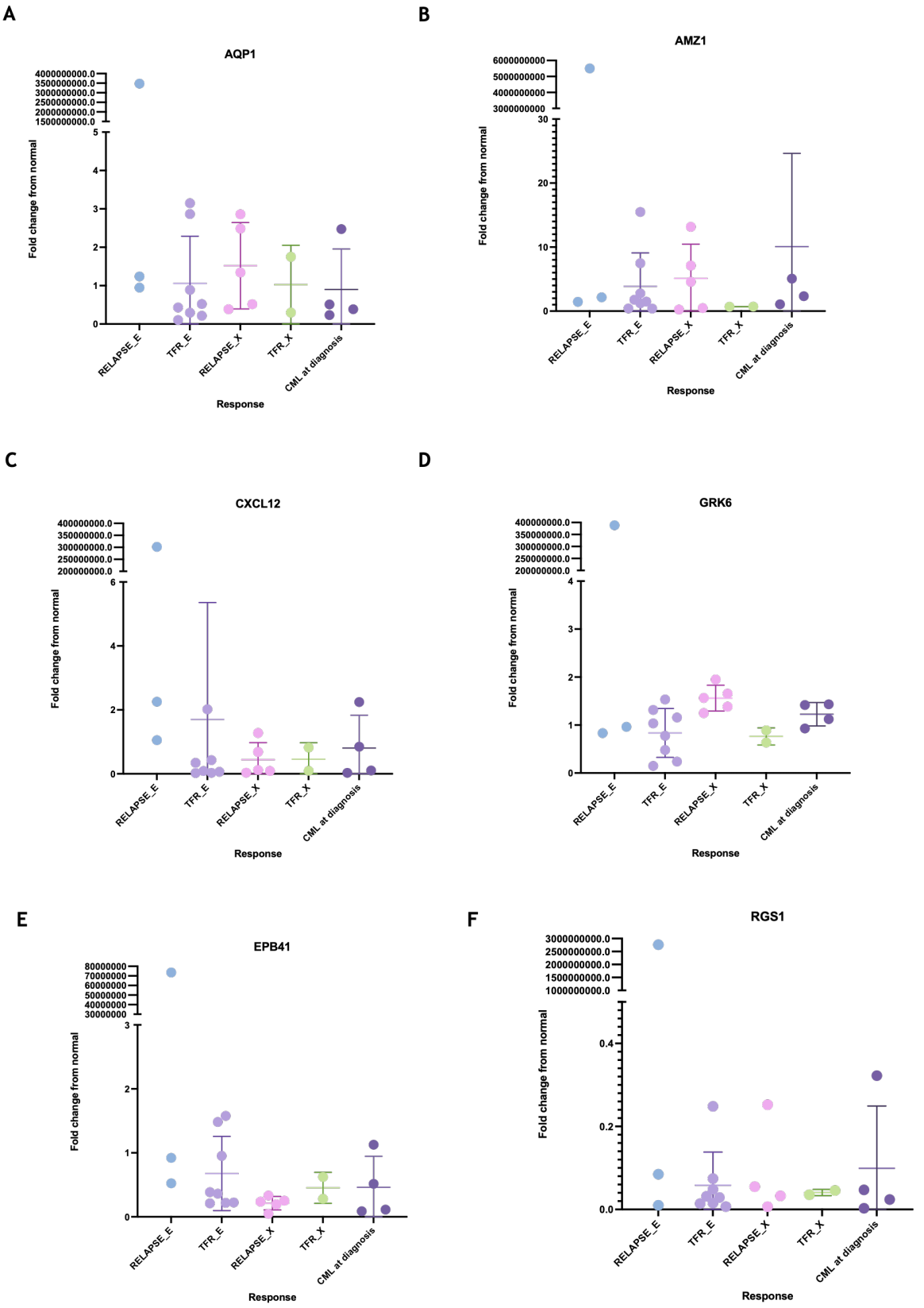

Figure 3-22 Changes to signficantly changed genes from Fluidigm data (A-F) Fold change ($2^{-\Delta\Delta Ct}$) of gene expression within all outcome groups. Samples normalised to normal BM MSCs. **(A)** *AQP1*. **(B)** *AMZ1*. **(C)** *CXCL12*. **(D)** *GRK6*. **(E)** *EPB41*. **(F)** *RGS1*. Error bars are represented as mean with SD. R_E (blue) (n=4), TFR_E (purple) (n=8), R_X (pink) (n=5), TFR_X (green) (n=2), CML (dark purple) (n=4).

As was examined within the RNAseq data, the next comparison made was between R_X (relapse patients with samples taken at point of relapse) vs R_E (relapse patients with samples taken at entry into trial). Of the 9 R_E and 5 R_X samples added to the Fluidigm, 4 R_E samples and 5 R_X were suitable for analysis. These samples were all normalised to normal BM MSCs expression and analysis to compare the two outcome groups was carried out on PRISM to identify statistically significant genes. The genes that were identified were *CXCL12* and *GRK6*, this is different to the DEGs found in the previous RNAseq analysis (Table 3-6). All genes identified were upregulated within this comparison.

Gene	Comparison	Q value
CXCL12	Relapse_Entry – Relapse_Exit (normalised to normal)	0.0296
GRK6	Relapse_Entry – Relapse_Exit (normalised to normal)	0.0160

Table 3-8 Genes significantly changed in Fluidigm relapse at trial entry (R_E) vs relapse at point of relapse (R_X) comparison of MSCs Samples were all normalised to normal BM MSC samples. Outcomes were compared to each other using Two-Way ANOVA with Šídák's multiple comparisons test, using PRISM. Q values: >0.05 (ns), <0.05 (*), <0.01 (**), <0.001 (***), <0.0001 (****).

The relapse at entry samples appear to have an increase in gene expression for genes shown in the top left corner, the increased expression is found within the genes that were previously identified in the PRISM analysis (*CXCL12* and *GRK6*). Again, as seen in the previous heatmap, it appears sample 44 (R_E) and 9 (R_E) have a more notable increase in expression throughout the genes being analysed. Most of the R_X samples have minimal expression changes from these genes. The heatmap of this is shown in Figure 3-23 (using heatmap.2 on RStudio) with the $\log_2$ fold change for each sample with each gene.

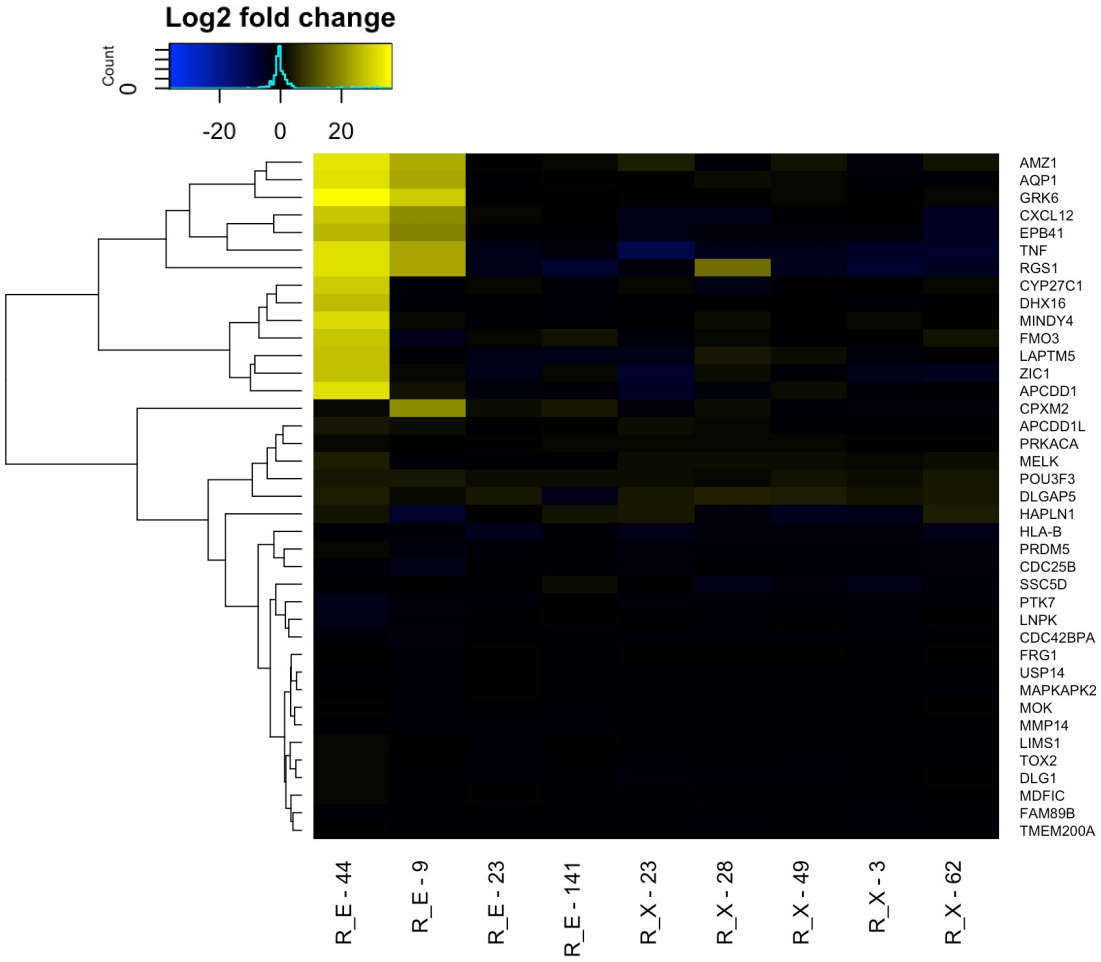

Figure 3-23 Expression level of MSC samples within R_E vs R_X Heatmap of log_2 fold change of comparison of relapse patients from trial entry (R_E) (n=4) vs relapse at point of relapse (R-X) (n=5) samples. The scale at the side shows the colour intensity based on the expression level, yellow is the highest expression and blue is the lowest. The heatmap has row clustering of the genes within these samples. Heatmap made in RStudio using heatmap.2.

3.5 Discussion

This chapter aimed to characterise MSCs as well as looking at changes to gene expression levels in samples taken at different timepoints to try to pinpoint how these changes could be affecting the BMM and potentially affecting how patients could maintain TFR. It was found that not only were there tangible changes in patients who maintained remission versus those who didn't in samples before they attempted TFR i.e., trial entry, but there were also changes seen at point of relapse. As CML is a disease that begins and progresses within the BMM it is important to further elucidate the changes that are happening in the BMM and how these could be causing patients to respond to treatment differently. This could open a host of opportunities for understanding CML, leukaemia and onco-haematopoiesis in more depth. The supportive stroma of the BMM is an excellent vantage point to begin this exploration.

Once the phenotype of the isolated MSCs had been confirmed (Figure 3-2) these samples could be profiled looking at their senescent and metabolic changes. Due to the nature of MSCs, senescence is a strong marker of their health and quality. The data showed that when comparing relapse to TFR at point of trial entry alone, the relapse patients had an increase of senescence in their MSCs with respect to patients that maintain TFR (Figure 3-3). Potentially the microenvironment of the BM is playing a significant role in disease progression and the MSCs could be involved in creating an environment that is inhibiting LSC proliferation in certain patients. Increases in senescence in relapse patients' MSCs could be showing more defective MSC activity as well as an increased inflammatory profile in the BMM which is contributing to relapse. However, when compared among the other outcome groups the only significant change was between TFR_E and normal MSCs, with TFR_E MSCs having a significantly lower senescence than normal MSCs. Due to previous research showing increased senescence decreases the effectiveness of MSCs and increases their pro-inflammatory profile, and the fact that within the relapse and TFR comparison TFR patients had lower senescence, this brings into question, if there is *increased* senescence in MSCs from healthy patients, does this mean senescence is a bad thing in MSCs and within the BMM? And if not, why do relapse patients have an increase in the senescence of their MSCs as the trial progressed? However, it can be seen from images that the normal BM MSCs have a higher

proliferation rate and increased confluency on the plate which could mean that the higher the cell number potentially the higher the number of senescent cells that are visible. Meaning the normal MSCs have more cells than the DESTINY MSCs which is what is being picked up by the staining. This also confirms a known limitation with the ß-galactosidase staining which is that it can introduce false positives/negatives and may not always be the best method of measuring senescence (Yang and Hu 2005; Hildebrand et al. 2013; Lee et al. 2006).

Additionally, the ROS levels produced by the cells directly links to the senescence of the cells. A significant increase was found in the ROS levels of MSCs from R_X compared to R_E patients and TFR_E patients, suggesting ROS levels secreted by MSCs is increased at point of relapse (Figure 3-5). It has previously been found that LSCs are as sensitive as HSC to excess ROS production and maintain quiescence to avoid this, however leukaemic cells that are proliferating have high ROS (Testa et al. 2016). In patients with CML it has been found that the BCR::ABL1 tyrosine kinase induces ROS production from several signalling pathways (Prieto-Bermejo et al. 2018), increased glucose metabolism (Kim et al. 2005), mitochondria (Sattler et al. 2000) and increased NAPDH oxidase activity (Naughton et al. 2009). Interestingly, a study found that in CML the BCR::ABL1 mediated increase in activation of STAT5 led to an increase in ROS production which was caused by an inhibition of the antioxidant enzymes, catalase and glutaredoxin-1 (Glrx1) (Bourgeais et al. 2016). They also discovered when co-culturing the CML cells with BM stromal cells this caused a decrease of STAT5 phosphorylation and increase in the antioxidant enzymes (Bourgeais et al. 2016). This also indicates a role the stromal cells are playing in the BMM with ROS production. Additionally, it was found that patients in DMR had significantly increased ROS production at the start of the trial compared to at the point of relapse (Figure 3-6), this suggests patients that are in the deepest remission and have previously had the best response to TKIs possible have increased expression of ROS in the BMM at the point of relapse. It is unsurprising that this increase is being seen in patients who are relapsing, the ROS production appears to be one driving factor in relapse. However, whether it is the MSCs secreting ROS or the changes to the BMM that are causing increased ROS production from the MSCs and how this could lead to TFR or relapse is yet to be determined.

It is known that mitochondria are one of the primary sites of ROS production (Tirichen et al. 2021), and due to the close links both have to senescence of MSCs this makes mitochondrial health an interesting area of research within the MSCs. Although no significant changes were seen within the data, the MMP for patients at point of relapse (R_E) was higher than any other outcome group (Figure 3-7). This is consistent with increased ROS levels that were also seen in this outcome group, as previously mentioned these go hand-in hand with metabolic function. This could potentially indicate active mitochondria that are producing increased ROS which could be driving the senescence of the MSCs leading to an increased pro-inflammatory profile within the BMM. Kolba *et al.*, reported that in CML the stroma facilitated transfer of vesicles, including mitochondria, to CML cells via TNTs (Kolba et al. 2019). This transfer appeared to protect the CML cells from the imatinib and prevented apoptosis, suggesting this is enhancing the survival of these leukaemic cells. Similar discoveries were reported in AML (Moschoi et al. 2016). The MSCs were then tested for MMP to provide a quantitative method to determine the mitochondrial health within the MSCs. However, these changes to MMP were not significant. As there was a significant increase in ROS production in R_X patients compared to R_E it would also be expected the MMP would decrease in R_X patients within the same MSCs. The lack of expected change in the MMP highlights one potential limitation of the JC1 stain. While a common stain for the evaluation of MMP, JC1 has one drawback that is its ratiometric nature which means that if the readings are taken at a single moment in time, yet the ratio may be fluctuating the value may be inaccurate. As well as this, in situations where drug efflux pumps such as ABCB1 and ABCG2, JC1 could be removed from the cytoplasm, reducing the production of red fluorescence and potentially showing a greater loss of MMP. For future work, instead of JC1 a stain like TMRE could be used, this is a fluorescent dye that produces a fluorescence which directly corresponds to the MMP. Additionally, a MitoTracker dye is a good option, which stains active mitochondria, higher MMP produces a higher fluorescence.

While there were minimal transcriptional changes when doing the RNAseq the changes seen did offer some interesting insight into the transformation of the MSCs between the outcome groups and how it could be altering the BMM and potentially affecting how patients respond to attempting TFR. Identification of

upregulation of *CXCL12* in relapse MSCs is unsurprising but significant as this is a chemoattractant produced by MSCs in the BM that regulates homing of HSCs to specific niches of the BM (Sugiyama et al. 2006). It has previously been identified within the BMM of CML patients that CXCL12 is essential on BM MSCs for maintaining quiescence of LSCs and maintaining their TKI-resistance (Agarwal et al. 2019). Additionally, this change was also identified in the Fluidigm data, where an increase in CXCL12 in relapse samples compared to TFR was seen, although there was a decrease in relapse samples at trial exit. Potentially there is an increase in CXCL12 from BM MSCs in relapse patients compared to TFR that is leading to relapse. CXCL12 is known to be involved in the maturation and proliferation of stem and progenitor cells and decrease of CXCL12 could contribute to proliferation of these leukaemic cells which is causing relapse. There was also an increase in *FMO3* in relapse patients compared to TFR, this is interesting as FMO3 has previously been found to increase the metabolism of dasatinib (Kamath et al. 2008), a drug commonly used to treat CML. This could have a potential link to the response of some patients to treatment. Furthermore, *HAPLN1* also had upregulated expression in relapse MSCs, it has previously been found that increased expression of HAPLN1 inhibits osteogenic differentiation of BM MSCs (G. Zhou et al. 2023) also causing a more pro-inflammatory phenotype (Chen et al. 2022). Increased osteogenic differentiation and a pro-inflammatory profile is beneficial for LSC protection and self-renewal. Additionally, ZIC1 overexpression leads to increased osteogenesis over adipogenesis within mesenchymal progenitor cells (Thottappillil et al. 2023), there was also an increased expression of this gene within our relapse BM MSCs.

The HLA-B, which is a part of the MHC and is involved in presenting to cytotoxic $CD8^+$ T lymphocytes was previously found to have very low expression on MSCs however this could be increased with stimulation with interferon gamma (IFN-γ) (Isa et al. 2010). In this study there was a decreased expression found in relapse MSCs. This further suggests a decrease of the immunomodulatory effects of MSCs in patients with CML, which appears to be increased in relapse patients. Additionally, there was also a decrease in *DHX16* expression; DHX16 plays a crucial role in maintaining HSCs within the BM, inhibition of DHX16 impairs HSCs quiescence, cell cycle arrest and apoptosis (Zhigang Li et al. 2024). The data

suggest that MSCs of patients that are relapsing are producing more factors that dysregulate HSCs, immune response and inflammation.

Due to the initial experiment having samples that failed and could not be analysed, it was essential to repeat this and compare the DEGs found. This allowed for additional samples to be assessed. However, this does not invalidate the changes seen within the initial RNAseq analysis, although it is the same comparison and they do show different genes both datasets are valid as it most probably reflects the heterogeneity associated with primary MSC BM samples and how the cDNA libraries were prepared and read depth of the sequencing. RNA sequencing is an excellent way to identify global changes, but findings then require validation at the transcriptional and translational level in a larger cohort to verify the changes. Additionally, there was slight differences to the MSC samples used in the first (Table 3-2) and second (Table 3-4) RNAseq run that could account for the differing DEGs seen.

Perhaps the most important factor to consider here is the differing samples used in the first RNAseq analysis compared to the second (Table 3-2 and Table 3-4), this is a potential reason differences of DEGs that were seen. MSCs are multipotent cells, we do not know at what point in ontogeny they may exist as well as this they are extracted from the BM of patients samples, making them potentially even more heterogeneous. The change of having differing samples within the second run could account for the difference of gene expression seen. It is for these reasons, that while the data for both the RNAseq runs are seen as valid individually, they were not combined. While both datasets were aligned to the same reference genome and only samples that passed QC were used in analysis, these variations of the two rounds of RNAseq may account for the differing results produced and is a potential limitation of the work.

Furthermore, prior to the first round of RNAseq the library prep was completed in-house in our lab, which is unaccustomed to the process, and as it is a sensitive process small errors could be magnified. This may well attribute to the failure of some samples for the first RNAseq as well as the variation of sequencing produced. Within the second round of RNAseq the RNA samples were processed commercially by University of Glasgow – Shared Research Facilities, a different facility than the first round, who are experienced in library preparation.

Although there was some overlap in samples between the two RNAseq runs it would have been better if the samples analysed were identical between rounds. Pragmatically samples were not always available for RNA extraction.

There were several transcriptional changes identified that could provide an interesting interpretation of the changes occurring in these MSCs. Firstly, it is known that the inhibition of CDC42 improved mitochondrial function and the function of mesenchymal stem and progenitor cells and bone volume post haematopoietic stem cell transplantation (Landspersky et al. 2024). This is interesting considering the increase of *CDC42BPA* in R_E patients compared to TFR_E patients was identified in these MSCs. As this gene has previously been found to increase the mitochondrial health and function of MSCs it would be expected that this would be increased within the TFR_E group rather than R_E. Additionally, upregulation of *PTK7* in relapse patients is interesting as this belongs to a receptor tyrosine kinase family and is seen to be upregulated in colon carcinoma cells (Mossie et al. 1995). There has also been an upregulation of *PTK7* found in CML cells (H. Zhou et al. 2014). Furthermore, it has been shown that PTK7 is a SASP factor that also activates the Wnt/Ca^{2+} pathway (Yun et al. 2023). Further indicating an increased pro-inflammatory profile is seen in patients with relapse compared to TFR before TFR is attempted. There was also an upregulation of *TOX2*, which has been found to play a role in NK cell development (Vong et al. 2014) as well as being involved in leukaemogenesis in T-ALL (A. Li et al. 2024).

While looking at the question of finding predictive biomarkers of TFR, it proposes an interesting question of how the BMM changes/is affected when attempting TFR that leads to relapse. To answer this question additional MSC samples were sent away with the second round of RNAseq with the addition of samples from patients at point of relapse (R_X). An upregulation of *APCDD1* was also observed, which has been found to be an inhibitor of the Wnt signalling pathway (Shimomura et al. 2010) and the BMP signalling pathway (Vonica et al. 2020). Additionally, *AQP1* was increased in relapse samples in RNAseq analysis and this was also seen in the Fluidigm data, this is interesting as it has been reported that an increase of AQP1 expression stimulated MSC migration through the Fak and ß-catenin pathway (Meng et al. 2014). Migration of MSCs typically occurs in response to increase inflammatory signals and injury, this stimulates

the migration of MSCs to this site (X. Yang et al. 2023). Therefore, the potential increased migration in relapse patients could be signifying an increased inflammatory profile within the BMM.

For the validation of these DEGs within a larger patient cohort, MSCs were tested on a Fluidigm chip. There were a few genes found to be upregulated in relapse samples that were not seen in the RNAseq data but were identified with Fluidigm data. The differences of gene expression found between the RNAseq and Fluidigm data could be because the gene expression for Fluidigm was normalised to normal BM MSCs, while the RNAseq was not. The genes that were not found within the RNAseq data were *GRK6, RGS1 and EPB41*. Interestingly, Le et al., previously found that GRK6 is involved in ROS signalling as well as maintaining the self-renewal of HSCs (Le et al. 2016). An important note for the Fluidigm results is the indication of an outlier in R_E cohort (Figure 3-22), this could be a limitation of results and may have skewed analysis. Dixon's Q-test could have been used to identify and reject the single suspected outlier from the dataset.

The findings from transcriptional changes found in relapse vs TFR samples at trial entry appear to produce more pro-inflammatory MSCs, with potential changes to differentiation and immunomodulatory effects. This also appear to continue within relapse sample at point of exit from the trial.

Additionally, due to the clear increased senesce in relapse patients and suggestions of an increased senescent profile within RNAseq, the MSCs are demonstrating at point of relapse, the SASP factors could be assessed to gain a deeper understanding of exact what is being secreted into the BMM and how this is effecting patients that relapse. The transcriptional changes could be assessed at a protein level by examining these genes as well as common SASP factors using a custom LUMINEX panel.

Overall, from the study of MSCs it appears the patients maintaining remission (TFR_E) may have MSCs with a less pro-inflammatory profile. This patient cohort also appears to have a less senescent MSCs with less changes to metabolic processes linked to senescence like ROS production. Additionally, TFR patient cohort have less markers of changes to immunomodulatory changes and changes

to MSC differentiation and proliferation potential. Importantly, the patients who relapsed appeared to have changes to genes involved in regulation of HSPC, while this did not appear to be the case with TFR MSCs. Therefore, the changes to these senescent and metabolic factors could be contributing to changes to the BMM and disease progression in patients who are relapsing. Patients who are maintaining remission appear to have a more robust immune response and more stable MSCs that are more like MSCs from someone without CML.

4 Results II – Stem and progenitor cells

4.1 Introduction

CML patients, even with the best response to TKIs in DMR, must still have remaining disease as evidenced by relapse of some patients that attempt TFR. The *BCR::ABL1* expressing stem cells play an important role in disease recrudescence, as they are able to persist even after treatment. Hence one major obstacle to achieving cure of CML is the inability to fully eradicate LSCs with TKIs. These LSCs can evade being targeted by treatment through dormancy and self-renewing properties within the BMM. As discussed it would be ideal for all patients to be able to achieve TFR. Furthermore, for patients that cannot achieve as deep of a remission in response to TKIs, if LSCs could be targeted in a more precise way this could open the potential for fully eradicating LSCs and potentially CML in all patients.

The LSCs in patients with CML can be identified with their expression profile of $CD34^{+}38^{-}$, however, HSCs also have the same expression profile. This is a problem when distinguishing LSCs from HSCs as they are so phenotypically and functionally similar yet LSCs need to be the cellular target for potential therapy while leaving HSCs unharmed. One of the ways in which targeting LSCs is being approached is the identification of specific CD markers found on LSCs but not on HSCs to distinguish between these two stem cell populations. Over the years there have been several potential cell surface markers identified as potentials for differentiating between LSCs and HSCs, this would be extremely valuable in several ways including for identifying the leukaemic burden within patients, monitoring their response to TKIs, deepening the understanding of changes to LSCs and also potentially offering an additional treatment target within this typically hard to target population of cells. Another important aspect of identification of these markers is their ability to predict TFR, due to their specificity to LSCs the change of expression of these markers could be examined in patients attempting TFR to identify changes to the expression in patients who maintain/fail TFR. Additionally, many of these markers on LSCs have an impact on the functionality of LSCs and can affect the growth and self-renewal of LSCs. An example of this is CD26, a surface enzyme that is expressed on CML LSC (H. Herrmann et al. 2014) it has been found to cleave and inactivate CXCL12 (Shioda

et al. 1998), preventing the interaction of CXCL12 and CXCR4 which is essential for HSC and LSC homing within the BM. This encourages the migration and proliferation of these stem cells. Additionally, the inhibitor WNT974, which targets Wnt ligands, was found to inhibit the proliferation of $CD34^{+}38^{-}26^{+}$ population from CML cells but did not affect the $CD34^{+}38^{-}26^{-}$ population, which indicates this inhibitor has specific inhibitory effect on LSCs which could be useful as a novel treatment (Agarwal et al. 2017). Overall, this is one example of the usefulness of identifying these CD markers, and how they can offer novel understanding of how CML and LSCs progress, be specifically targeted within LSCs as well as offer alternative treatment options for targeting LSCs. The surface markers present on LSCs are an area of interest for biomarker discovery for their role in CML and their diagnostic properties for the prediction of TFR outcome (Table 4-1).

Marker	Findings	Reference
CD25	Higher expression of CD25 found on LSCs in CML, very low expression on HSCs	(Sadovnik et al. 2017)
CD26	In CML stem cells all had CD26 marker but not found on normal HSCs.	(H. Herrmann et al. 2014)
CD35	Marker of HSC/LSC and potentially predictive of TFR	(Warfvinge et al. 2024)
CD36	Upregulated in primitive CML LSCs and have decreased sensitivity to imatinib	(Landberg et al. 2018)
CD44	Required for BCR::ABL1 LSCs homing and engraftment more than HSCs	(Krause et al. 2006)
CD45RA	CML LSCs that were CD45RA- were TKI-insensitive	(Warfvinge et al. 2017)
CD47	Increased expression on LSCs in AML/CML	(H. Herrmann et al. 2020)
CD49d	Used as a prognostic marker of survival in CLL	(Bulian et al. 2014)
CD93	Novel marker of LSCs and found on LSCs even after TKI therapy. Needed for self-renewal of LSCs	(Kinstrie et al. 2020)
CD117	The inhibition of CD117 (c-kit) may be a target to achieve optimal response in CML patients taking imatinib.	(Dybko et al. 2013)
CXCR4	Increase survival of quiescent LSCs from up-regulation of CXCR4	(L. Jin et al. 2008)
IL-1RAP	Can discriminate between Ph(+) and Ph(-) CML stem cells.	(Järås et al. 2010, 1)

Table 4-1 Table of HSC/LSC CD markers of research interest based on published literature.

The uncontrolled proliferation of CML stem and progenitor cells is a marker of disease progression and controlling this is the first step to treating CML. While TKIs have provided an excellent job of eradicating mature CML cells they are unable to target and eradicate all LSCs. This is due to quiescence LSCs, dysregulated signalling pathways and changes to the BMM and their role in protecting these LSCs from being targeted by TKIs and allows for disease progression in the absence of TKIs. CML originates from the LSCs as was proven when it was found that progenitor cells do not have the self-renewal capacity of LSCs and were not able to cause CML in mice (Huntly et al. 2004). Although they do not possess the ability to cause or maintain CP-CML, in patients that develop blast crisis CML progenitor cells develop self-renewal capacity through the ß-catenin signalling pathway (Jamieson et al. 2004). It is expansion of these primitive progenitors and their corresponding production of mature myeloid cells that is the initial manifestation of CML, once this is controlled by TKIs, patients are considered to be in remission and haematopoiesis can occur normally. The degree to which the stem and progenitor population is targeted by TKIs corresponds to their ability to attempt TFR.

Further elucidating the activity and behaviour of these stem and progenitor CML cells through marker profiling could be used to provide potential clarity to identify how they differ in TFR and relapse and whether they offer the potential to distinguish between the two outcomes.

4.2 Aims

1. To enumerate and characterise the stem and progenitor population of patients to identify predictive cellular signature of TFR.

4.3 Objective/ sub aims

1. Using MPFC, identify and enumerate LSC/HSC markers in the BM of all DESTINY trial patients to reveal if the presence of these markers was linked to TFR success or relapse.

2. Study if the differentiation potential and proliferative capacity of BM MNC from DESTINY trial patients predicts TFR.

3. Quantify the *BCR::ABL1* within the stem and progenitor population from all outcomes of the DESTINY patients. Evaluate the leukaemic burden within the colony forming assays for the sample outcome groups to identify if the number of leukaemic cells is higher in the relapsing groups and therefore driving relapse.

4.4 Results

4.4.1 Transcriptional changes to IL1-RAP and CD26 were higher in CML LSCs compared to normal HSCs

Before completing analysis of stem cell markers by MPFC, the Gerber *et.al* (accession: GSE43754E/GEOD-43754) publicly available dataset hosted by the Stemformatics platform was used to identify transcriptional changes to the markers of interest (Table 4-1) within the stem and progenitor populations of CML patients and normal donors (Gerber et al. 2013). This was later used as a comparison to the MPFC analysis of the DESTINY samples.

This dataset used exon microarrays to compare BM CML and normal stem ($CD34^+CD38^-$ALDH-high) and progenitor ($CD34^+CD38^+$) cells. The log_2 normalised expression of *CD93, IL1-RAP, CD25, CD90, CD36, CD26, CD45RA, CD44, CD47, CD49d, CXCR4, CD117* and *CD35* genes were looked at in these patient/donor groups (Figure 4-1). From the analysis a significantly increased expression of *IL1-RAP* in CML progenitor population vs normal stem cell population (p=0.0197) and within the CML stem population vs normal stem cell population (p=0.0277). With CD25, there was a significant increase in the CML stem population compared to the CML progenitor population (p=0.0025). Previous work also found, CD25 has been shown to have the highest expression on LSCs ($CD34^+38^-$) compared to normal stem cells ($CD34^+38^-$), the normal stem cells had little to no CD25 expression (Sadovnik et al. 2017). Furthermore, the expression of CD26 was significantly higher in the CML stem population compared to the normal stem population (p=0.0011). This finding is consistent with previous research, where CD26 expression was found on CML LSCs but not present on HSCs (H. Herrmann et al. 2014). The presence of CD26 on CML LSCs but not HSCs was found at both a transcriptional level, with gene array and q-PCR analysis of $CD34^+38^-$ cells, and at a protein level when the expression of CD26 was assessed by flow cytometry (H. Herrmann et al. 2014). There was a significant change with CD45RA where the expression was increased in CML stem vs CML progenitor (p=0.0385). With CD44 there was an increased expression in CML stem vs CML progenitor (p=0.0385). Additionally, CXCR4 had an increased expression within the normal progenitor population compared to the CML progenitor population (p=0.0277).

The expression of CD35 was reduced in the CML stem population compared to the CML progenitor population ($p=0.0139$).

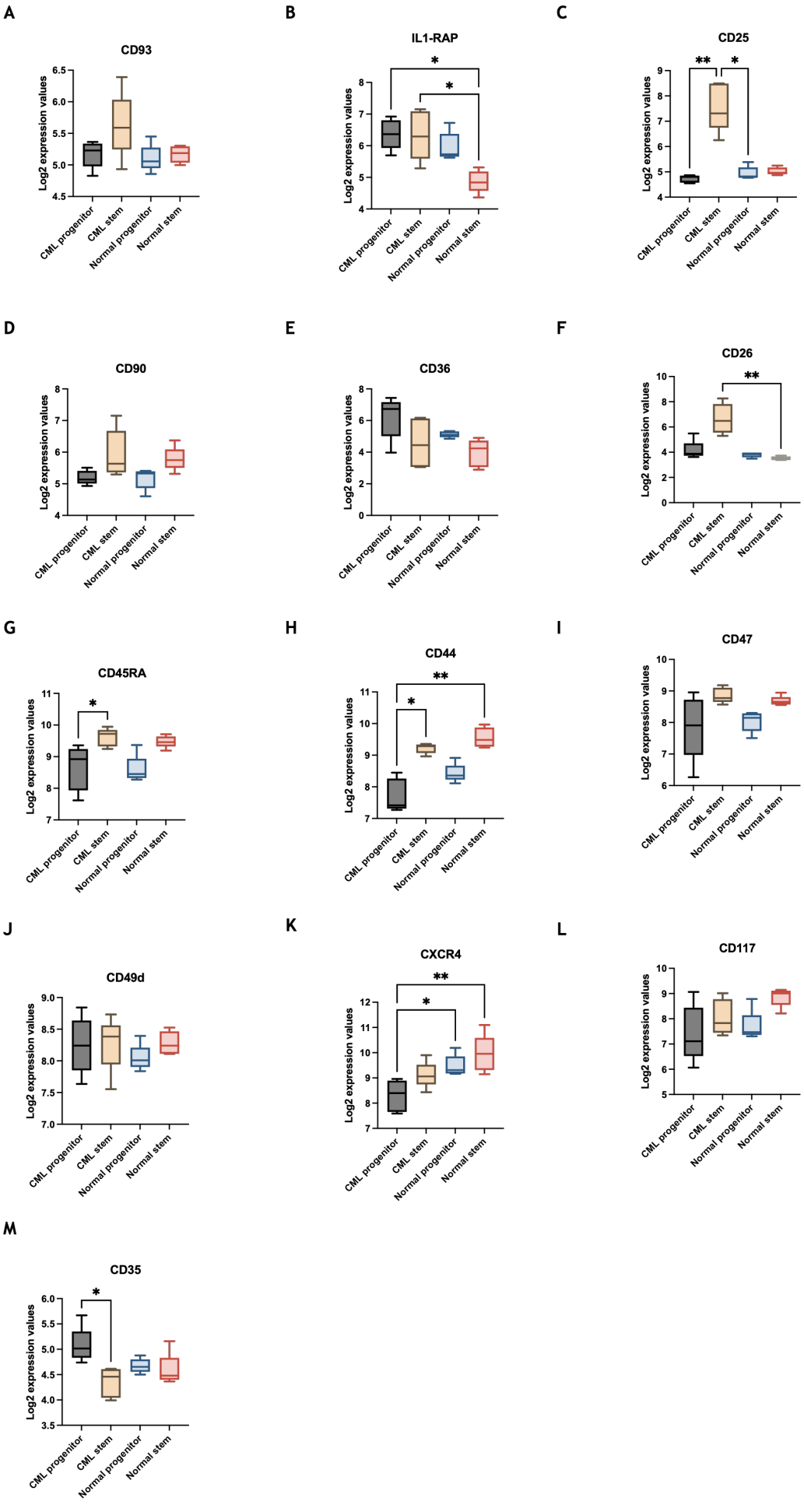
A
CD93
B
IL1-RAP
C
CD25
D
CD90
E
CD36
F
CD26
G
CD45RA
H
CD44
I
CD47
J
CD49d
K
CXCR4
L
CD117
M
CD35
Log2 expression values
CML progenitor
CML stem
Normal progenitor
Normal stem

Figure 4-1 Changes to gene expression of markers of interest using CML and normal stem and progenitor populations using data set from Stemformatics The boxplots demonstrate the minimum to maximum of the log_2 normalised gene expression values from the Gerber et al., (2013) data set looking at CML and normal stem and progenitor BM samples using exon microarrays. **(A)** *CD93* **(B)** *IL1_RAP* **(C)** *CD25* **(D)** *CD90* **(E)** *CD36* **(F)** *CD26* **(G)** *CD45RA* **(H)** *CD44* **(I)** *CD47* **(J)** *CD49d* **(K)** *CXCR4* **(L)** *CD117* **(M)** *CD35.* Samples from CML progenitor (black) (n=5), CML stem (yellow) (n=5), normal progenitor (blue) (n=5), normal stem (red) (n=5) cells. Statistical tests carried out were one-way ANOVA, Kruskal-Wallis test. P values: >0.05 (ns), <0.05 (*), <0.01 (**), <0.001 (***), <0.0001 (****).

From the transcriptional data it can be seen that *CD93, IL1-RAP, CD25* and *CD26* appear to have a higher expression level within the CML LSCs than the normal HSCs, although only *IL1-RAP* and *CD26* had a statistically significant change. These findings from the Stemformatics analysis demonstrates the changes to gene expression of these markers of interest is consistent with changes to the expression profiles of these markers which has previously been demonstrated in the literature (Table 4-1) which identified these markers as being specific to LSCs. This initial analysis of these markers from an external dataset provided an overview of the transcriptions changes to these markers and how their expression profile is changed in LSCs vs HSCs within the BM. As a continuation of this work the next stage was to confirm the expression through protein level expression analysis using MPFC and the DESTINY samples.

4.4.2 CD44 expression is increased after TKI use in CML patients

Samples of BM MNCs were thawed and stained with HSC/LSC panels for markers identified to alter in CML and AML stem and progenitor cells in the literature. The interest in these panels was to identify the expression levels, how they differ between the outcome groups and if they could potentially be used as a marker of TFR or relapse. The intention of using these panels was to identify the live cells, remove any doublets, and isolate the stem cell population marked by $Lin^-CD34^+38^-$ that is representative of all HSCs including LSCs within the sample. Cells from these panels were also sorted and used for functional assays which will be described below (section 4.4.5). From here the aim was to quantify the level of expression of the markers of interest were present within the $Lin^-CD34^+38^-$ primitive population.

These markers distinguish between HSC and LSCs, the data examined if any of these LSC specific markers were changed during TFR/relapse and therefore could they be used as biomarkers of TFR.

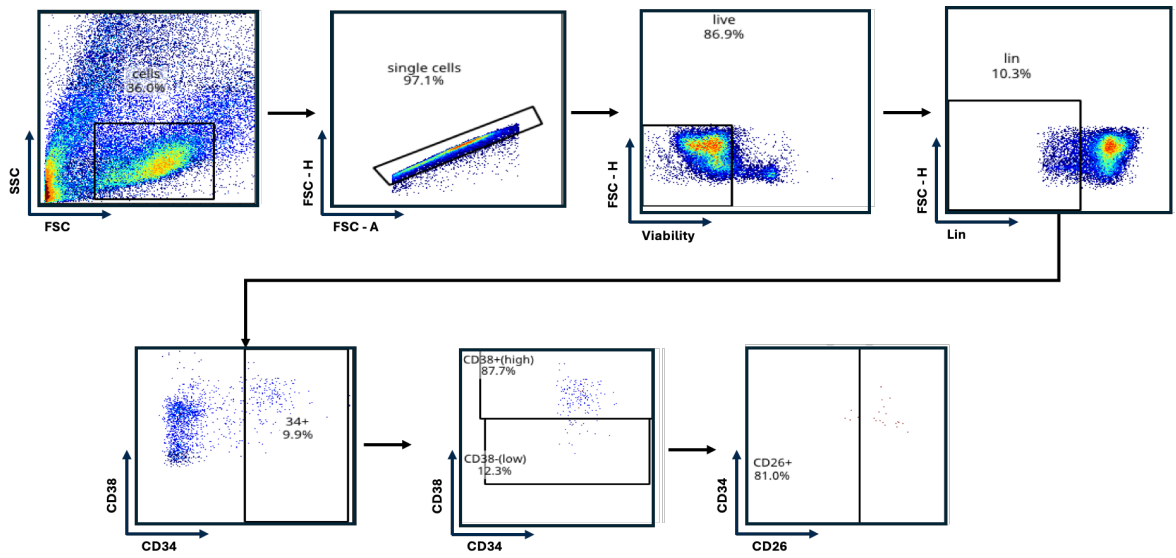

Figure 4-2 Multiparameter flow cytometry gating strategy using HSC panel An example using HSC/LSC panel 1 to obtain stem cell marker (CD26) expression data.

Sample number	Trial Response	Timepoint of sampling	Days to relapse	HSC1	HSC2	HSC3	LTC-IC	ST-CFC	BCR::ABL1 LTC-IC - Fluidigm	BCR::ABL1 ST-CFC - Fluidigm
CML254	-	-								
CML341	-	-								
CML438	-	-								
CML454	-	-								
CML520	-	-								
CML533	-	-								
CML535	-	-								
RB1119	-	-								
RB1120	-	-								
RB768	-	-								
RB769										
RB771	-	-								
RB810	-	-								
RB900	-	-								
3	Relapse in stopping	Entry – at start point of trial	455							
3X	Relapse in stopping	Exit – relapse during trial	455							
9	Relapse in stopping	Entry – at start point of trial	449							
10	TFR	Entry – at start point of trial	-							
14	TFR	Entry – at start point of trial	-							

15	Relapse in stopping	Entry – at start point of trial	449							
17	TFR	Entry – at start point of trial	-							
20	TFR	Entry – at start point of trial	-							
21	TFR	Entry – at start point of trial	-							
23	Relapse in de-escalation	Entry – at start point of trial	244							
23X	Relapse in de-escalation	Exit – relapse during trial	244							
24	TFR	Entry – at start point of trial	-							
25	Relapse in stopping	Entry – at start point of trial	1022							
30	TFR	Entry – at start point of trial	-							
31	Relapse in stopping	Entry – at start point of trial	465							
33	TFR	Entry – at start point of trial	-							
34	TFR	Entry – at start point of trial	-							
34	TFR	Exit – end point of trial	-							
36	TFR	Entry – at start point of trial	-							

37	TFR	Entry – at start point of trial	-							
38	Relapse in stopping	Entry – at start point of trial	404							
41	TFR	Entry – at start point of trial	-							
44	Relapse in de-escalation	Entry – at start point of trial	124							
44X	Relapse in de-escalation	Exit – relapse during trial	124							
49	Relapse in stopping	Entry – at start point of trial	475							
49X	Relapse in stopping	Exit – relapse during trial	475							
51	Relapse in de-escalation	Entry – at start point of trial	56							
53	TFR	Entry – at start point of trial	-							
56	TFR	Entry – at start point of trial	-							
56X	TFR	Exit – end point of trial	-							
60	Relapse in stopping	Entry – at start point of trial	485							
62	Relapse in stopping	Entry – at start point of trial	828							

62X	Relapse in stopping	Exit – relapse during trial	828							
64	TFR	Entry – at start point of trial	-							
66	TFR	Entry – at start point of trial	-							
67	TFR	Entry – at start point of trial	-							
68	TFR	Entry – at start point of trial	-							
68X	TFR	Exit – end point of trial	-							
72	TFR	Entry – at start point of trial	-							
73	TFR	Entry – at start point of trial	-							
75	TFR	Entry – at start point of trial	-							
76	Relapse in de-escalation	Entry – at start point of trial	130							
78	Relapse in de-escalation	Entry – at start point of trial	75							
79	TFR	Entry – at start point of trial	-							
82	TFR	Entry – at start point of trial	-							
82X	TFR	Exit – end point of trial	-							

83	TFR	Entry – at start point of trial	-							
84	TFR	Entry – at start point of trial	-							
84X	TFR	Exit – end point of trial	-							
85	Relapse in stopping	Exit – relapse during trial	476							
87	TFR	Exit – end point of trial	-							
89	Relapse in de-escalation	Entry – at start point of trial	245							
89X	Relapse in de-escalation	Exit – relapse during trial	245							
90	Relapse in stopping	Entry – at start point of trial	399							
90X	Relapse in stopping	Exit – relapse during trial	399							
93	TFR	Entry – at start point of trial	-							
93X	TFR	Exit – end point of trial	-							
105	Relapse in stopping	Entry – at start point of trial	483							
107	Relapse in de-escalation	Entry – at start point of trial	96							

109	TFR	Entry – at start point of trial	-							
115	TFR	Entry – at start point of trial	-							
116	TFR	Entry – at start point of trial	-							
117	TFR	Entry – at start point of trial	-							
118	TFR	Entry – at start point of trial	-							
119	TFR	Entry – at start point of trial	-							
121	TFR	Entry – at start point of trial	-							
122	Relapse in stopping	Entry – at start point of trial	483							
131	Relapse in stopping	Entry – at start point of trial	562							
138	Relapse in de-escalation	Entry – at start point of trial	181							
141	Relapse in stopping	Entry – at start point of trial	472							
141X	Relapse in stopping	Exit – end point of trial	472							
142	Relapse in stopping	Entry – at start point of trial	496							
142X	Relapse in stopping	Exit – relapse during trial	496							

148	TFR	Entry – at start point of trial	-							
149	Relapse in stopping	Entry – at start point of trial	440							
149X	Relapse in stopping	Exit – relapse during trial	440							
151	TFR	Entry – at start point of trial	-							
152	Relapse in stopping	Entry – at start point of trial	403							
152X	Relapse in stopping	Exit – relapse during trial	403							
154	Relapse in stopping	Entry – at start point of trial	1081							
154X	Relapse in stopping	Exit – relapse during trial	1081							
161	Relapse in stopping	Entry – at start point of trial	440							
161X	Relapse in stopping	Exit – relapse during trial	534							
163	TFR	Entry – at start point of trial	-							
166	TFR	Entry – at start point of trial	-							

Table 4-2 BM samples used for each experiment Samples and the experiments they were used for. The information for each sample is also shown. Boxes highlighted in green indicate this sample was used for this technique.

The HSC/LSC 1 panel consisted of:

Target	Fluorochrome
Lineage	FITC
CD34	BV421
CD38	BV786
CD90	PE-Cy7
CD25	BV605
CD26	APC
CD93	BB700
IL1-RAP	PE
CD36	BV711
VIABILITY	7-AAD

Table 4-3 HSC/LSC 1 Panel

The HSC/LSC 2 panel consisted of:

Target	Fluorochrome
Lineage	FITC
CD34	BV421
CD38	BV786
CD45RA	BV510
CD49d	BV711
CD44	APC-H7
CD47	Alexa Fl 647
CXCR4	PE
CD117	PE/Dazzle 594
VIABILITY	7-AAD

Table 4-4 HSC/LSC Panel 2

To begin with there were two HSC/LSC marker panels (created by Dr Shaun Patterson). The panels HSC/LSC 1 and 2 included markers identified from the literature as being of interest within poor response, CML, stem cells and TFR, therefore worthy of consideration as biomarkers for TFR. Due to the number of markers of interest these were split between two panels. Comparisons of these panels was carried out to compare DESTINY samples to determine if any of these markers could be predictive of TFR. Unfortunately, no statistically significant changes were found, however changes were seen between DESTINY patients compared to normal and at diagnosis samples, therefore the data was separated to show the changes found in relapse patients and TFR patients separately.

From the HSC/LSC1 panel it could be seen that there was a significant increase of the $CD25^+$ population within the 'CML at diagnosis' (samples from CML patients at point of diagnosis, independent to DESTINY patients) group compared to DESTINY patients who maintain TFR (TFR_E) ($p=0.0446$). Across the other DESTINY patient groups, the level of $CD25^+$ appears to be the same to that of non CML donors. Thus, indicating $CD25^+$ appears to be a marker that is highest before treatment with TKIs. The assessment of the $CD90^+$ marker showed a significant increase ($p=0.0368$) in levels within samples from relapse patients taken at the point of their relapse and trial exit (R_X) compared to trial entry (R_E). Increased levels of $CD90^+$ could be a potential biomarker for patients who are about to relapse and lose their TFR. Additionally, there is an increase in $CD93^+$ in normal HSCs compared to relapsed patients' samples taken at trial entry (R_E) ($p=0.0174$), suggesting it to be a marker found predominantly on HSCs with respect to LSCs. This is interesting as previously CD93 has been associated with being a marker of LSCs, increased expression on normal HSCs suggests it may not be exclusive to LSCs and therefore not a useful biomarker of TFR.

With the HSC/LSC2 panel, the only marker that showed any significant changes was $CD44^+$ (Figure 4-3 and Figure 4-4). All the DESTINY samples appeared to have similar levels of $CD44^+$ however it was almost completely absent in CML at diagnosis and normal BM samples. The significant changes were seen between Relapse_E, Relapse_X, TFR_E, TFR_X versus CML at diagnosis ($p=0.0336$; 0.0337; 0.0109; 0.0337, respectively), and TFR_E vs normal ($p=0.0366$). The CD45RA marker appeared to have the lowest expression, with the levels being lower than the other markers across the outcome groups. Markers like CD47, CD49d, CXCR4 and CD117 all appeared to have similar expression levels across DESTINY samples, suggesting these markers may not be useful as potential biomarkers for TFR prediction.

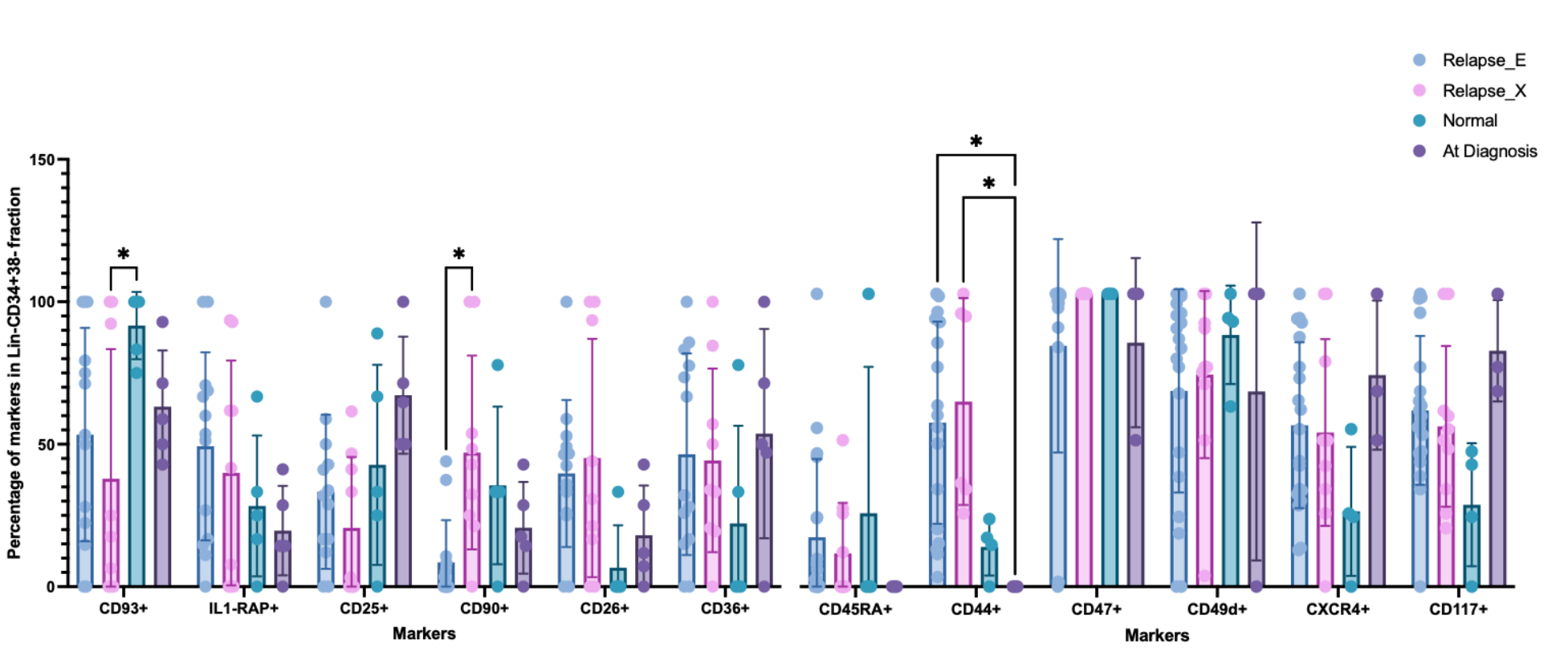

Figure 4-3 Changes to markers in Lin$^-$CD34$^+$38$^-$ fraction from HSC/LSC panel 1 and 2 of BM MNCs in relapse, normal and at diagnosis outcome groups Bar graph showing the percentage of markers in Lin$^-$CD34$^+$38$^-$ fraction using BM MNC samples. Markers CD93$^+$ to CD36$^+$ are from HSC/LSC panel 1. HSC/LSC panel 1 = samples from Relapse_E (relapse at point of trial entry) (blue) (n=13), Relapse_X (relapse at point of relapse) (pink) (n=9), Normal (turquoise) (n=5), and At diangosis (patients at point of dianosis) (dark purple) (n=5). Markers from CD45RA$^+$ to CD117$^+$ are markers from HSC/LSC panel 2. HSC/LSC panel 2 = samples from Relapse_E (relapse at point of trial entry) (blue) (n=19), Relapse_X (relapse at point of relapse) (pink) (n=10), Normal (turquoise) (n=4), and At diangosis (patients at point of dianosis) (dark purple) (n=3). Bars show Mean with SD. Carried out two-way ANOVA, Tukey's multiple comparison test. P values: >0.05 (ns), <0.05 (*), <0.01 (**), <0.001 (***), <0.0001 (****).

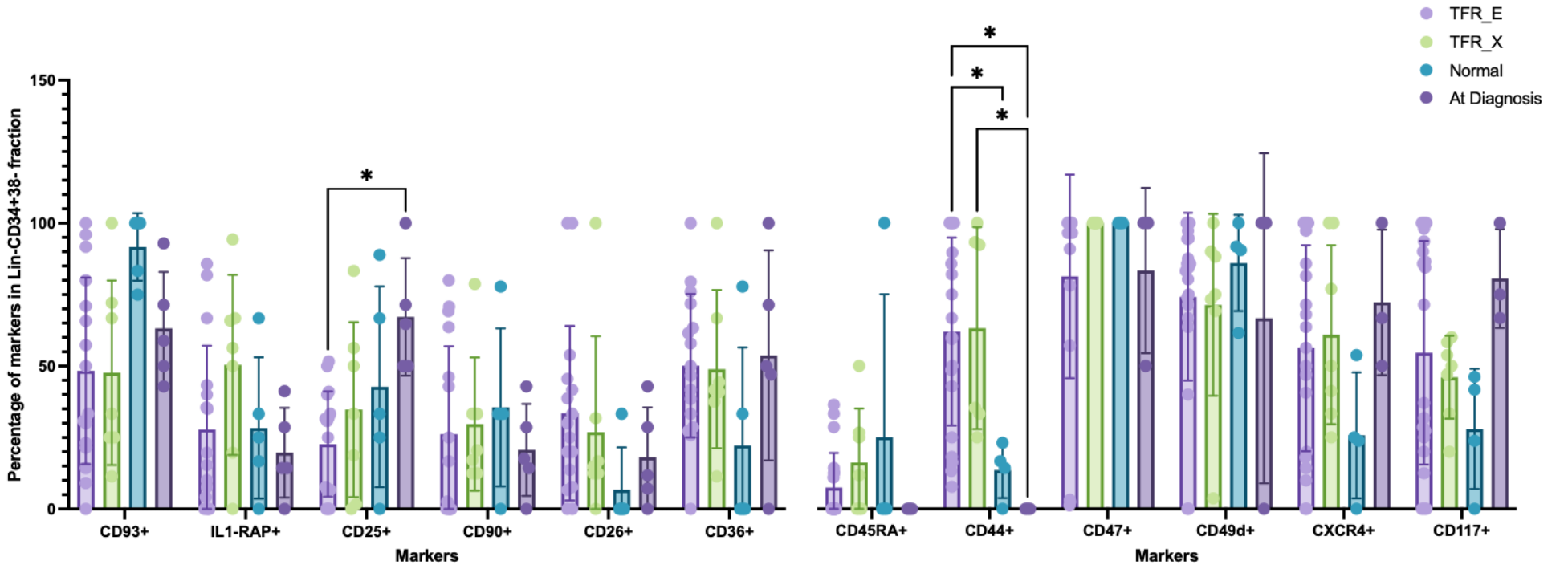

Figure 4-4 Changes to markers in Lin$^-$CD34$^+$38$^-$ fraction from HSC/LSC panel 1 and 2 of BM MNCs in TFR, normal and at diangosis outcome groups Bar graph showing the percentage of markers in Lin$^-$CD34$^+$38$^-$ fraction using BM MNC samples. Markers CD93$^+$ to CD36$^+$ are from HSC/LSC panel 1. HSC/LSC panel 1 = samples from TFR_E (TFR at point of trial entry) (purple) (n=16), TFR_X (TFR at trial exit) (green) (n=7), Normal (turquoise) (n=5), and At diangosis (patients at point of dianosis) (dark purple) (n=5). Markers from CD45RA$^+$ to CD117$^+$ are markers from HSC/LSC panel 2. HSC/LSC panel 2 = samples from TFR_E (TFR at point of trial entry) (purple) (n=20), TFR_X (TFR at trial exit) (green) (n=7), Normal (turquoise) (n=4), and At diangosis (patients at point of dianosis) (dark purple) (n=3). Bars show Mean with SD. Carried out two-way ANOVA, Tukey's multiple comparison test. P values: >0.05 (ns), <0.05 (*), <0.01 (**), <0.001 (***), <0.0001 (****).

By MPFC, the CD marker expression level was indicated as a percentage of the markers within the 'parent' live $Lin^-CD34^+38^-$ gate to identify the expression of markers within the stem cell population. While small numbers of cells are therefore represented as seemingly large percentages it demonstrates specifically the percentage of positive cells within the $CD38^-$ (primitive) population. To present another representation of the numbers the raw counts for these markers was also reported. From this it can be seen that the presence of markers like $CD25^+$ and $CD26^+$ were actually very low within normal samples and the numbers being seen could be due to debris, compensation etc. An additional limitation of presenting the data in this way is for some samples they had no stem cell ($Lin^-CD34^+38^-$) population, so there were no cells/events in the sample in the $CD38^-$ gate. As a result of this there can be no data produced for the markers within these samples. While these samples were still included in the analysis for counts they were left removed for the percentage graphs.

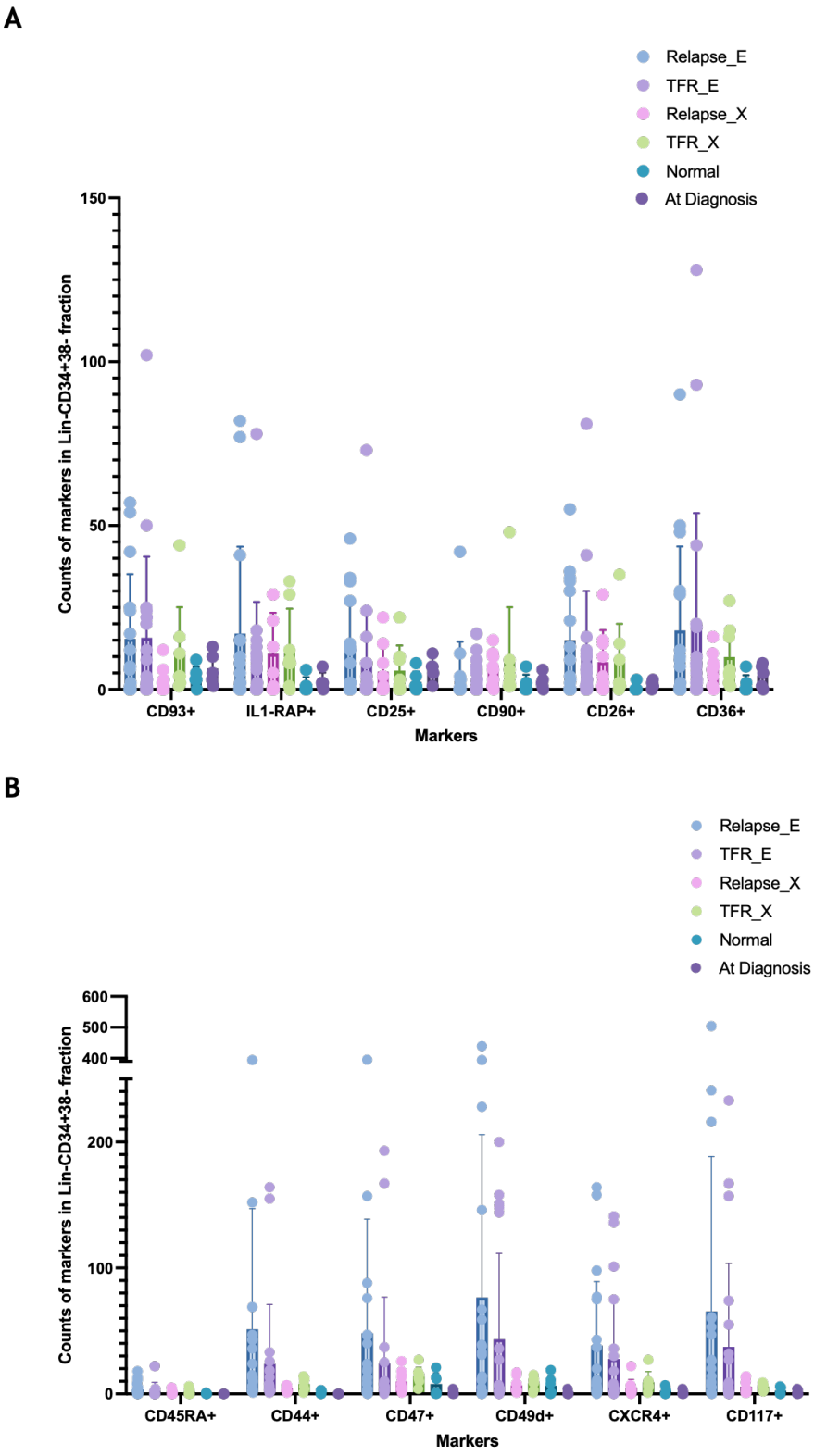

Figure 4-5 Changes to counts of markers within HSC/LSC panel 1 and 2 of BM MNCs in all patient outcome groups (A) Bar graph showing the counts of live cells in $Lin^{-}CD34^{+}38^{-}$ fraction and the markers using BM MNC samples. Samples from Relapse_E (relapse at point of trial entry) (blue) (n=16), TFR_E (TFR at point of trial entry) (purple) (n=19), Relapse_X (relapse at point of relapse) (pink) (n=9), TFR_X (TFR at trial exit) (green) (n=7), Normal (turquoise) (n=6), and CML at diagnosis (dark purple) (n=5). **(B)** Bar graph showing the counts of HSC/LSC panel 2 in $Lin^{-}CD34^{+}38^{-}$ fraction and the markers using BM MNC samples. Samples from Relapse_E (relapse at point of trial entry) (blue) (n=16), TFR_E (TFR at point of trial entry) (purple) (n=19), Relapse_X (relapse at point of relapse) (pink) (n=9), TFR_X (TFR at trial exit) (green) (n=7), Normal (turquoise) (n=6), and CML at diagnosis (dark purple) (n=5). Bars show Mean with SD. Carried out two-way ANOVA, Tukey's multiple comparison test. P values: >0.05 (ns), <0.05 (*), <0.01 (**), <0.001 (***), <0.0001 (****).

Using the same data for the HSC/LSC1 panel changes were identified within the relapse and TFR patient groups from the start of the trial to the end/point of relapse. Firstly, this demonstrates with all samples (Figure 4-6 A-B) and then with specifically paired samples from the same patient groups (Figure 4-6 C-D). There was a significant increase of $CD90^{+}$ marker within the relapse (R_X) patients at point of relapse compared to relapse patients at start of trial (R_E) (p=0.0462). Suggesting a potential biomarker for predicting/monitoring relapse. The rest of the comparisons did not show a significant change between the outcome groups.

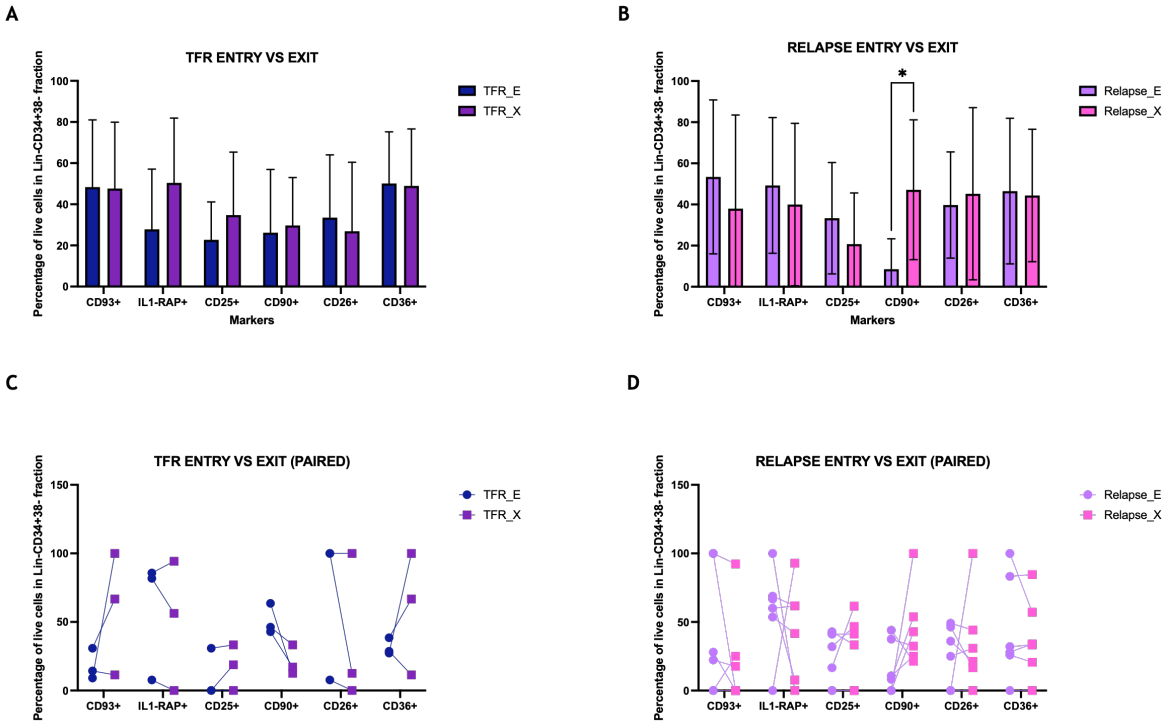

Figure 4-6 Changes to markers within LSC/HSC panel 1 of BM MNCs in TFR and relapse patients Bar graph of the CD marker data produced from BM MNC samples from TFR and relapse samples only. **(A)** Comaprison of TFR at trial entry (TFR_E) (n=16) vs TFR at end point of trial (TFR_X) (n=7). **(B)** Comparison of relapse at trial entry (R_E) (n=13) vs at point of relapse (R_X) (n=9). **(C)** Comaprison of TFR at trial entry (TFR_E) (n=3) vs TFR at end point of trial (TFR_X) (n=3) of paired samples only. **(D)** Comparison of relapse at trial entry (R_E) (n=3) vs at point of relapse (R_X) (n=3) of paired samples only. TFR_E shown in dark blue, TFR_X shown in dark purple. Relapse_E shown in light purple, Relapse_X shown in pink. Bars show Mean with SD. Carried out two-way ANOVA, Tukey's multiple comparison test. P values: >0.05 (ns), <0.05 (*), <0.01 (**), <0.001 (***), <0.0001 (****).

Using the HSC/LSC2 panel the changes in cell surface markers from trial entry to exit for TFR (Figure 4-7 A) and relapse (Figure 4-7 B) patient groups were investigated. There were no statistically significant changes identified indicating

that these markers may not be useful for monitoring TFR, and are not invovled in maintaining TFR or causing relapse.

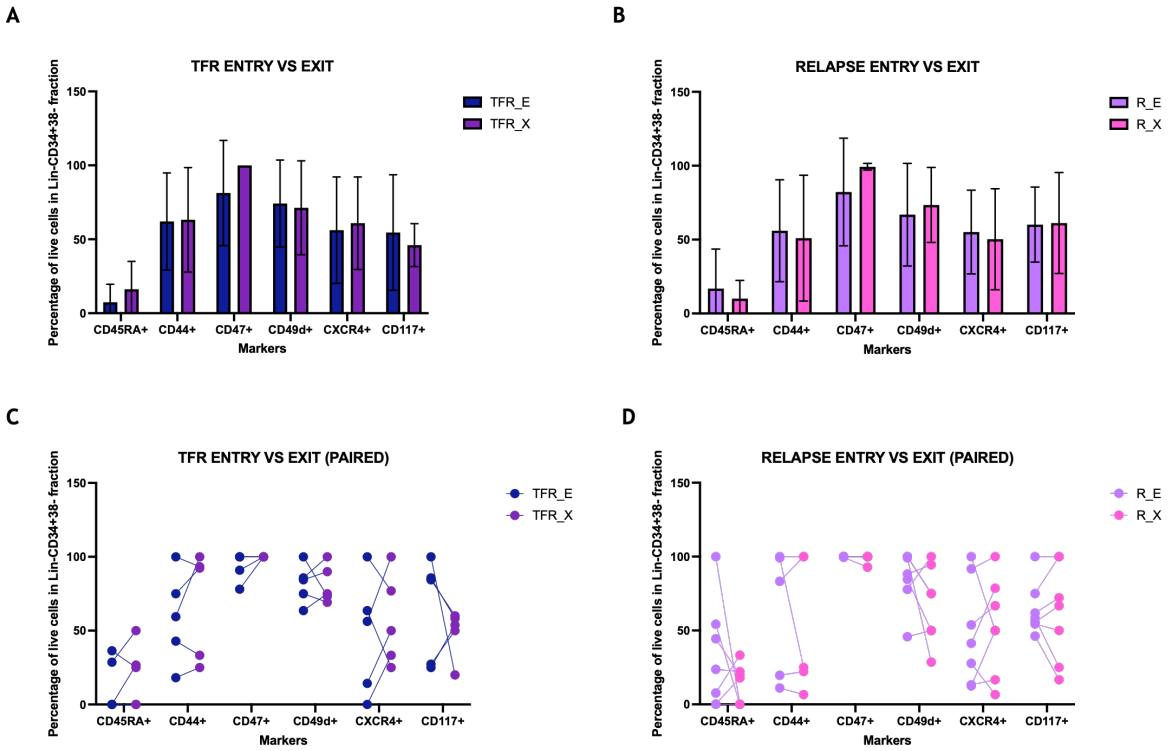

Figure 4-7 Changes to markers within LSC/HSC panel 2 of BM MNCs in TFR and relapse patients Bar graph of the CD marker data produced from BM MNC samples from TFR and relapse samples only. **(A)** Comaprison of TFR at trial entry (TFR_E) (n=21) vs TFR at end point of trial (TFR_X) (n=7). **(B)** Comparison of relapse at trial entry (R_E) (n=19) vs at point of relapse (R_X) (n=10). **(C)** Comaprison of TFR at trial entry (TFR_E) (n=6) vs TFR at end point of trial (TFR_X) (n=6) of paired samples only. **(D)** Comparison of relapse at trial entry (R_E) (n=5) vs at point of relapse (R_X) (n=5) of paired samples only. TFR_E shown in dark blue, TFR_X shown in dark purple. Relapse_E shown in light purple, Relapse_X shown in pink. Bars show Mean with SD. Carried out two-way ANOVA, Tukey's multiple comparison test. P values: >0.05 (ns), <0.05 (*), <0.01 (**), <0.001 (***), <0.0001 (****).

In pursuit of stem cell marker for the prediction of TFR, each marker was examined individually to monitor its change of expression. However, the data could also be examined as a whole to determine broader changes to the population. To do this all samples of interest were examined on a tsne plot which allowed each data point from the samples to be visualised together for each marker and to gain a visual representation of the change of expression to the markers within the $Lin^{-}CD34^{+}38^{-}$ population. This was done using Omiq software, the samples for each sample group were concatenated together for each marker. An example of a marker is shown in Figure 4-8 (A) demonstrates the markers with all samples concatenated within the live cells filter (B) Lin^{-}

filter and (C) $CD34^+$ filter. Markers were ultimately examined within the $CD34^+38^-$ filter to determine changes within the stem cell population.

Initially, all markers were examined together to identify trends in change of expression. Within HSC/LSC1 markers it was found that CD36 expression (Figure 4-9) had a high expression in relapse and TFR patients at start of the trial, as seen in the top left corner (black circle). However, after TKI cessation in both TFR and relapse samples this high expression was no longer seen. Additionally, analysis of CD26 and IL1-RAP together (Figure 4-10) found there is a small cluster of cells in the bottom left corner of the plots (black circle) for TFR_E, R_X and TFR_X outcomes, however this is lacking in R_E. In the outcome groups that have this cluster it appears the expression of these markers is increasing after stopping TKIs. It is not determined if these are leukaemic cells, their presence in R_X and TFR_X could be because they are normal HSCs.

From the HSC/LSC 2 markers CD47 expression was found to have high expression of this marker on the right side (orange circle) and low expression of the marker on the left side (green circle) from R_E and TFR_E patients, however at R_X and TFR_X the low expression of CD47 was no longer present while the high expression found on the right side of the plot remained (Figure 4-11).

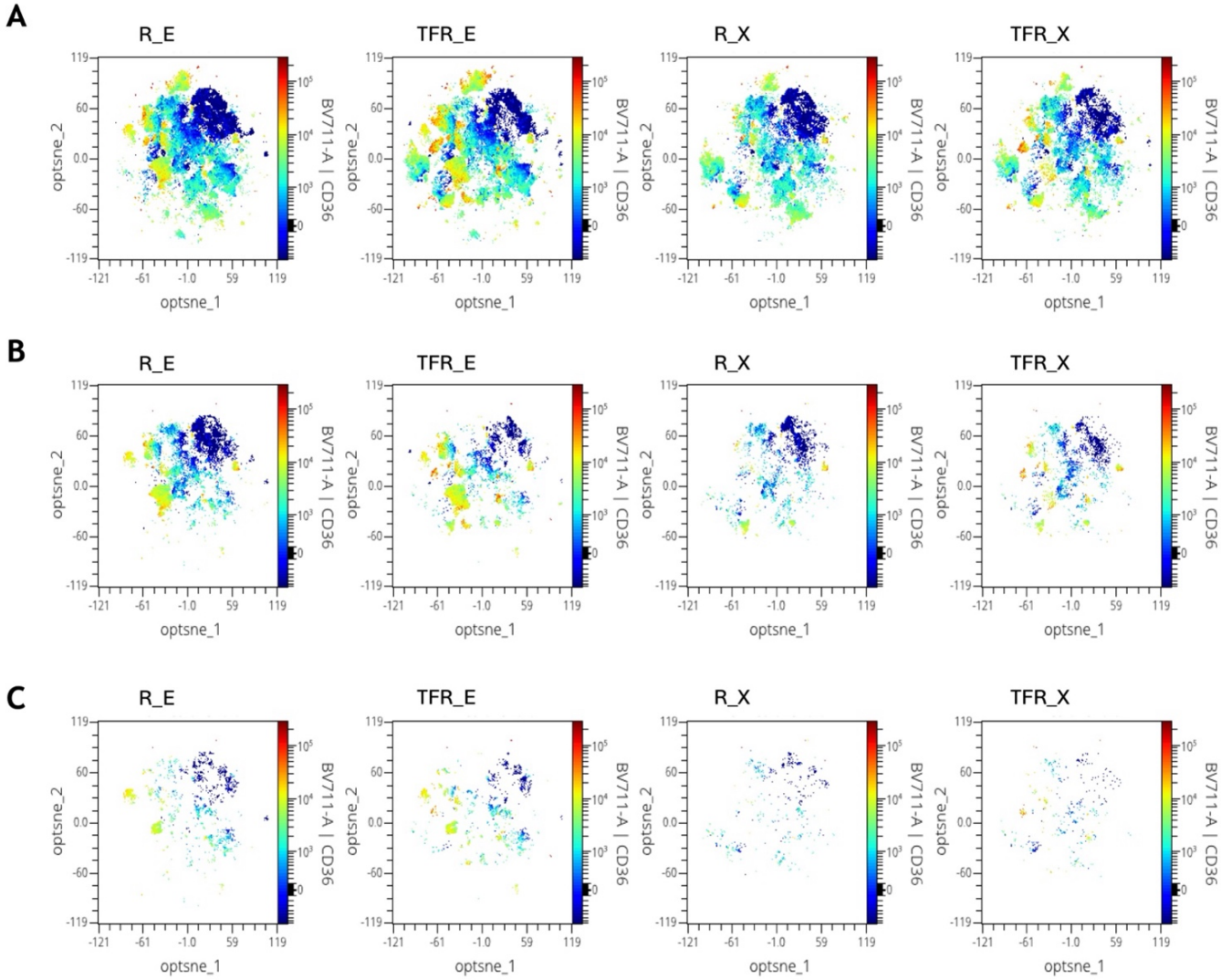

Figure 4-8 Breakdown of filtering concatenated samples within CD36 marker across all DESTINY samples Tsne plots of CD36 expression from the HSC/LSC 1 panel in each outcome group within the **(A)** Live cells filter **(B)** Lin^- filter and **(C)** $CD34^+$ filter.

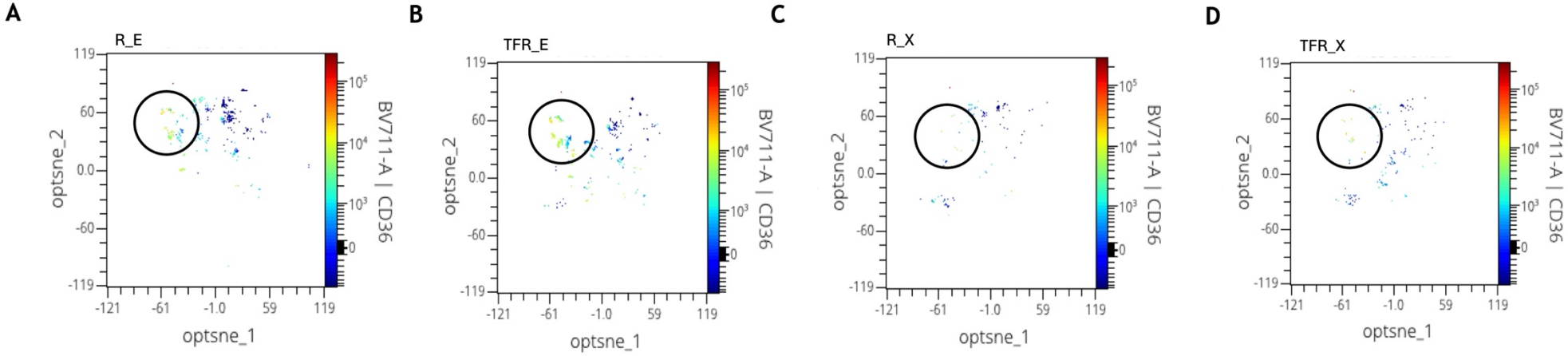

Figure 4-9 Expression changes of CD36 within live Lin$^-$CD34$^+$38$^-$ gates across all DESTINY patients Tsne plots of CD36 expression, from HSC/LSC 1 panel in **(A)** R_E (relapse at point of trial entry) **(B)** TFR_E (TFR at point of trial entry) **(C)** Relapse_X (relapse at point of relapse) **(D)** TFR_X (TFR at trial exit). Samples from each outcome group were concatonated. Black circle represents cluster of interest.

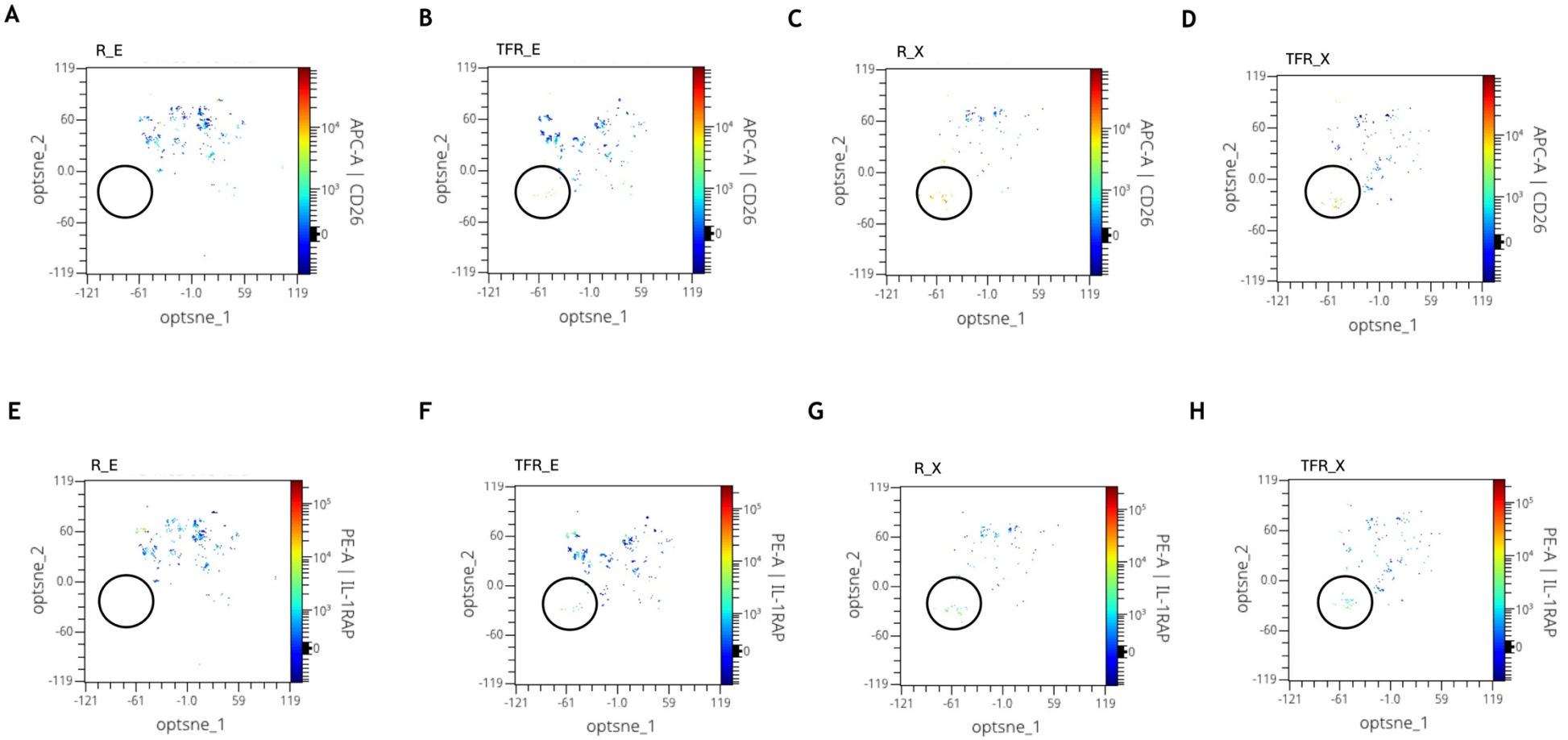

Figure 4-10 Expression changes of IL1-RAP and CD26 within live Lin$^-$CD34$^+$38$^-$ across all DESTINY patients Tsne plots of CD36 **(A-D)** and IL1-RAP **(E_H)** expression, from HSC/LSC 1 panel in **(A + E)** R_E (relapse at point of trial entry) **(B + F)** TFR_E (TFR at point of trial entry) **(C + G)** Relapse_X (relapse at point of relapse) **(D + H)** TFR_X (TFR at trial exit). Samples from each outcome group were concatonated. Black circle represents cluster of interest.

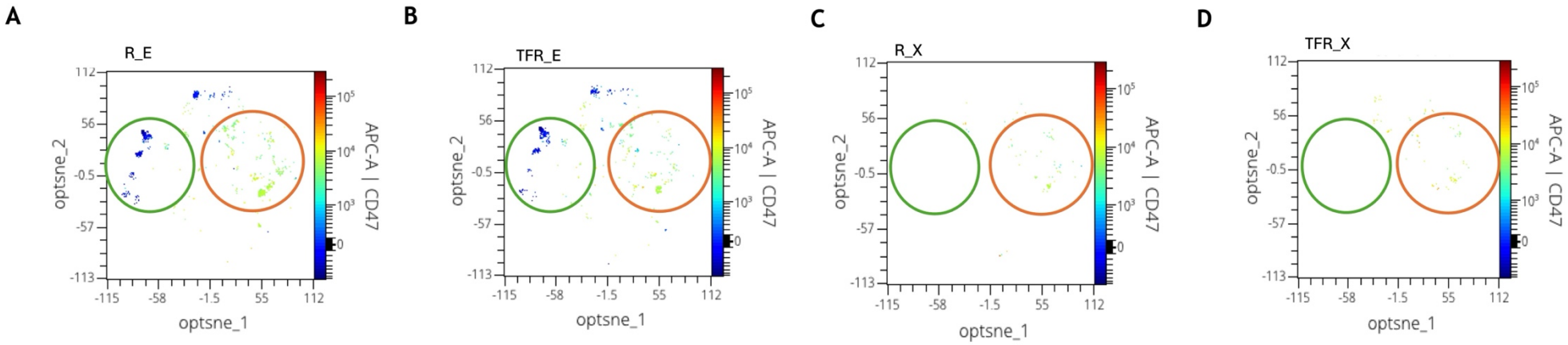

Figure 4-11 Expression changes of CD47 within live Lin$^-$CD34$^+$38$^-$ across all DESTINY patients Tsne plots of CD47 expression, from HSC/LSC 2 panel in **(A)** R_E (relapse at point of trial entry) **(B)** TFR_E (TFR at point of trial entry) **(C)** Relapse_X (relapse at point of relapse) **(D)** TFR_X (TFR at trial exit). Samples from each outcome group were concatonated. Green and orange circles represents clusters of interest.

As the CD93, IL1-RAP, CD25 and CD26 markers were the most important and had the most significant changes within Stemformatics analysis (Figure 4-1), these were also looked at within the outcome groups (Appendix - Figure 6-1). However, these did not show obvious clustering or patterning.

The Stemformatics data (Figure 4-1) found significant changes to the gene expression of the markers of interest within the progenitor populations of CML and normal patients. In order to examine the progenitor population within The DESTINY samples, the same markers were looked at within the $CD34^{+}38^{+}$ profile. This was to identify changes within the CML progenitors and how they vary.

For the IL1-RAP marker, CML patients at diagnosis (outwith DESTINY trial) had significantly increased expression compared to R_E (p=0.0140) and R_X (p=0.0373) DESTINY patients (Figure 4-12). Similarly, this increase was also seen within TFR patients at trial entry (TFR_E) (p=0.0024) (Figure 4-13).

Additionally, the CD25 marker was higher within the progenitor population of normal donors (p=0.0151) and patients at diagnosis (p=0.0054) compared to TFR_E (Figure 4-13).

Similar to the stem cell ($CD34^{+}38^{-}$) population there were significant changes seen within the CD44 marker within the progenitor ($CD34^{+}38^{+}$) population. There was lower expression in normal (p=0.0234) and at diagnosis (p=0.0226) samples when compared to TFR_E. Similarly, the CD44 expression was lower in the progenitor population of normal (p=0.0404) and at diagnosis (p=0.0331) samples in comparison to TFR_X.

The CD90 expression was also higher within normal progenitors compared to R_E (p=0.0006) (Figure 4-12) and TFR_E (p=0.0152).

Direct comparison of markers between entry and exit samples of TFR and relapse did not show any significant differences (Appendix - Figure 6-2 and Figure 6-3).

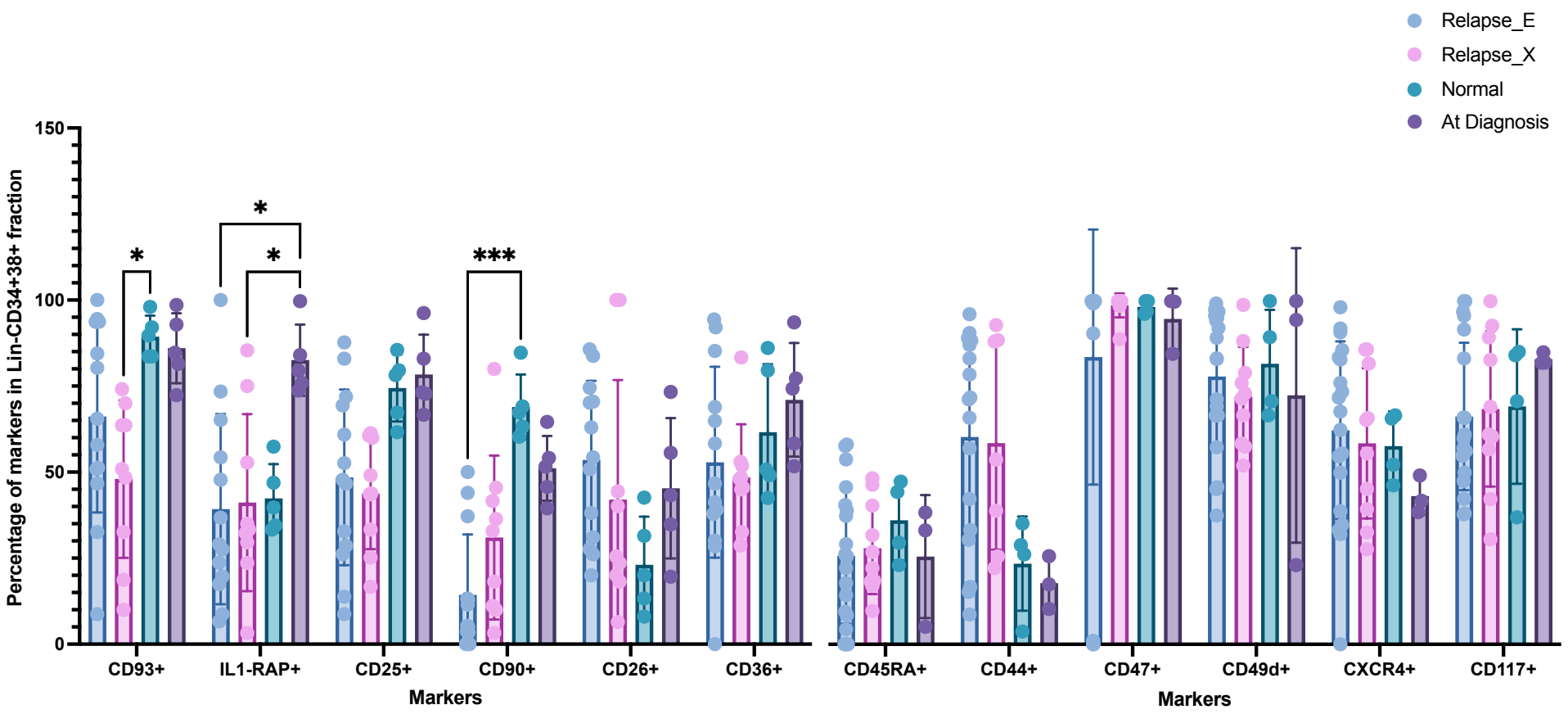

Figure 4-12 Changes to markers within Lin$^-$CD34$^+$38$^+$ fraction from HSC/LSC panel 1 and 2 of BM MNCs in relapse, normal and at diagnosis outcome groups
Bar graph showing the percentage of markers in Lin$^-$CD34$^+$38$^+$ fraction using BM MNC samples. Markers CD93$^+$ to CD36$^+$ are from HSC/LSC panel 1. HSC/LSC panel 1 = samples from Relapse_E (relapse at point of trial entry) (blue) (n=13), Relapse_X (relapse at point of relapse) (pink) (n=9), Normal (turquoise) (n=5), and At diangosis (patients at point of dianosis) (dark purple) (n=5). Markers from CD45RA$^+$ to CD117$^+$ are markers from HSC/LSC panel 2. HSC/LSC panel 2 = samples from Relapse_E (relapse at point of trial entry) (blue) (n=19), Relapse_X (relapse at point of relapse) (pink) (n=10), Normal (turquoise) (n=4), and At diangosis (patients at point of dianosis) (dark purple) (n=3). Bars show Mean with SD. Carried out two-way ANOVA, Tukey's multiple comparison test. P values: >0.05 (ns), <0.05 (*), <0.01 (**), <0.001 (***), <0.0001 (****).

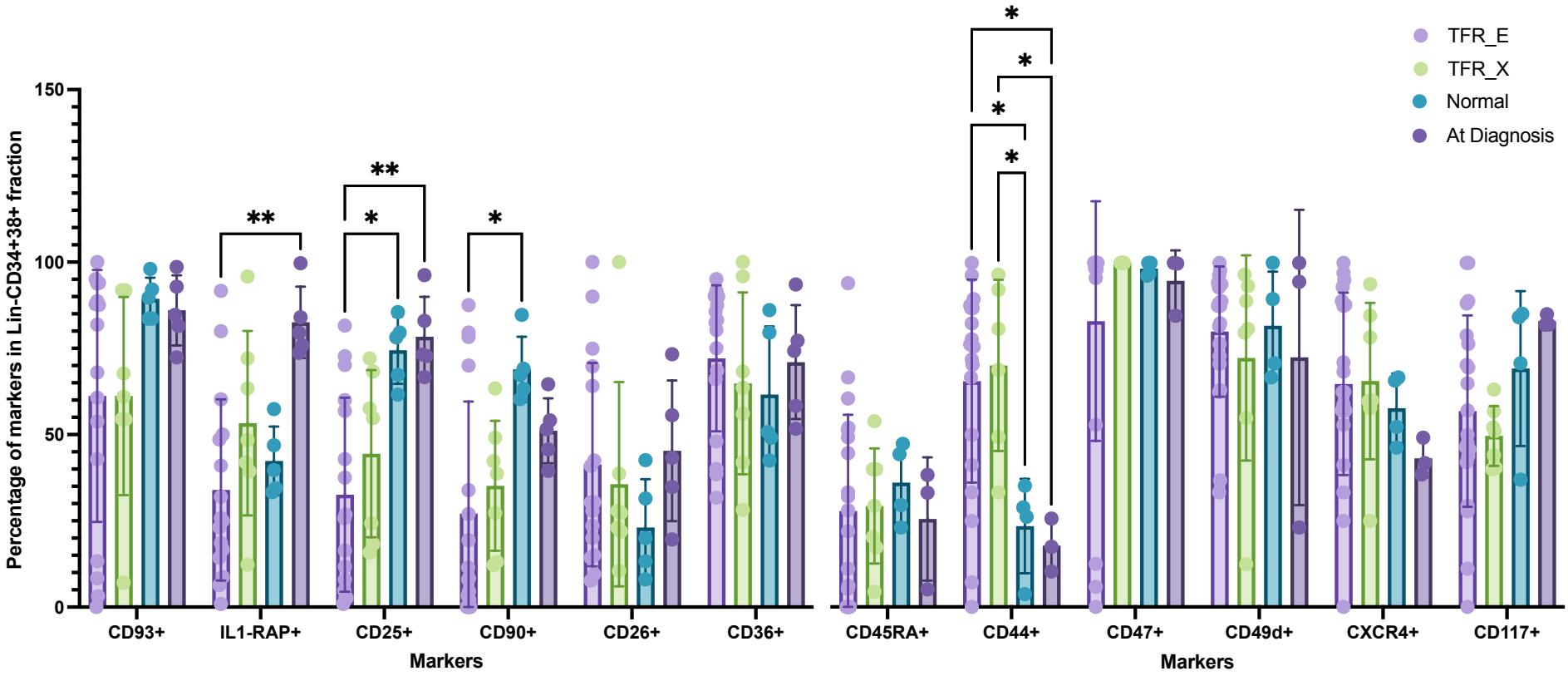

Figure 4-13 Changes to markers within Lin$^-$CD34$^+$38$^+$ fraction from HSC/LSC panel 1 and 2 of BM MNCs in TFR, normal and at diangosis outcome groups
Bar graph showing the percentage of markers in Lin$^-$CD34$^+$38$^+$ fraction using BM MNC samples. Markers CD93$^+$ to CD36$^+$ are from HSC/LSC panel 1. HSC/LSC panel 1 = samples from TFR_E (TFR at point of trial entry) (purple) (n=16), TFR_X (TFR at trial exit) (green) (n=7), Normal (turquoise) (n=5), and At diangosis (patients at point of dianosis) (dark purple) (n=5). Markers from CD45RA$^+$ to CD117$^+$ are markers from HSC/LSC panel 2. HSC/LSC panel 2 = samples from TFR_E (TFR at point of trial entry) (purple) (n=20), TFR_X (TFR at trial exit) (green) (n=7), Normal (turquoise) (n=4), and At diangosis (patients at point of dianosis) (dark purple) (n=3). Bars show Mean with SD. Carried out two-way ANOVA, Tukey's multiple comparison test. P values: >0.05 (ns), <0.05 (*), <0.01 (**), <0.001 (***), <0.0001 (****).

4.4.3 CD35 is not a useful marker for the prediction of TFR

After data had been gathered with the HSC/LSC1 and HSC/LSC2 panels, Warfvinge *et al.*, described the role of CD35 as a predictive marker of CML. It was found that $CD26^{+}CD35^{-}$ determined $BCR::ABL1^{+}$ population and $CD26^{-}CD35^{+}$ was representative of a $BCR::ABL1^{-}$ population (Warfvinge et al. 2024). The ratio of $CD26^{+}CD35^{-}$ to $CD26^{-}CD35^{+}$ was much higher in patients who experiences TKI failure than those with optimal response (Warfvinge et al. 2024), indicating $CD35^{+}$ was higher in patients who have a better response to TKIs. Due to this published finding, IL1-RAP was replaced with CD35 in creating an HSC/LSC3 panel to identify the usefulness of this putative biomarker of TFR within the DESTINY trial samples.

The new panel, HSC/LSC 3 had the markers:

Target	Fluorochrome
Lineage	FITC
CD34	BV421
CD38	BV786
CD90	PE-Cy7
CD25	BV605
CD26	APC
CD93	BB700
CD35	PE
VIABILITY	7-AAD

Table 4-5 HSC/LSC3 panel

Due to sample availability, there were no TFR patient samples at point of end of trial (TFR_X) available for testing with this panel. Interestingly, with the $CD35^{+}$ marker the expression of TFR_E and Relapse_E samples had no significant differences, and their expression levels were also similar to that of the normal samples. Additionally, the $CD35^{+}$ appeared to have a decrease trend in relapse patients' cell samples at point of relapse (R_X) akin to the levels seen in CML at diagnosis samples. This is perhaps unsurprising as previously mentioned $CD35^{+}$ expression is associated with $BCR::ABL1^{-}$ population, so it would make sense for patients at point of relapse and at diagnosis to have lower expression than normal donors and DESTINY patients still in remission from TKIs. Hence $CD35^{+}$ may not be a useful marker of TFR, and patients in remission have similar $CD35^{+}$

expression levels to normal. Additionally, the lowest expression of $CD35^+$ was identified in the R_X samples and patients at diagnosis, both groups are not using TKIs indicating the loss of $CD35^+$ expression could be associated with active disease state of CML, which could suggest loss of $CD35^+$ could be used to be monitored for relapse. However, these changes seen were not significant.

Unlike the HCS/LSC 1 panel significant changes were not seen within the $CD90^+$ marker, but there were changes in markers $CD25^+$ and $CD26^+$. Previously there were not any changes for $CD26^+$ however with the HSC3 panel there was significant decrease in $CD26^+$ at point of relapse compared to normal BM samples ($p=0.0404$). These differences within the markers between panels HSC/LSC1 and HSC/LSC 3 could be due to the expression profile in which they are tested, for more specific and consistent HSC/LSC examination a more stringent gating profile is perhaps required. While the results from the matching markers is slightly different than previously, the inconsistency and lack of statistical significance indicate there are no markers that would be useful as a potential biomarker of TFR or relapse.

A

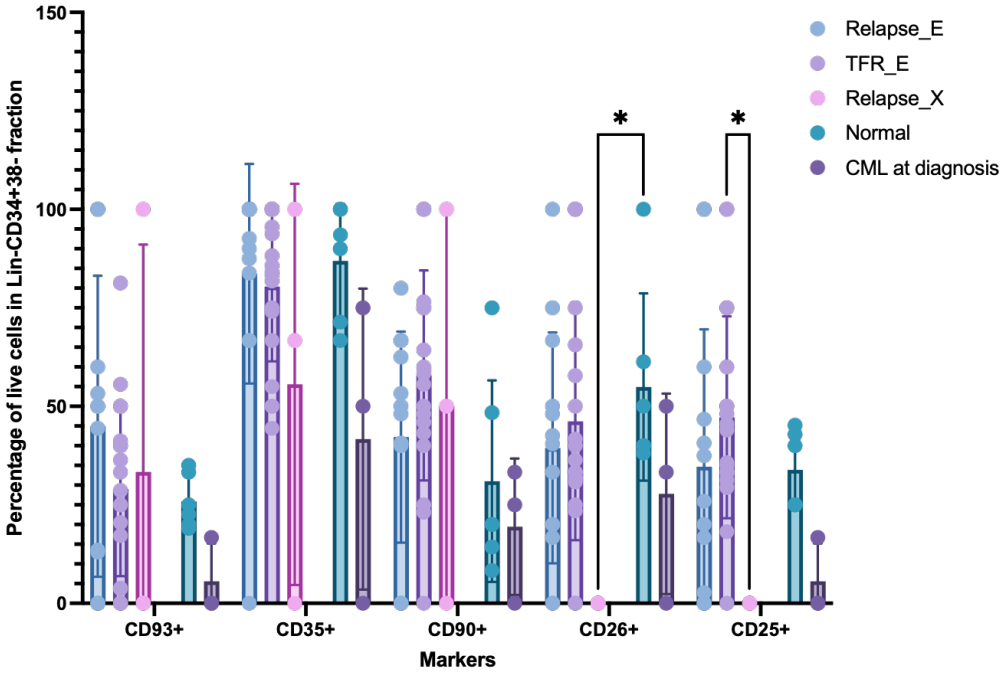

B

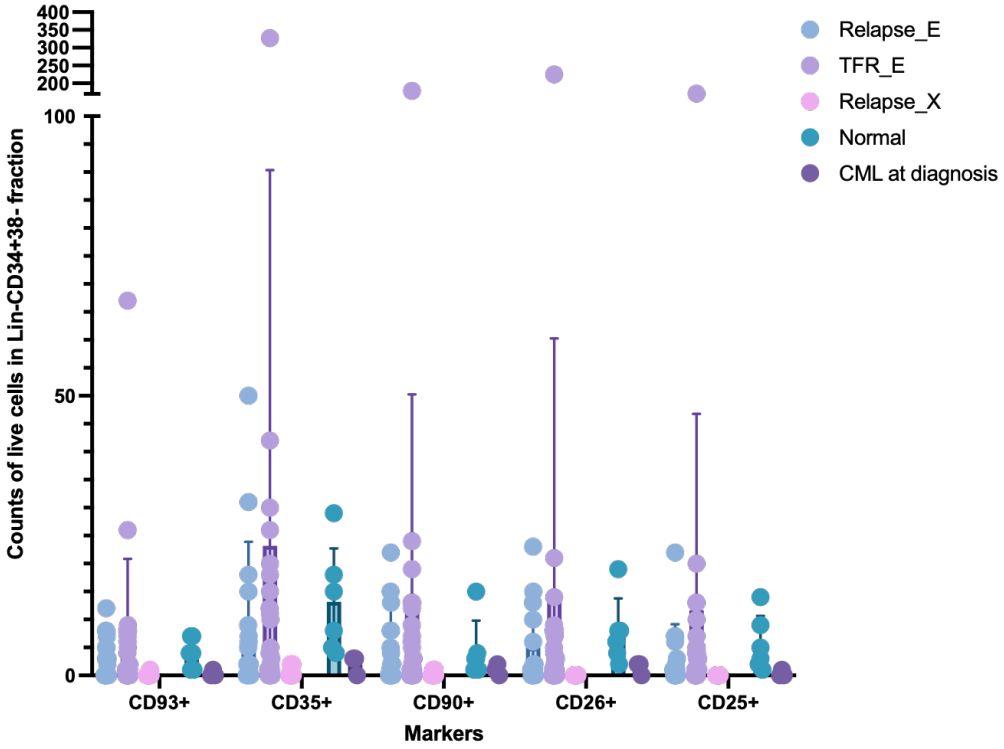

Figure 4-14 Changes to markers within HSC/LSC panel 3 population of BM MNCs in all patient outcome groups (A) Bar graph showing the percentage of live cells in Lin$^-$CD34$^+$38$^-$ fraction and the markers using BM MNC samples. **(B)** Bar graph showing the counts of live cells in Lin$^-$CD34$^+$38$^-$ fraction and the markers using BM MNC samples. Samples from Relapse_E (blue) (n=13), TFR_E (purple) (n=19), Relapse_X (pink) (n=3), TFR_X (green) (n=0), Normal (turquoise) (n=6), and CML at diagnosis (dark purple) (n=3). Bars show Mean with SD. Carried out two-way ANOVA, Tukey's multiple comparison test. P values: >0.05 (ns), <0.05 (*), <0.01 (**), <0.001 (***), <0.0001 (****).

The samples were compared at trial entry with exit with relapse samples, which ultimately did not show any significant changes. These markers would not be useful for predicting relapse.

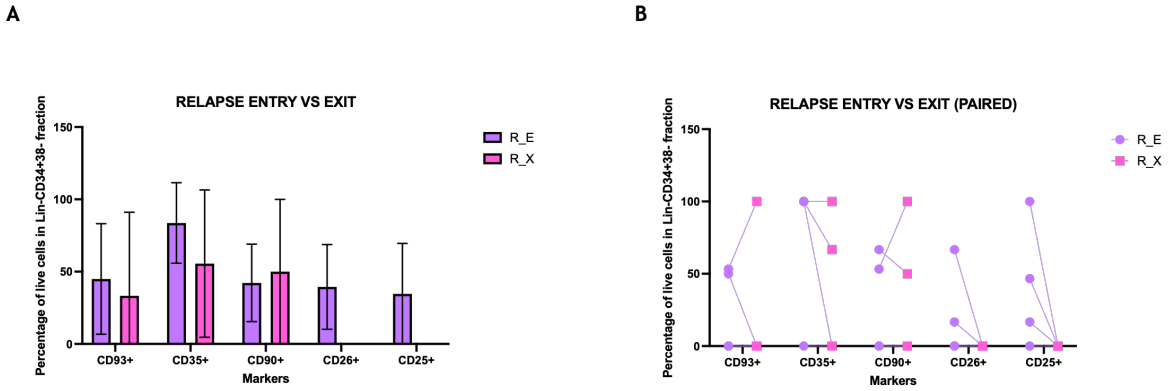

Figure 4-15 Changes to markers within LSC/HSC panel 3 of BM MNCs in relapse patients Bar graph of the CD marker data produced from BM MNC samples from relapse samples only. **(A)** Comparison of relapse at trial entry (R_E) (n=13) vs at point of relapse (R_X) (n=3). **(B)** Comparison of relapse at trial entry (R_E) (n=4) vs at point of relapse (R_X) (n=4) of paired samples only. TFR_E shown in dark blue, TFR_X shown in dark purple. Relapse_E shown in light purple, Relapse_X shown in pink. Bars show Mean with SD. Carried out two-way ANOVA, Tukey's multiple comparison test. P values: >0.05 (ns), <0.05 (*), <0.01 (**), <0.001 (***), <0.0001 (****).

Analysis of stem cell markers continued with HSC/LSC 3 panel. From the tsne plots it can be seen that at trial entry TFR and relapse patients have similar expression levels of CD35 however, by the point of relapse this expression appears to be almost completely lost (black circle).

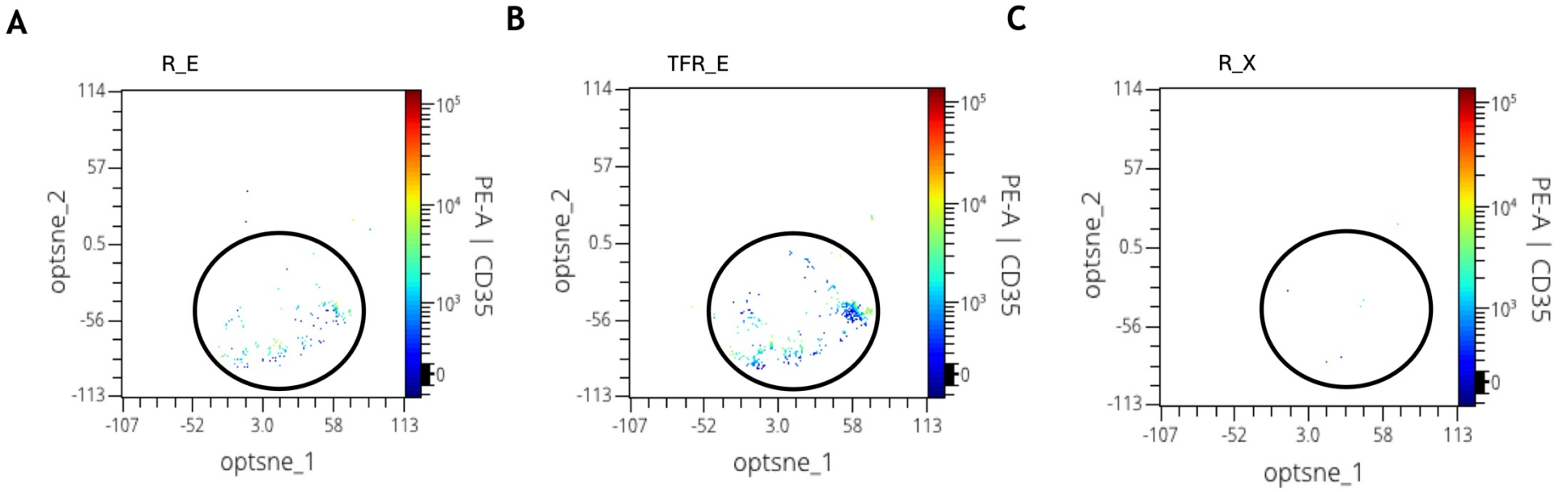

Figure 4-16 Expression changes of CD35 within live Lin$^-$CD34$^+$38$^-$ across all DESTINY patients Tsne plots of CD35 expression, from HSC/LSC 3 panel in **(A)** R_E (relapse at point of trial entry). **(B)** TFR_E (TFR at point of trial entry). **(C)** Relapse_X (relapse at point of relapse). Samples from each outcome group were concatonated. Black circle represents cluster of interest.

The progenitor population was also examined within the HSC/LSC 3 panel of markers. The CD35 marker had the highest expression within the patients at diagnosis and was significantly lower in R_E (p=0.0008), TFR_E (p=0.0045), R_X (p=<0.0001) and normal (p=0.0003).

Interestingly, the CD90 marker appears to have a significantly reduced expression within normal patients compared to TFR at trial entry (p=0.0225).

The CD26 marker expression is significantly higher on the patients at diagnosis, compared to all other outcome groups tested, R_E (p=0.0032), TFR_E (p=0.0097), R_X (p=<0.0001) and normal (p=0.0119). Similarly, the CD25 expression is highest in patients at diagnosis with respect to R_E and R_X patients.

Direction comparison of TFR and relapse groups at trial entry and at trial endpoint or relapse did not show any statistically significant changes (Appendix - Figure 6-4).

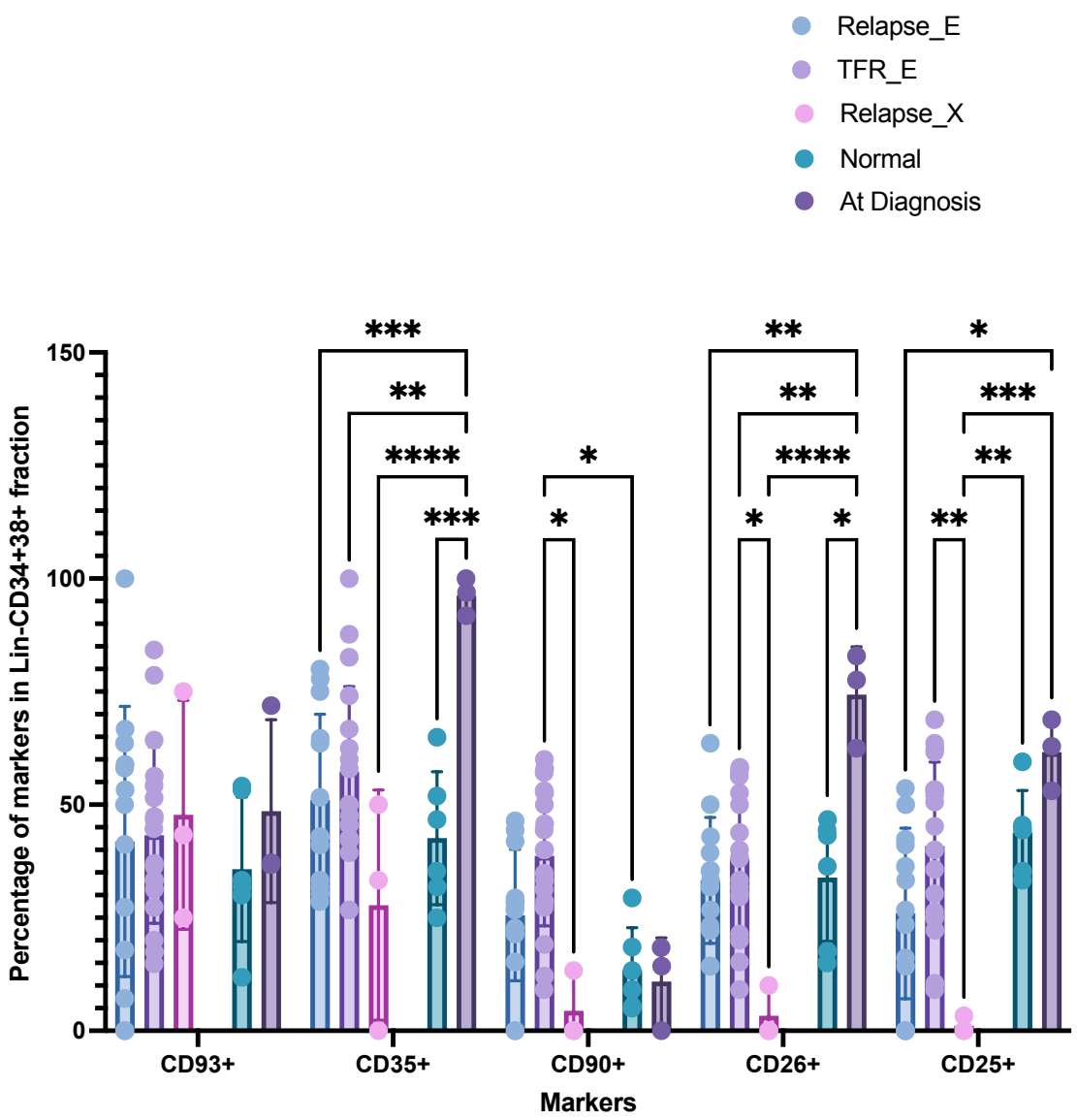

Figure 4-17 Changes to markers within Lin$^-$CD34$^+$38$^+$ fraction from HSC/LSC panel 3 population of BM MNCs in all patient outcome groups Bar graph showing the percentage of live cells in Lin$^-$CD34$^+$38$^+$ fraction and the markers using BM MNC samples. Samples from Relapse_E (blue) (n=13), TFR_E (purple) (n=19), Relapse_X (pink) (n=3), TFR_X (green) (n=0), Normal (turquoise) (n=6), and CML at diagnosis (dark purple) (n=3). Bars show Mean with SD. Carried out two-way ANOVA, Tukey's multiple comparison test. P values: >0.05 (ns), <0.05 (*), <0.01 (**), <0.001 (***), <0.0001 (****).

4.4.4 Determining progenitor proliferation and differentiation potential of in TFR versus relapse

Functional colony forming assays give a better idea of the clonogenicity of stem and progenitor cells.

The frequency of progenitors (ST-CFC) and stem cells (LTC-IC) as well as the proliferation and differentiation potential of these cells were investigated to determine the differences between the two patient outcome groups. As well as

looking at the number of colonies produced the colony type was also determined to examine the differentiation capacity of the samples (BFU-E, CFU-M, CFU-G, CFU-GM and CFU-GEMM).

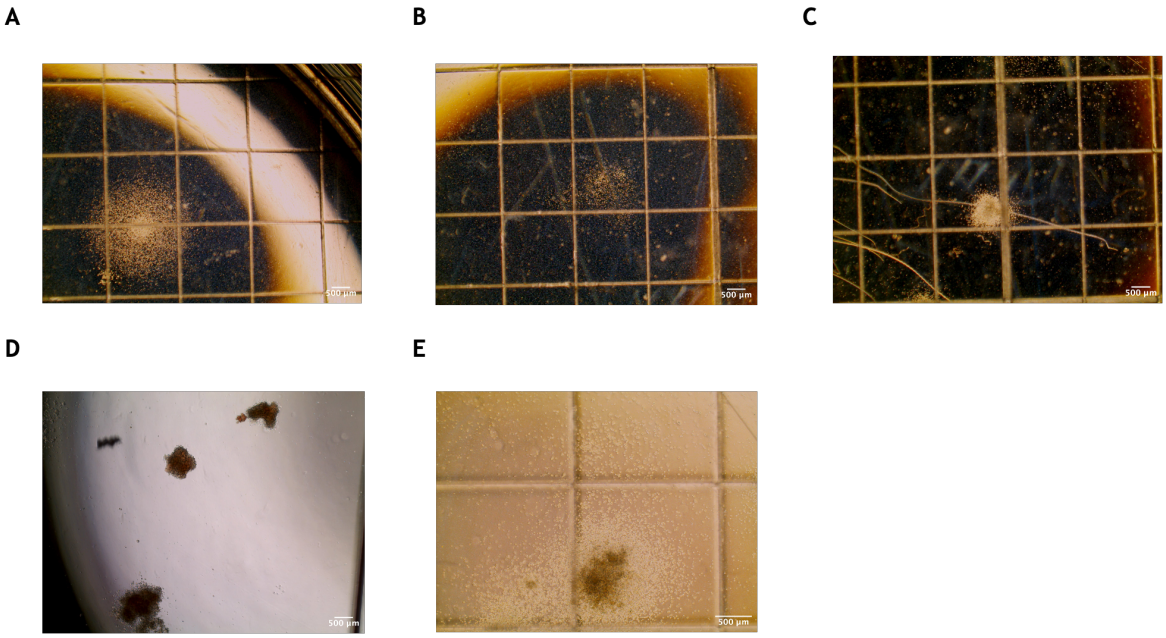

Figure 4-18 Colonies identified within ST-CFC and LTC-IC assays Images of colony types identified and counted from LTC-IC and ST-CFC assays. Taken on EVOS microscope **(A-D)** at 2X and **(E)** at 4X magnification. Scale bar - 500 µm. **(A)** CFU-GM **(B)** CFU-M **(C)** CFU-G **(D)** BFU-E **(E)** CFU-GEMM.

For the ST-CFC assay 10,000 MNCs were counted and placed into Methocult for 14 days after which colonies were counted. A marked increase in the total number of colonies produced by samples from CML patients at diagnosis compared to normal was seen (Figure 4-15), which was expected as *BCR::ABL1* drives proliferation of haematopoietic cells. Overall, there was lower scoring of CFU-GEMM and BFU-E compared to CFU-M, CFU-G and CFU-GM. This was also expected as BFU-E would indicate erythroid skewing and CML patients have more myeloid cells and less erythroid cells. Furthermore, the CFU-GEMM forms from a more primitive cell that is less frequent hence less likely to be seen in this type of assay. The differences seen were not statistically significant. Average number of CFU-G and CFU-M colonies per 10,000 cells appeared to be similar between the R_E and TFR_E patient outcome cohorts. Within the total colonies produced the cohort with the lowest number of colonies was from normal patients, all CML patients treated or not (at diagnosis and within DESTINY) had higher colony forming capacity within their progenitor cells.

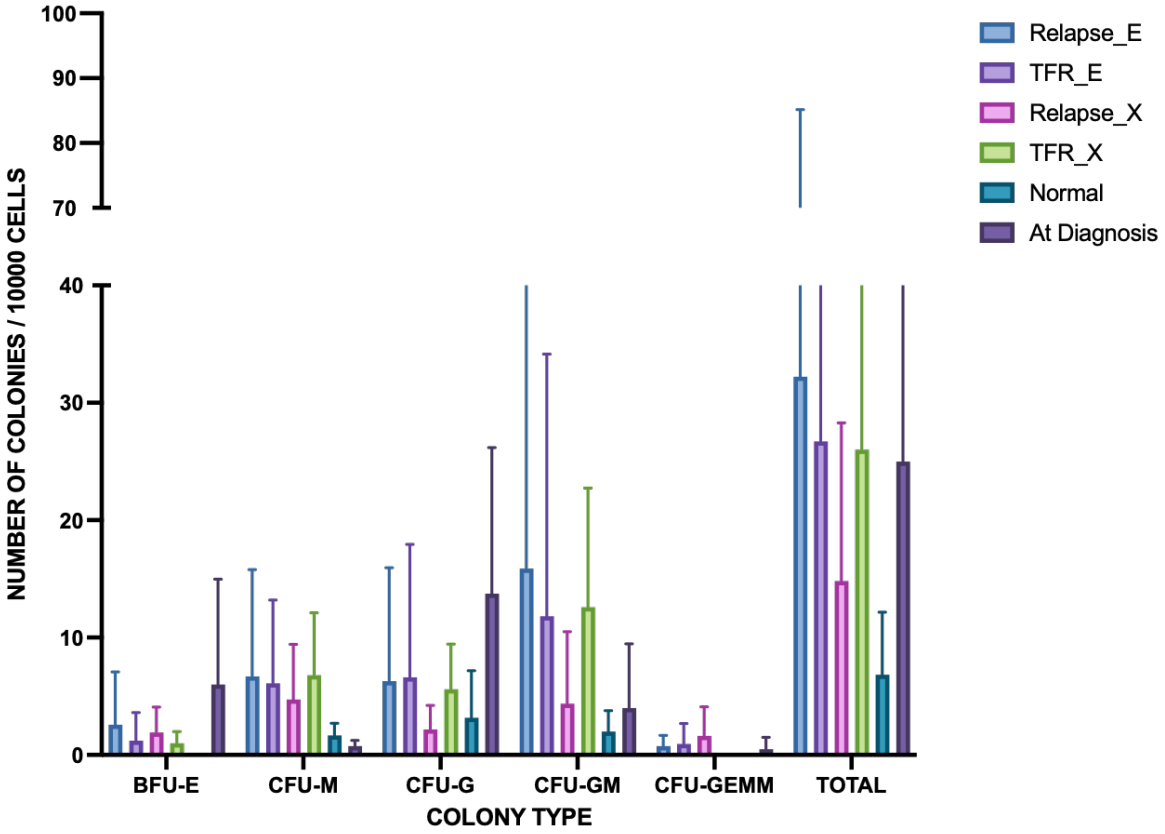

Figure 4-19 Changes to colonies produced by ST-CFC with all patient outcome groups Bar graph of the ST-CFC data produced from BM MNC samples from Relaspe_E (n=17), TFR_E (n=18), Relapse_X (n=11), TFR_X (n=5), Normal (n=6), CML at diagnosis (n=4). The colony types examined were BFU-E, CFU-M, CFU-G, CFU-GM, CFU-GEMM and the total number of colonies. Bars show Mean with SD. Carried out two-way ANOVA, Tukey's multiple comparison test. P values: >0.05 (ns), <0.05 (*), <0.01 (**), <0.001 (***), <0.0001 (****).

Additionally, the relapse and TFR samples were looked at individually at the start of the trial compared to the end of the trial / point of relapse (Figure 4-20 A&B). This was done for all samples as a group and additionally for paired samples. As before there was lower levels of BFU-E and CFU-GEMM compared to the other colony types. There was a significant increase in total colonies produced when comparing paired TFR patients at entry into trial (TFR_E) with end of trial (TFR_X) (p=0.0003) (Figure 4-20 C). While an increase in progenitor proliferation is usually associated with worse prognosis this appears to be associated with maintenance of TFR. However, as these patients are maintaining TFR the increased proliferation is not being driven by BCR::ABL1 therefore is not leading to loss of TFR. When looking at individual colony types it appears the increase in total colony number scored was owing to an uplift in CFU-M, CFU-G

and CFU-GM colonies specifically. There were no significant changes seen within the relapse patients' samples from the start of trial (R_E) compared to point of relapse (R_X) with respect to proliferation or differentiation capacity of the cells.

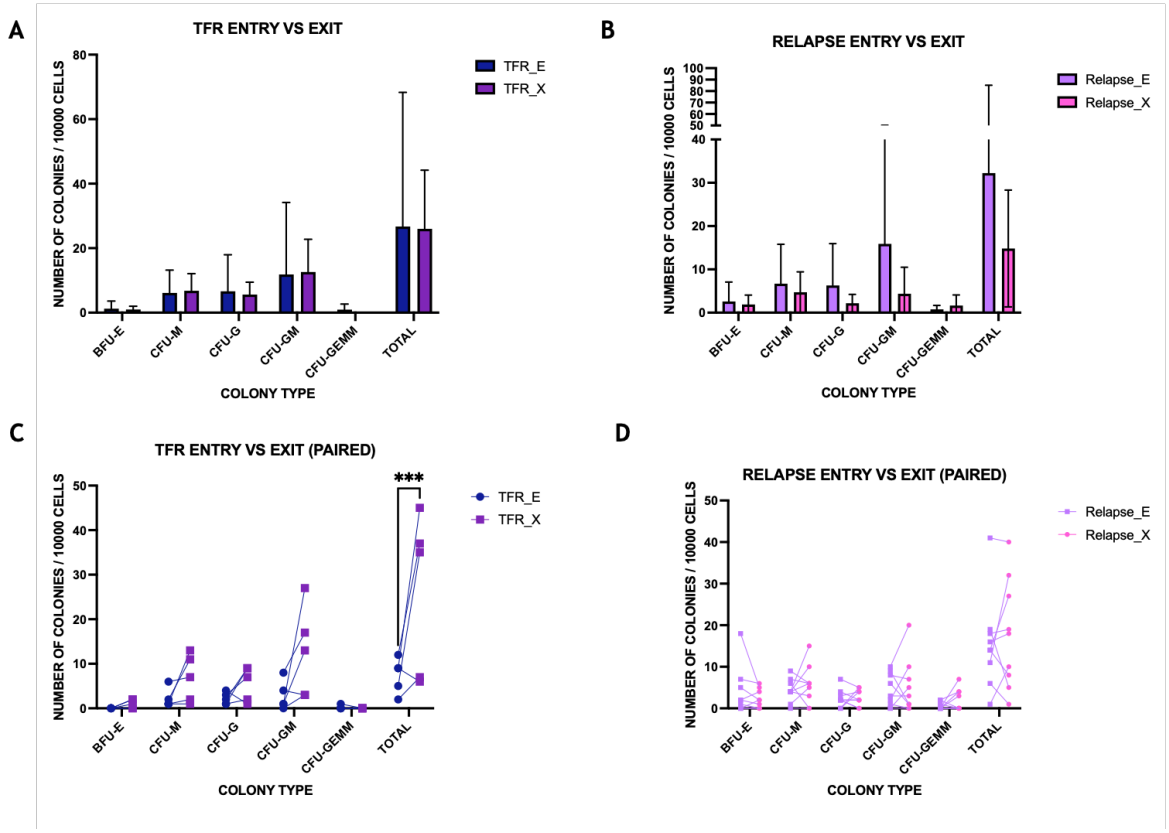

Figure 4-20 Changes to colonies produced by ST-CFC in TFR and relapse patients Bar graph of the ST-CFC data produced from BM MNC samples from TFR and relapse samples only. **(A)** Comaprison of TFR at trial entry (TFR_E) (n=18) vs TFR at end point of trial (TFR_X) (n=5). **(B)** Comparison of relapse at trial entry (R_E) (n=17) vs at point of relapse (R_X) (n=11). **(C)** Comaprison of TFR at trial entry (TFR_E) (n=5) vs TFR at end point of trial (TFR_X) (n=5) of paired samples only. **(D)** Comparison of relapse at trial entry (R_E) (n=9) vs at point of relapse (R_X) (n=9) of paired samples only. The colony types examined were BFU-E, CFU-M, CFU-G, CFU-GM, CFU-GEMM and the total number of colonies. TFR_E shown in dark blue, TFR_X shown in dark purple. Relapse_E shown in light purple, Relapse_X shown in pink. Bars show Mean with SD. Carried out two-way ANOVA, Tukey's multiple comparison test. P values: >0.05 (ns), <0.05 (*), <0.01 (**), <0.001 (***), <0.0001 (****).

4.4.5 Determining the proliferation and differentiation potential of stem cells in TFR vs relapse patients

LTC-IC conditions allow the primitive cells to proliferate and differentiate and produce colonies which allow us to see not only how many cells of colony forming potential were left but also the type of cells they produced. When setting up this assay the number of $Lin^{-}CD34^{+}$ cells produced was variable between samples, therefore the analysis of the number of colonies was

normalised to 5000 cells as this was the average number of $Lin^{-}CD34^{+}$ cells that was able to be sorted from most samples.

There were no statistically significant changes seen between of the number of the different colony types produced within any of the patient cohorts (Figure 4-21). TFR_E had the highest level of CFU-GM than any other patient cohort. Additionally, TFR_X patients at the end point of trial have the highest level of BFU-E colonies produced. The colony type with the lowest numbers throughout all outcome groups tested was the most primitive population (CFU-GEMM). Additionally, within the CFU-GEMM colonies the highest number of colonies counted came from the relapse samples at entry (R_E). The levels of CFU-M and CFU-G appear to have similar colony numbers in relapse and TFR samples before the trial.

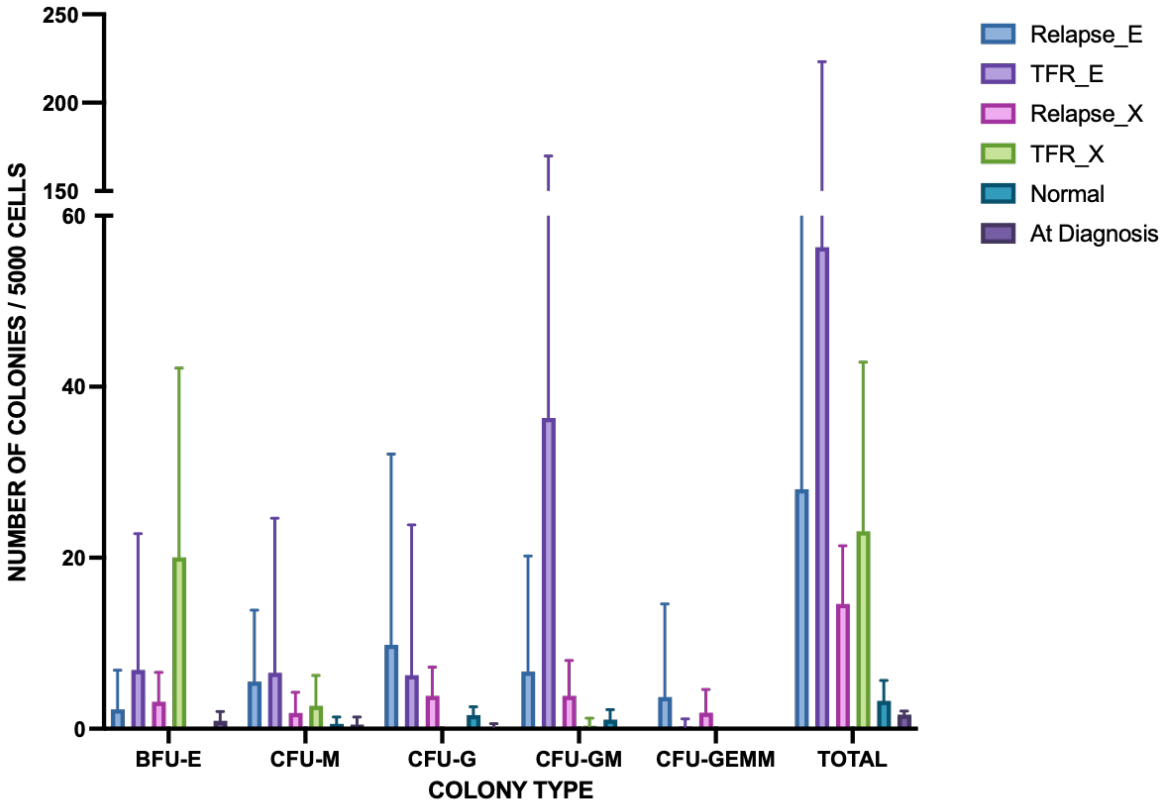

Figure 4-21 Changes to colonies produced by LTC-IC with all patient outcome groups Bar graph of the LTC-IC data produced from BM MNC samples from Relapse_E (n=12), TFR_E (n=14), Relapse_X (n=7), TFR_X (n=6), Normal (n=5), and CML at diagnosis (n=3). The colony types examined were BFU-E, CFU-M, CFU-G, CFU-GM, CFU-GEMM and the total number of colonies. Bars show Mean with SD. Carried out two-way ANOVA, Tukey's multiple comparison test. P values: >0.05 (ns), <0.05 (*), <0.01 (**), <0.001 (***), <0.0001 (****).

Paired comparison of individual relapse patients at entry into trial (R_E) compared to the point of relapse (R_X) showed a significant decrease in the total number of colonies (Figure 4-22 D; p=0.0257).

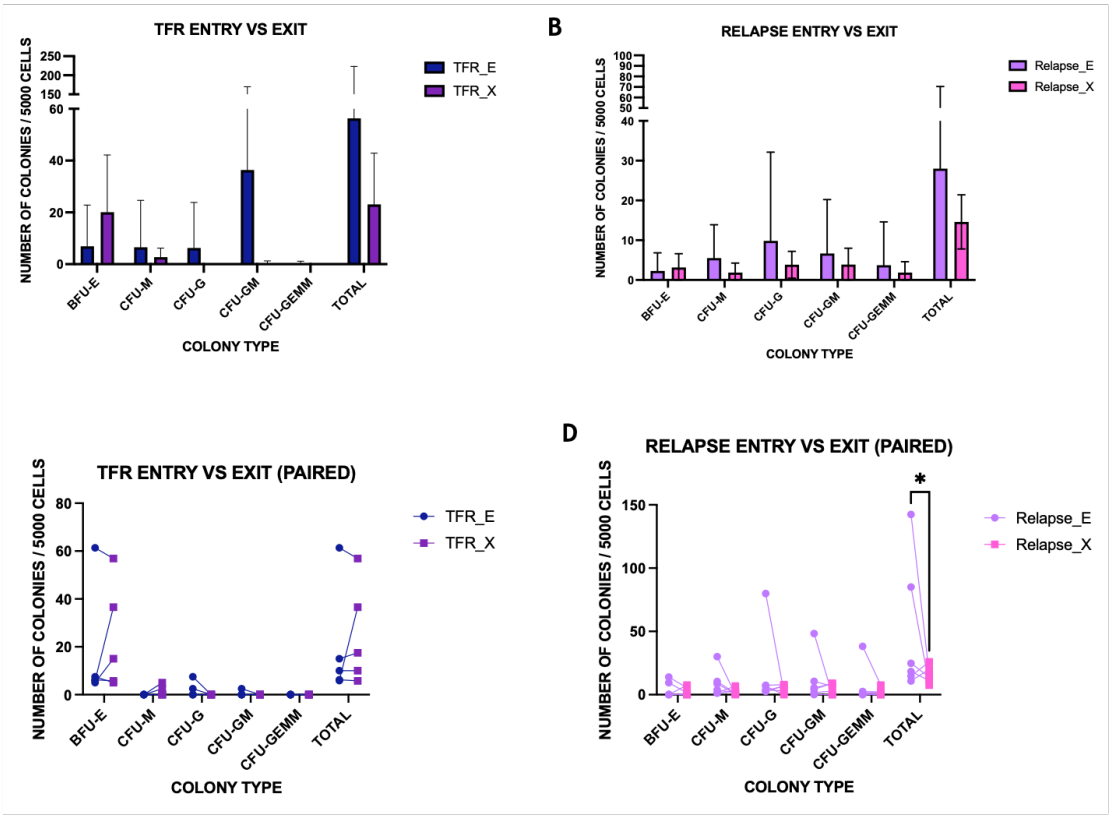

Figure 4-22 Changes to colonies produced after LTC-IC in TFR and relapse patients Bar graph of the LTC-IC data produced from BM MNC samples from TFR and relapse samples only. **(A)** Comaprison of TFR at trial entry (TFR_E) (n=14) vs TFR at end point of trial (TFR_X) (n=6). **(B)** Comparison of relapse at trial entry (R_E) (n=12) vs at point of relapse (R_X) (n=7). **(C)** Comaprison of TFR at trial entry (TFR_E) (n=5) vs TFR at end point of trial (TFR_X) (n=5) of paired samples only. **(D)** Comparison of relapse at trial entry (R_E) (n=6) vs at point of relapse (R_X) (n=6) of paired samples only. The colony types examined were BFU-E, CFU-M, CFU-G, CFU-GM, CFU-GEMM and the total number of colonies. TFR_E shown in dark blue, TFR_X shown in dark purple. Relapse_E shown in light purple, Relapse_X shown in pink. Bars show Mean with SD. Carried out two-way ANOVA, Tukey's multiple comparison test. P values: >0.05 (ns), <0.05 (*), <0.01 (**), <0.001 (***), <0.0001 (****).

4.4.6 BCR::ABL1 is not the driving factor of colony formation within stem and progenitor cells of DESTINY patients

While colony formation assays examine the differentiation and proliferation capacity of stem and progenitor cells, it is unclear if the changes seen are from leukaemic or normal cells. One way of enumerating the leukaemic burden of these colonies to determine if this is involved in patients achieving TFR or not is to quantify these *BCR::ABL1* expressing cells present within the BM and identifying if they are associated with relapse. The *BCR::ABL1* expression levels

from pooled colonies for each sample from the ST-CFC and LTC-IC assays were tested using the Fluidigm Biomark system. The RNA extracted from these samples was very low due to the low cell and colony numbers, for the purposes of a Fluidigm chip, usually 300-500ng of RNA is used for optimum and consistent results. For the purposes of this experiment and due to the sensitive nature of the chip, the maximum volume of RNA had to be used. A study that developed a SMART-Seq2 method to analyse just 2,000 stem/progenitor cells successfully identified gene signatures whilst simultaneously distinguishing between BCR::ABL negative and BCR::ABL positive cells in the sample (Giustacchini et al. 2017). Based on this seminal study, the top 86 most correlated genes to *BCR::ABL1* were used in the chip. Therefore, the interest was in how these levels change between the two outcome groups, and less so about quantifying absolute expression. The genes chosen were described as *BCR::ABL1* associated genes, these were looked at further to identify what is currently known about their association to BCR::ABL1 and CML, or if not what is known about these genes in disease (Appendix - Table 6-1). Many have been previously associated with CML and disease progression.

The -ΔCt was calculated to provide the accurate representation of the expression levels. From this the samples were ordered into TFR and relapse at start of trial and TFR and relapse at end of trial/point of relapse. Normal samples were also included with the hopes of normalising the DESTINY groups to normal values however these samples failed. This was thought to be due to RNA extraction of the colony samples, due to low cell numbers RNA extraction of colonies produced low quantity RNA, while most samples were able to be analysed by Fluidigm, the one normal sample included did not produce any expression for any of the genes in the panel, including the housekeeping genes showing this sample had failed. Therefore, the best representation of the changes to *BCR::ABL1* related gene expression levels was -ΔCt. This was represented in a heatmap to display how the expression levels change between the outcome groups (Figure 4-23). The genes used are ranked from most relevant to least from the top down, the ranking of these genes was identified by the study which identified the genes which correlate to BCR::ABL, these genes were also ranked (Giustacchini et al. 2017).

As can be seen from the heatmap below from the ST-CFC colony samples there are no visible patterning in the expression levels of the relapse and TFR samples at trial entry. The TFR_E and R_E samples (from TFR_E -163 to R_E -23) appear to have similar expression levels of the BCR::ABL1 associated genes. Additionally in columns for TFR_X and R_X samples while you do see increased gene expression in specific samples like R_E – 44X and R_E – 141X, overall, these samples also do not appear to have evident differences based on the outcome groups, suggesting the BCR::ABL1 is not a driving factor of the colony formation within the pooled colonies from the ST-CFC assays.

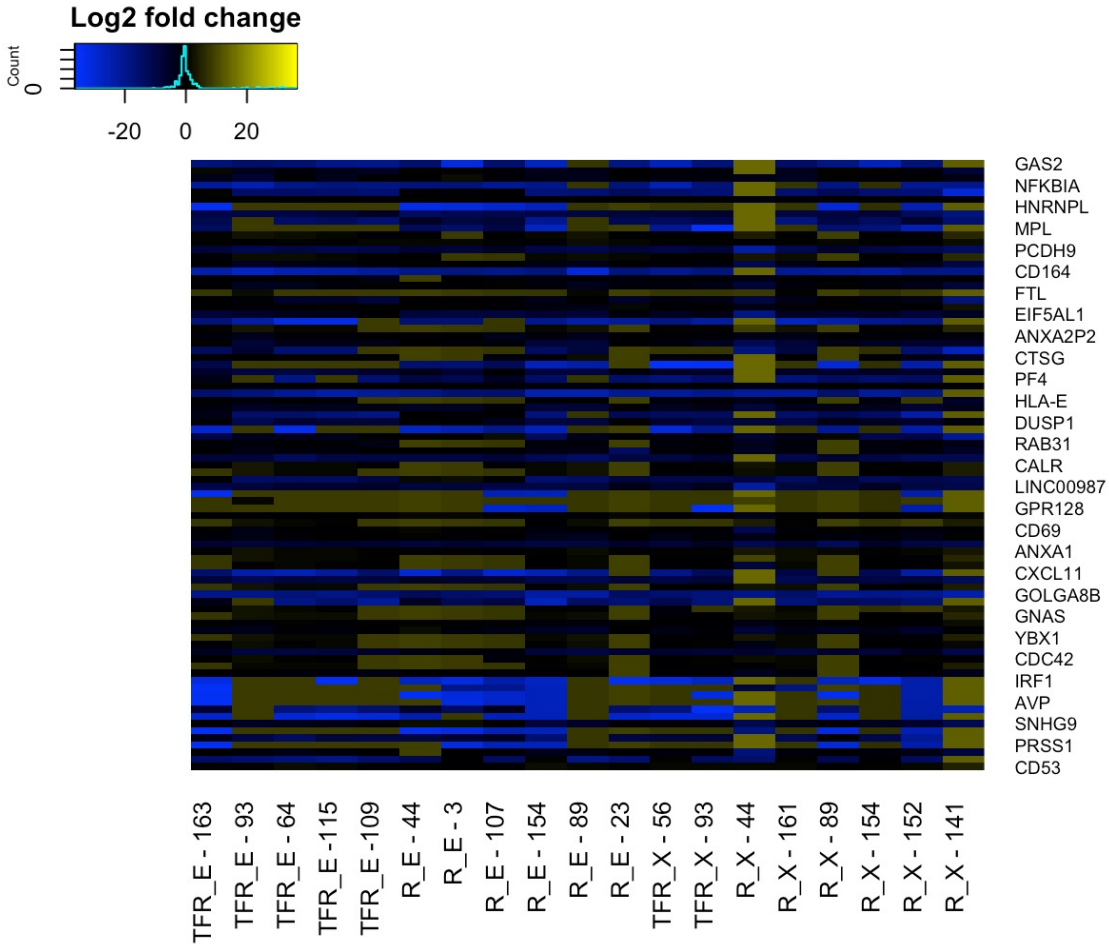

Figure 4-23 Expression of RNA of ST-CFC colonies and their BCR::ABL1 gene signature
Heatmap showing gene expression of RNA samples from the colonies from the ST-CFC assay were tested against a BCR::ABL1 gene signature. The expression values are represented as -ΔCt from Fluidigm. The genes are ranked from most to least important from top to bottom. Samples used include TFR_E (TFR samples at trial entry) (n=5), R_E (relapse samples at trial entry) (n=6), TFR_X (TFR samples at trial end point) (n=2) and R_X (relapse samples at point of relapse) (n=6). Increased expression is shown in yellow, decreased expression is shown in blue. Heatmap made in RStudio using heatmap.2.

For the LTC-IC assays the same analysis of *BCR::ABL1* associated genes was carried out on the colonies from the sample groups (Figure 4-24). In sample R_E – 149 and R_E – 62 the expression levels of all BCR::ABL1 associated genes appear to be higher than the TFR samples. However, the other R_E samples (R_E -138, R_E -25, R_E -76) do display similar expression to the TFR_E samples, showing lower expression of these genes, indicating the increase of BCR::ABL1 might be specific to these samples. Interestingly, within the TFR_X samples it appears the two samples tested have the highest expression of BCR::ABL1 associated genes than the other samples being tested. Additionally, the samples at R_X also seem to have higher *BCR::ABL1* associated gene expression visible compared to the samples (R_E -138, R_E -25, R_E -76) at trial entry but similar gene expression to R_E -149 and R_E -62 at trial entry. Suggesting leukaemic burden may not be associated with driving relapse in stem cells. While this analysis of the more primitive colony samples appears to have increased expression of the BCR::ABL1 associated genes being tested, there is no clear suggestion the leukaemic burden within these samples is driving colony formation.

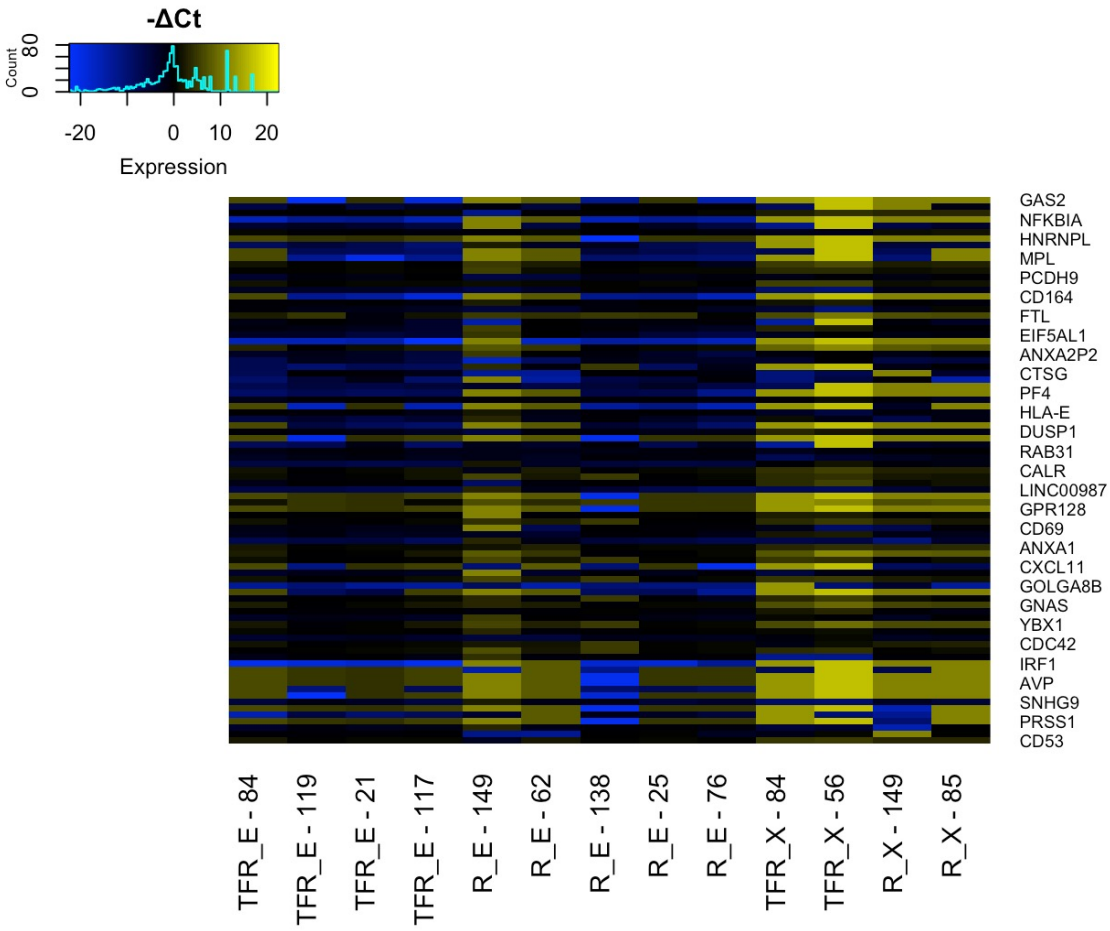

Figure 4-24 Expression of RNA of LTC-IC colonies and their BCR::ABL1 gene signature
Heatmap showing gene expression of RNA from the colonies from the LTC-IC assay were tested against a BCR::ABL1 gene signature. The expression values are represented as -ΔCt from Fluidigm. The genes are ranked from most to least important from top to bottom. Samples used include TFR_E (TFR samples at trial entry) (n=4), R_E (relapse samples at trial entry) (n=5), TFR_X (TFR samples at trial end point) (n=2) and R_X (relapse samples at point of relapse) (n=2). Increased expression is shown in yellow, decreased expression is shown in blue. Heatmap made in RStudio using heatmap.2.

4.5 Discussion

The stem and progenitor population of the BM is one of the most vital aspects of CML treatment discovery and disease research. It is from stem cells that the disease begins and from progenitor cells that disease maintenance occurs. While it is known that TKIs are able to target most of the *BCR::ABL1* carrying cells, it is a persistent population of quiescent LSCs that preclude complete remission of CML. With TFR there is a subgroup of patients (about 50% who attempt treatment stopping) that can maintain their deep remission off therapy. This suggests there are differences between patients who respond optimally to TKIs, potentially within their stem and progenitor population, and understanding these changes could offer a target for LSCs and a potential for TFR biomarker.

4.5.1 Stem cell markers

In the search for stem cell markers that can be used for predicting TFR there were no statistically significant changes of markers between TFR and relapse patients at trial entry that could be identified as potential biomarkers. There were however changes seen between the DESTINY samples and normal donors and patients at diagnosis. While there were no changes to the markers which would indicate a potential biomarker, the changes that were seen could provide essential insight into the behaviour of the LSCs and their interaction within the BMM.

The suggestion that CD25 could potentially be a good diagnostic marker for LSCs in CML comes from the findings that normal BM stem cells had little to no expression of CD25 (Sadovnik et al. 2017) and more mature myeloid cells CD25 expression was undetectable except for basophils which did have CD25 expression (Sadovnik et al. 2016). The data from this project did identify CD25 expression on the normal cells which indicates this marker may not be useful as a specific LSC identifier. CD25 expression was significantly increased in the CML at diagnosis samples compared to samples from patients who maintained TFR taken at trial entry (TFR_E). The expression of CD25 was also seen to have a consistent trend across the DESTINY outcome patient sample, comparable to normal, and at its highest in CML at diagnosis samples. This indicates CD25 is a marker that appears to be at its highest on cells before TKI treatment, upon

which it decreases and normalises in patients' cells after they stop treatment. This is consistent with previous work which has also found upon treatment with TKIs the percentage of $CD25^+$ decreased in LSCs compared to levels at diagnosis (Sadovnik et al. 2016). It has also been shown that while imatinib did not have any effect on the expression of CD25 on CML LSCs, nilotinib and ponatinib did lower the expression (Sadovnik et al. 2017). This could be due to the increased potency of second-generation TKIs and their heightened ability to target BCR::ABL1. However, when CD25 was assessed in DESTINY samples with the HSC/LSC3 panel the trend of expression values differed. The lowest expression of CD25 was found within the samples at point of relapse (R_X), while the R_E and TFR_E samples had similar expression levels to normal, but failed to reach significance. In this case, the samples from CML patients at diagnosis did not have the highest expression of CD25. While the IL1-RAP marker was swapped for CD35 marker in the HSC/LSC3 panel, this should not have provided such different results within the panel to affect the CD25 marker. The varying results and lack of consistency of this marker between the two panels suggests that CD25 wouldn't be a useful predictive biomarker of TFR or LSC marker as is it does not give reproducible results. The changes identified in HSC/LSC panel 1 were different to the changes seen in HSC/LSC panel 3. Furthermore, due to the presence of CD25 on HSCs which could cause variability of results due to lack of specificity to LSCs, the recommendation for using CD25 as a marker in CML was to use it alongside additional diagnostic markers like IL1-RAP and CD26 which would make CD25 a more accurate and precise marker of LSCs (Sadovnik et al. 2017) which in the case of this project would provide better identification of the predictive nature of CD25 and its use as a biomarker of TFR.

The analysis of HSC/LSC 1 panel showed a significant increase of the CD90 marker in relapse patients at the point of relapse (R_X) compared to at the start of trial (R_E) (Figure 4-6) potentially pointing to increasing levels of $CD90^+$ as a marker of relapse during attempted TFR. However, CD90 is known for being a prominent marker of HSCs (Baum et al. 1992) as well as other stem cells like MSCs (Dominici et al. 2006), even lymphoid cells (Schroeder et al. 2023), its inability to act as a LSC marker in isolation was further confirmed when the same changes were not seen in HSC/LSC panel 3. However, $CD90^+$ as an addition alongside $CD34^+38^-$ profile as a marker of LSCs has been successfully used in

previous biomarker discovery with CD93 (Kinstrie et al. 2020), although alone it cannot be used as a predictive biomarker of TFR.

The CD93 marker has been previously investigated as a prominent marker of LSCs in CML (Riether et al. 2021; Kinstrie et al. 2020); the expression of CD93 was found to be increased in DESTINY patients' BM samples who experienced molecular recurrence after attempting TFR (Kinstrie et al. 2020). However, analysis of the HSC/LSC1 panel did not find the same changes as there was not any statistically significant changes in CD93 expression between TFR patients at the start of the trial (TFR_E) compared relapse patients at point of relapse (R_E). Additionally, the expression of CD93 appeared to have a decreased trend from R_E to R_X, although this was not statistically significant. Interestingly, a significant increase in CD93 on normal HSCs compared to relapse at entry (R_E) was found, which could indicate that the number of LSCs was low and therefore the CD93 expression was also lower. This also demonstrates the CD93 marker was not specific to LSCs. It is important to note that these results could differ from the findings by Kinstrie et al., because their research into CD93 looked at the stem cell population within a $Lin^{-}CD34^{+}38^{-}90^{+}$ population, whereas this analysis used in this project used a $Lin^{-}CD34^{+}38^{-}$ population, by additionally having the $CD90^{+}$ this demonstrates a more primitive population than the one being looked at here and could account for the variability seen. The HSC/LSC 1 and 3 panel includes $CD90^{+}$ as a marker therefore in future work this data could be reanalysed including $CD90^{+}$ within the population to look at this marker.

A potentially interesting finding within the HSC/LSC2 panel was the significant increase in expression in R_E vs CML at diagnosis of CD44. This marker has previously been found to be associated with imatinib resistance (independent of BCR::ABL1) (W. Li et al. 2018) and is required for homing and engraftment of LSCs, more so than HSCs (Krause et al. 2006). Indeed, inhibiting CD44 reduced the survival of LSCs, this was demonstrated when mice with CML were treated with mAb CD44 which caused a significant reduction in CML LSCs within the bone marrow, spleen and PB (Hellqvist et al. 2013). Considering its importance in the survival and homing of LSCs it is unsurprising the levels of $CD44^{+}$ were at their lowest in patients with CML at diagnosis but have a significant increase when compared to R_E, TFR_E, R_X and TFR_X. The R_E and TFR_E patients who are

all in a stable long-term remission and have higher expression of CD44 than CML at diagnosis. One of the effects of TKIs on LSCs is causing increased quiescence, it appears after treatment the increased CD44 expression is responsible for increased protection of these LSCs. Additionally, the DESTINY patient samples also do not appear to have any change to the trend of CD44 expression between these outcome groups. However, as CD44 expression was lower in patients at diagnosis (before treatment), it suggests increased CD44 expression is induced by treatment and could potentially be responsible for the survival of the LSCs after treatment helping them remain quiescent to avoid TKI induced cell death. Additionally, the expression of CD44 in normal samples was significantly lower when compared to TFR_E and was also visibly lower when compared to the remaining DESTINY samples: R_E, R_X and TFR_X. Again, this could indicate the levels of CD44 are not highly expressed but after TKI treatment they increase and could be involved in the survival of LSCs.

The analysis of the markers was carried out looking at the percentage of markers within the $CD34^{+}CD38^{-}$ gate, which was the parent gate (Figure 4-2). While this is the best way of analysing and describing this data as the interest in this case is to look at these markers within the HSC/LSC population it may visually distort results. A small number of cells could present as a very high percentage of the parent gate hence the cell counts of each marker were also included. For example, the markers $CD25^{+}$ and $CD26^{+}$ are known for lack of expression on HSCs and exclusively being found on LSCs, however there is a presence of these markers visible within the normal BM samples in the analysis. Additionally, markers like CD93 appeared to be higher percentage of parent in the normal group than the DESTINY samples, however, the counts show the opposite with no significant change between all patient cohorts. The counts analysis was much more varied but without any significant changes. While there is potential for over/under representation of certain markers with looking at percentage of the parent population this remains the best method for analysing these markers as ultimately the interest was to assess how many of these markers are present within this stem cell population ($Lin^{-}CD34^{+}38^{-}$) which is what this analysis does.

Ultimately, none of these markers appeared to be potentially useful biomarkers in isolation. Based on the current analysis the markers: CD45RA, CD47, CD49d, CXCR4, CD117 had similar expression levels across DESTINY samples suggesting

these markers may not be useful as potential biomarkers. Additionally, within the current LSC/HSC population ($Lin^-CD34^+38^-$) the CD44 marker, while not showing potential as a predictive biomarker of TFR, could instead be providing an insight into the behaviour of LSCs and their ability to evade TKIs under the protection of the BMM.

A potential limitation of the staining procedure is that Fluorescence Minus One (FMO) approach should have been used alongside single stains for flow cytometry multi-plex panels. With large panels with multiple fluorescence stains the spill over from some stains into other channels can cause false positives. While FMOs were used initially when creating panels, they were not used alongside single stains when running samples. By including an FMO alongside the single stains this will give a more in-depth look at the spillover and any background noise allowing for more accurate gating and eliminating false positives.

As previously mentioned the inability to identify a predictive LSC marker could be due to the stem cell population ($Lin^-CD34^+38^-$) in which the markers have been assessed, the examination of these markers with additional markers of the stem cell population could provide a more specific look at the LSC population and produce a more promising result for the identification of TFR predictive biomarkers. For example, papers have also used different profiles for identifying LSCs like: $Lin^-CD34^+CD38^{-/low}CD45RA^-cKIT^-CD26^+$ (Warfvinge et al. 2017) and $Lin^-CD34^+CD38^-CD90^+$ (Kinstrie et al. 2020).

Another factor to consider with these samples in the intra-patient variability. This can be seen with HSC/LSC panel 1 and 3 where even though many of the same samples were used in the panels, a lot of the same markers produce slightly varying results. This could be due to things like time in transit, transit conditions and contamination of blood within the BM samples based on who took the sample, while measures were taken to ensure processing was standardised there were certain factors that could not be controlled. With clinical samples these variabilities must always be considered with the data.

Alongside identification of markers on an individual basis, markers were examined together with looking at the samples for the outcome group combined. This allowed for the expression change of these markers to be visualised on a

broader basis and allows a more rounded view of the data. The initial approach for other markers didn't see differential changes for a biomarker of TFR therefore a new approach was tried to gain a new perspective of the data. One finding was the CD36 expression that has a cluster of high expression in both TFR and relapse patients at trial entry which is then gone in both outcome groups when patients stop taking TKIs. This suggests CD36 is related to a deep remission and good response to TKIs. CD36 has previously been found to have increased expression on primitive CML cells and cells with higher expression of CD36 were imatinib resistant (Landberg et al. 2018). It is therefore interesting that this data suggests CD36 expression is decreasing after patients stop TKIs and perhaps LSCs express this marker as a result of TKIs. The same thing was seen in CD47 expression, which again has been identified as a marker of LSCs in CML. The expression of CD47 on cells has been identified as a "don't eat me" signal (Yu'e Liu et al. 2023). The increase of these markers specifically in response to TKIs could indicate these are markers involved in maintaining the quiescence and anti-apoptotic effects of LSCs. This also potentially presents an interesting finding that many of these LSC markers that have previously described are not specific to LSCs but in actual fact are a protective mechanism in response to TKIs. This is perhaps an important and significant point to consider for all future CD marker work.

Additionally, the analysis of IL1-RAP and CD26 together found within the same cluster the expression of these markers is high in R_E, TFR_E and TFR_X patients but not in R_X. This is particularly interesting as out of these cohorts, R_X is the only patient with active disease, the other three cohorts are all in remission either with or without TKIs. The increased expression of this marker in patients in remission suggests together these markers could be markers of good response to TKIs. It also proposes an interesting suggestion that instead of looking at changing expression of CD markers individually perhaps there would be more strength in examining the predictive ability in combination. The analysis for this was purely observational and would require further analysis, furthermore the stem cell population that is being examined is a small minority of the BM sample so gaining an in-depth understanding of changes within this population is limited. Additionally, there is no certain way to confirm if the SCs being looked at are leukaemic or not.

The expression of these known stem cell markers was examined within the progenitor population ($CD34^{+}38^{+}$) of the samples, the Stemformatics data found significant gene changes within the stem and progenitor populations of the CD markers of interest. However, within this dataset these surface markers did not show predictive ability for distinguishing between TFR and relapse patients at point of trial entry. The IL1-RAP expression was at its highest in patients at diagnosis and was significantly lower in comparison to R_E, TFR_E and R_X patients (Figure 4-12). It has previously been found that IL1-RAP is expressed on CML progenitor cells as well as LSCs (K. Zhao et al. 2014). Furthermore, it was also reported that IL1-RAP expression is associated with *BCR::ABL1* and the patients with further progression of CML (i.e. in BP and AP) had higher expression of IL1-RAP (K. Zhao et al. 2014). Therefore, it is perhaps not surprising that patients that had previously never had TKI treatment had the most expression of IL1-RAP.

The CD35 marker has specifically been identified on HSCs and LSCs thus far, however within these DESTINY samples it was also seen on the progenitor population. It was found to have a significantly higher expression on patients at diagnosis compared to R_E, TFR_E, R_X and normal samples. Previous work looking at this marker found $CD35^{+}$ cells were associated with BCR::$ABL1^{-}$ HSCs in the BM (Warfvinge et al. 2024), therefore it is interesting that the patients at diagnosis had highest expression of $CD35^{+}$. However, as this is an assessment of the progenitor population and CD35 is expressed in B cells, monocytes, neutrophils, eosinophils etc (Kremlitzka et al. 2013) it is likely due to the high number of granulocytes from CML this increased expression is seen within the patients at diagnosis. Similar to results from analysis of the LSC population, the progenitor analysis also produced different results from HSC/LSC panel 1 and 3. The CD90 expression shows a significant increase in normal donors compared to R_E in HSC/LSC 1, while HSC/LSC 3 panel found a decreased trend in the expression of CD90 in normal donors compared to relapse patients at trial entry, further suggesting these are not useful predictive biomarkers.

From this data it can be said that as expression of HSC/LSC markers showed small statistically insignificant changes, the markers on these panels may not be

useful as predictive biomarkers of TFR from BM samples at trial entry when patients are still on their TKI prior to attempting TFR.

4.5.2 Colony formation

As CML arises in a primitive haematopoietic cell it is essential to determine if progenitors and stem cells differ between TFR and relapse patients, and if their differentiation and proliferation capacity changes. The quantitative and qualitative assessment of this was completed through ST-CFC and LTC-IC assays to examine how changes to colony forming ability might relate to DESTINY patient outcome.

Overall, analysis of the ST-CFC found progenitor cells did not produce significant differences in the total number of colonies produced or within each colony type across any of the outcome groups tested. Although the total number of colonies produced had an increased trend in R_E patients compared to TFR_E, this was not significant and indicates there was no difference in proliferation capacity between TFR and relapse patients at the start of the trial and the proliferation is not predictive of TFR. While there were no significant changes between the DESTINY samples tested, there was a decreased trend in the total number of colonies produced from R_E to R_X, while TFR_E to TFR_X did not appear to have any change. Additionally, there was an increased trend in the total number of colonies produced in CML at diagnosis patients' samples compared to normal. This is unsurprising as an increase in the proliferation of haematopoietic cells is expected as it is a characteristic of CML before treatment. The cohort with the lowest number of total number of colonies produced was from the normal samples. While this is not surprising in comparison to samples at point of relapse (R_X) or at diagnosis, it is perhaps surprising when compared to patients at entry into trial (R_E and TFR_E) as these patients are in deep, stable remission for a number of years with no detectable signs of disease so it would be expected that they would perhaps have similar number of colonies/progenitors as normal patients, although as it has been established this does not appear to play a role in relapse. Furthermore, a direct comparison of paired TFR samples found there was a significant increase in the total number of colonies produced in TFR_X samples compared to TFR_E, suggesting patients that are maintaining their remission during TFR have an increase in proliferation of progenitor cells. It is

perhaps surprising that this increased proliferation is seen in patients maintaining remission, this may be expected in patients relapsing, however as these patients are not relapsing this suggests the increased proliferation of progenitors is consistent with normal haematopoiesis. Further work could be done to identify what this increased cell proliferation is being driven by. Finally, the number of CFU-GEMM and BFU-E colonies was lower than the CFU-M, CFU-G and CFU-GM across all the sample groups, which is in keeping with the knowledge that the CFU-GEMM colonies are the most primitive and are more likely to be seen in LTC-IC than ST-CFC which is designed to show progenitor functionality. Additionally, the BFU-E colonies are erythroid progenitors and as previously discussed the CML patients having an increased production of myeloid cells and less erythroid cells.

Alongside the analysis of the progenitors, the stem cell population and activity were also assessed through LTC-IC assays. The comparison of the DESTINY outcome groups within each colony type and total number of colonies produced did not show any statistically significant differences. Analysis of the total number of colonies produced found an increased trend in TFR_E patients compared to R_E. However, this was not significant and therefore it cannot be said that stem cell activity is predictive of TFR.

Moreover, when looking at the paired relapse samples the patients at point of relapse had significantly decreased number of total colonies formed compared to relapse at trial entry (R_E). Although this is consistent with previous findings from paired analysis of progenitors (Figure 4-20) where proliferation/colony formation was found to be increased at trial exit in TFR patients compared to trial entry, this result is still surprising. It was expected that patients relapsing would have had increased proliferation of cells however the data shows the opposite for both the stem and progenitor cells. The decreased stem cell activity at point of relapse could suggest increased quiescence of SCs in response to relapsing. However, it is not clear if this increased quiescence is from the HSCs or LSCs, it is known that increased LSCs quiescence occurs due to TKI treatment therefore it would not be expected that LSCs have an increased quiescence after TKI cessation however investigation into the BCR::ABL1 activity of these stem cells would be required to determine this.

Within this analysis, CFU-GM colonies produced at TFR_E appeared to have a higher number of CFU-GM colonies out of all other cohorts, although this was not significant. It is expected and has previously been reported that untreated CML patients in CP produce more CFU-GM colonies than normal samples (Strife et al. 1988) the increased proliferation and self-renewal capacity seen in the primitive population is not expected from patients maintaining their remission, making increased CFU-GM colonies in TFR_E patients surprising. This could be understood as being due to the number of *BCR::ABL1*$^{-}$ CFU-GMs increasing in preference to the *BCR::ABL1*$^{+}$ ones. As it is known this patient cohort goes on to maintain remission, the increased production of these colonies could be associated with normal haematopoiesis as was suggested with increased progenitor production at end point of trial (Figure 4-20). This is consistent with findings of decreased stem cell activity within relapse patients at point of relapse which is hypothesised to be a result of increase quiescence due to relapse. Additionally, DESTINY patients at the end point of trial (TFR_X) produced the highest number of BFU-E colonies compared to the other patient groups. While this is not a significant change, it is interesting as the BFU-E progenitor cell is committed to differentiation into red blood cell (Dulmovits et al. 2017). In CML there is an increased proliferation of granulocytes and as a result this commonly causes the presentation of anaemia in patients, this increased BFU-E could be involved in the maintenance of normal haematopoiesis in patients after TKI cessation. Similar findings were reported when Krishnan et al., found single-cell RNA sequencing of LSCs from good responders (patients who achieved MMR) had increased erythroid progenitor expansion when compared to patients who progressed to BP. The ‘good responders’ also had erythroid lineage skewing (instead of myeloid) and the erythroid progenitors were more sensitive than myeloid progenitors to TKIs (Krishnan et al. 2023). Erythroid progenitors could potentially be associated with better prognosis to TKIs, additional work would be required to identify if they are also predictive of TFR success.

From the colony assays assessed, any samples that did not produce any colonies were removed from analysis. This is because the samples used were all BM samples for the colony forming assays, therefore all assays should produce colonies, any that did not, it was assumed the assay had either failed or the

stem cells present were quiescent/nonfunctional stem cells, regardless the data was not included as it did not seem reasonable that some vials did not have stem progenitor cells. For some patient samples the first vial used did not produce any colonies, yet the next duplicate vial did. This is not uncommon as patient samples are heterogenous therefore variations are possible within the samples i.e. having stem population of quiescent cells.

Overall, the data shows the colony forming ability of the stem and progenitor cells does not change with a patient's ability to maintain TFR or relapse and therefore cannot be used in a predictive approach for TFR.

4.5.3 *BCR::ABL1* associated gene expression within stem and progenitor colonies

The colony forming assays did not produce statistically significant changes that could differentiate the relapse and TFR outcome groups. However, there were data that identified increased proliferation of progenitor cells in TFR samples and reduced proliferation of stem cells in relapse when comparing trial entry to trial exit. It can be hypothesised why these changes are being seen however, understanding the BCR::ABL1 activity of these cells would provide insight into the leukaemic burden of the colonies produced from these patient cohort samples and may help elucidate if it contributes to driving expansion of the cells. Initially, q-PCR was attempted to measure the BCR::ABL1 expression within the colonies (as described by (Pagani et al. 2023)), however due to the low cell number and low RNA quantity produced from each sample this test was not sensitive enough and did not detect *BCR::ABL1*, even in positive controls with the colony samples. Additionally, the BCR::ABL1 transcripts can be variable due to different transcripts making identification of it more difficult with q-PCR, a more sensitive machine would be required for this. To overcome this a Fluidigm chip was used which is a high-throughput, high sensitivity method that can detect very low cell numbers. This was used alongside BCR::ABL1 related genes identified by (Giustacchini et al. 2017) as a surrogate readout for the BCR::ABL1 activity within the samples.

RNA was extracted from the pooled colonies grown for each sample from LTC-IC and ST-CFC assays, and tested for *BCR::ABL1* related genes (Giustacchini et al.

2017) using a Fluidigm chip. While the quantity of the RNA added was variable this was not a drawback to the analysis as the aim of this experiment was not to quantify gene expression but to discover a representation of the expression changes within the outcome groups. From the genes identified several are currently known for their association with CML and BCR::ABL1 (Appendix - Table 6-1) including *ANXA2*, *CALR*, *CLEC4GP1*, *CTNNB1*, *CTSG*, *CYP51A1*, *DNTT*, *DUSP1*, *EIF5A*, *GAS2*, *HNRNPH1*, *IFITM1*, *KIAA0125*, *LGALS1*, *NFKBIA*, *NOG*, *PF4*, *RPL18A*, *SELL*, *SOCS2*, *TRA2A*, *CD69*, *ANXA1*, *GNAS*, *LRRC75A*, *YBX1*, *CDC42*, *RPL10A*, *WTAP* and *CK52*. Several genes were involved in dysregulation of signalling pathways like *AAMDC*, *AREG*, *ARRDC3*, *GAS5*, *STON2*, *IFITM2*, *RTN4* and *EIF2S*. Additionally, there was genes associated with haematopoiesis, HSCs, immune cell regulation and other cancers.

Nonetheless within the LTC-IC (Figure 4-24) samples it appeared that TFR_X patients had the highest expression of BCR::ABL1 genes than any of the other outcome groups. Additionally, the R_X samples also had increased expression of *BCR::ABL1* when compared to all TFR_E samples, this was also the case when R_X samples were compared to certain R_E samples (R_E -138, R_E -25, R_E -76). However, the expression of *BCR::ABL1* genes within R_X samples did have similar expression compared to the R_E samples: 149 and 62. These findings suggest not all relapse patients have the same level/activity of BCR::ABL1 within their stem cell population before attempting relapse. Furthermore, the stem cells of TFR and relapse patients at end point of trial samples appeared to have high expression of BCR::ABL1 related genes compared to the samples at the start of the trial, which suggests in the most primitive population of stem cells in DESTINY patients at least, appear to have increased *BCR::ABL1* expression after stopping TKIs. Although TKI use has stopped, it would have been expected that patients maintaining TFR would not have increased *BCR::ABL1* expression as they are not relapsing which is evidence by their steady *BCR::ABL1* expression levels that were seen during the DESTINY trial. This finding could suggest that the lack of TKI caused a resurgence of BCR::ABL1 activity within the stem cells however another factor is patients maintaining TFR are able to control this. Additionally, within the R_E vs R_X paired comparison the total number of colonies from SCs decreased at point of relapse, therefore seeing an increased *BCR::ABL1* associated gene expression was surprising, and this could further prove the

hypothesis that indicates there is an increase BCR::ABL1 activity in LSCs though these are quiescent. Perhaps a more predictable result was increase *BCR::ABL1* associated gene expression in some of the relapse at trial entry samples as this could have been an indication that although they were in deep remission they had more BCR::ABL1 activity which led to their relapse. However, most of the samples from both outcome groups before the trial started, appear to have consistent *BCR::ABL1* associated gene expression, suggesting the leukaemic burden of these stem cells before TKI cessation does not differ and isn't associated with TFR success. It is Important to consider that as the samples being tested are pooled from the assays and cells were not separated into BCR::ABL1$^-$ and BCR::ABL1$^+$ prior to adding to the assay it is difficult to definitively determine the activity of the BCR::ABL1 cells within these stem and progenitor populations.

Furthermore, within the ST-CFC the progenitor population from both TFR and relapse samples before the trial did not show considerable changes in *BCR::ABL1* associated gene expression. There was, however, an increased trend in expression in two of the relapse samples at point of relapse (R_X – 44 and R_X – 141) which appeared to have higher expression compared to the other R_X samples. While it would be expected to see increased BCR::ABL1 number/activity in cells at point of relapse it is surprising that other R_X samples did not show the same increased expression. Interestingly, there was no trend in expression identified within the TFR_X patient cohort when compared to TFR_E, although there was a significant increase of progenitor colonies produced from the start to the end of the trial, this further validates the hypothesis that the increased progenitor proliferation seen here is in line with normal haematopoiesis as the increase in proliferation is not driven by BCR::ABL1.

As with the LTC-IC analysis, the findings from the *BCR::ABL1* expression of these ST-CFC results is difficult to distinguish how many of the colonies tested were all *BCR::ABL1*$^+$ or *BCR::ABL1*$^-$ colonies. As the colonies for each sample were all tested together as a pool and not as individual colonies, this introduces variability of *BCR::ABL1* within each sample, which is not necessarily representative of the leukaemic burden within the stem and progenitor

population of these samples. To overcome this, healthy normal samples were included on the Fluidigm chip, unfortunately these samples failed and could not be used. This could have provided informative data, the use of normal samples would be useful to normalise the gene expression and allow the ΔCt value to be examined, this would allow statistical analysis of the expression changes to be calculated and overcomes variations within the samples by accounting for the baseline.

Interestingly, previous research found at CML diagnosis within the BCR::ABL1$^-$ stem cell population there was distinct clustering of good responders (patients who achieved MMR) and poor responders (patients who did not achieve MMR) (Giustacchini et al. 2017). There was enrichment of TGF-β and TNF-α pathways in the BCR::ABL1$^-$ stem cell population in poor responders when compared to good responders, suggesting there is an increase quiescence within these SCs (Giustacchini et al. 2017). This is predictive of TKI response and is showing the poor response to TKIs is also associated with BCR::ABL1$^-$ SCs. These findings suggest the response to TKIs in patients may also be related to BCR::ABL1$^-$ population. Another reason for BCR::ABL1$^-$ and BCR::ABL1$^+$ cells to be separated and analysed within independently as this may provide more comprehensive understanding of the role of these stem and progenitor cells in TFR.

Overall, a detailed exploration was carried out on the stem and progenitor population of these DESTINY samples. From the chosen markers based on the literature, at this point in the study it was considered that the panels were not useful as predictive biomarkers of TFR. Similarly, the investigation into the differentiation and proliferation capacity of the stem and progenitor population from these samples show any significant changes between the outcome groups that would be useful as potential predictive biomarker of TFR success. However, this analysis has provided noteworthy findings of changes within the primitive population of CML patients that could identify novel mechanisms by which relapse and TFR occur and stem cells survive. Further work investigating these changes may provide essential information in future experimentation for finding predictive biomarkers of TFR.

5 Results III – Proteomics

5.1 Introduction

The BMM is made up of cellular and non-cellular components which create specific niches for HSCs and because of this the BMM provides precise and tight regulation of the process of haematopoiesis. One factor involved in this precise regulation is the proteome. The proteome includes the intrinsic cellular proteins as well as the extrinsic ECM, enzymes, and soluble factors (such as cytokines, chemokines and growth factors) (Ho et al. 2023). This extrinsic protein production plays an essential part of the BMM and an integral role in maintaining homeostasis for the normal progression of haematopoiesis, the dysregulation of which drives haematological disease.

The interaction of these soluble factors and CML cells in the BMM results in changes which are essential for maintenance of disease. For CML the changes to the BMM are essential for the protection of LSCs. The protein expression/proteome of the BMM are an essential aspect of the changes seen in CML. One such change is the increase in a pro-inflammatory environment that is a driver for CML disease persistence, with enhanced secretion of several pro-inflammatory cytokines and chemokines. The pro-inflammatory profile of the BMM of someone with CML and how this contributes to preventing LSC eradication has been previously described. This includes IL-6, VEGF, IL-1α and TNF- α cytokines and CXCL12 and CCL3 chemokines which are increased in the BM of CML patients (Aguayo et al. 2000; Järås et al. 2010; Reynaud et al. 2011; B. Zhang et al. 2012; Baba et al. 2013; Hoermann et al. 2015; Guo et al. 2016; Peled et al. 2018; Staversky et al. 2018). This increased pro-inflammatory profile can also alter patients response to TKIs. Additionally, through examination of changes to protein expression, changes to immune response have been identified in patients on TKI treatment with regards to how deep the remission they can achieve. Patients that achieved optimal response of DMR were found to have higher expression of NK cells and T cells and lower expression of programmed death -1 (PD-1) and MDSCs, which are immunosuppressive (A. Hughes et al. 2017). Within the BM most of the proteome is secreted from MSCs (Hennrich et al. 2018), which are known as multi-potent cells involved in maintaining the BMM, haematopoiesis and HSCs. The MSCs release cytokines, chemokines and

growth factors all collectively known as the secretome (the soluble part of the proteome).

There are thought to be many other changes to the proteome of patients with CML within the BMM and identifying these would be essential to further elucidating CML disease characteristics and improving patient outcomes. Additionally, it is not well understood how these changes within the BMM differ between patients that maintain TFR and those who relapse. Due to this the proteome of the BMM has clearly been identified to be an essential aspect of understanding patients treatment response and disease progression.

While aspects of the proteome of CML patients have been assessed separately, there is an unfulfilled need for a comprehensive analysis to aid understanding of the changes to the proteome. Unbiased analysis looks at a wide range of proteins that otherwise may have been missed if a more targeted panel is used. DIA is a type of MS-based quantitative proteomics (Li et al. 2021) that offers a high-throughput approach for the identification and quantification of proteins. Using an MS-based proteomics approach is ideal for the analysis of the BM plasma of the DESTINY patients to identify quantitative changes within and between the proteome of patients that maintain TFR and those that relapse.

5.2 Aims

1. To identify a predictive protein signature within BMM of TFR patients.

5.3 Objectives/sub aims

1. Discover protein expression within the BM plasma of DESTINY CML patients and evaluate if there is a protein expression signature which predicts patients able to maintain TFR or relapse.

2. Identify predictability of protein signatures within pathways of interest as potential biomarkers of TFR.

5.4 Results

5.4.1 Decreased expression of proteins involved in immune response pathways in BM plasma relapse vs TFR patients at trial entry

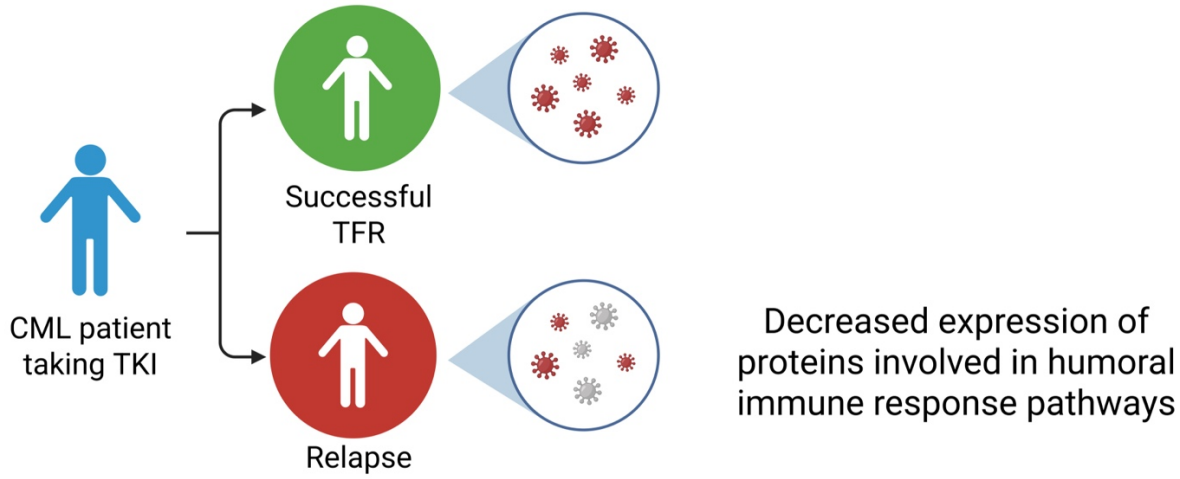

Figure 5-1 Take home message of proteomics analysis for R_E vs TFR_E

The proteomics results were analysed using Spectronaut software, a high-performance proteomics software that is able to provide in-depth analysis of proteomics data. From the software used over 5000 proteins were identified from the proteomics analysis. Using this data, several comparisons were made between relapse and TFR samples at trial entry, relapse and TFR at trial exit/point of relapse, and normal BM plasma samples.

Sample number	Trial Response	Timepoint of sampling	Days to relapse	Proteomics
NORMAL 1	-	-		
NORMAL 2	-	-	-	
NORMAL 4	-	-	-	
3	Relapse in stopping	Entry – at start point of trial	455	
3X	Relapse in stopping	Entry – at start point of trial	455	
4	TFR	Entry – at start point of trial	-	
10	TFR	Entry – at start point of trial	-	
14	TFR	Entry – at start point of trial	-	
15	Relapse in stopping	Entry – at start point of trial	449	
15X	Relapse in stopping	Exit – relapse during trial	449	
18	TFR	Entry – at start point of trial	-	
028	Relapse in de-escalation	Entry – at start point of trial	262	
34	TFR	Entry – at start point of trial	-	
34X	TFR	Exit – end point of trial	-	
37	TFR	Entry – at start point of trial	-	

38	Relapse in stopping	Entry – at start point of trial	404	
38X	Relapse in stopping	Entry – at start point of trial	404	
40	TFR	Entry – at start point of trial	-	
44	Relapse in de-escalation	Entry – at start point of trial	124	
44X	Relapse in de-escalation	Exit – relapse during trial	124	
49	Relapse in stopping	Entry – at start point of trial	475	
49X	Relapse in stopping	Exit – relapse during trial	475	
56	TFR	Entry – at start point of trial	-	
56X	TFR	Exit – end point of trial	-	
62	Relapse in stopping	Entry – at start point of trial	828	
62X	Relapse in stopping	Exit – relapse during trial	828	
64	TFR	Entry – at start point of trial	-	
64X	TFR	Exit – end point of trial	-	
67	TFR	Entry – at start point of trial	-	
67X	TFR	Exit – end point of trial	-	
68	TFR	Entry – at start point of trial	-	
68X	TFR	Exit – end point of trial	-	
73	TFR	Entry – at start point of trial	-	

73X	TFR	Exit – end point of trial	-	
78	Relapse in de-escalation	Entry – at start point of trial	75	
080	Relapse in stopping	Entry – at start point of trial	449	
80X	Relapse in stopping	Exit – relapse during trial	449	
82	TFR	Entry – at start point of trial	-	
82X	TFR	Exit – end point of trial	-	
84	TFR	Entry – at start point of trial	-	
84X	TFR	Exit – end point of trial	-	
89	Relapse in de-escalation	Entry – at start point of trial	245	
89X	Relapse in de-escalation	Exit – relapse during trial	245	
93	TFR	Entry – at start point of trial	-	
93X	TFR	Exit – end point of trial	-	
100	Relapse in stopping	Entry – at start point of trial	417	
100X	Relapse in stopping	Exit – relapse during trial	417	
101	TFR	Entry – at start point of trial	-	
103	TFR	Entry – at start point of trial	-	
112	Relapse in stopping	Entry – at start point of trial	762	
117	TFR	Entry – at start point of trial	-	

122	Relapse in stopping	Entry – at start point of trial	483	
122X	Relapse in stopping	Entry – at start point of trial	483	
122X	Relapse in stopping	Entry – at start point of trial	483	
125	Relapse in stopping	Entry – at start point of trial	488	
125X	Relapse in stopping	Exit – relapse during trial	488	
136	TFR	Entry – at start point of trial	-	
136X	TFR	Exit – end point of trial		
140	Relapse in stopping	Entry – at start point of trial	659	
140X	Relapse in stopping	Exit – relapse during trial	659	
141	Relapse in stopping	Entry – at start point of trial	472	
149	Relapse in stopping	Entry – at start point of trial	440	
149X	Relapse in stopping	Exit – relapse during trial	440	
151	TFR	Entry – at start point of trial	-	
159	Relapse in stopping	Entry – at start point of trial	485	
159X	Relapse in stopping	Exit – relapse during trial	485	
161	Relapse in stopping	Entry – at start point of trial	440	
161X	Relapse in stopping	Exit – relapse during trial	534	
172	Relapse in stopping	Entry – at start point of trial	426	

172X	Relapse in stopping	Exit – relapse during trial	426	

Table 5-1 BM plasma samples used for each experiment BM plasma samples used for the proteomics analysis. The information about each sample is also shown. Boxes highlighted in green indicate this sample was used with this technique.

PCA plot showed no major grouping between relapse (R_E) and TFR (TFR_E) samples at trial entry. The samples did not cluster as outcome groups, instead are mixed in with each other indicating there is a high similarity between groups in the variables being measured. Additionally, this could indicate noisy samples which is not surprising as BM plasma samples have high levels of proteins. Using the Orbitrap™ Astral™ MS and Spectronaut software can remove noise thus allow changes to be identified.

To begin with the relapse vs TFR at trial entry comparison was assessed, for this there were 20 relapse and 20 TFR samples. For analysis of the data RStudio was used to identify DEPs, using a cutoff of p.adj<0.05 and log_2fold>0.5. Of the DEPs 108 were upregulated and 144 downregulated within the threshold for this data (Figure 5-2 B).

The expression of the 252 DEPs was normalised to get the z-score which allows the expression to be compared more directly across the samples. The samples were then clustered by row, using RStudio to allow grouping of similar expression values to show similarity of the samples. The heatmap shows the changes identified in this comparison of proteins within these samples. There are certain ‘outlier’ samples with higher expression like T_073 and R_141.

The STRING database is used to identify any protein-protein interactions within a dataset. It allows a visual representation of the proteins that are present and potential group clustering of these proteins. The upregulated and downregulated proteins did not show many clusters.

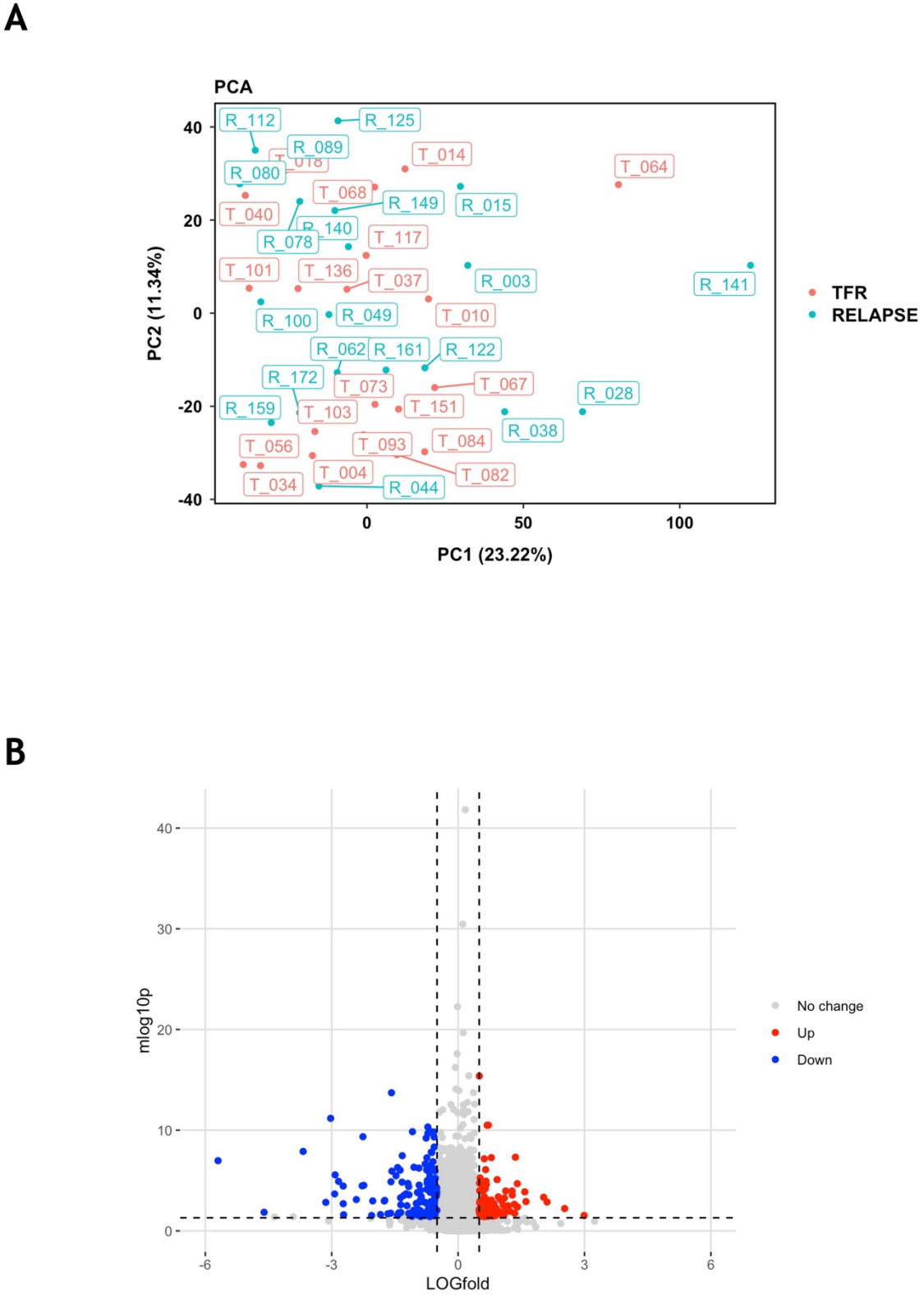

Figure 5-2 Proteins changed in BM plasma of relapse with respect to TFR at trial entry (A) PCA plot of protein expression data between (R_E) (blue) and TFR (TFR_E) (n=20) (red). Showing PC1 (23.22%) and PC2 (11.34%). **(B)** Volcano plot of comparison of relapse (R_E) vs TFR (TFR_E) at trial entry. DEPs were established at p.adj<0.05 and $\log_2$ fold>0.5. These are shown as upregulated (red), downregulated (blue) and no change (grey). Volcano and PCA plot were made on RStudio. R_E (n=20) and TFR_E (n=20).

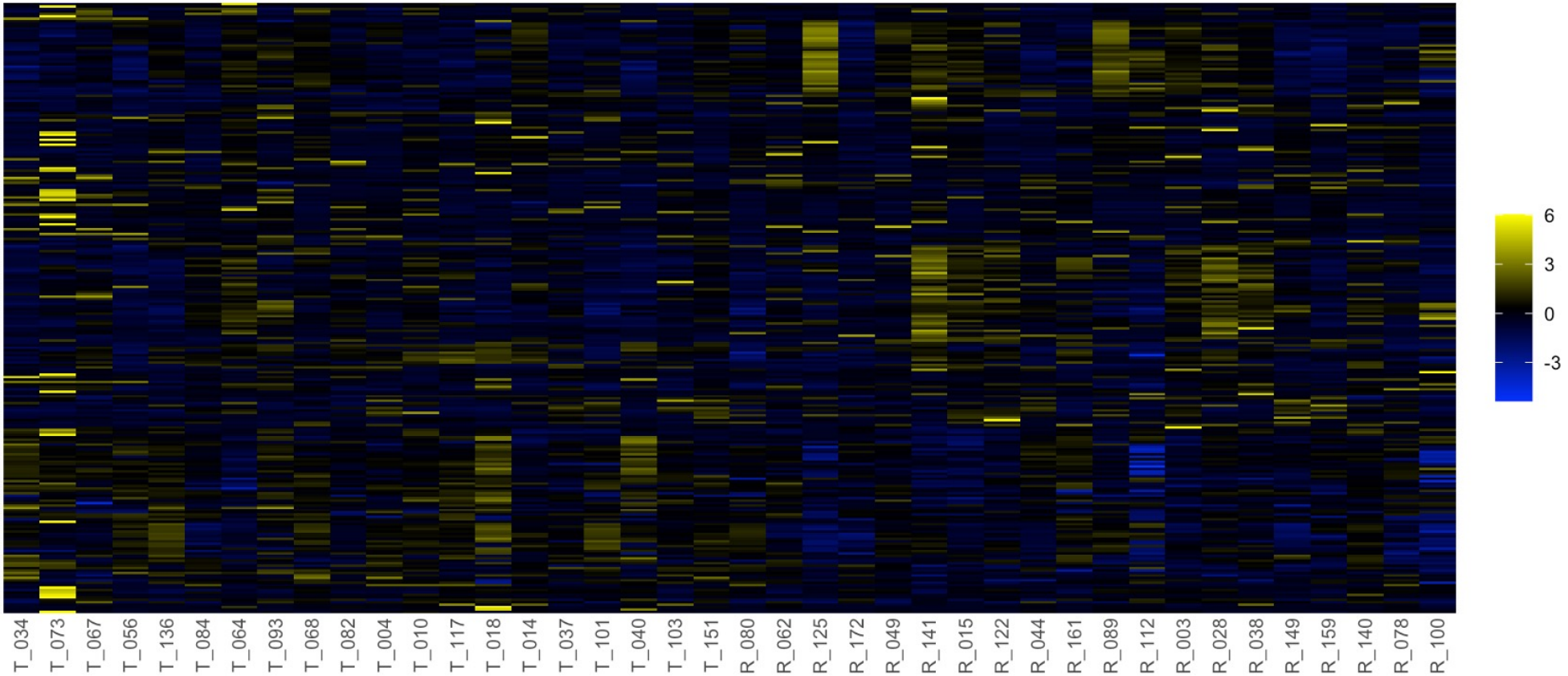

Figure 5-3 Expression change of DEPs relapse at trial entry with respect to TFR at trial entry A heatmap showing the expression change of all significant proteins within the relapse at trial entry (R_E) (n=20) TFR at trial entry (TFR_E) (n=20). Samples are shown on the x-axis, proteins are shown on the y-axis. The scale shows the expression level by colour and intensity; yellow is the highest expression (upregulated) and blue is the lowest (downregulated). The expression values have been normalised into z-scores. The heatmap has y-clustering of the rows, this clustered related proteins together. DEPs were identified at p.adj<0.05 and log_2fold>0.5. Heatmap and clustering was done on RStudio.

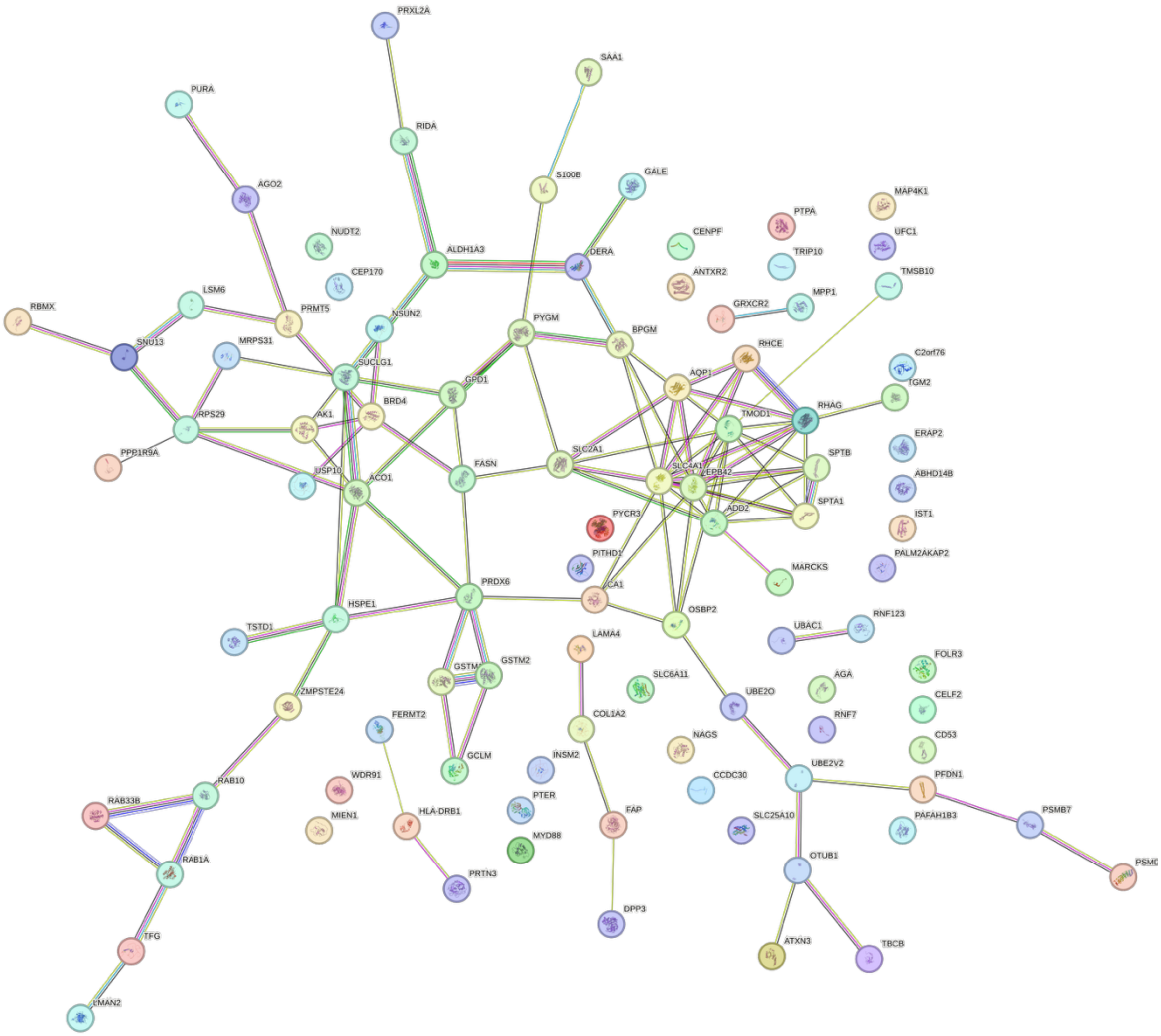

Figure 5-4 Interaction of 108 upregulated DEPs in relapse patients with respect to TFR patients at trial entry STRING network showing the interactions of the 108 upregulated DEPs in relapse patients at trial entry (R_E) vs TFR at trial entry (TFR_E). All proteins within this comparison were put into the STRING database, the 108 proteins were used to identify their relationship to each other. Each colour for the lines identifies a different type of association that is predicted about two proteins, the thickness of the line is related to the confidence of this prediction.

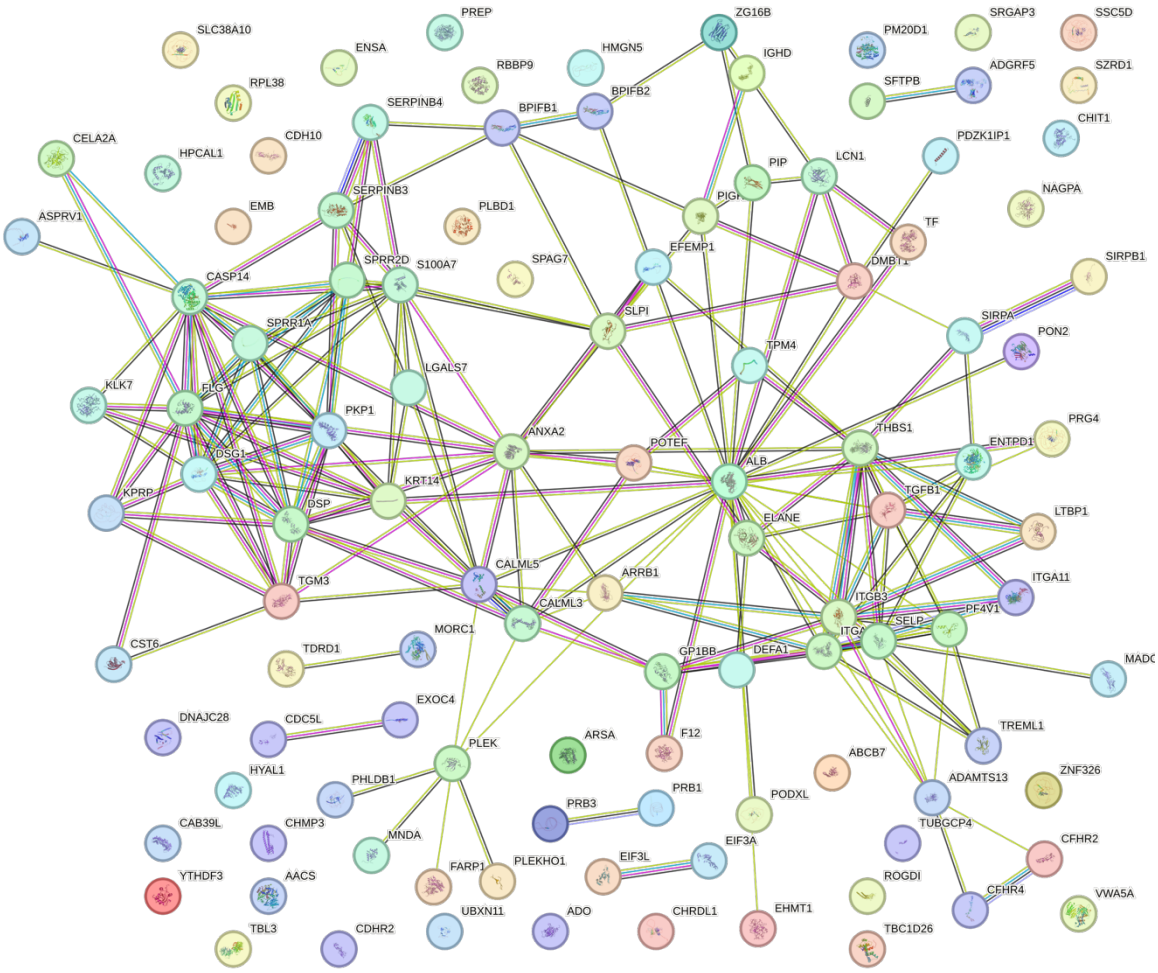

Figure 5-5 Interaction of 144 downregulated DEPs in relapse patients with respect to TFR patients at trial entry STRING network showing the interactions of the 144 downregulated DEPs in relapse patients at trial entry (R_E) vs TFR at trial entry (TFR_E). All proteins within this comparison were put into the STRING database, the 144 proteins were used to identify their relationship to each other. Each colour for the lines identifies a different type of association that is predicted about two proteins, the thickness of the line is related to the confidence of this prediction.

The identified DEPs were inputted to the Gene Ontology (GO) database so that associated pathways could be identified. These proteins were compared to biological processes (BP) within the GO database using RStudio. To do this over-representation analysis (ORA) was used, this looks at if genes from the data are over-represented within a pre-determined pathway that includes specific genes. The significant proteins were categorised into upregulated ($p.adj<0.05$ and $log_2fold>0.5$) and downregulated ($p.adj<0.05$ and $log_2fold>-0.5$), and each dataset was individually assessed.

For this data, all analysis was done using RStudio where the input when doing pathway analysis must be genes. With proteomics data sometimes there can be multiple genes associated with different isoforms of proteins; to remove

‘duplicates’ data were sorted by p.adj levels and the gene/protein with the lowest p.adj number was kept while the rest were removed (only for pathway analysis purposes) thus allowing only the most significant data to be used and still allowing the genes of interest to be acknowledged within the analysis. Although the input for pathway analysis used genes the analysis still all corresponds to proteins.

Initial analysis of relapse vs TFR at trial entry found DEPs in relapse samples were involved in the increased proliferation and differentiation of myeloid cells, with pathways such as ‘myeloid cell differentiation’ and ‘erythrocyte development’ upregulated (Figure 5-6 A). There was also an upregulation of the metabolic process ‘sulfur compound metabolic process’ seen. These are perhaps unsurprising results for being over-represented within the relapse cohort compared to TFR, as this suggests patients that are relapsing have an increase in the activity and production of myeloid cells. Additionally, there was upregulation of pathways such as ‘actin filament capping’, ‘ammonium transmembrane transport’ and ‘regulation of actin filament polymerisation’ that are also linked to increased myeloid cell activation suggesting the proteins within the BMM of relapsing patients are producing a more proliferative environment, even before TKI cessation, which is prohibiting the maintenance of TFR.

On the other side, the downregulated pathways (Figure 5-6 B) from this comparison shows over-representation of ‘humoral immune response’, ‘antimicrobial humoral response’ and ‘antibacterial humoral response’. The humoral response is the process by which B cells within the body are activated by foreign antigens and release antibodies to clear any threat. This integral part of the immune response is decreased in relapsing patients, and conversely relatively increased in TFR patients. Hence, the humoral immune response could play a part in maintaining TFR. Additional pathways such as ‘wound healing’, ‘blood coagulation’ and ‘coagulation’ are all closely linked to each other within GO hierarchy and are more likely related to normal BMM homeostasis.

A

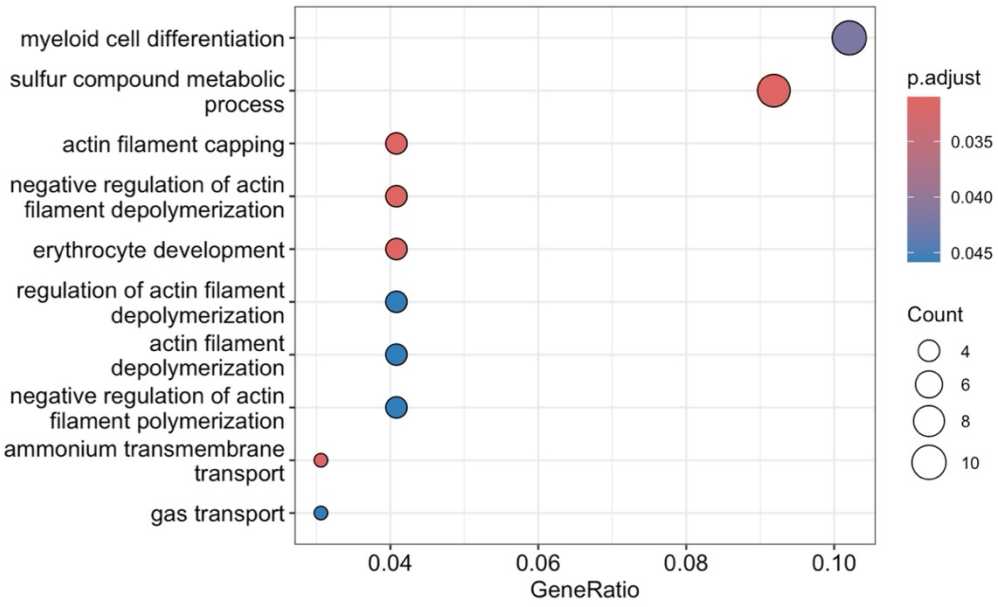

B

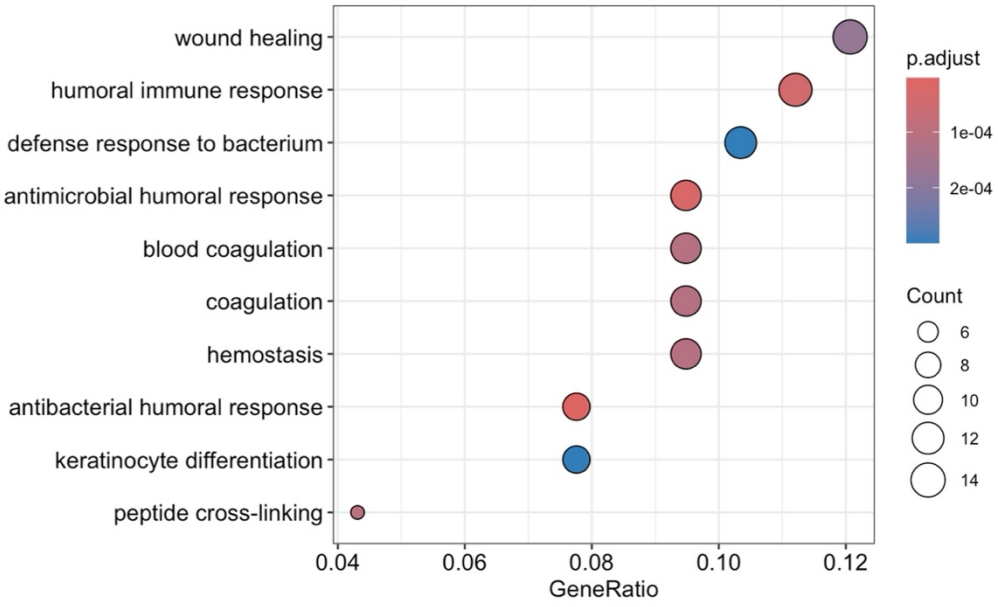

Figure 5-6 Gene ontology biological processes pathway analysis of DEPs discovered from relapse proteomics DEPs were used to identify top 10 enriched pathways (using RStudio) that were **(A)** upregulated, and **(B)** downregulated in relapse patients at trial entry (R_E) (n=20) compared to patients who maintained TFR (TFR_E) (n=20). Gene ratio = ratio of DEPs in pathway to all target proteins. Count demonstrated the number of proteins identified within the pathway.

Once the pathways of interest had been established, the discriminatory power of the proteins to distinguish between the outcome groups was evaluated. To do this, ROC (receiver operating characteristic) curves were generated that measure the sensitivity (true positive rate) against the specificity (false positive rate) (Hoo et al. 2017). This can be used as a measure of the diagnostic ability when comparing two outcome groups (Hoo et al. 2017). The proteins found within these pathways were as follows:

GO ID	Description	Gene ratio	GeneID
GO:0048821	erythrocyte development	4/98 (0.04)	**RHAG**/**EPB42**/**BPGM**/**SLC4A1**
GO:0030099	myeloid cell differentiation	10/98 (0.1)	PRXL2A/PRTN3/HLA-DRB1/**RHAG**/MYD88/**EPB42**/**BPGM**/**SLC4A1**/PITHD1/FASN

Table 5-2 Upregulated proteins from pathways of interest using ORA analysis (Figure 5-6 A) of R_E vs TFR_E.

When the area under the curve (AUC) of a ROC curve is 0.5, it shows the data doesn't have discriminating ability and is not predictive (Hoo et al. 2017). Less than 0.7 is considered 'poor' while 0.8 and above is considered excellent, with an AUC of 1 being perfect (Çorbacıoğlu and Aksel 2023).

The AUC for 'erythrocyte development' was 0.49 and for 'myeloid cell differentiation' was 0.6 (Figure 5-7) suggesting the proteins in the 'erythrocyte development' pathway were not useful for distinguishing between relapse and TFR. Although 'myeloid cell differentiation', that includes all the proteins of 'erythrocyte development' along with 6 other proteins, had a higher AUC, which suggests the 'combination' of these proteins that is present in the 'myeloid cell differentiation' pathway is more useful, the higher AUC is still not considered useful for prediction.

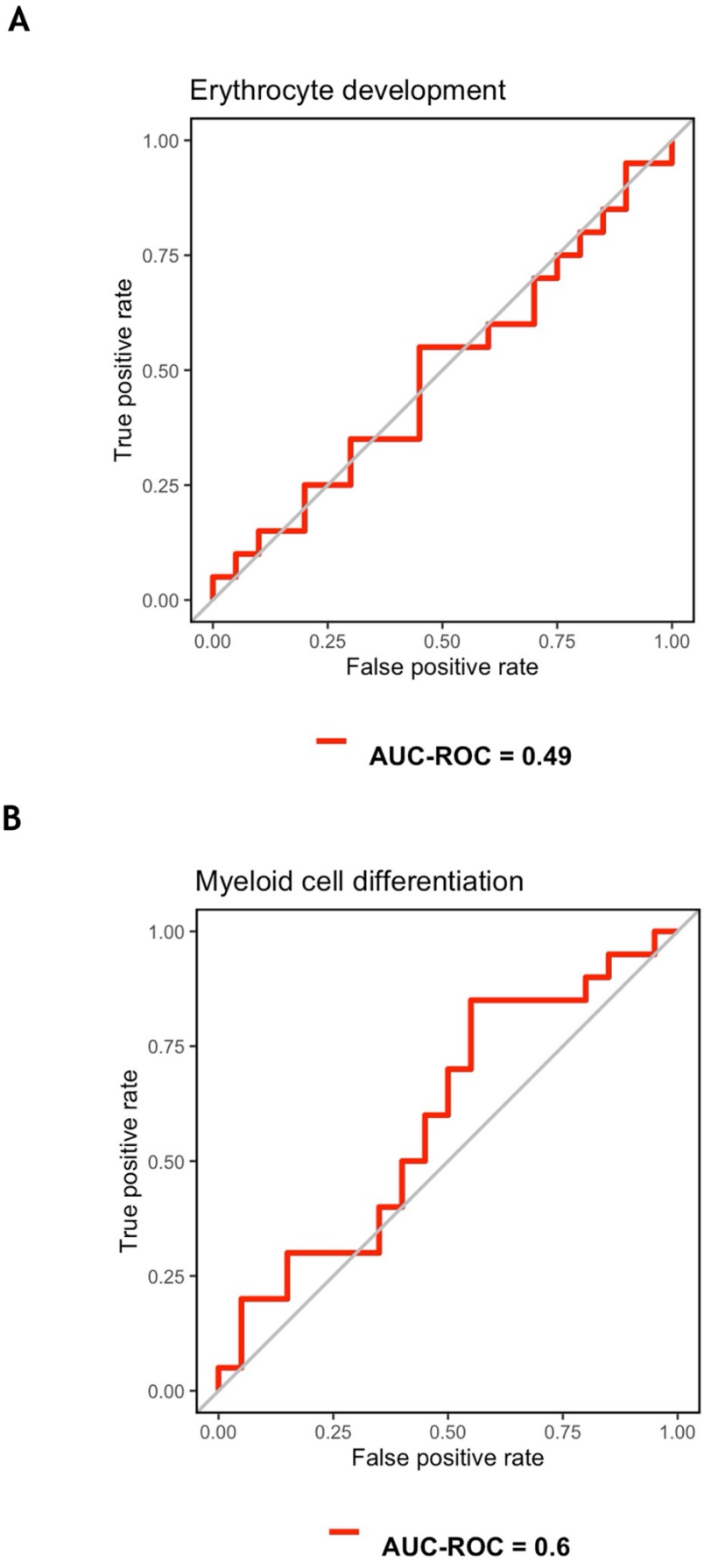

Figure 5-7 BM plasma DEPs from pathways were used to generate ROC curves for the prediction of TFR (A) ROC curve analysis of proteins in upregulated 'erythrocyte development' (GO:0048821) pathway from GO analysis; **(B)** ROC curve analysis of proteins in upregulated 'myeloid cell differentiation' (GO:0030099) pathway from GO analysis.

With the over-representation of pathways from the downregulated proteins, the pathways of interest were selected (Table 5-3). As seen below, many of the pathways share proteins.

GO ID	Description	Gene ratio	GeneID
GO:0019731	antibacterial humoral response	9/116 (0.08)	**IGHA2/TF/DEFA1/SLPI/ELANE/DMBT1 IGHD/KLK7/IGHE**
GO:0019730	antimicrobial humoral response	11/116 (0.09)	**IGHA2**/PF4V1/**TF/DEFA1/SLPI/ELANE** S100A7/**DMBT1/IGHD/KLK7/IGHE**
GO:0006959	humoral immune response	13/116 (0.1)	**IGHA2**/CFHR2/PF4V1/**TF/DEFA1/SLPI** CFHR4/**ELANE**/S100A7/**DMBT1/IGHD KLK7/IGHE**

Table 5-3 Downregulated proteins from pathways of interest using ORA analysis of R_E vs TFR_E.

From these pathways the ROC curves demonstrate 'antibacterial humoral response' has an AUC of 0.71, 'antimicrobial humoral response' has an AUC of 0.8 and 'humoral immune response' has an AUC of 0.8. The proteins within the 'humoral immune response' pathway included the proteins found in the other two pathways as well as additional proteins, this is unsurprising as these pathways are descendants of the 'humoral immune response' pathway. Additionally, the 'humoral immune response' and 'antimicrobial humoral response' produced an AUC of 0.8 which means this protein combination is a potential option to predict between TFR and relapse at trial entry.

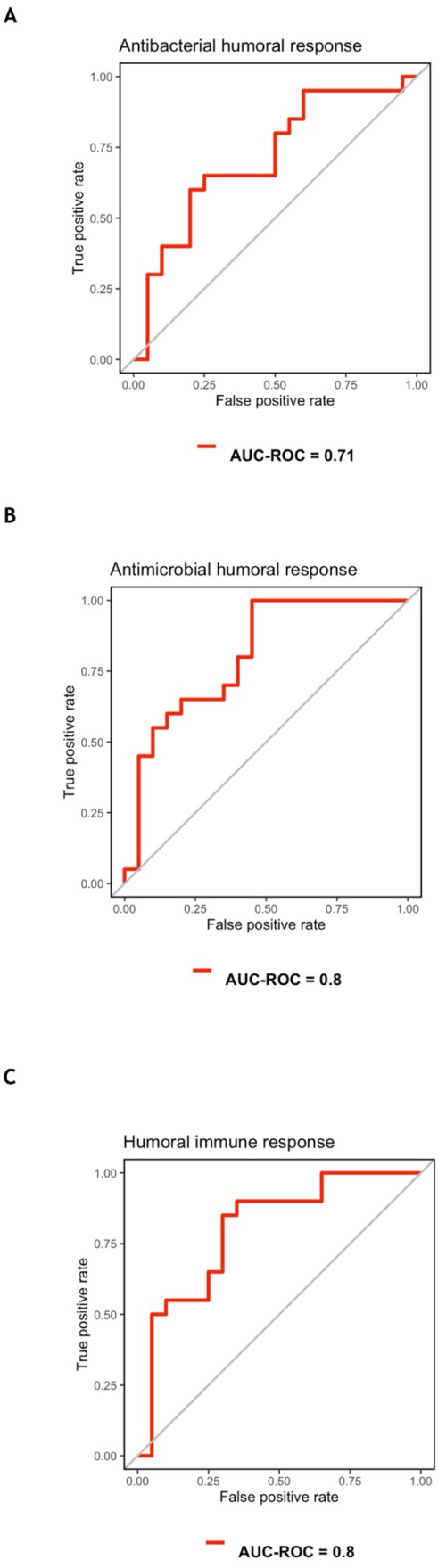

Figure 5-8 BM plasma DEPs from pathways were used to generate ROC curves for the prediction of TFR (A) ROC curve analysis of proteins in downregulated 'humoral immune response' (GO:0006959) pathway from GO analysis. **(B)** ROC curve analysis of proteins in downregulated 'antibacterial humoral response' (GO:0019731) pathway from GO analysis. **(C)** ROC curve analysis of proteins in downregulated 'antimicrobial humoral response' (GO:0019730) pathway from GO analysis.

The analysis was initially done using ORA, however, to provide a broader understanding of the data, GSEA was also measured. GSEA takes all the genes and ranks them based on their direction of change and their significance that is then compared to pre-defined gene lists. The gene list used was all the genes within the proteomics data, as necessarily the genes were used as input to represent proteomic changes.

As GSEA method uses all genes, this allows the analysis to focus on small changes that ORA may miss. While ORA is an excellent initial analysis, using both ORA and GSEA gives a more thorough, in-depth analysis of the data. GO software was also used that once again focussed on biological processes (BP).

For the positively enriched pathways in the comparison of R_E vs TFR_E, an increase in metabolic and catabolic pathways can be seen (Figure 5-9 A). This includes 'purine nucleotide metabolic process' and 'purine-containing compound metabolic process', purines are molecules for the synthesis of nucleic acid used for DNA and RNA production. Additionally, enrichment of 'nucleoside phosphate metabolic process', 'nucleobase-containing small molecule metabolic process' and 'nucleotide metabolic process' are all pathways also involved in DNA synthesis. An increase of these pathways could suggest there is an increase in cell proliferation and metabolic activity within relapsing patients even before TFR is attempted.

Within the negatively enriched BP pathways there was: 'humoral immune response', 'complement activation', 'complement activation, classical pathway' and 'humoral immune response mediated by circulating immunoglobulin'. Downregulation of 'humoral immune response' was seen with the ORA analysis (Figure 5-6 B). Additionally, the complement pathways identified here are unsurprising as complement can be involved in activating the humoral immune response that suggests the immune response of relapsing patients is less robust than patients maintaining TFR even before TKIs have been stopped. Hence it may be said that before attempting TFR, some patients are predicted more likely to relapse owing to their immune response.

Unlike ORA which focuses on upregulated and downregulated lists, GSEA uses entire dataset, therefore ROC curves were not generated for the proteins

identified within these pathways. GSEA does not have a cut-off and so does not provide a binary result like ORA; a ROC curve that is assessing the ability of these proteins to discriminate between the two outcome groups is more useful with ORA than GSEA.

A

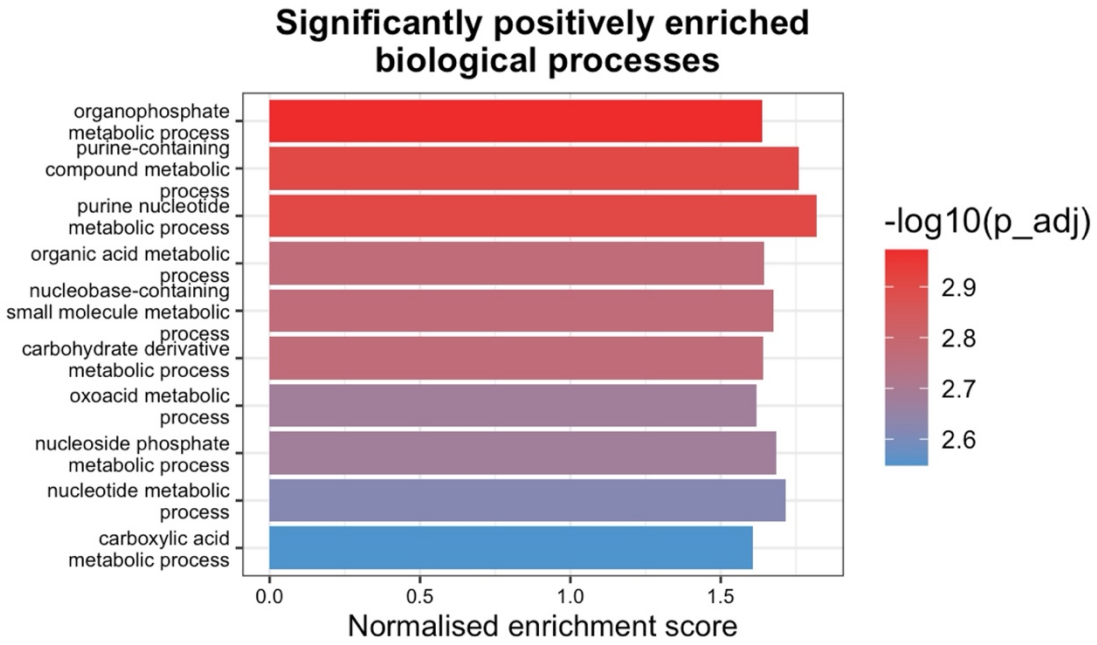

B

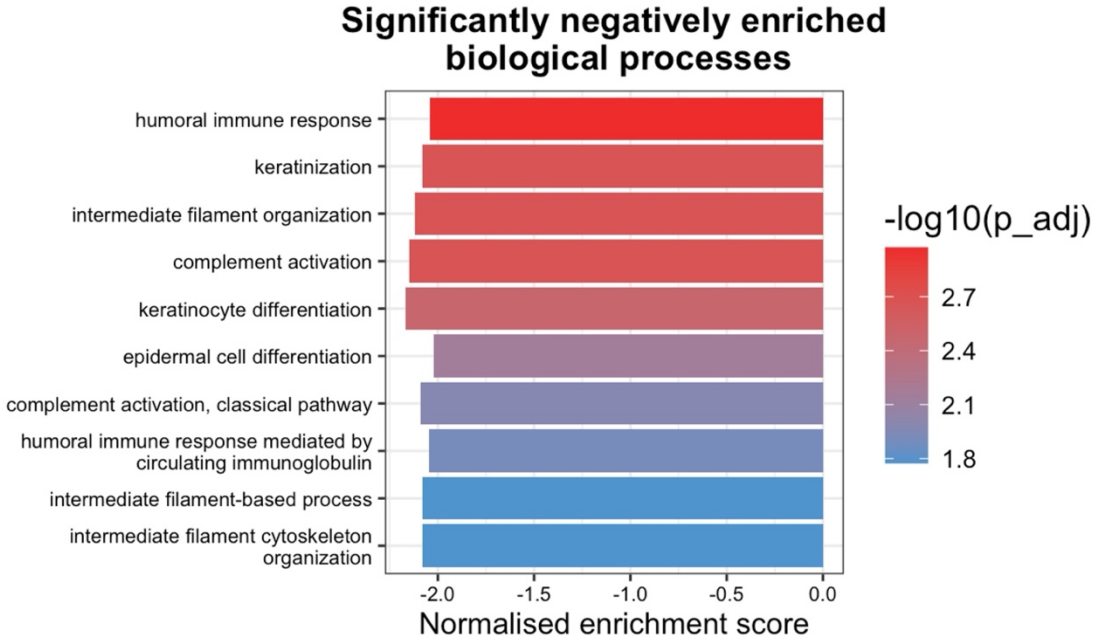

Figure 5-9 Enrichment analysis of BM plasma using gene set enrichment analysis GSEA (GSEA) tool DEPs were used to identify top 10 enriched pathways (using RStudio) found to be positively and negatively enriched at R_E (n=20) vs TFR_E (n=20).

Pathway	NES	p.adj
purine nucleotide metabolic process	1.8	0.0017
organophosphate metabolic process	1.6	0.0017
purine-containing compound metabolic process	1.7	0.0019
nucleoside phosphate metabolic process	1.7	0.0019
nucleobase-containing small molecule metabolic process	1.7	0.0019
carbohydrate derivative metabolic process	1.6	0.0019
organic acid metabolic process	1.6	0.0019
nucleotide metabolic process	1.7	0.0024
oxoacid metabolic process	1.6	0.0024
carboxylic acid metabolic process	1.6	0.0024

Table 5-4 Top 10 positively enriched pathways of GSEA comparing relapse (R_E) vs TFR (TFR_E) at trial entry.

Pathway	NES	p.adj
humoral immune response	-2.2	0.0019
complement activation	-2.2	0.0019
intermediate filament organization	-2.2	0.0019
keratinocyte differentiation	-2.1	0.0019
keratinization	-2.1	0.0020
epidermal cell differentiation	-2.1	0.0070
complement activation, classical pathway	-2.1	0.0104
humoral immune response mediated by circulating immunoglobulin	-2.1	0.0151
intermediate filament-based process	-2.1	0.0163
intermediate filament cytoskeleton organization	-2.1	0.0163

Table 5-5 Top 10 negatively enriched pathways of GSEA comparing relapse (R_E) vs TFR (TFR_E) at trial entry.

5.4.2 Pro-inflammatory protein profile in BM plasma at Relapse exit (R_X) vs Relapse entry (R_E)

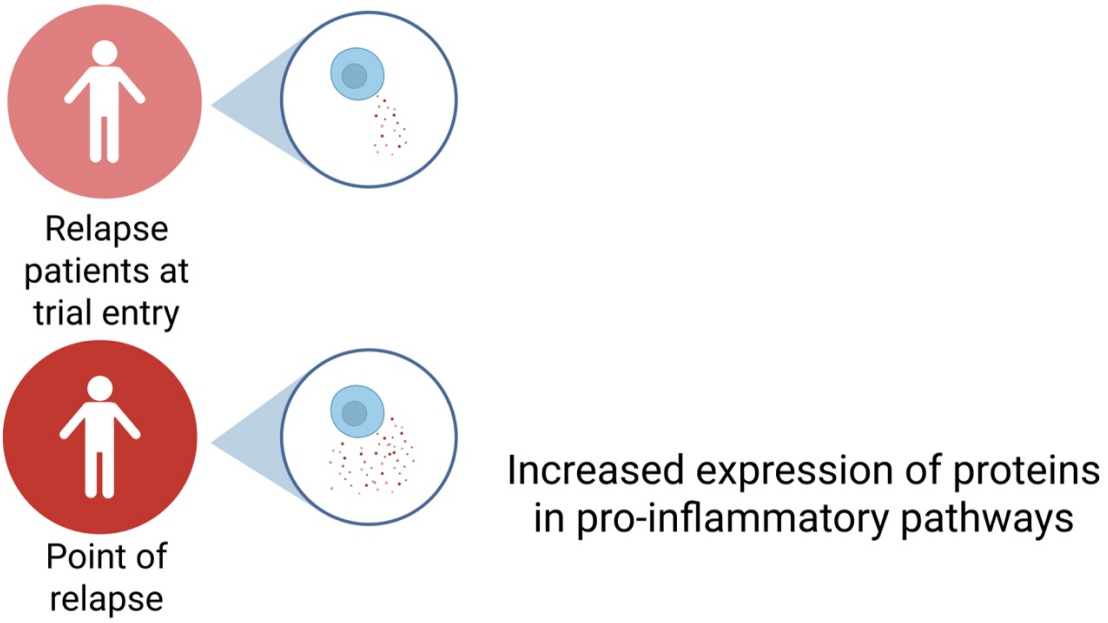

Figure 5-10 Take home message of proteomics analysis for R_X vs R_E

Once the initial analysis of how relapse and TFR patients differ at the common start point of the trial before stopping TKIs, exit data was then analysed to compare changes in proteins within the BMM of relapse patients from the start of the trial to their point of relapse and what pathways were changed. For this a comparison of 17 patient samples taken at point relapse (R_X) and 20 samples taken at start of trial (R_E) were compared. For analysis of the data RStudio was used to identify DEPs, using a cutoff of p.adj<0.05 and $\log_2$fold>0.5.

The PCA plot shows no grouping between R_X and R_E samples, indicating high similarity between samples. Additionally, by volcano plot, 111 upregulated DEPs were identified and 201 downregulated DEPs within the threshold for this data. The comparison of the relapse samples has produced 312 DEPs which is more DEPs than the 252 found with R_E vs TFR_E (Figure 5-2). The increased DEPs within this comparison suggests there are more changes found within patients when they relapse.

Only DEP data was visualised on a heatmap (Figure 5-12). The STRING network of downregulated proteins showed two major clusters, one was associated with

ribosomes, and the other cluster is proteins associated with histones (Figure 5-14).

A

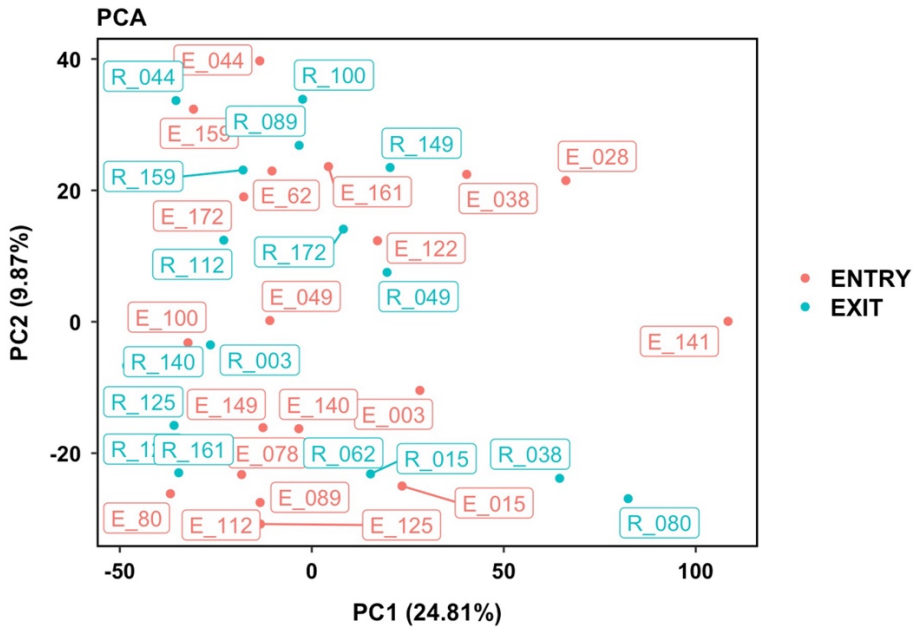

B

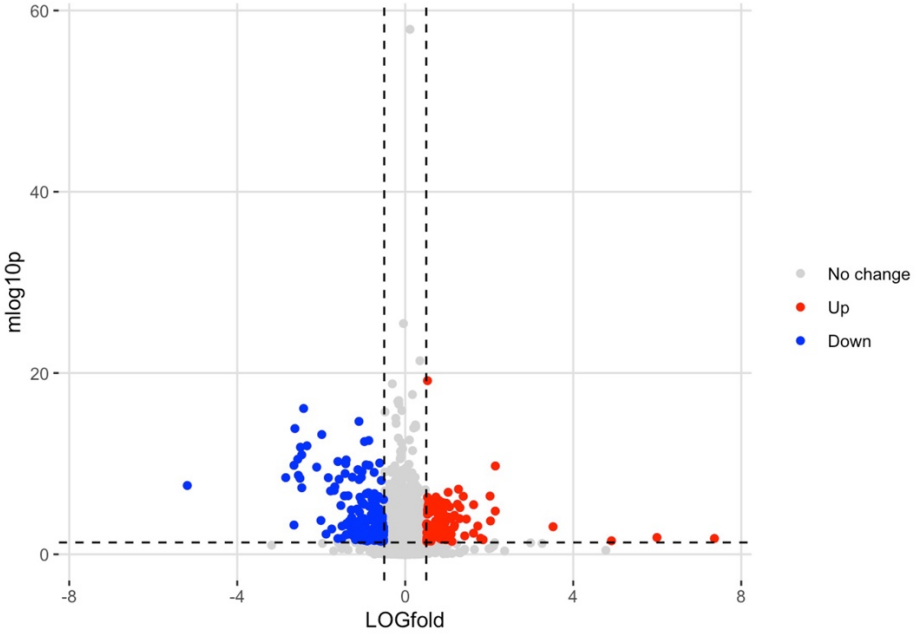

Figure 5-11 Proteins changed in BM plasma at point of relapse with respect to relapse at trial entry (A) PCA plot of protein expression data between relapse at point of relapse (R_X) (blue) and relapse at trial entry (R_E) (n=20) (red). Showing PC1 (24.81%) and PC2 (9.87%). **(B)** Volcano plot of comparison of relapse at point of relapse (R_X) vs relapse at trial entry (R_E) at trial entry. DEPs were established at p.adj<0.05 and $\log_2$ fold>0.5. These are shown as upregulated (red), downregulated (blue) and no change (grey). Volcano and PCA plot were made on RStudio. R_X (n=17) and R_E (n=20).

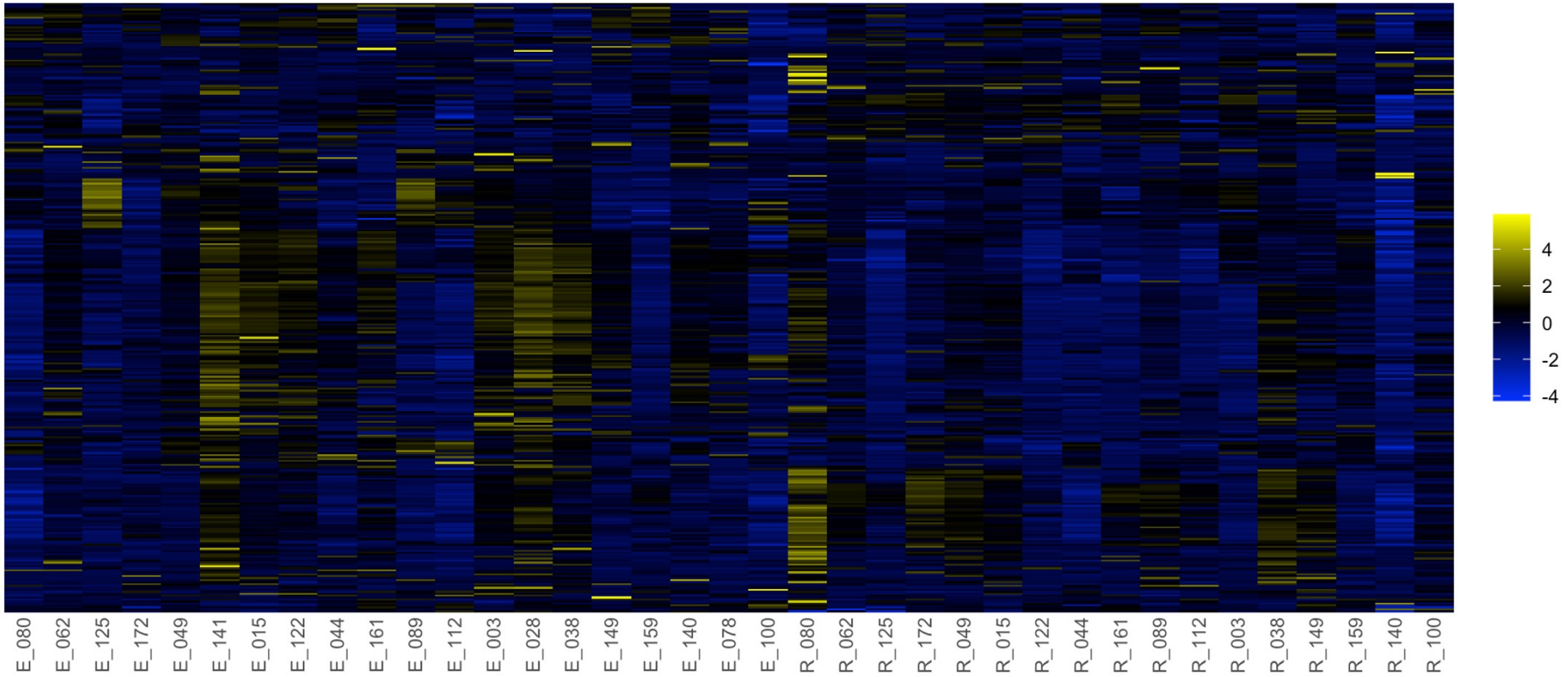

Figure 5-12 Expression levels of the DEPs found to be changed in BM plasma at point of relapse with respect to relapse at trial entry The expression values have been normalised into z-scores. The heatmap shows the expression of all significant proteins within the relapse at point of relapse (R_X) (n=17) and relapse at trial entry (R_E) (n=20) comparison. Samples are shown on the x-axis, proteins are shown on the y-axis. The scale at the side shows the colour intensity based on the expression level, highest expression (upregulated) and blue is the lowest (downregulated). The heatmap has y-clustering of the rows, this clustered related proteins together, based on the expression levels. DEPs were identified at p.adj<0.05 and $\log_2$fold>0.5. Heatmap and clustering was done on RStudio.

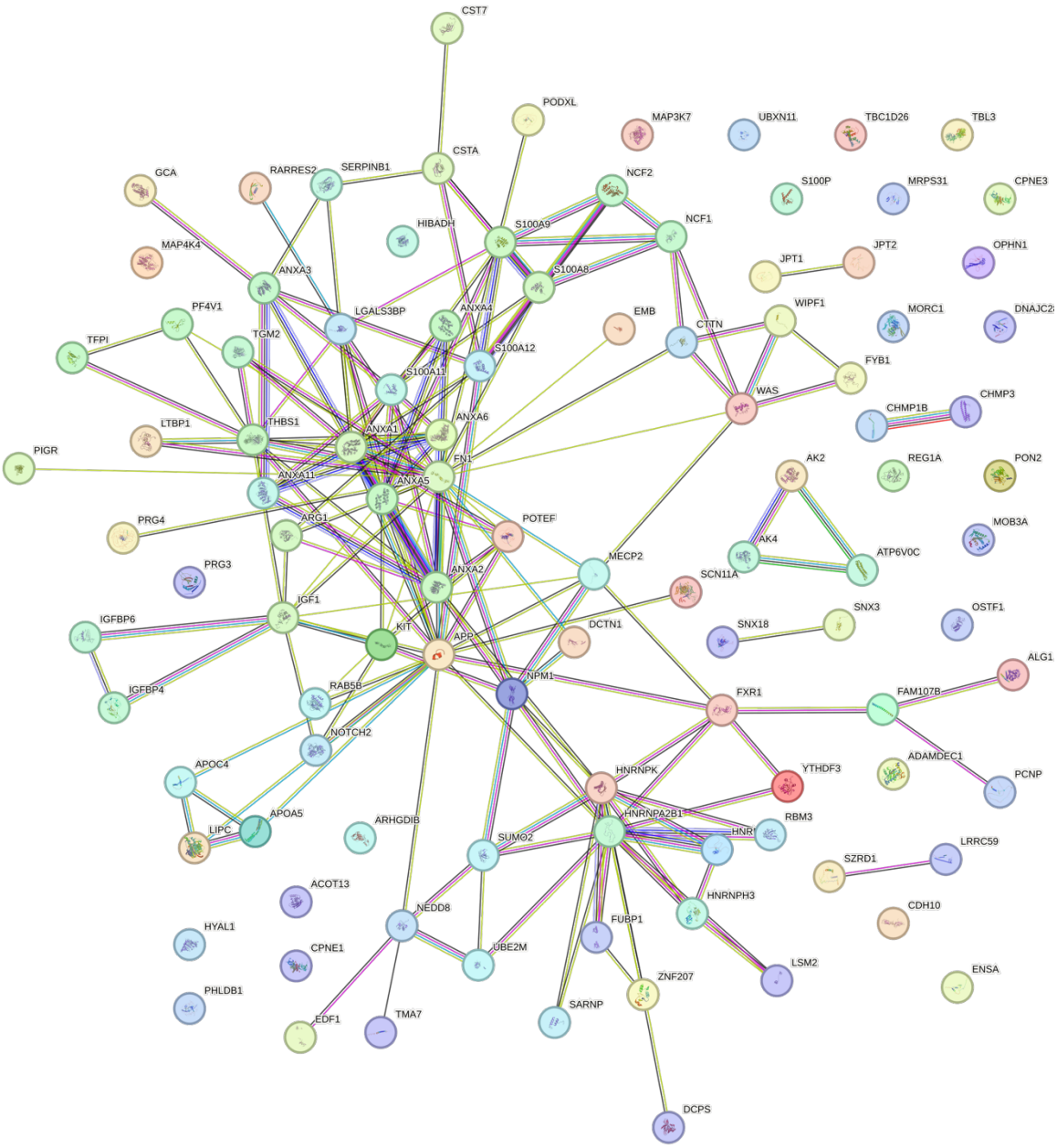

Figure 5-13 Interaction of 111 upregulated DEPs in relapse patients at point of relapse with respect to relapse patients at trial entry STRING network showing the interaction of 111 upregulated DEPs in relapse patients at point of relapse (R_X) vs relapse patients at trial entry (R_E). All proteins within this comparison were put into the STRING database, the 111 proteins were used to identify their relationship to each other. Each colour for the lines identifies a different type of association that is predicted about two proteins, the thickness of the line is related to the confidence of this prediction.

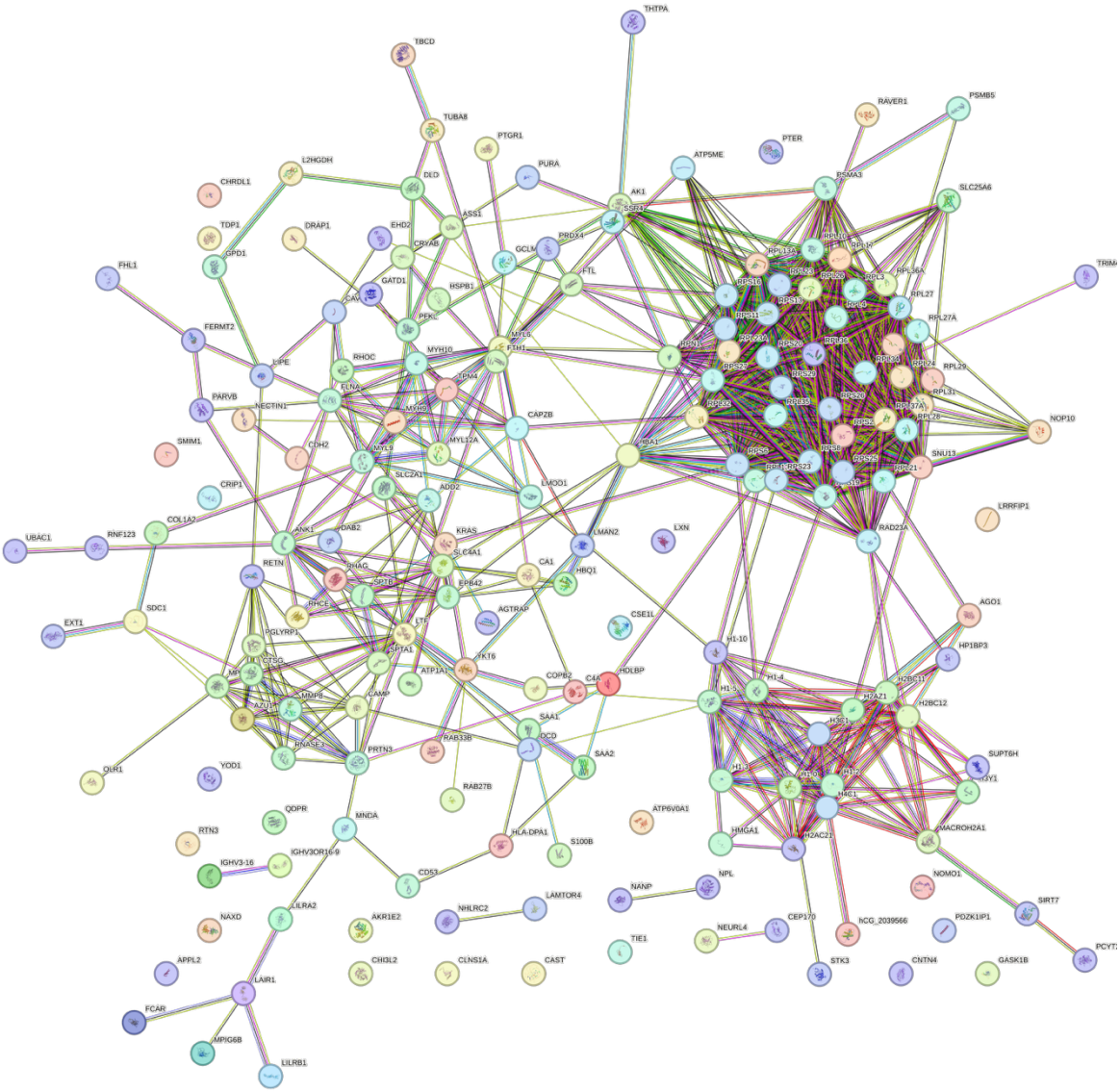

Figure 5-14 Interaction of 201 downregulated DEPs in relapse patients at point of relapse with respect to relapse patients at trial entry STRING network showing the interaction of 201 downregulated DEPs in relapse patients at point of relapse (R_X) vs relapse patients at trial entry (R_E). All proteins within this comparison were put into the STRING database, the 201 proteins were used to identify their relationship to each other. Each colour for the lines identifies a different type of association that is predicted about two proteins, the thickness of the line is related to the confidence of this prediction.

Looking at R_X vs R_E for pathway analysis using GO with BP, there is a clear increase of granulocyte activity (Figure 5-15 A) as evidenced by the increased representation of pathways such as ‘myeloid leukocyte activation’, ‘leukocyte chemotaxis’, ‘myeloid leukocyte migration’, ‘granulocyte chemotaxis’ and ‘granulocyte migration’. This suggests increased inflammation in BMM of patients at the point of relapse as well as increase in activity of granulocytes, which would be expected as relapsing patients have active disease progression.

Downregulated pathways such as ‘ribonucleoprotein complex biogenesis’, ‘ribosome biogenesis’, ‘rRNA metabolic process’, ‘rRNA processing’ and ‘ribosomal small subunit biogenesis’ are involved in the formation, alteration, disassembly of ribosomes, suggesting dysregulation of ribosomes and their production could be involved in relapse. Perhaps most surprisingly in this data, ‘cytoplasmic translation’, ‘protein-DNA complex organisation’, ‘nucleosome organisation’ and ‘nucleosome assembly’ pathways were also downregulated. These pathways are all related to DNA and protein production which would be expected to be upregulated at point of relapse as there is increased production of BCR::ABL^{+} cells.

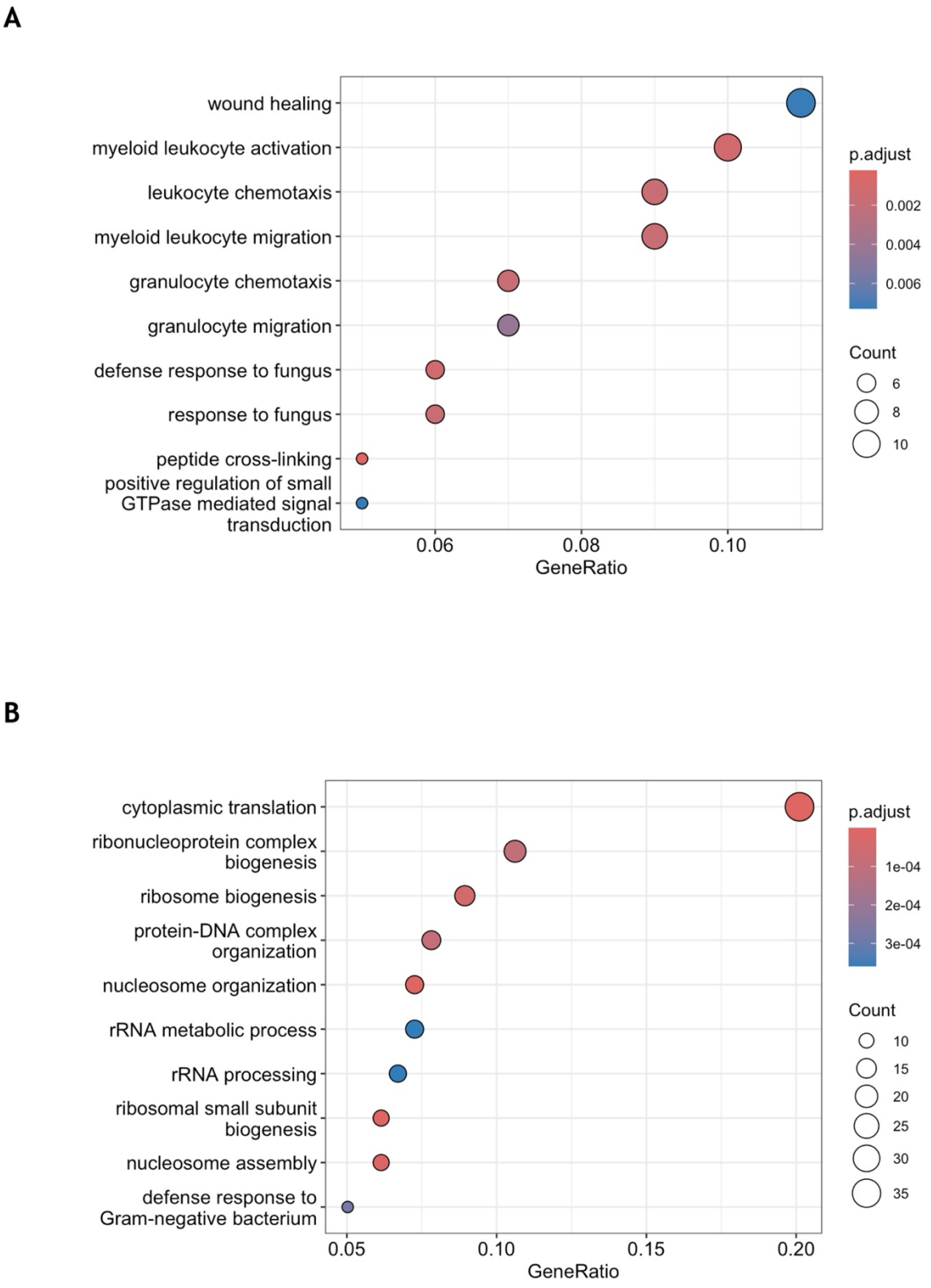

Figure 5-15 Gene ontology (GO) biological processes (BP) pathway analysis of Relapse_X vs Relapse_E proteomics DEPs were used to identify top 10 enriched pathways (using RStudio) **(A)** upregulated and **(B)** downregulated in relapse patients at point of relapse (R_X) (n=17) compared to relapse at trial entry (R_E) (n=20). Gene ratio = ratio of DEPs in pathway to all target proteins. Count demonstrated the number of proteins identified within the pathway.

GO ID	Description	Gene ratio	GeneID
GO:0002274	Myeloid leukocyte activation	10/100 (0.1)	**ANXA1**/ANXA3/FN1/THBS1/**S100A12 KIT**/CST7/NOTCH2/PRG3/**APP**
GO:0071621	Granulocyte chemotaxis	7/100 (0.07)	**ANXA1/S100A9/S100A8/PF4V1/RARRES2THBS1/S100A12**
GO:0097530	Granulocyte migration	7/100 (0.07)	**ANXA1/S100A9/S100A8/PF4V1/RARRES2THBS1/S100A12**
GO:0030595	Leukocyte chemotaxis	9/100 (0.09)	**ANXA1/S100A9/S100A8/PF4V1/RARRES2THBS1/S100A12/KIT/APP**
GO:0097529	Myeloid leukocyte migration	9/100 (0.09)	**ANXA1/S100A9/S100A8/PF4V1/RARRES2THBS1/S100A12/KIT/APP**

Table 5-6 Upregulated proteins from pathways of interest using ORA analysis of R_X vs R_E. Many GO pathways have a hierarchical relationship therefore the proteins associated with these pathways can be similar amongst a group of pathways.

Once the pathways of interest had been established (Table 5-6 and Table 5-7), the usefulness for the proteins to distinguish between patients at point of relapse compared to same patients at the start of the trial. To do this, the dysregulated proteins within these pathways were used to generate ROC curves allowing identification of proteins related to relapse.

The AUC for ‘myeloid leukocyte activation’ was 0.78. The AUC for ‘granulocyte chemotaxis’/’granulocyte migration’ was 0.76. The AUC for ‘leukocyte chemotaxis’/ ‘myeloid leukocyte migration’ was 0.73. Overall, these pathways are moderate in their effectiveness of predictability for R_X and R_E and potentially could be used to further elucidate the mechanisms that lead to relapse.

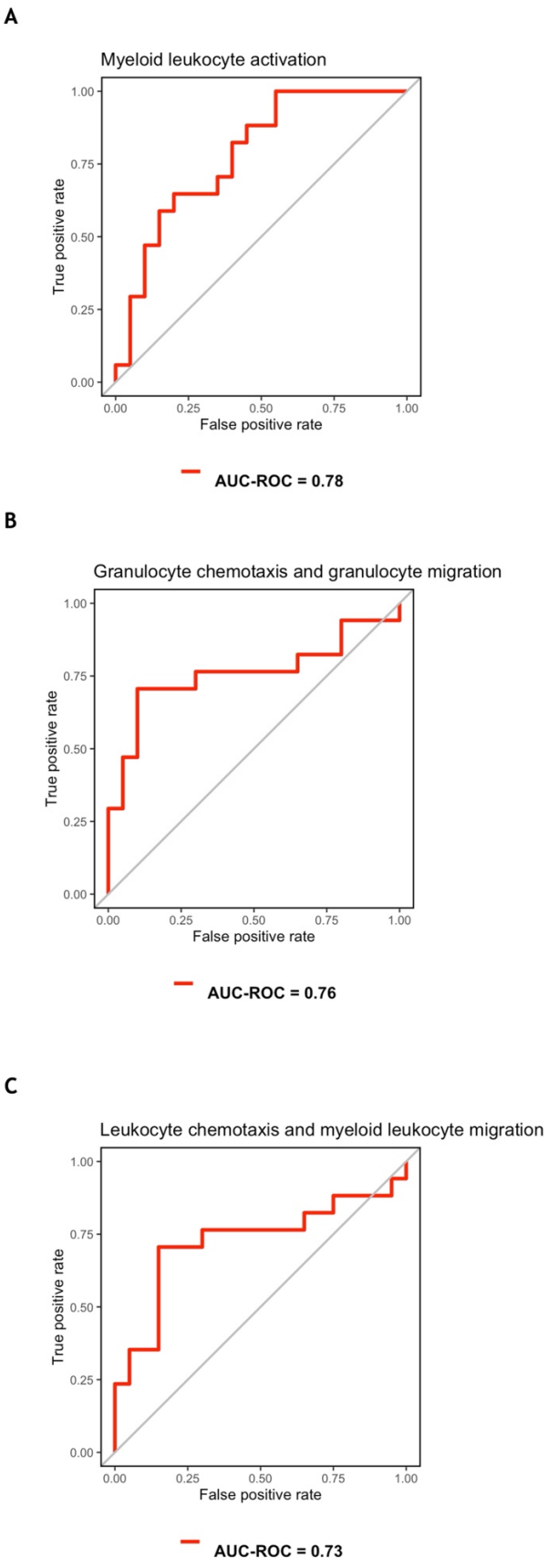

Figure 5-16 BM plasma DEPs from pathways were used to generate ROC curves for the prediction of relapse (A) ROC curve analysis of proteins in upregulated 'myeloid leukocyte activation' (GO:0002274) pathway from GO analysis. **(B)** ROC curve analysis of proteins in upregulated 'granulocyte chemotaxis' (GO:0071621) and 'granulocyte migration' (GO:0097530) pathway from GO analysis. **(C)** ROC curve analysis of proteins in upregulated 'leukocyte chemotaxis' (GO:0030595) and 'myeloid leukocyte migration' (GO:0097529) pathway from GO analysis.

GO ID	Description	Gene ratio	GeneID
GO:0042274	ribosomal small subunit biogenesis	11/179 (0.06)	**RPS19/RPS13/RPS8/RPS27/RPS6/RPS11 RPS23/RPS16/RPS25/RPS24**/SNU13
GO:0042254	ribosome biogenesis	16/179 (0.09)	**RPS19/RPS13/RPS8/RPL26/RPS27/RPS6 RPL27/RPL35**/RPL24/**NOP10/RPS11 RPS23/RPS16/RPS25/RPS24**/SNU13
GO:0002181	cytoplasmic translation	36/179 (0.2)	RPL37A/**RPS19/RPS13/RPS8**/RPS29 RPL26/RPL36A/**RPS27/RPS6**/RPL13 RPL4/RPL17/RPL21/RPL10/RPL27/RPL35 RPL24/RPL34/RPL3/**RPS11/RPS23** RPL27A/RPL23A/**RPS16/RPS25/RPS24** RPL19/RPL13A/RPL36/RPS20/RPL31 RPL29/RPL28/RPL32/RPL23/RPS26
GO:0006334	nucleosome assembly	11/179 (0.06)	**H1-2/H1-4/H4C1/H2BC11 H1-10/HP1BP3/H1-5/H1-3/H3C1 H1-0/MACROH2A1**
GO:0034728	nucleosome organization	13/179 (0.07)	**H1-2/H1-4/H4C1/H2BC11 H1-10/HP1BP3/H1-5/H1-3/H3C1 H1-0**/HMGA1/**MACROH2A1**/SUPT6H
GO:0071824	protein-DNA complex organization	14/179 (0.08)	**H1-2/H1-4/H4C1/H2BC11 H1-10/HP1BP3/H1-5/H1-3/H3C1 H10**/HMGA1/**MACROH2A1**/SUPT6H RPL23
GO:0006364	rRNA processing	12/179 (0.07)	**RPS19/RPS8/RPL26/RPS27/RPS6/RPL27 RPL35/NOP10/RPS16/RPS25/RPS24 SNU13**
GO:0016072	rRNA metabolic process	13/179 (0.07)	**RPS19/RPS8/RPL26/RPS27/RPS6/RPL27 RPL35/NOP10/RPS16/RPS25/RPS24 MACROH2A1/SNU13**
GO:0022613	ribonucleoprotein complex biogenesis	19/179 (0.1)	**RPS19/RPS13/RPS8/RPL26/RPS27/RPS6 RPL27/RPL35/RPL24/NOP10/RPS11 RPS23/RPS16/RPS25/RPS24**/RPL13A CLNS1A/SNU13/AGO1

Table 5-7 Downregulated proteins from pathways of interest using ORA analysis of R_X vs R_E.

The pathways can be separated into DNA/protein synthesis and ribosome biogenesis, many of the proteins within these pathways are almost identical owing to common proteins. One pathway chosen to look at the proteins within it in a ROC curve was 'cytoplasmic translation' [GO:0002181] as this pathway included unique proteins, some of which were not seen in other pathways, the other proteins within the other pathways will be looked at with a ROC curve

also. The ‘protein-DNA complex organisation’ [GO:0071824] was also chosen for similar reasons to ‘cytoplasmic translation’ however the protein list was different. Finally, ‘ribonucleoprotein complex biogenesis’ [GO:0022613] was selected as this included the 12 common proteins found within the other ribonuclease associated pathways as well as 7 additional proteins. ROC curves were generated for these pathways to identify the ability of these proteins to distinguish between the changes to proteins between trial entry and trial exit for patients who relapse. The AUC of ‘cytoplasmic translation’ was 0.72, for ‘protein-DNA complex organisation’ it was 0.79 and for ‘ribonucleoprotein complex biogenesis’ it was 0.71. These are all reasonable scores for indicating the predictability of these proteins for causing molecular relapse from deep remission when off TKI therapy.

A

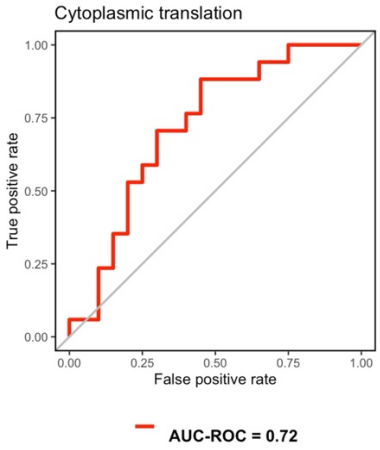

B

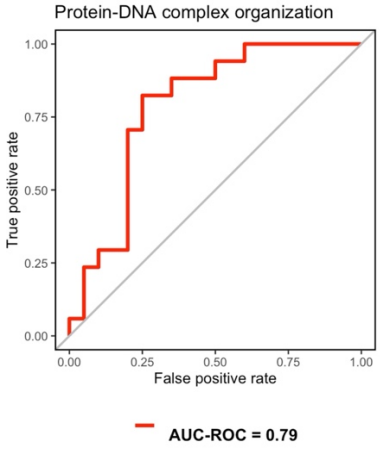

C

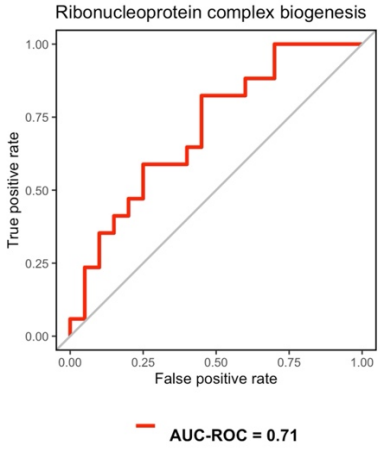

Figure 5-17 BM plasma DEPs from pathways were using to generate ROC curves for the prediction of relapse (A) ROC curve analysis of proteins in downregulated 'cytoplasmic translation' (GO:0002181) pathway from GP analysis. **(B)** ROC curve analysis of proteins in downregulated 'protein-DNA complex organization' (GO:0071824) pathway from GO analysis. **(C)** ROC curve analysis of proteins in downregulated 'ribonucleoprotein complex biogenesis' (GO:0022613) pathway from GO analysis.

Analysis by GSEA found only 7 positively enriched BPs within R_X vs R_E analysis (Figure 5-18 A). From this comparison the majority (6 out of 7) of positively enriched pathways were related to cell motility and migration. Pathways including ‘positive regulation of cell motility’, ‘regulation of cell migration’ ‘positive regulation of cell migration’, ‘regulation of cell motility’ and ‘positive regulation of locomotion’ were all positively enriched indicating potentially increased activity in the BM of R_X patients. These pathways are all involved in the upregulation of cell activity and within the BMM. Additionally, there is the presence of the ‘toll-like receptor signalling pathway’ known to be able to activate MAPK pathway, which is also upregulated, as seen with the ‘regulation of MAPK cascade’, that may lead to release of pro-inflammatory cytokines.

Similar to ORA analysis, the negatively enriched pathways are all involved in DNA and protein formation including ‘cytoplasmic translation’, ‘nucleosome assembly’, ‘protein-DNA complex organisation’ and more. The decrease of these pathways could be due to dysregulation of the normal cell production.

A

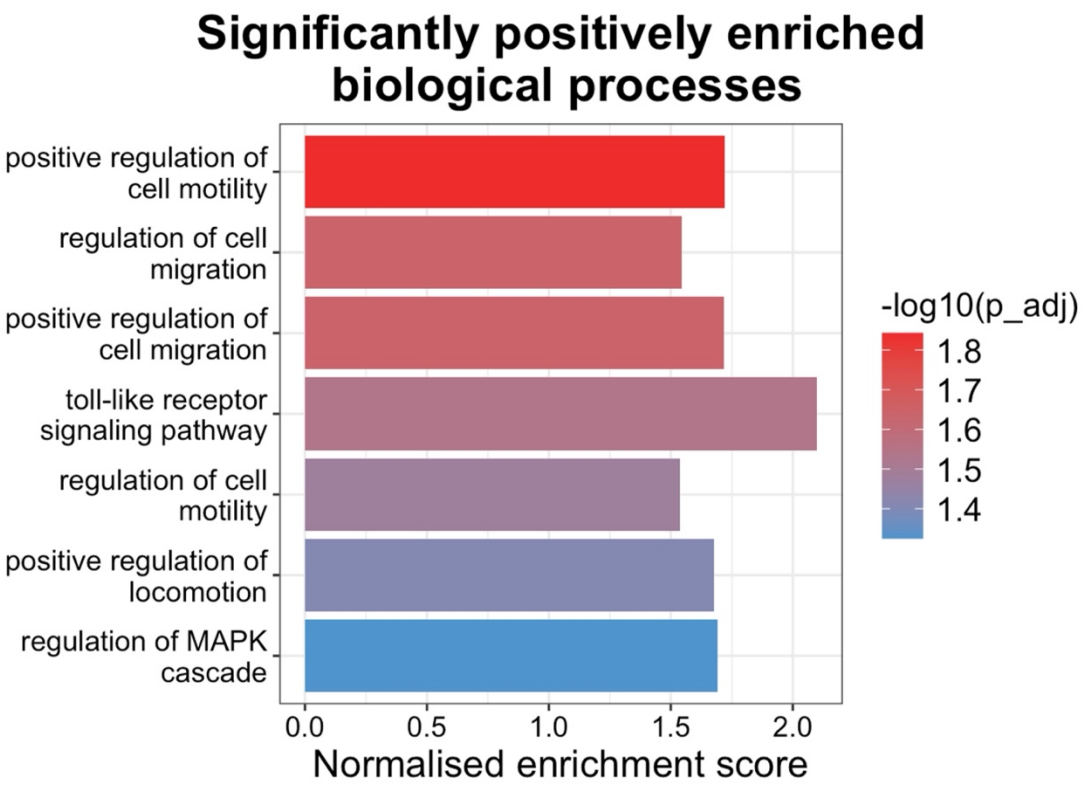

B

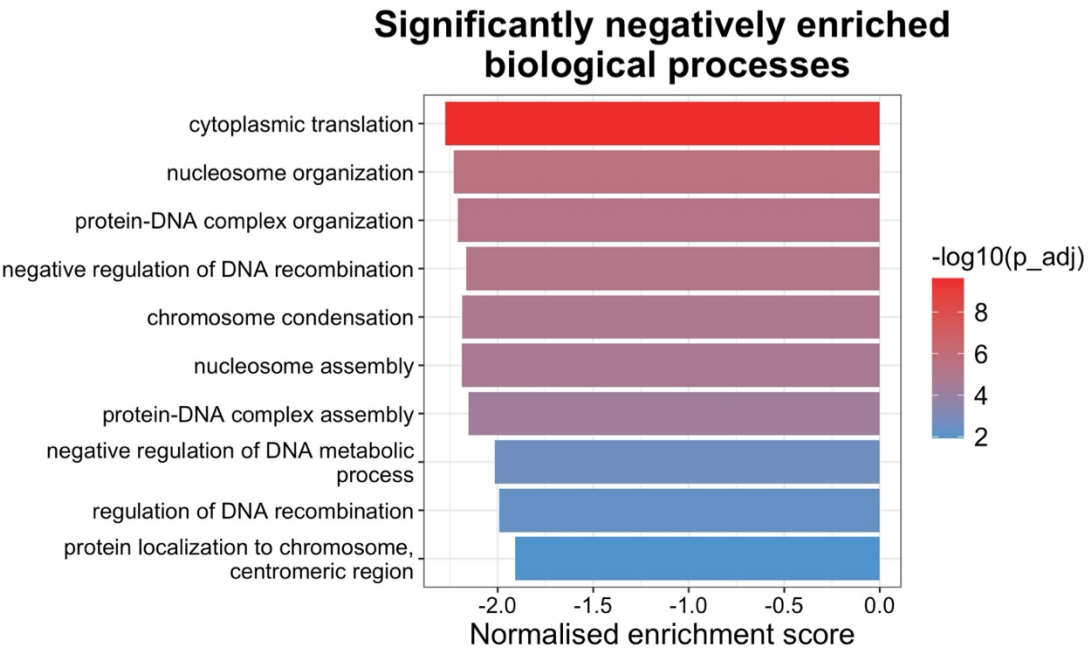

Figure 5-18 Enrichment analysis of BM plasma using GSEA tools DEPs were used to identify top 10 enriched pathways (using RStudio) found to be positively and negatively enriched in comparison of R_X (n=17) vs R_E (n=20).

Pathway	NES	p.adj
positive regulation of cell motility	1.7	0.0202
positive regulation of cell migration	1.7	0.0202
positive regulation of locomotion	1.7	0.0282
regulation of cell motility	1.5	0.0282
toll-like receptor signalling pathway	2.1	0.0346
regulation of cell migration	1.5	0.0475
regulation of MAPK cascade	1.7	0.0495

Table 5-8 The 7 positively enriched pathways of GSEA comparing R_X vs R_E.

Pathway	NES	p.adj
cytoplasmic translation	-2.3	2E-10
nucleosome organization	-2.2	3E-6
protein-DNA complex organization	-2.2	6E-6
negative regulation of DNA recombination	-2.2	8E-6
chromosome condensation	-2.2	1E-5
nucleosome assembly	-2.2	2E-5
protein-DNA complex assembly	-2.2	6E-5
negative regulation of DNA metabolic process	-2.0	0.0029
regulation of DNA recombination	-2.0	0.0053
protein localization to chromosome, centromeric region	-1.9	0.0117

Table 5-9 Top 10 negatively enriched pathways of GSEA comparing R_X vs R_E.

5.4.3 Increase of proteins associated with immune response pathway at trial end point compared to TFR patients at the start of the trial

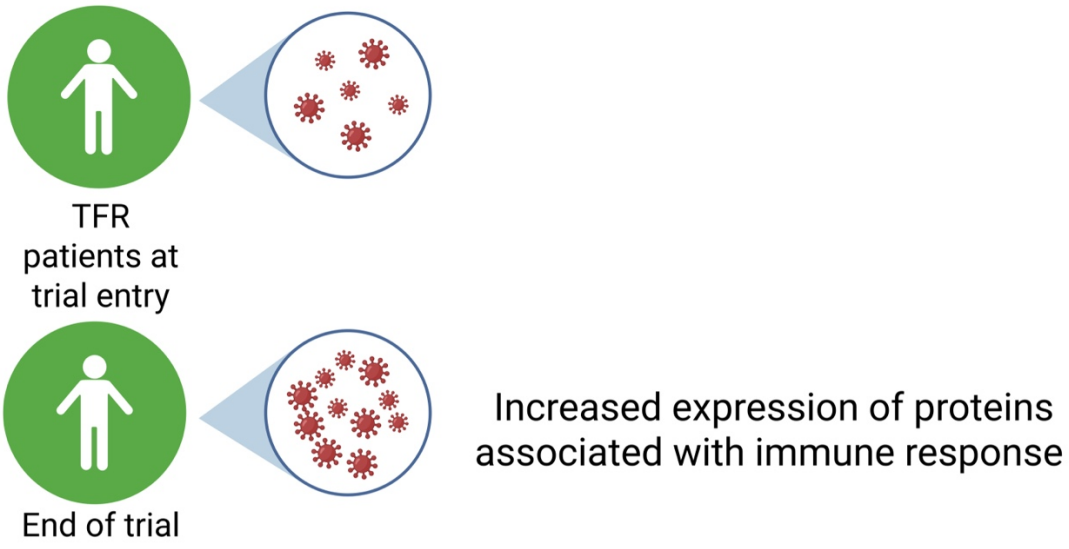

Figure 5-19 Take home message of proteomics analysis for TFR_X vs TFR_E

Following on from the analysis of relapse samples, the proteomic changes within the TFR samples was evaluated. For this 10 TFR at end point of trial (TFR_X) were compared to 20 TFR at trial entry (TFR_E) to uncover changes that may occur within the BMM to maintain remission during TFR. There was no visible clustering by PCAs of the TFR_X and TFR_E indicating their similarities/lack of trend between outcome groups (Figure 5-20 A). To distinguish the DEPs a threshold of p.adj<0.05 and $\log_2$fold>0.5 was set for significant proteins; there were 51 upregulated and 302 downregulated DEPs within the threshold (Figure 5-20 B). The split of DEPs here differs from before. R_E vs TFR_E had an almost even split of upregulated and downregulated DEPs, R_X vs R_E had a 1:2 split and now the TFR_X vs TFR_E has a 1:6 split.

The number of upregulated proteins at point of TFR_X was low with respect to at trial entry (TFR_E), this can also be seen on the heatmap below (Figure 5-21) where at trial exit there is almost no increased expression of these proteins additionally, the STRING network shows the low number of upregulated DEPs. The STRING network of the downregulated proteins has three major clusters with the two smaller clusters containing proteins involved in ribosomes, and the other proteins associated with histones.

A

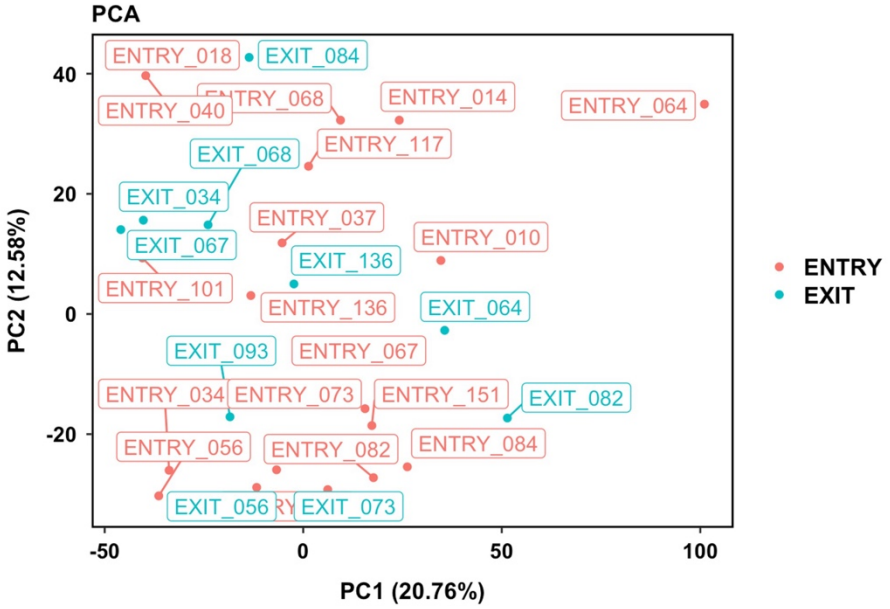

B

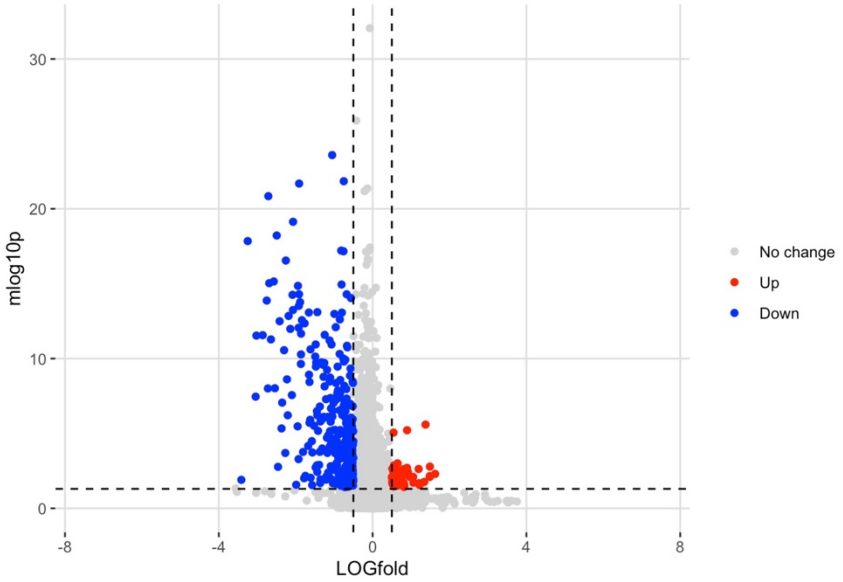

Figure 5-20 Proteins changed in TFR at end of trial with respect to start of trial (A) PCA plot of protein expression data between TFR at end of trial (TFR_X) (blue) and TFR at trial entry (TFR_E) (red). Showing PC1 (20.76%) and PC2 (12.58%). **(B)** Volcano plot of comparison of TFR at end of trial (TFR_X) vs TFR (TFR_E) at trial entry. DEPs were established at p.adj<0.05 and $\log_2$ fold>0.5. These are shown as upregulated (red), downregulated (blue) and no change (grey). Volcano and PCA plot were made on RStudio. TFR_X (n=10) and TFR_E (n=20).

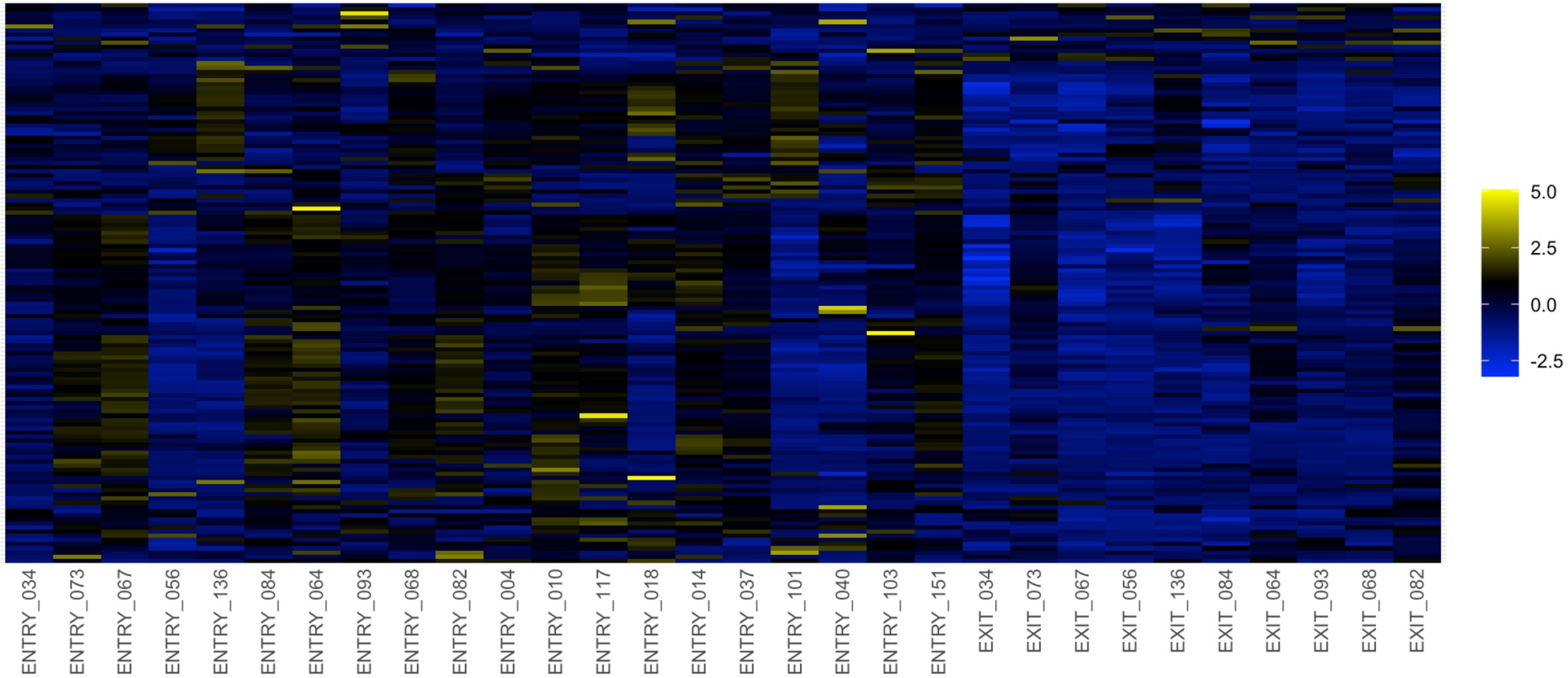

Figure 5-21 Expression change of DEPs in TFR at end of trial with respect to start of trial The heatmap shows the expression of all proteins significant proteins within the TFR at end of trial (TFR_X) (n=10) vs TFR at trial entry (TFR_E) (n=20) comparison. Samples are shown on the x-axis, proteins are shown on the y-axis. The scale at the side shows the colour intensity based on the expression level, highest expression (upregulated) and blue is the lowest (downregulated). The expression values have been normalised into z-scores. The heatmap has y-clustering of the rows, this clustered related proteins together. DEPs were identified at p.adj<0.05 and $\log_2$fold>0.5. Heatmap and clustering was done on RStudio.

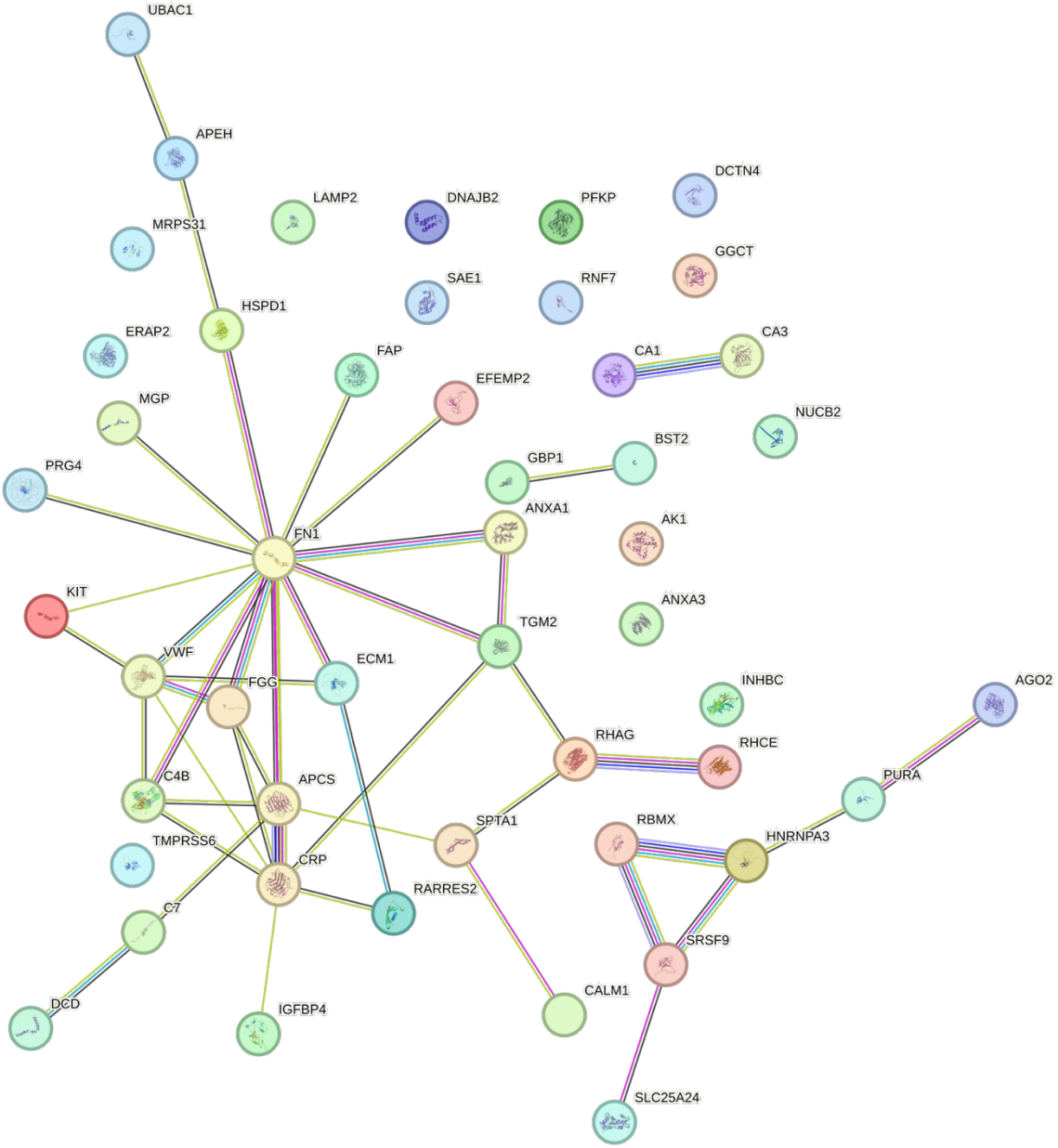

Figure 5-22 Interaction of 51 upregulated DEPs in TFR patients at end of trial with respect to TFR patients at trial entry STRING network showing the interaction of 51 upregulated DEPs in TFR patients at end point of the trial (TFR_X) vs TFR patients at trial entry (TFR_E). All proteins within this comparison were put into the STRING database, the 51 proteins were used to identify their relationship to each other. Each colour for the lines identifies a different type of association that is predicted about two proteins, the thickness of the line is related to the confidence of this prediction.

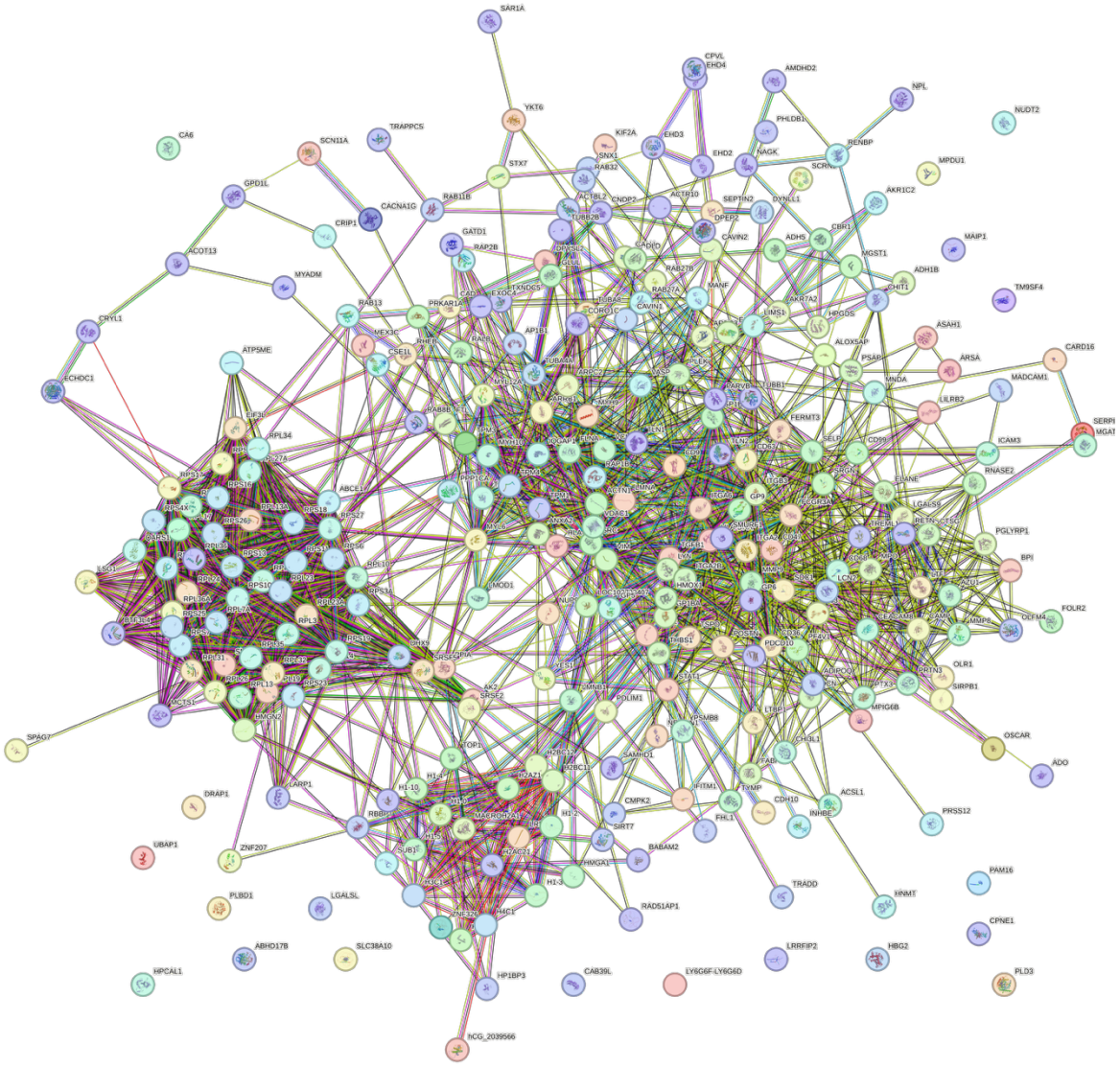

Figure 5-23 Interaction of 302 downregulated DEPS in TFR patients at end of trial with respect to TFR patients at trial entry STRING network showing the interaction of 302 downregulated DEPs in TFR patients at end point of the trial (TFR_X) vs TFR patients at trial entry (TFR_E). All 302 downregulated proteins within this comparison were put into the STRING database to identify their relationship to each other. Each colour for the lines identifies a different type of association that is predicted about two proteins, the thickness of the line is related to the confidence of this prediction.

As it was seen at the start of the trial (Figure 5-6) there is a decrease in proteins involved in immune response in relapse patients compared to TFR patients at the start of the trial, the reverse of this therefore suggests TFR patients have an increase of proteins involved in the immune response at the start of the trial. Therefore, the increase in 'acute-phase response' pathway which is an innate immune reaction in TFR patients at the end of the trial indicates an increased expression of proteins associated with immune response at the end point of the trial in patients that maintain TFR. The increase of 'leukocyte proliferation' and

‘myeloid leukocyte activation’, which are also involved in activating the immune response further suggests patients maintaining TFR have increased activity of immune associated proteins. This increased immune response could imply there is a continuation of increase immune response in TFR patients after TKI cessation which is responsible for maintaining TFR. The upregulation of the immune response pathways after it was already established at trial entry to be increased in TFR patients indicates this is essential for maintaining TFR.

The pathway analysis using GO with BP revealed a perhaps surprising increase in myeloid activity and proliferation with pathways: ‘leukocyte proliferation’ and ‘myeloid leukocyte activation’ increased at end point of trial in TFR patients. Additionally, although there is an increase in activity of the granulocyte cells there is also an increase of ‘phagocytosis’, ‘apoptotic cell clearance’ and ‘regulation of apoptotic cell clearance’. This could suggest in patients maintaining TFR the pathways regulating an increase in granulocyte proliferation is perhaps working in alongside normal apoptotic pathways and immune regulation pathways which is results in normal haematopoiesis being maintained.

Interestingly, there was also an increase in the ‘positive regulation of cell adhesion’ pathway; within the BM adhesion molecules keep HSCs within their own niche to maintain haematopoiesis (Kulkarni and Kale 2020). Increase of this normal haematopoietic regulatory pathway could be responsible for maintaining remission.

Pathways downregulated in this comparison included ‘cytoplasmic translation’ and ‘ribosomal small subunit biogenesis’. This was unexpected as these same pathways were also downregulated in the R_X vs R_E comparison (Figure 5-15). Perhaps in patients destined to relapse these pathways are completely dysregulated while in patients maintaining remission the same pathways are only part of the maintenance of the BMM along with the other pathways allowing TFR to continue.

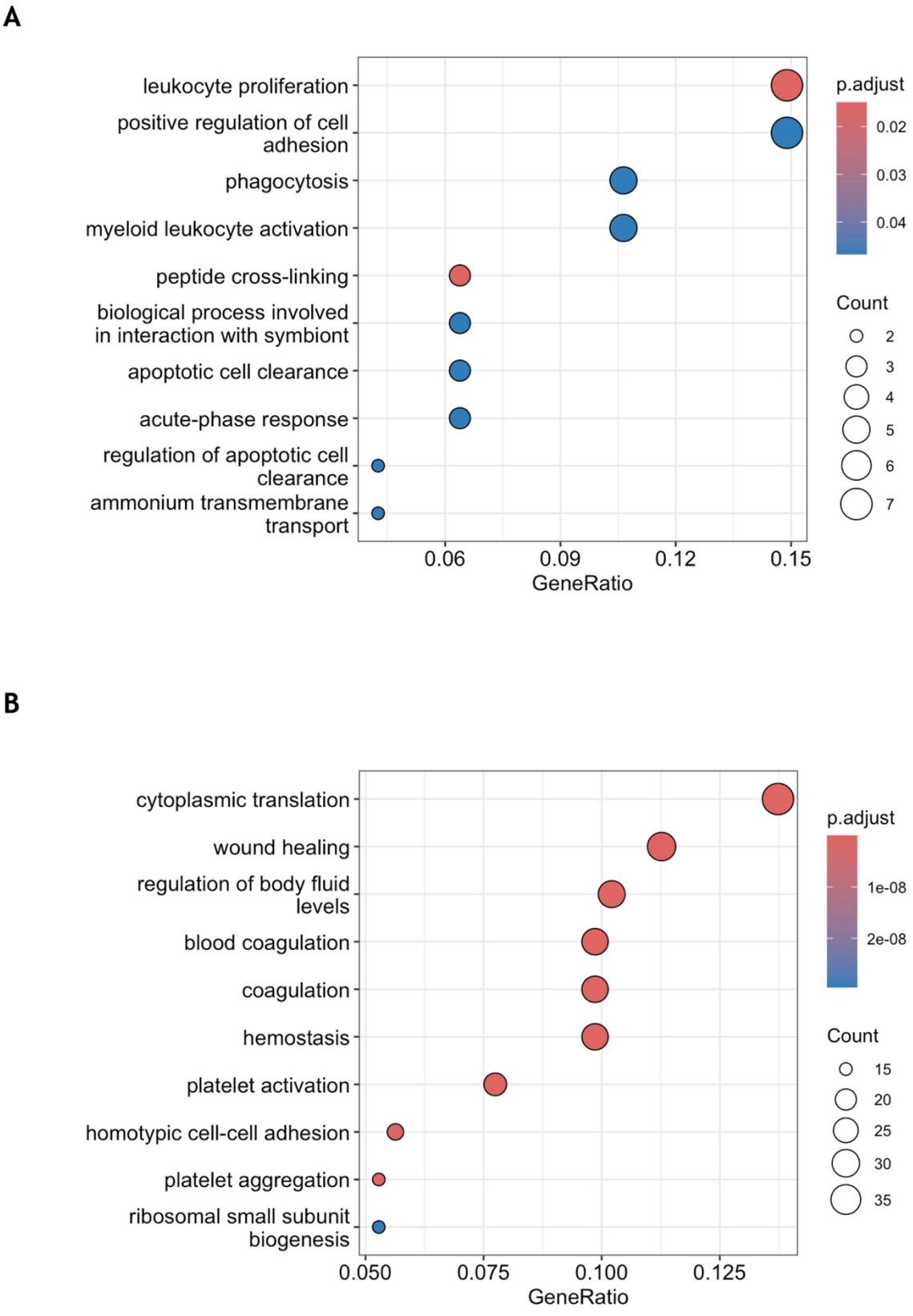

Figure 5-24 Gene ontology (GO) biological processes (BP) pathway analysis of TFR_X vs TFR_E proteomics DEPs were used to identify top 10 enriched pathways (using RStudio) **(A)** upregulated and **(B)** downregulated in TFR patients at trial exit (TFR_X) (n=10) compared to TFR at trial entry (TFR_E) (n=20). Gene ratio = ratio of DEPs in pathway to all target proteins. Count demonstrated the number of proteins identified within the pathway.

GO ID	Description	Gene ratio	GeneID
GO:0043277	apoptotic cell clearance	3/47	**ANXA1**/TGM2/C4B
GO:0070661	leukocyte proliferation	7/47	**ANXA1**/PURA/BST2/**HSPD1**/KIT/ **SPTA1**/CRP
GO:0045785	positive regulation of cell adhesion	7/47	FN1/**ANXA1**/EFEMP2/TGM2/**HSPD1**/ FGG/**SPTA1**

Table 5-10 Upregulated proteins from pathways of interest using ORA analysis of TFR_X vs TFR_E

The proteins were tested using ROC curves which found 'leukocyte proliferation' had an AUC of 0.75, a good score. Additionally, apoptotic cell clearance had an AUC of 0.88, this is excellent and demonstrates potential biomarkers for maintenance of TFR. However, 'positive regulation of cell adhesion' had the highest AUC of any proteins within a pathway that was tested with a score of 0.94. This would suggest that the combination of the proteins in 'positive regulation of cell adhesion' provides the best opportunity for potential biomarkers for prediction of maintaining TFR.

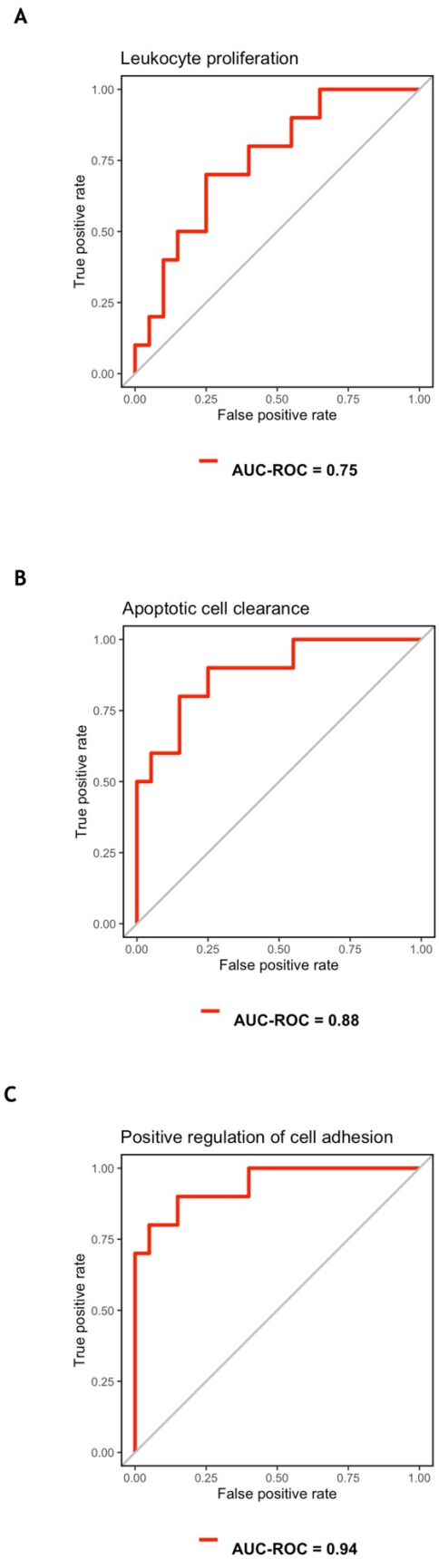

Figure 5-25 BM plasma DEPs from pathways were used to generate ROC curve for distinguishing between TFR patients (A) ROC curve analysis of proteins in upregulated 'leukocyte proliferation' (GO:0070661) pathway from GO analysis. **(B)** ROC curve analysis of proteins in upregulated 'apoptotic cell clearance' (GO:0043277) pathway from GO analysis. **(C)** ROC curve analysis of proteins in upregulated 'positive regulation of cell adhesion' (GO:0045785) pathway from GO analysis.

GO ID	Description	Gene ratio	GeneID
GO:0042274	ribosomal small subunit biogenesis	15/284 (0.05)	**RPS13/RPS19/**SNU13**/RPS6/RPS16/ RPS23/RPS27/RPS25/RPS11/RPS7/ RPS17/RPS27L/RPS4X/RPS12/RPS3A**
GO:0002181	cytoplasmic translation	39/284 (0.1)	DHX9/RPL26/RPS26/RPL10/**RPS13/ RPS19**/RPL19/RPL32/**RPS6**/RPL35/ RPL4/**RPS16**/RPS10/**RPS23**/RPL36A/ RPL13/**RPS27**/RPS25/**RPS11**/RPL13A/ RPS7/RPL34/**RPS17**/RPL36/RPL27A/ RPL17/RPS18/RPL7A/RPL31/RPL24/ RPL27/**RPS4X**/RPL3/RPL23/MCTS1/ RPL23A/EIF3L/**RPS12/RPS3A**

Table 5-11 Downregulated proteins from pathways of interest using ORA analysis of TFR_X vs TFR_E

The ROC curves for these indicated an AUC of 0.84 for ‘cytoplasmic translation’ and an AUC of 0.87 for ‘ribosomal small subunit biogenesis’ pathway. These are both very high AUC scores and indicate there is potential for the use of the proteins within these pathways for understanding the difference between TFR patients before they stop TKIs and later as they preserve TFR.

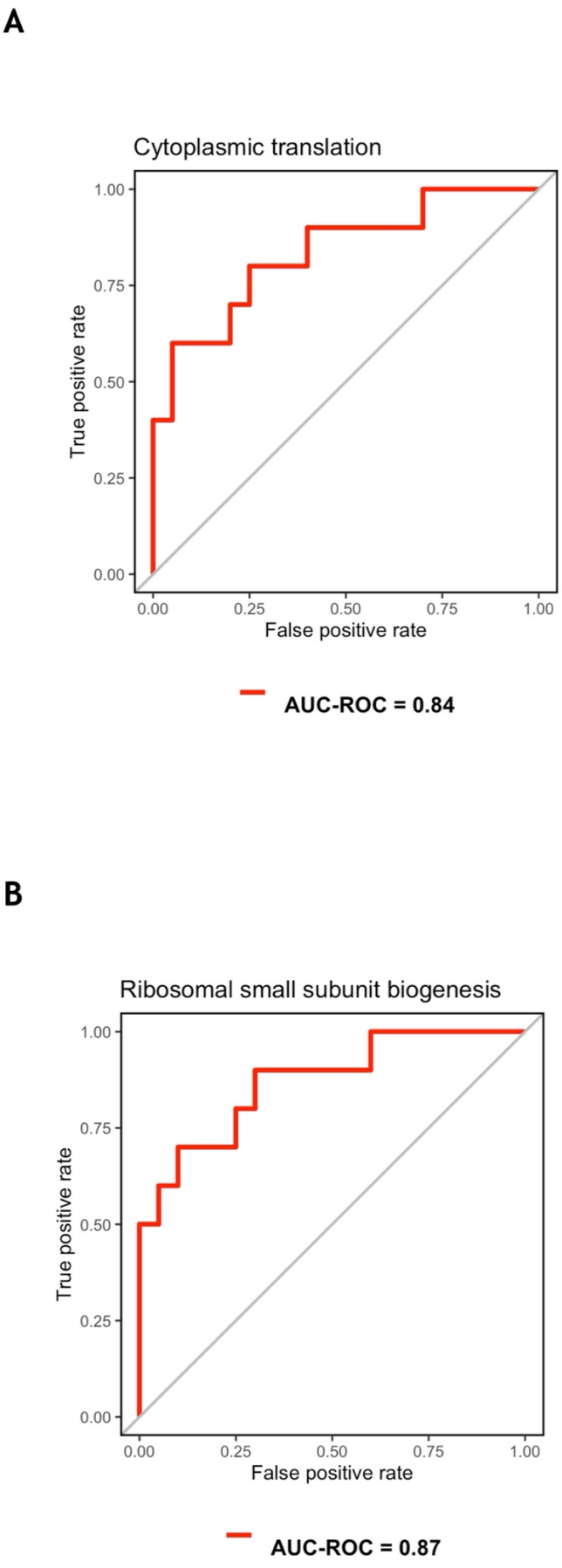

Figure 5-26 BM plasma DEPs from pathways were used to generate ROC curves for the prediction of TFR (A) ROC curve analysis of proteins downregulated in 'cytoplasmic translation' (GO:0002181) pathway from GO analysis. **(B)** ROC curve analysis of proteins in downregulated 'ribosomal small subunit biogenesis' (GO:0042274) pathway from GO analysis.

For the comparison of TFR_X vs TFR_E the GSEA found only 2 positively enriched BPs. The pathway ‘regulation of peptidase activity’ is interesting as peptidase are involved in the maintenance of HSCs and the BMM. Increase in the regulatory pathway suggests that TFR patients express proteins that are involved in normal haematopoiesis and the regulation of BMM.

It was previously found by GSEA analysis of R_X vs R_E comparison that there was an increase of DNA replication pathways. Therefore, it is interesting to find in here, when comparing TFR_X to TFR_E there is negative enrichment of ‘cytoplasmic translation’, ‘chromosome condensation’, ‘translation’ ‘nucleosome organisation’ and ‘nucleosome assembly’. These pathways are involved in DNA replication and assembly, the decrease expression could indicate these pathways are involved in preventing increased cell proliferation to uphold TFR.

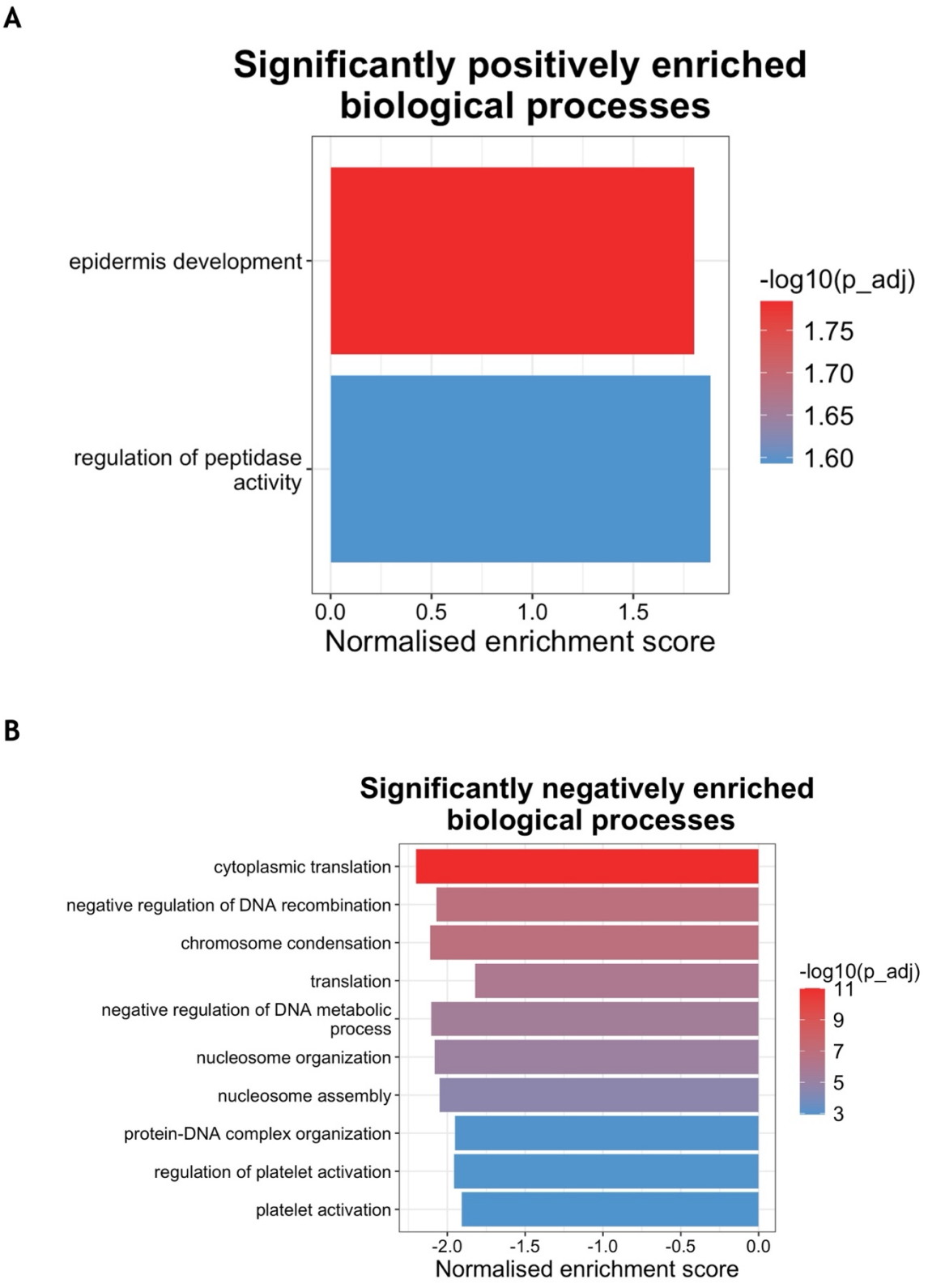

Figure 5-27 Enrichment analysis of BM plasma using GSEA tools DEPs were used to identify top 10 enriched pathways (using RStudio) found to be positively and negatively enriched in TFR_X (n=10) vs TFR_E (n=20).

Pathway	NES	p.adj
epidermis development	1.81	0.024
peptide cross-linking	1.971	0.049

Table 5-12 The 2 positively enriched pathways of GSEA comparing TFR_X vs TFR_E

Pathway	NES	p.adj
cytoplasmic translation	-2.2	1E-11
chromosome condensation	-2.1	1E-7
negative regulation of DNA recombination	-2.1	1E-7
translation	-1.8	1E-6
negative regulation of DNA metabolic process	-2.1	3E-6
nucleosome organization	-2.1	8E-6
nucleosome assembly	-2.0	3E-5
protein-DNA complex organization	-1.9	0.001
regulation of platelet activation	-2.0	0.001
platelet activation	-1.9	0.001

Table 5-13 Top 10 negatively enriched pathways of GSEA comparing TFR_X vs TFR_E

5.5 Discussion

This study provides an unparalleled examination into the proteomic changes that occur within the BMM of optimally responding CML patients who attempt TFR from before de-escalating the TKI to the point of maintenance/relapse as exit points from the DESTINY stopping trial. The value of this lies in providing an in-depth insight into the soluble factors released within the BMM that are essential for maintaining a harmonious, healthy BMM. In this the environment, prevention or disease progression can take place. Understanding this could open doors to predicting TFR or potentially understanding better the ways in which more patients may maintain remission off therapy.

5.5.1 R_E vs TFR_E

The initial examination of relapse (R_E) vs TFR (TFR_E) at trial entry demonstrated increase proliferation and differentiation of myeloid and erythrocyte cells with the 'myeloid cell differentiation' and 'erythrocyte development' in those patients destined to relapse off therapy. Additionally, the increase in the expression of sulfur metabolism can be linked to increased proliferation of cancer cells (Kaleta et al. 2024). While it is well established in CP-CML, progenitors have increased and uncontrolled proliferation, this is well controlled in most patients after TKI treatment and was controlled well in all DESTINY patients prior to the trial. An increase of these pathways in relapse patients could indicate increased activity of these myeloid cells even before TKIs have been stopped which could presage relapse. However, the 'erythrocyte development' pathway is surprising, while an increase in leukaemic granulocytes is typical of CML, normal red blood cell development can be negatively affected as uncontrolled proliferation of granulocytes leaves little room for erythrocytes, often causing anaemia which is associated with more aggressive CML (Liu et al. 2020) and a risk factor for progression to blast crisis (Copland 2022). The usefulness of these proteins to differentiate between relapse and TFR was examined. The proteins within the 'erythrocyte development' pathway were all also found within the 'myeloid cell differentiation pathway' (Table 5-2) this is not uncommon as the 'erythrocyte development' pathway is a part of the 'myeloid cell differentiation' pathway within the GO hierarchy. Additionally, when using ROC curve to examine these proteins 'erythrocyte development' had

low predictive power (with an AUC of 0.49) and ‘myeloid cell differentiation’ was only slightly higher AUC at 0.6, however neither was high enough to be considered useful for predicting between the two outcome groups. While the over-representation of these pathways provides an interesting consideration for the difference between TFR and relapse patients even before attempting TFR, they do not appear to be useful for separating the cohorts.

Additionally, there was also an increase in pathways such as ‘actin filament capping’ and ‘regulation of actin filament polymerisation’. It is known that in the activation of myeloid cells one of the results of this is rearrangement of the actin cytoskeleton as well as an increase inflammatory profile (release of ROS, nitric oxide and cytokines) (Greene et al. 2021). Therefore, the increase of these actin pathways indicates there is increased myeloid cell activation and inflammation in the BMM in patients that initially present as optimally responding patients that go on to relapse during TFR (Greene et al. 2021).

Perhaps most interesting within the R_E vs TFR_E comparison was the over-representation of the downregulated pathways ‘humoral immune response’, ‘antimicrobial humoral response’ and ‘antibacterial humoral response’. The proteins within ‘antimicrobial humoral response’ and ‘antibacterial humoral response’ are all found within the ‘humoral immune response’, but the latter included additional proteins; the first two pathways are a branch of the ‘humoral immune response’ being closely linked (Table 5-3). The humoral immune response occurs when foreign antigens are presented to B cells which produced antibodies to fight the foreign infection (Charles A Janeway et al. 2001). This is a key part of the body’s immune system and is essential for maintaining health. This reduced immune response was also seen in RNAseq analysis of MSCs where *HLA-B* gene was downregulated in R_E patients compared to TFR_E (Figure 3-10), this gene is involved in activating $CD8^+$ T cells. This is consistent with research that found patients that were able to achieve deeper remission (DMR) during TKI use had higher $CD8^+$ T cell numbers than those that did not achieve DMR (Cayssials et al. 2025). It has also been reported that $CD8^+$ T cells were increased in patients that maintained TFR (Cayssials et al. 2019). The AUC for the ‘humoral immune response’ was 0.8, this is a high score and indicates that the proteins within this pathway could be used in combination as predictive markers of TFR prior to TKI cessation.

Similar results were seen with GSEA where the negatively enriched pathways included ‘humoral immune response’, ‘complement activation’, ‘complement activation, classical pathway’ and ‘humoral immune response mediated by circulating immunoglobulin’. Complement pathways can activate the humoral immune response, so the decrease in these is unsurprising and corroborating when the latter was also seen as a downregulated pathway. This supports the finding that the immune response in patients that go on to relapse is less robust even before TFR is attempted. Specifically, it appears their humoral immune response is affected. This was also found in previous work whereby DESTINY patients that maintained TFR had an increase of B cells in their BM (Patterson et al. 2024). The immune system of patients who relapse appears to be less strong than patients that maintain TFR and potentially this could be why they are unable to continue TFR. These findings suggest the proteins of the immune response could be predictive for those who relapse.

Additionally, a range of metabolic and catabolic processes such as ‘purine nucleotide metabolic process’, ‘purine-containing compound metabolic process’, nucleoside phosphate metabolic process’, ‘nucleobase-containing small molecule metabolic process’ and ‘nucleotide metabolic process’ were positively enriched from the protein list of relapse patients. These pathways are all involved in DNA and RNA production. As CML is characterised as a haematological disorder with uncontrolled proliferation of granulocytes the upregulation of these pathways could already be present within the BMM of relapse patients and without the counteractive mechanism of TKIs, could be driving relapse. Additionally, altered metabolic activity in CML has been previously identified and linked to treatment response. Sayın et.al., looked at two patient groups, separated by *BCR::ABL1* IS levels called T1 (≤0.0032%, MR4.5 or better) and T2 (>0.0032%, <1%). They found an increased nucleotide metabolism within the T2 group, suggesting there is an increased nucleotide metabolism in patients that do not achieve deeper remission (Sayın et al. 2025).

5.5.2 R_X vs R_E

The comparison of point of relapse (R_X) vs relapse patients at trial entry (R_E), provided an understanding of the changes that occur in patients that leads to molecular recurrence. The R_X group had an increase in myeloid and leukocyte

activity. There was an increase in pathways including ‘myeloid leukocyte activation’, ‘leukocyte chemotaxis’, ‘myeloid leukocyte migration’, ‘granulocyte chemotaxis’ and ‘granulocyte migration’. Myeloid cells and leukocytes are responsible for monitoring the body for infection, tissue damage etc., when they are activated there is release of ROS and pro-inflammatory cytokines, and phagocytosis (Greene et al. 2021). Additionally, chemotaxis occurs when granulocytes move toward chemoattractant signals to initiate an immune response (T. Jin et al. 2008) while granulocyte migration is the process where leukocytes move to the site of infection/damage to repair this by evoking an immune response (Radtke and Voehringer 2023). These pathways are heavily related as the granulocytes would migrate in response to a chemotactic gradient. Overall, the upregulation of these pathways would suggest that the R_X patients have an increased inflammatory profile within the BMM, which would be expected as these patients have relapsed and they have active disease. It is important to note that this increase of ROS production which is seen when myeloid cells and leukocytes are activated is in line with increased ROS production from MSCs (Figure 3-5). This increased inflammatory profile was first suggested in the R_E vs TFR_E analysis where R_E patients appeared to have markers of this, the increase at point of relapse suggests these proteins are associated with relapse and they are present before TFR is attempted, suggesting relapse could be predicted.

Downregulation of pathways such as ‘ribonucleoprotein complex biogenesis’, ‘ribosome biogenesis’, ‘rRNA metabolic process’, ‘rRNA processing’ and ‘ribosomal small subunit biogenesis’ is interesting as it has previously been found that dysregulation of ribosomal biogenesis is an underlying cause of marrow failure syndromes (Ruggero and Shimamura 2014). Therefore, the decrease of ribosome biogenesis could be harming the BM leading to relapse. Additionally, the downregulation of pathways ‘cytoplasmic translation’, ‘protein-DNA complex organisation’, ‘nucleosome organisation’ and ‘nucleosome assembly’ are all related to the formation and alteration of DNA and proteins. This decrease of DNA metabolism occurs in patients at point of relapse, this is surprising as patients are in active disease state, therefore it may be assumed that they would have increased cell proliferation which should mean their DNA and protein metabolism is increased. However, Bilousova et al., found that impairing DNA

replication in haematopoietic progenitors gave an advantage where BCR::ABL1 was able to increase production of leukaemic cells (Bilousova et al. 2005). They found that knockout of a transcription factor involved in promoting cell cycle caused an increased production of BCR::ABL1^{+} myeloid cells, BCR::ABL1 restored the S phase progression of cell cycle, therefore bypassing the transcription factors and continuing cell cycle. It could be assumed that when the regulation of the cell cycle has been disrupted the apoptosis and DNA repair mechanisms that this pathway is associated with is now also reduced/disrupted, meaning there is increased cell proliferation without the regulatory mechanisms. It is believed that the reduction of these cell proliferation pathways also decreases the regulation of cell proliferation pathways which is involved in maintaining homeostasis of blood cell production. Therefore, this could indicate impaired DNA metabolism in relapsing patients allows for molecular recurrence. Also, in the previous chapter of this thesis it was found that at point of relapse the stem cell activity had decreased compared to start of trial (Figure 4-22), it was suggested that this could be due to increased quiescence of SCs, however now it could also be suggested that this is due to decreased normal regulation of proliferation pathways.

Regarding the GSEA analysis for R_X vs R_E, the positively enriched pathways included ‘positive regulation of cell motility’, ‘positive regulation of cell migration’ and ‘positive regulation of locomotion’. These pathways are all related to increase cell migration and motility. The increase in mobility of HSPCs is often triggered by inflammation, cytokines, chemokines, or injury and causes the movement of HSPCs from their niches in the BMM to the PB (Ratajczak et al. 2018). In CML it is found that the oncogenic translocation event causes dysregulation of migration (Chomel and Turhan 2011), it was reported that with treatment of imatinib, CML cells have increased CXCR4 expression which leads to homing of cells to BMM niches allowing the cells to become quiescent (L. Jin et al. 2008). This indicates that without TKIs, there is an increase in the pro-inflammatory profile of the BMM in patients who relapse alongside an increased cell motility and migration. There was also the upregulation of ‘toll-like receptor signalling pathway’, this is part of the innate immune response and activation of this leads to increased inflammation (Kawasaki and Kawai 2014). Additionally, this pathway is involved in the activation of MAPK cascades which causes an

increase in the expression of genes involved in inflammation (Kawasaki and Kawai 2014). This corresponds with the upregulation of ‘regulation of MAPK cascade’ that is also seen in GSEA. The upregulation of these both further indicates that patients at point of relapse have an increased pro-inflammatory profile and dysregulated immune response within the BMM. This corresponds nicely with the increase inflammatory profile that was suggested from ORA analysis due to the increased granulocyte activation and migration and perhaps offers an idea of the exact signalling pathways that are causing this increased inflammation. As well, the decreased immune response seen at the start of the trail seems to continue to decrease at point of relapse further suggesting an essential role for the immune response in protecting TFR. Generally, when relapse at trial entry samples were assessed there was evidence of increased inflammatory profile as well as increased cell proliferation and decreased immune response, while this appears to be under control with the use of TKIs, after stopping treatment these pathways continue and could lead to relapse. These markers could be predictive of relapsing occurring in patients before TKI cessation.

As previously seen in the ORA analysis, there was also negatively enriched pathways including ‘cytoplasmic translation’, ‘nucleosome assembly’, ‘protein-DNA complex organisation’. The decrease of these pathways associated with DNA and protein production could be due to over-production of leukaemic cells in these patients and potentially a decrease in normal haematopoiesis. Also, it was previously mentioned that this may be due to BCR::ABL1 overriding normal DNA and protein production pathways to cause aberration.

5.5.3 TFR_X vs TFR_E

An investigation into understanding pathways involved in maintaining TFR could potentially be utilised to identify how these patients differ from those who relapse and to predict which patients can maintain TFR before they attempt stopping TKI. To investigate this TFR at end point of trial (TFR_X) was compared to TFR at trial entry (TFR_E). The initial ORA pathway analysis showed a surprising increase of ‘leukocyte proliferation’ and ‘myeloid leukocyte activation’. These pathways could indicate there is an increase in leukocyte expansion and activation of myeloid cells which usually occurs in response to an

external stimulus which increases a pro-inflammatory and immune response. This increased cell proliferation is consistent with findings from the colony assay which demonstrated an increased production of progenitor cells in TFR_X patients compared to TFR_E (Figure 4-20). While an increase in myeloid cell proliferation and increase of production of inflammatory cytokines is seen in expected to be seen relapsing patients, in TFR patients there is also an increase of 'phagocytosis', 'apoptotic cell clearance' and 'regulation of apoptotic cell clearance' pathways. This indicates that although there is increased cell proliferation there is also pathways involved in the regulation and maintenance of these pathways that create a homeostasis that is required in BMM to prevent disease progression and maintain normal haematopoiesis. Additionally, these pathways involved in increased myeloid cell proliferation and increased pro-inflammatory response are also normal pathways seen within the BMM of healthy individuals and are required for the normal regulation of haematopoiesis, this alongside the pathways involved in regulation of cell production indicates these pathways are maintaining TFR in the absence of TKIs. The upregulation of 'acute phase response' within this comparison shows that not only is the immune response upregulated in TFR patients at the start of the trial (point of de-escalation) upregulation of the innate immune response is maintained in TFR_E patients at the end of the trial. Additionally, the 'leukocyte proliferation' and 'myeloid leukocyte activation' pathways, while being associated with pro-inflammatory response are also responsible for the innate immune response. It appears the 'acute phase response' alongside increased myeloid/granulocyte activity then continues the activation of the immune system in the TFR patients in the TFR_X cohort. The increased immune response in TFR patients appears to be a staple in maintained remission and suggest a more robust immune response in patients who attempt TFR is a predictor of those who can maintain remission after stopping their TKIs.

Another interesting finding was the increase of 'positive regulation of cell adhesion' pathway. Within the BM, adhesion mechanisms maintain HSCs to cells within their niche depending on extraneous stimulation (Kulkarni and Kale 2020). The cues from the BMM can alter the adhesion of the HSCs and change their position within the BMM based on the HSC fate, cells can migrate, self-renew, undergo haematopoiesis etc. (Kulkarni and Kale 2020), adhesion of HSCs within

the BMM directly corresponds to their activity. The increase of this pathway suggests the HSCs of patients who maintain TFR are maintained within their appropriate niches which allows the normal process of haematopoiesis to occur thus sustaining TFR. These results are like the HSC/LSC marker work which found an increase in CD44 marker in TFR_X vs CML at diagnosis along with several other cohort comparisons (Figure 4-3 and Figure 4-4). While previous literature has found an increased adhesion in CML LSCs mediated by CD44 which increases their homing to, and engraftment within, the BM (Krause et al. 2006). Interestingly, this data suggests patients who maintain TFR have increased cell adhesion within the BMM, which could be sustaining remission. Additionally, from all the proteins of pathways tested 'positive regulation of cell adhesion' produced the highest AUC of 0.94, this is an excellent score and indicates this combination of proteins can distinguish between the two outcomes tested and could potentially be useful predictive biomarkers of TFR. The proteins included in this pathway (Table 5-10) includes FN1 (fibronectin 1) which is an ECM protein found within the BMM in stem cell niches responsible for maintaining SCs within their niche by binding to integrins like CD44 (Wirth et al. 2020). ANAXA1 (Annexin A1) is a cell membrane protein T cell regulation (Xia Liu et al. 2024) and immune response (Araújo et al. 2021) within the bone marrow. EFEMP2 (EGF-containing fibulin-like extracellular matrix protein 2) is a protein found in connective tissues in BM (Karnik et al. 2025). TGM2 (Transglutaminase 2) is an enzyme involved in the differentiation of MSCs (F. Liu et al. 2023). HSPD1 (Heat Shock Protein Family D Member 1) encodes the mitochondrial chaperone heat shock protein 60 (HSP60) which is responsible for folding proteins in the mitochondrial matrix (Cömert et al. 2020), overexpression of this protein has been identified in osteosarcoma (Yiming Zhang et al. 2024). FGG (Fibrinogen Gamma Chain) this is the gamma part of fibrinogen which is found within the BM and is involved in endothelial cell adhesion (Y.-Q. Zhou et al. 1993). SPTA1 (Spectrin alpha 1) is one of the proteins that links the membrane to the cytoskeleton in RBCs, responsible for maintaining the cell shape (Chonat et al. 2019). These proteins are all part of the 'positive regulation of cell adhesion' pathway and are all upregulated in the comparison of TFR_X to TFR_E, in combination they offer potential as predictive biomarkers for maintaining TFR after TKI cessation.

Another positively enriched pathway within the TFR_X vs TFR_E comparison was ‘regulation of peptidase activity’. There are several peptidases found within the BM including the most researched peptidase in CML, namely dipeptidyl peptidase-4 (DPP4)/CD26. This is a neural endopeptidase and ubiquitin specific peptidases which plays a role in maintaining haematopoiesis and is also a marker of LSCs. CD26 has been found to potentially play a role in bone metabolism as it was expressed on osteoclasts in the BM and was involved in the development of osteoclasts (Nishida et al. 2014). Additionally, research shows that proteases are a factor involved in the mobilisation of HSPCs through G-CSF (Christopher et al. 2009). The ‘regulation of peptidase activity’ pathway being positively enriched suggests this is another mechanism of sustaining normal haematopoiesis that is found within the BMM of patients with TFR that allows them to maintain remission.

Another stand out from the GSEA of TFR_X vs TFR_E data was negatively enriched pathways related to DNA replication and assembly including ‘cytoplasmic translation’, ‘chromosome condensation’, ‘translation’ ‘nucleosome organisation’ and ‘nucleosome assembly’ pathways. The decrease of these pathways suggests the BMM of patients who maintain TFR have more control over cell proliferation and are able to maintain normal haematopoietic environment which allows the continuation of TFR. Interestingly, the same/similar pathways were also downregulated in ORA and GSEA of R_X vs R_E. It could be hypothesised that the dysregulation of the BMM that occurs in relapsing patients leads to a decrease in these pathways however, this does not explain why the same changes are seen in TFR patients at the end point of trial. As previously mentioned within the ORA analysis, there is also upregulation of pathways involved in apoptosis and phagocytosis which could indicate there is a more harmonious balance of DNA replication and cell death in the TFR patients that has allowed them to maintain remission, unlike relapse patients who appear to only have a decrease in the DNA replication pathways. Additionally, in relapse patients this could be due to a decrease of DNA repair mechanisms, while in TFR it could be involved in the maintenance of TFR.

Overall, the findings of this study provide possibilities for potential predictors of TFR/relapse. The data shows patients that relapse, even before TKI cessation, have an increased inflammatory profile compared to patients that maintain TFR. Furthermore, at the point of relapse these patients have continued increase in a pro-inflammatory profile in the BMM as well as dysregulation to normal DNA and ribosome production, causing disorder within the BMM and preventing TFR from being maintained. Moreover, the patients who maintain TFR have a more robust immune response at the start of the trial and by the end have an increase in a range of pathways involved in normal haematopoiesis and immune response which could be related to maintaining their remission. This means there are several potential predictive mechanisms that could be used for TFR.

6 Discussion and future directions

This thesis aimed to understand the changes within the treated CML BMM that contribute to TFR or relapse, and if these changes can be used to predict TFR success. Within this thesis the BMM was evaluated in a three-part approach, that is examination of the supportive stroma (MSCs), the LSCs and the proteins. It was hoped from this wide-ranging investigation of the BMM that an in-depth integrated approach to identifying predictive biomarkers of TFR would be achieved.

To identify the changes within the supportive stroma of the BMM the detailed characterisation of the MSCs of the BM was carried out. As has been described throughout this thesis the MSCs are an essential part of the BMM and have various roles in creating the BMM, maintaining HSCs and supporting the process of haematopoiesis. Additionally, in patients with CML the BMM has been reported to be dysregulated in order to maintain quiescent LSCs and MSCs are critical to these changes. The initial characterisation of MSCs was focussed on the metabolic and senescent changes within the patient cohorts. Analysis of the senescence found the MSCs of relapse patients (R_E) had an increased senescence at trial entry compared to TFR at trial entry (TFR_E). This increased senescence of MSCs leads to increased pro-inflammatory secretion. Furthermore, the ROS production of the MSCs was significantly increased within relapse patients at point of relapse (R_X) compared to relapse at trial entry (R_E), suggesting at point of relapse there is increased ROS production within the BMM creating increased oxidative stress, HSC exhaustion and an increased pro-inflammatory profile. The RNAseq data of MSCs found a decrease of HLA-B in relapse patients compared to TFR; HLA-B is involved in activating $CD8^+$ T cells which induce an immune response. Previous research has found that $CD8^+$ T cells could be useful predictors of DMR in patients with CML, this was because within PB MNCs there is an increase in $CD8^+$ T cells after patients have been on TKIs for three months compared to at the point of diagnosis (Cayssials et al. 2025). Furthermore, it was found that patients that achieved DMR had increased $CD8^+$ T cells compared to patients that did not achieve DMR during the entire 24 months of treatment that this was tested (Cayssials et al. 2025). This increase was seen at diagnosis, indicating its predictive nature for DMR which is one of the requisites of TFR (Cayssials et al. 2025). This is similar to the RNAseq findings of

this thesis which found HLA-B was lower in relapse patients than patients that maintained TFR

The MPFC analysis found that while none of the markers individually was a valid predictive biomarker of TFR, enlightening trends pertaining to the changes of the BMM were identified. The increased expression of CD44 in all DESTINY samples compared to CML patients at diagnosis suggests an increased expression induced by TKI treatment. Due to the known role of CD44 in homing and engraftment of LSCs, this could be suggestive of how LSCs are surviving in CML patients owing to an increase in their engraftment in the BMM preventing their eradication by TKIs. From the data, the increased CD44 expression appears to be present in both patients that maintain TFR and those who relapse, therefore while this may not be a marker for relapse it could provide enlightenment on the survival mechanisms of LSCs within the BMM. Additionally, in the data, CD25 expression was found to be specific to LSCs as the highest expression was seen in patients with CML at diagnosis after which expression in DESTINY samples was reduced being comparable to levels seen in normal samples. This was initially thought to be a good marker of LSCs, as it has been demonstrated in previous research (Sadovnik et al. 2017). However, the same trends in expression levels were not reproducible between HSC/LSC 1 and HSC/LSC 3, which disputes its potential as a LSC marker. This did however lead to a larger discussion about the profile in which the markers are being examined and potentially examining these LSC markers along with CD45RA, cKIT, CD26, IL1-RAP and CD90. The addition of these markers to the $Lin^{-}CD34^{+}38^{-}$ population when examining HSC/LSCs has been previously looked at (Kinstrie et al. 2020; Sadovnik et al. 2017; Warfvinge et al. 2017) and even found useful predictive biomarkers of TFR, to properly examine these markers as worthwhile biomarkers, further analysis would be required using a more specific population of LSCs.

The proteomics data of the BM plasma GO analysis found a downregulation of ‘humoral immune response’ pathway at trial entry in patients who relapse compared to those who have successful TFR. Within the same comparison the GSEA found negatively enriched pathways ‘humoral immune response’, ‘complement activation’, ‘complement activation, classical pathway’ and ‘humoral immune response mediated by circulating immunoglobulin’. These pathways show relapse patients have dysregulation of immune response at start

point of trial regardless of good clinical response to TKIs which could potentially contribute to relapse and could be predicted. Again, for patients that are relapsing it appears the increase of pro-inflammatory profile is seen at point of relapse. When comparing patients at point of relapse (R_X) to patients that relapse at point of trial entry (R_E) there is an increase of 'toll-like receptor signalling pathway' and 'regulation of MAPK cascade' which are known for producing pro-inflammatory cytokines. This increased pro-inflammatory cytokine production was also seen with a group examining results of the AST- Argentina Stop Trial found that in PB samples before TKI cessation there was an increased expression in monocyte chemoattractant protein-1 (MCP-1) (CCL2) and IL-6 in relapse patients compared to patients who maintained TFR (Pavlovsky et al. 2025). Activation of the MAPK signalling pathway increased the production of MCP-1 (S. Singh et al. 2021) and toll-like receptor activation also causes an increased production of MCP-1 (Lee et al. 2008) which has downstream pro-inflammatory effects. IL-6 binds to the IL-6 receptor and activates the intracellular JAK-MAPK pathway (S. Kang et al. 2019) and activation of toll-like receptor 2 causes increased production of IL-6 (Flynn et al. 2019), with IL-6 causing increased inflammatory response in the BMM. The combination of these cytokines was found to produce a Positive Predictive Value of 100% in predictive TFR in patients (Pavlovsky et al. 2025). While these changes were seen before the attempt of TFR not after relapse this further suggests the importance and predictive value of increase inflammatory profile in patients with CML and how this is a potential biomarker of TFR.

Together, it can be said the patients in R_E have a more pro-inflammatory profile than TFR_E at the start of the trial which is also seen through increased MSC senescence. This pro-inflammatory profile appears to increase through to point of relapse as demonstrated by the proteomics analysis comparing R_X and R_E patients which had enrichment of pathways that produce pro-inflammatory cytokines as well as increased ROS production from MSCs. Additionally, transcriptional changes to MSCs along with pathway analysis of proteomic data both suggested there is an increased immune response in patients who maintain TFR compared to patients who relapse that can be identified before TKI cessation. Patients who go on to relapse during TFR appear to have more

markers of immune dysregulation. These results suggest immune response may be the most evident route for identifying a predictive biomarker.

To understand the results of this thesis attention should be drawn to the previous work that has been attempted at examining TFR and identifying a predictive biomarker. In an examination of samples from the TWISTER and RESIST trials, Irani et al., found within the RESIST cohort the number of NK cells within the PB were significantly higher in patients who maintained TFR vs those who relapsed (Irani et al. 2020). They additionally found T-regs and monocytic MDSCs (MO-MDSCs), which are both suppressors of the immune response had a higher expression in patients who relapsed compared to those in TFR (Irani et al. 2020). These further confirm the findings previously seen within this data from this thesis, that patients that maintain remission have a more robust immune response and this is found before attempting TFR. When investigating a statistical predictive model using the STRING cohort, the combination of increased NK cells and decreased T-regs and MO-MDSCs was found to be predictive of TFR (Irani et al. 2020). Another indication of the importance of the immune changes in TFR indicating these can be used as predictive biomarkers.

Additionally, work by Giustacchini et al., in analysis of stem cell signatures found that in patients at diagnosis the BCR::ABL1^{+} stem cell population could be split into two groups: group A and group B. GSEA found group A had increase quiescent associated genes while group B had increase proliferation associated genes (Giustacchini et al. 2017). Patients were then treated with TKIs, and after 3 months and 1 year of TKI treatment there was an increase in group A enrichment (i.e. there was an increase in group A compared to group B), which shows TKI treatment causes increased persistence of quiescent BCR::ABL1^{+} population in patients with CML (Giustacchini et al. 2017). The work from Giustacchini et al., also identified a distinct cluster of BCR::ABL1^{-} stem cell that could be predictive of poor response to TKIs, GSEA of the BCR::ABL1^{-} grouping of the poor responders showed enrichment of inflammatory pathways within these cells. Once again suggesting the significant importance of a pro-inflammaotry profile within the BMM, its role in relapse and therefore the potential to exploit this as a predictive biomarker of TFR.

As was previously mentioned previous analysis of the DESTINY BM samples found the naïve B cells were reduced while memory B cells were increased in relapse patients compared to patients who maintained TFR (Patterson et al. 2024). This correlates with the current findings of the proteomics analysis of this thesis which found an decreased immune response in relapse patients compared to TFR, in the form of negatively enriched 'humoral immune response' and 'complement activation' pathways. Further indicating that these changes to immune cells have also been identified within the DESTINY cohort in separate experiments using these patient samples.

Due to the in-depth understanding using BM samples provides within the examination of CML and its progression as a disease without TKI use, the analysis done has provided additional avenues that were not within the initial scope of this project for potential treatment of CML and potentially ensuring TFR. Not only could this provide a marker for TFR but also a deeper understanding of what is lacking in some patients and a novel therapeutic approach to this possibly finding a cure. Also, present options of novel treatment opportunities for certain patients to achieve a deeper remission.

As there is a deep understanding and appreciation for the importance of immune changes in how CML patients respond to TKIs, there has been research and clinical trials carried out focussed on improving and targeting the immune response in CML patients alongside the use of TKIs. Promising results have been found from treatment combinations alongside TKIs to target LSCs and the immune response (Mu et al. 2021). One example of a combination treatment was to use IFN-α alongside TKIs, before the discovery of TKIs patients were treated with IFN-α and while not nearly as effective as TKIs, it did delay disease progression in most patients. Interestingly, a study found PB analysis of patients treated with TKIs and IFN-α had increased immunosuppression with increased MO-MDSCs in patients only taking TKIs and increased granulocytic MDSCs in patients on TKIs and IFN-α (Alves et al. 2020). Additionally, it was demonstrated that treatment of IFN-α in mice caused dormant HSCs to re-enter the cell cycle (Essers et al. 2009), this could offer another mechanism of treatment alongside TKIs. As well as this, TKIs have also been examined with BCL-2 inhibitors and JAK2 inhibitors (Mu et al. 2021). BCL-2 is involved in the regulation of apoptosis (Vogler et al. 2025). The combination of a BCL-2 inhibitor, sabutoclax, with

dasatinib was found to increase the apoptosis of LSCs in blast crisis CML patients (Goff et al. 2013). The effectiveness of JAK2 inhibitors was examined when a combination of nilotinib with ruxolitinib were tested on CML cells, finding increased apoptosis of $CD34^{+}38^{-}$ cells (Gallipoli et al. 2014). By using two separate treatment options that are able to target separate things, this provides an option for increased opportunity of targeting LSCs by different mechanisms instead of one.

The potential for combining TKIs with other drugs in order to enhance the effects to provide deeper remission and potentially increase the chances of TFR is another aspect of this thesis that could be examined in the future. Based on the understanding of the changes within the BMM like decreased humoral immune response, increased to ROS levels from MSCs and increased pro-inflammatory profile in relapse patients these provide novel therapeutic targets that could be exploited to produce a deeper remission and potentially lead to TFR. This could be done by targeting specific inflammatory pathways, however inflammation also plays an essential role within HSCs to encourage their quiescence which prevents exhaustion and maintains their self-renewal capacity. Any investigation to target a reduction of inflammation within the BMM would need to be done while ensuring HSCs health and normal haematopoiesis is maintained.

6.1 Future directions

A general verdict that can be said about the biomarker identification based on the analysis done on this thesis is that there is currently no clear biomarker signature that can be used as a predictor of TFR. All future work of finding predictive biomarkers should take into consideration the biomarker may be a combination of factors that when examined together are responsible for predicting TFR. Furthermore, these findings may not all be within the same direction, for example some changes identified might be associated with an increase of certain markers and others may be associated with a decrease. Going forward a more holistic approach should be considered in the search for biomarkers, using the findings from this thesis where a three-pronged approach as a guide for the immune response and changes to the supportive stroma. Additionally, an important consideration in the pursuit for identification of a

biomarker of TFR is it should also be understood that a biomarker of relapse may be better. This would mean finding changes that occur in patients that relapse when attempting TFR may be the best biomarkers for separating patients that achieve TFR from those who relapse.

While no stem cell markers were found to be useful predictive biomarkers of TFR, this area of the thesis perhaps requires a different approach. Future work could be done by looking at these markers within a different profile and not just within $Lin^{-}CD34^{+}38^{-}$. As previously mentioned, other research has used different stem cell profiles to establish their LSC population and has had success in identifying predictive markers of TFR from this, such as $CD93^{+}$ which was identified within the $CD34^{+}38^{-}90^{+}$ profile. Adjusting the profile for future work may provide a more precise and targeted representation of the LSCs and their markers and even within the markers previously tested could show differences in the outcome groups.

Patients were separated into TFR and relapse based on knowledge of outcomes from the trial. For future work it would be interesting to have more current follow-up data of patients to see if the same patients are still in TFR and if possible re-analysis would need to take place based on new patients outcomes to see if this produces different results.

The analysis of the stem and progenitor populations of the DESTINY samples did not provide any predictive results of how TFR is maintained within CML patients. However, as has been discussed the idea that the $BCR::ABL1^{-}$ and $BCR::ABL1^{+}$ population play separate roles in the BMM and within the response of CML patients to TFR, this provides a unique future direction where patient samples could first be separated into $BCR::ABL1^{+}$ and $^{-}$ populations using flow cytometry (by tagging BCR::ABL1 cells with an antibody as described by (Recchia et al. 2015)) before examination of the stem and progenitor populations using functional assays.

While the present work of the MSCs provided an interesting initial introduction into the role of the supportive stroma in the BMM and how this affects TFR and relapse, additional work could be done to further elucidate these findings. Due to the multipotent nature of MSCs and the wide range of roles MSCs can play in

the BMM, single-cell sequencing of these cells would be able to provide a more comprehensive understanding of the transcriptional changes within each cell and the different presentations of MSCs within the two outcome groups. Additionally examining the differentiation potential between the outcome groups could clarify the role of the MSCs and how their lineage skewing is altering the BMM. Furthermore, follow-up of the current RNAseq analysis to determine how these transcriptional changes are being translated at a protein level could be done using a custom LUMINEX panel. This could be used on the secretome of the MSCs which is released by the MSCs when they are in culture. To recreate a BMM model, $CD34^{+}$ HSCs could be placed in a co-culture with MSCs from relapse patients and separately from TFR patients and the viability of the HSCs could be examined to identify the relationship between the HSCs and MSCs. Additionally, a custom LUMINEX could be used to examine the secretome, identifying how the MSCs change their secretome to support/undermine HSC. Also, this co-culture could be set up with LSCs instead of HSCs, this could be used not only to test the LSCs viability, the secretome produced by the MSCs but also could be a potential model for different treatment options. Additionally, within these co-cultures different treatment combinations could be tried, for example TKI with IFN-α, BCL-2 inhibitors or JAK2 inhibitors, to identify how this affects the stem cell viability and as this is slightly more representative of the BMM the changes based on treatment can be assessed in more detail based on the MSC secretome.

Consistent with previous findings, this thesis has shown consistent evidence of the dysregulation to the immune response in patients who relapse. While previous work has demonstrated how this can also be seen within the PB this thesis analysis has focused on changes within the BM plasma which consistently corresponds with the findings shown above and perhaps demonstrates a more in-depth portrayal of these changes. While there have been some substantial findings for using the immune response as a potential predictive biomarker of TFR, these remain theories and have not yet been able to be translated into a clinical setting as further investigation is required. Furthermore, current examination of the proteomic analysis, while an excellent initial scope of the proteins changes, requires further validation with a larger patient cohort to ensure changes seen can be translated to all CML patients. To validate the findings of the proteomics data creating a custom LUMINEX panel with select

proteins of interest that have been identified within the pathways, specifically associated with immune changes/dysregulation, would provide a closer step to identification of a biomarker. Due to limitations of analyte availability of this method, specific proteins of interest that are available would need to be selected. Finally, with successful validation of these proteins validation would be required using PB samples from patients within the DESTINY trial and any other patients who have attempted TFR to ensure the changes seen within the BMM can be identified within the PB. This is particularly important for movement of these understandings into a clinical setting as a routine practice as use of BM aspirates is not a reasonable long-term option for patients due to the invasiveness of this procedure. The goal would be to identify a biomarker of TFR within the BM which can be tested within the PB and used routinely.

Overall, this thesis has clearly identified significant differences within the BMM of patients that maintain TFR compared to those who do not. Before TKI cessation has begun TFR patients have a more robust immune response that is ultimately believed to be the differing factor which allows for TFR success. Additionally, pro-inflammatory changes can be seen that occur in patients who relapse from the start of the trial to the point of relapse. While further work is required, the findings of this thesis have provided a unique and in-depth understanding of CML that has introduced several potential avenues for identification of predictive biomarkers for the success of TFR.

Appendices

Gene	Association	Reference
AAMDC	Oncogene involved in PI3K-AKT-mTOR signalling.	(Golden et al. 2021)
ANXA2	Involved in survival of BCR::ABL1^{+} leukaemia	(Minciacchi et al. 2024)
ANXA2P2	Potential prognostic for ovarian serous cystadenocarcinoma (OV)	(Yanna Zhang et al. 2022)
AREG	Part of EGF family and associated with cancer	(L. Wang et al. 2020)
ARRDC3	Tumour suppressor, regulates GPCR signalling	(Arakaki et al. 2021)
C16orf54	Associated with immune cell infiltration in tumours	(Ershov et al. 2023)
CALR	CALR mutation associated with BCR::ABL1 CML	(Saal et al. 2023)
CD164	Found on haematopoietic cells, involved in cell proliferation and adhesion. Involved in tumour progression of bladder cancer	(Xiao-Guang Zhang et al. 2018)
CLEC4GP1	Associated with CML	(Ma et al. 2022)
CRHBP	Demonstrated anti-tumour effects	(Yoo et al. 2024)
CTNNB1	Encodes ß-catenin which is involved in maintenance of CML LICs	(Luong-Gardiol et al. 2019)
CTSG	Upregulated in CML 34^{+} cells	(Benjamin et al. 2026)
CYP51A1	Involved in TKI resistance	(Hossain et al. 2026)
DNTT	Upregulated in BCR::ABL1 positive lymphoid cells	(Shahrin et al. 2019)
DUSP1	Involved in TKI resistance in CML	(Kesarwani et al. 2017)
EIF5A	Thought to drive proliferation in BCR::ABL1 positive cells	(Balabanov et al. 2006)
EIF5AL1	Decreased proliferation and migration in HeLa cell line	(Y.-Y. Wu et al. 2023)
ERAP2	Immuno-supportive in Squamous cell lung carcinoma	(Z. Yang et al. 2021)
FTH1	Increased expression in AML and LSCs	(Bertoli et al. 2019)
FTH1P3	Involved in cell differentiation	(Di Sanzo et al. 2016)
FTL	Increased expression in AML and LSCs	(Bertoli et al. 2019)
GAS2	Upregulated in CML	(H. Zhou et al. 2014)
GAS5	Upregulated STAT5 expression and caused increased Treg differentiation	(Chi et al. 2021)
GMNN	Found in various cancers, thought to be part of S phase of cell cycle	(Di Bonito et al. 2012)
HLA-E	Overexpressed in several cancers	(Sætersmoen et al. 2025)

HNRNPH1	Increased expression in CML cell lines	(M. Liu et al. 2021)
HNRNPL	High expression in tumour cells, promotes proliferation and migration	(Gu et al. 2020)
HOPX	Increased expression associated with poor prognosis in AML	(Lin et al. 2017)
IFITM1	One of the genes identified as BCR::ABL1 like signature	(Chiaretti et al. 2018)
KIAA0125	Associated with leukaemia. Increased expression in some paediatric ALL (BCR::ABL1 positive)	(Hung et al. 2021; Batista-Gomes et al. 2020)
LGALS1	Involved in chemoresistance in CML	(Luo et al. 2016)
LINC00987	Involved in proliferation of AML cells, inhibits their apoptosis	(C. Liu et al. 2022)
MRPL16	Downregulated in AML	(H. Wu et al. 2025)
NFKBIA	Inhibitor of NF-κβ. BCR::ABL1 activates NF-κβ pathway.	(Carrà et al. 2016; Bin Wang et al. 2024)
NOG	Inhibitors of BMPs, which are dysregulated in CML	(Lowery and Rosen 2018)
PF4	Involved in TKI resistance in CML	(Weisberg et al. 2012)
RAB31	Increased levels seen in cancers	(Chua and Tang 2015)
RPL18A	Increased expression in BC vs AP CML	(Schwarz et al. 2022)
RSL1D1	Inhibitor of senescence. Increased expression in several cancers	(Xunhua Liu et al. 2022)
SELL	Investigated for predictive marker of molecular response in CML	(Sopper et al. 2017)
SOCS2	Increased expression BCR::ABL1^{+} cell lines	(Schultheis et al. 2002)
SPINK2	High expression associated with poor prognosis in AML	(Pitts et al. 2023)
STON2	Increased expression in oral cancer, activates mTOR pathway	(Mahapatra et al. 2023)
TSC22D3	AML patients had higher expression	(Xu et al. 2023)
ADGRG7	Increased expression in BRCA patients	(Shi et al. 2024)
TRA2A	Splices CHK1 in K562 cells	(Lei et al. 2025)
TMSB10	Upregulated in several cancers	(Bingwei Wang et al. 2019)
CD69	Knockdown increased apoptosis of CML cells	(S.-Y. Huang et al. 2018)
GOLGA8A	Involved in lung squamous cell carcinoma	(Zhanzhan Li et al. 2022)
ANXA1	Higher expression in imatinib sensitive CML cell line than imatinib resistant CML cell line	(Colavita et al. 2010)
IFITM2	Increased expression seen in colorectal cancer, involved in PI3K/AKT pathway.	(Yonggang Liu et al. 2024)
CXCL11	Overexpressed in several cancers	(J. Wang et al. 2024)

RTN4	Causes cell proliferation through AKT pathway in cancers	(Pathak et al. 2018)
RPL37A	Downregulated expression in nasopharyngeal carcinomas	(Sim et al. 2010)
GOLGA8B	Associated with drug resistant prostate cancer	(Haopeng Li et al. 2024)
CD74	Upregulated in most cancers, associated with infiltration of M1 macrophages	(R. Q. Li et al. 2024)
GNAS	Mutation of this has been identified in CML	(Bidikian et al. 2022)
PIP4K2A	Inhibitor of PIP4K2A caused antileukaemic effect in AML and ALL	(Lima et al. 2022)
LRRC75A	Increased expression of SNHG29 in CML cell lines	(XueFeng Feng et al. 2024)
YBX1	Highly expressed in CML cells, removal caused apoptosis of LSCs	(Chai et al. 2023)
NCF4	Associated with SAT3 in CML	(Xiaoyun Feng et al. 2025)
TSC22D1	Increased expression in AML tissues	(Xu et al. 2023)
CDC42	Inhibition of BCR::ABL1 inhibited CXC42 activity	(Chang et al. 2009)
RPL10A	Associated with NPM1 in CML	(L. W. Chan et al. 2015)
EIF2S3	Anti-tumour effect via MAPK/ERK pathway in AML	(Lu et al. 2021)
RSPO1	Activates Wnt/ß-catenin pathway	(Geng et al., n.d.)
DAZAP2	Regulator of p53	(Liebl et al. 2021)
AVP	Promotes myeloid differentiation in HSCs	(Mou et al. 2024)
MPIG6B	Involved in megakaryocyte differentiation	(Becker et al. 2022)
RPS15	Mutated in patients with CLL	(Ntoufa et al. 2021)
PROM1	Marker found on both HSCs and LSCs	(Arrigoni et al. 2018)
PRSS1	Mutation leads to increased risk of pancreatic cancer	(Weiss 2014)
PCDH9	Mutations associated with several cancers and other diseases	(Haohan Li et al. 2025)
HLA-DRB1	Regulates $CD4^+$ T cells in melanoma	(Lester et al. 2023)
CD53	Expressed on immune cells	(Dunlock 2020)
WTAP	Involved in abnormal protein translation associated with BCR::ABL1	(Fernandez Rodriguez et al. 2024)
CKS2	Overexpressed in CML and other leukaemia's	(Cai et al. 2025)
ALG11	Associated with congenital disorders	(P. Zhao et al. 2024)

Table 6-1 BCR::ABL1 associated genes Table of genes associated with BCR::ABL1 (as described by (Giustacchini et al. 2017)) and the current knowledge of these genes.

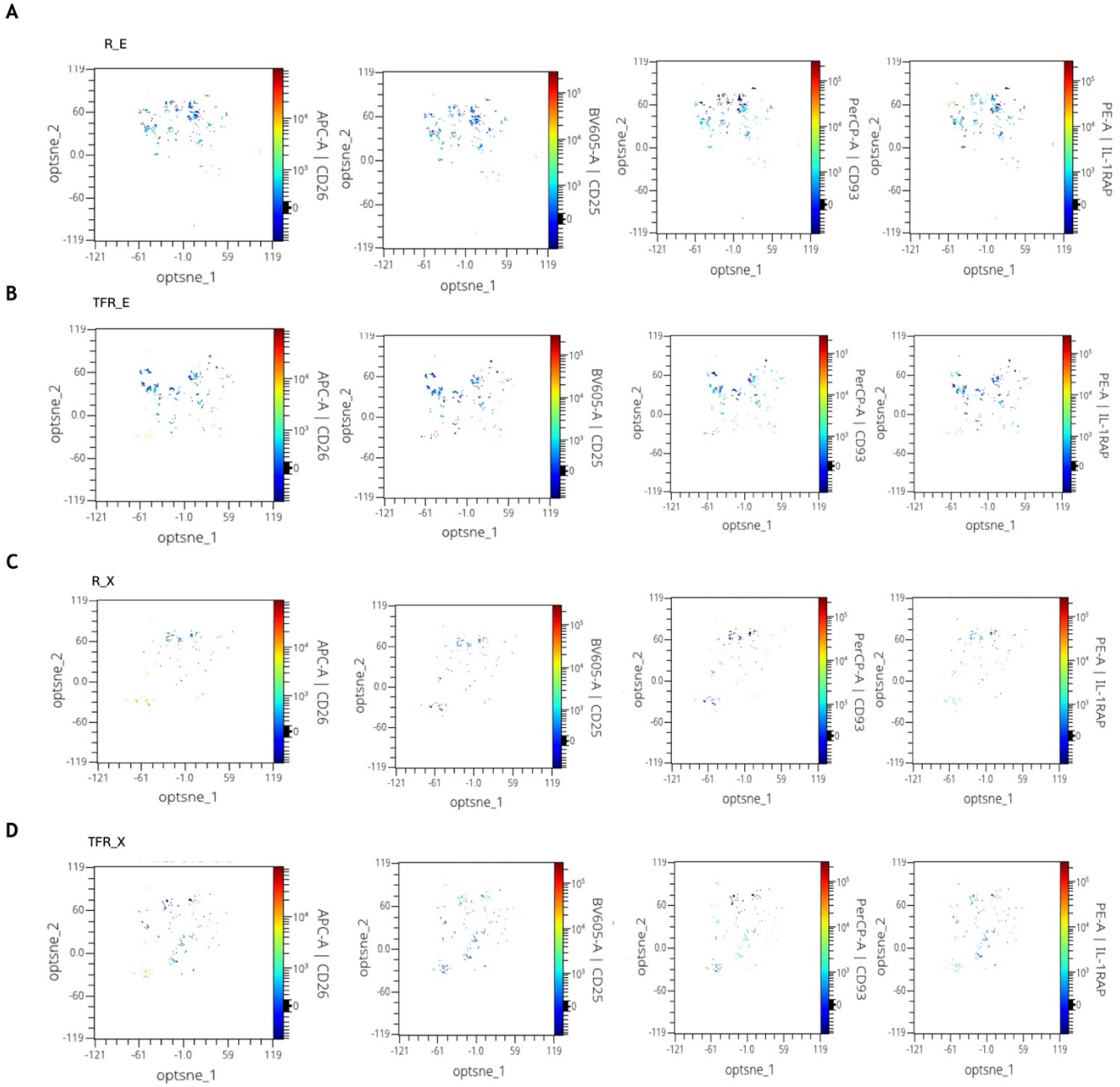
A
R_E
B
TFR_E
C
R_X
D
TFR_X
optsne_1
optsne_2
APC-A | CD26
BV605-A | CD25
PerCP-A | CD93
PE-A | IL-1RAP

Figure 6-1 Expression changes of CD26, CD25, CD93 and IL1-RAP across all DESTINY patients Tsne plots of CD26, CD25, CD93 and IL1-RAP expression, from HSC/LSC 1 panel in **(A)** R_E (relapse at point of trial entry) **(B)** TFR_E (TFR at point of trial entry) **(C)** Relapse_X (relapse at point of relapse) **(D)** TFR_X (TFR at trial exit). Samples from each outcome group were concatonated.

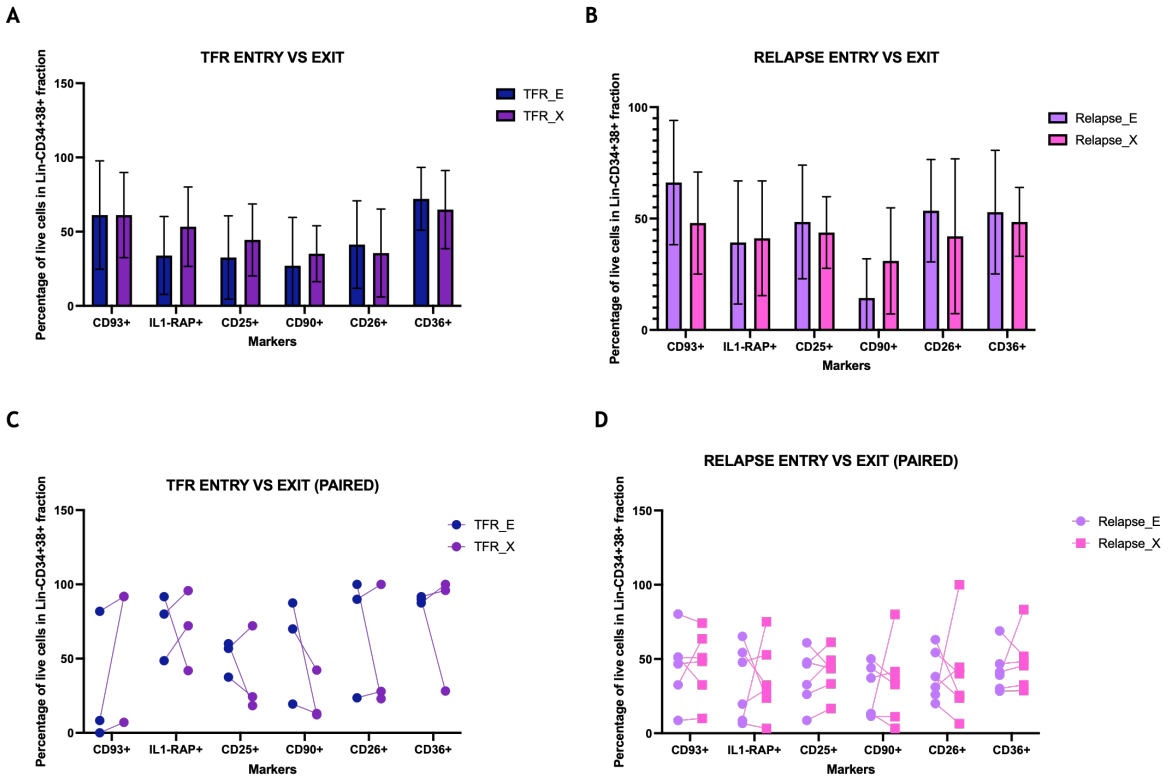

Figure 6-2 Changes to markers within progenitors from LSC/HSC panel 1 of BM MNCs in TFR and relapse patients Bar graph of the CD marker data produced from BM MNC samples from TFR and relapse samples only. **(A)** Comaprison of TFR at trial entry (TFR_E) (n=16) vs TFR at end point of trial (TFR_X) (n=7). **(B)** Comparison of relapse at trial entry (R_E) (n=13) vs at point of relapse (R_X) (n=9). **(C)** Comaprison of TFR at trial entry (TFR_E) (n=3) vs TFR at end point of trial (TFR_X) (n=3) of paired samples only. **(D)** Comparison of relapse at trial entry (R_E) (n=3) vs at point of relapse (R_X) (n=3) of paired samples only. TFR_E shown in dark blue, TFR_X shown in dark purple. Relapse_E shown in light purple, Relapse_X shown in pink. Bars show Mean with SD. Carried out two-way ANOVA, Tukey's multiple comparison test. P values: >0.05 (ns), <0.05 (*), <0.01 (**), <0.001 (***), <0.0001 (****).

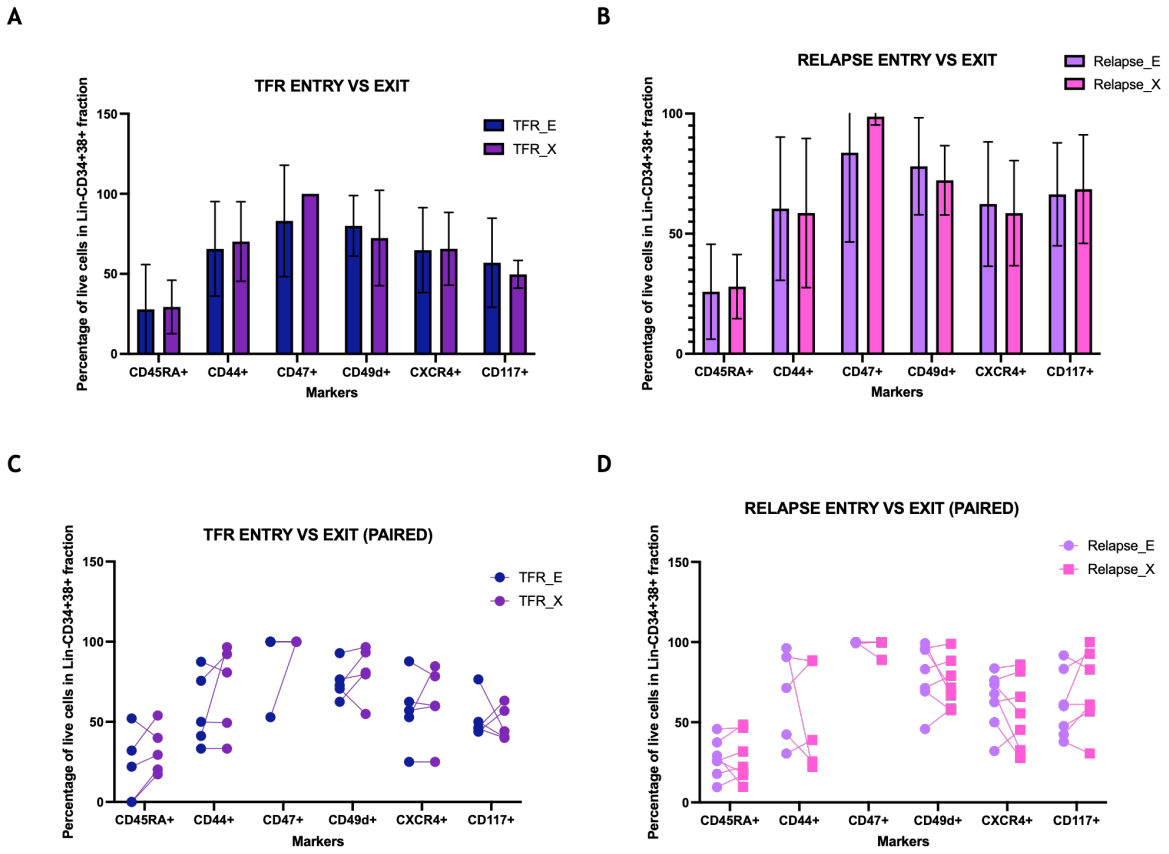

Figure 6-3 Changes to markers within progenitors from LSC/HSC panel 2 of BM MNCs in TFR and relapse patients Bar graph of the CD marker data produced from BM MNC samples from TFR and relapse samples only. **(A)** Comaprison of TFR at trial entry (TFR_E) (n=21) vs TFR at end point of trial (TFR_X) (n=7). **(B)** Comparison of relapse at trial entry (R_E) (n=19) vs at point of relapse (R_X) (n=10). **(C)** Comaprison of TFR at trial entry (TFR_E) (n=6) vs TFR at end point of trial (TFR_X) (n=6) of paired samples only. **(D)** Comparison of relapse at trial entry (R_E) (n=5) vs at point of relapse (R_X) (n=5) of paired samples only. TFR_E shown in dark blue, TFR_X shown in dark purple. Relapse_E shown in light purple, Relapse_X shown in pink. Bars show Mean with SD. Carried out two-way ANOVA, Tukey's multiple comparison test. P values: >0.05 (ns), <0.05 (*), <0.01 (**), <0.001 (***), <0.0001 (****).

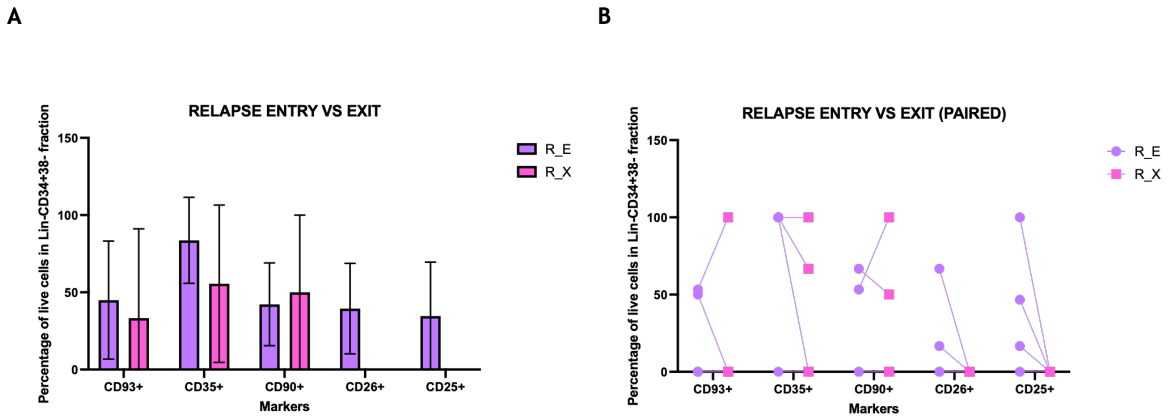

Figure 6-4 Changes to markers within progenitors from LSC/HSC panel 3 of BM MNCs in relapse patients Bar graph of the CD marker data produced from BM MNC samples from TFR and relapse samples only. **(A)** Comparison of relapse at trial entry (R_E) (n=13) vs at point of relapse (R_X) (n=3). **(B)** Comparison of relapse at trial entry (R_E) (n=4) vs at point of relapse (R_X) (n=4) of paired samples only. TFR_E shown in dark blue, TFR_X shown in dark purple. Relapse_E shown in light purple, Relapse_X shown in pink. Bars show Mean with SD. Carried out two-way ANOVA, Tukey's multiple comparison test. P values: >0.05 (ns), <0.05 (*), <0.01 (**), <0.001 (***), <0.0001 (****).

List of References

Agarwal, Puneet, Stephan Isringhausen, Hui Li, et al. 2019. 'Mesenchymal Niche-Specific Expression of Cxcl12 Controls Quiescence of Treatment-Resistant Leukemia Stem Cells'. *Cell Stem Cell* 24 (5): 769-784.e6. https://doi.org/10.1016/j.stem.2019.02.018.

Agarwal, Puneet, Hui Li, Kwangmin Choi, et al. 2021. 'TNF-α-Induced Alterations in Stromal Progenitors Enhance Leukemic Stem Cell Growth via CXCR2 Signaling'. *Cell Reports* 36 (2). https://doi.org/10.1016/j.celrep.2021.109386.

Agarwal, Puneet, Bin Zhang, Yinwei Ho, et al. 2017. 'Enhanced Targeting of CML Stem and Progenitor Cells by Inhibition of Porcupine Acyltransferase in Combination with TKI'. *Blood* 129 (8): 1008–20. https://doi.org/10.1182/blood-2016-05-714089.

Aguayo, Alvaro, Hagop Kantarjian, Taghi Manshouri, et al. 2000. 'Angiogenesis in Acute and Chronic Leukemias and Myelodysplastic Syndromes'. *Blood* 96 (6): 2240–45. https://doi.org/10.1182/blood.V96.6.2240.

Alves, Raquel, Stephanie E. B. McArdle, Jayakumar Vadakekolathu, et al. 2020. 'Flow Cytometry and Targeted Immune Transcriptomics Identify Distinct Profiles in Patients with Chronic Myeloid Leukemia Receiving Tyrosine Kinase Inhibitors with or without Interferon-α'. *Journal of Translational Medicine* 18 (1): 2. https://doi.org/10.1186/s12967-019-02194-x.

Ameziane-El-Hassani, Rabii, and Corinne Dupuy. 2013. 'Detection of Intracellular Reactive Oxygen Species (CM-H_2DCFDA)'. *Bio-Protocol* 3 (1). https://doi.org/10.21769/BioProtoc.313.

Anjo, Sandra Isabel, Cátia Santa, and Bruno Manadas. 2017. 'SWATH-MS as a Tool for Biomarker Discovery: From Basic Research to Clinical Applications'. *PROTEOMICS* 17 (3–4): 1600278. https://doi.org/10.1002/pmic.201600278.

Apperley, Jane F., Dragana Milojkovic, Nicholas C. P. Cross, et al. 2025. '2025 European LeukemiaNet Recommendations for the Management of Chronic Myeloid Leukemia'. *Leukemia* 39 (8): 1797–813. https://doi.org/10.1038/s41375-025-02664-w.

Arai, Fumio, Atsushi Hirao, Masako Ohmura, et al. 2004. 'Tie2/Angiopoietin-1 Signaling Regulates Hematopoietic Stem Cell Quiescence in the Bone Marrow Niche'. *Cell* 118 (2): 149–61. https://doi.org/10.1016/j.cell.2004.07.004.

Arakaki, Aleena K. S., Wen-An Pan, Helen Wedegaertner, et al. 2021. 'α-Arrestin ARRDC3 Tumor Suppressor Function Is Linked to GPCR-Induced TAZ Activation and Breast Cancer Metastasis'. *Journal of Cell Science* 134 (8): jcs254888. https://doi.org/10.1242/jcs.254888.

Araújo, Thaise Gonçalves, Sara Teixeira Soares Mota, Helen Soares Valença Ferreira, Matheus Alves Ribeiro, Luiz Ricardo Goulart, and Lara Vecchi.

2021. ‘Annexin A1 as a Regulator of Immune Response in Cancer’. *Cells* 10 (9). https://doi.org/10.3390/cells10092245.

Arrigoni, Elena, Marzia Del Re, Sara Galimberti, et al. 2018. ‘Concise Review: Chronic Myeloid Leukemia: Stem Cell Niche and Response to Pharmacologic Treatment’. *Stem Cells Translational Medicine* 7 (3): 305–14. https://doi.org/10.1002/sctm.17-0175.

Atallah, Ehab, Charles A. Schiffer, Jerald P. Radich, et al. 2021. ‘Assessment of Outcomes After Stopping Tyrosine Kinase Inhibitors Among Patients With Chronic Myeloid Leukemia: A Nonrandomized Clinical Trial’. *JAMA Oncology* 7 (1): 42–50. https://doi.org/10.1001/jamaoncol.2020.5774.

Atallah, Ehab, Charles A. Schiffer, Kevin P. Weinfurt, et al. 2018. ‘Design and Rationale for the Life after Stopping Tyrosine Kinase Inhibitors (LAST) Study, a Prospective, Single-Group Longitudinal Study in Patients with Chronic Myeloid Leukemia’. *BMC Cancer* 18 (1): 359. https://doi.org/10.1186/s12885-018-4273-1.

Atashi, Fatemeh, Ali Modarressi, and Michael S. Pepper. 2015. ‘The Role of Reactive Oxygen Species in Mesenchymal Stem Cell Adipogenic and Osteogenic Differentiation: A Review’. *Stem Cells and Development* 24 (10): 1150–63. https://doi.org/10.1089/scd.2014.0484.

Baba, Tomohisa, Kazuhito Naka, Soji Morishita, Norio Komatsu, Atsushi Hirao, and Naofumi Mukaida. 2013. ‘MIP-1α/CCL3-Mediated Maintenance of Leukemia-Initiating Cells in the Initiation Process of Chronic Myeloid Leukemia’. *The Journal of Experimental Medicine* 210 (12): 2661–73. https://doi.org/10.1084/jem.20130112.

Baberg, Falk, Stefanie Geyh, Daniel Waldera-Lupa, et al. 2019. ‘Secretome Analysis of Human Bone Marrow Derived Mesenchymal Stromal Cells’. *Biochimica et Biophysica Acta (BBA) - Proteins and Proteomics* 1867 (4): 434–41. https://doi.org/10.1016/j.bbapap.2019.01.013.

Balabanov, Stefan, Artur Gontarewicz, Patrick Ziegler, et al. 2006. ‘Hypusination of Eukaryotic Initiation Factor 5A (eIF5A): A Novel Therapeutic Target in BCR-ABL–Positive Leukemias Identified by a Proteomics Approach’. *Blood* 109 (4): 1701–11. https://doi.org/10.1182/blood-2005-03-037648.

Barilani, Mario, Christopher Lovejoy, Roberta Piras, Andrey Y. Abramov, Lorenza Lazzari, and Plamena R. Angelova. 2022. ‘Age-Related Changes in the Energy of Human Mesenchymal Stem Cells’. *Journal of Cellular Physiology* 237 (3): 1753–67. https://doi.org/10.1002/jcp.30638.

Batista-Gomes, Jéssica Almeida, Fernando Augusto Rodrigues Mello, Edivaldo Herculano Corrêa de Oliveira, et al. 2020. ‘Identifying Novel Genetic Alterations in Pediatric Acute Lymphoblastic Leukemia Based on Copy Number Analysis’. *Molecular Cytogenetics* 13 (June): 25. https://doi.org/10.1186/s13039-020-00491-5.

Baum, C. M., I. L. Weissman, A. S. Tsukamoto, A. M. Buckle, and B. Peault. 1992. ‘Isolation of a Candidate Human Hematopoietic Stem-Cell

Population.' *Proceedings of the National Academy of Sciences* 89 (7): 2804–8. https://doi.org/10.1073/pnas.89.7.2804.

Becker, Isabelle C., Zoltan Nagy, Georgi Manukjan, et al. 2022. 'G6b-B Regulates an Essential Step in Megakaryocyte Maturation'. *Blood Advances* 6 (10): 3155–61. https://doi.org/10.1182/bloodadvances.2021006151.

Benjamin, Esther Sathya Bama, Raveen Stephen Stallon Illangeswaran, Bharathi Rajamani, et al. 2026. 'Targeting Cathepsin-G to Overcome Leukemic Stem Cell Persistence in Chronic Myeloi'. Preprint. https://doi.org/10.21203/rs.3.rs-8580579/v1.

Benveniste, Patricia, Catherine Frelin, Salima Janmohamed, et al. 2010. 'Intermediate-Term Hematopoietic Stem Cells with Extended but Time-Limited Reconstitution Potential'. *Cell Stem Cell* 6 (1): 48–58. https://doi.org/10.1016/j.stem.2009.11.014.

Bertoli, Sarah, Etienne Paubelle, Emilie Bérard, et al. 2019. 'Ferritin Heavy/Light Chain (FTH1/FTL) Expression, Serum Ferritin Levels, and Their Functional as Well as Prognostic Roles in Acute Myeloid Leukemia'. *European Journal of Haematology* 102 (2): 131–42. https://doi.org/10.1111/ejh.13183.

Bi, Weimin, Jian Min Deng, Zhaoping Zhang, Richard R. Behringer, and Benoit de Crombrugghe. 1999. 'Sox9 Is Required for Cartilage Formation'. *Nature Genetics* 22 (1): 85–89. https://doi.org/10.1038/8792.

Bidikian, Aram, Hagop Kantarjian, Elias Jabbour, et al. 2022. 'CML-288 Impact of ASXL1 Mutations on Prognosis of Chronic Phase Chronic Myeloid Leukemia'. *Clinical Lymphoma Myeloma and Leukemia*, Proceedings of the Society of Hematologic Oncology 2022 Annual Meeting, vol. 22 (October): S291. https://doi.org/10.1016/S2152-2650(22)01371-4.

Bilousova, Ganna, Andriy Marusyk, Christopher C. Porter, Robert D. Cardiff, and James DeGregori. 2005. 'Impaired DNA Replication within Progenitor Cell Pools Promotes Leukemogenesis'. *PLOS Biology* 3 (12): e401. https://doi.org/10.1371/journal.pbio.0030401.

Bolton, Kelly L., Ryan N. Ptashkin, Teng Gao, et al. 2020. 'Cancer Therapy Shapes the Fitness Landscape of Clonal Hematopoiesis'. *Nature Genetics* 52 (11): 11. https://doi.org/10.1038/s41588-020-00710-0.

Bourgeais, Jerome, Nicole Ishac, Magdalena Medrzycki, et al. 2016. 'Oncogenic STAT5 Signaling Promotes Oxidative Stress in Chronic Myeloid Leukemia Cells by Repressing Antioxidant Defenses'. *Oncotarget* 8 (26): 41876–89. https://doi.org/10.18632/oncotarget.11480.

Bourne, Garrett, Ravi Bhatia, and Omer Jamy. 2024. 'Treatment-Free Remission in Chronic Myeloid Leukemia'. *Journal of Clinical Medicine* 13 (9): 2567. https://doi.org/10.3390/jcm13092567.

Bousounis, Pavlos, Veronica Bergo, and Eirini Trompouki. 2021. 'Inflammation, Aging and Hematopoiesis: A Complex Relationship'. *Cells* 10 (6): 6. https://doi.org/10.3390/cells10061386.

Bower, Hannah, Magnus Björkholm, Paul W. Dickman, Martin Höglund, Paul C. Lambert, and Therese M. L. Andersson. 2016. 'Life Expectancy of Patients With Chronic Myeloid Leukemia Approaches the Life Expectancy of the General Population'. *Journal of Clinical Oncology: Official Journal of the American Society of Clinical Oncology* 34 (24): 2851–57. https://doi.org/10.1200/JCO.2015.66.2866.

Bowie, Michelle B., David G. Kent, Michael R. Copley, and Connie J. Eaves. 2007. 'Steel Factor Responsiveness Regulates the High Self-Renewal Phenotype of Fetal Hematopoietic Stem Cells'. *Blood* 109 (11): 5043–48. https://doi.org/10.1182/blood-2006-08-037770.

Bowman, Robert L., Lambert Busque, and Ross L. Levine. 2018. 'Clonal Hematopoiesis and Evolution to Hematopoietic Malignancies'. *Cell Stem Cell* 22 (2): 157–70. https://doi.org/10.1016/j.stem.2018.01.011.

Breccia, Massimo, Rosalba Cucci, Giovanni Marsili, et al. 2025. 'Deep Molecular Response Rate in Chronic Phase Chronic Myeloid Leukemia: Eligibility to Discontinuation Related to Time to Response and Different Frontline TKI in the Experience of the Gimema Labnet CML National Network'. *Clinical Lymphoma, Myeloma and Leukemia* 25 (1): e34–39. https://doi.org/10.1016/j.clml.2024.08.009.

Bruns, Ingmar, Daniel Lucas, Sandra Pinho, et al. 2014. 'Megakaryocytes Regulate Hematopoietic Stem Cell Quiescence through CXCL4 Secretion'. *Nature Medicine* 20 (11): 1315–20. https://doi.org/10.1038/nm.3707.

Bulian, Pietro, Tait D. Shanafelt, Chris Fegan, et al. 2014. 'CD49d Is the Strongest Flow Cytometry–Based Predictor of Overall Survival in Chronic Lymphocytic Leukemia'. *Journal of Clinical Oncology* 32 (9): 897–904. https://doi.org/10.1200/JCO.2013.50.8515.

Busch, Caroline, and Helen Wheadon. 2019. 'Bone Marrow Niche Crosses Paths with BMPs: A Road to Protection and Persistence in CML'. *Biochemical Society Transactions* 47 (5): 1307–25. https://doi.org/10.1042/BST20190221.

Cai, Zhaoyi, Qiang Luo, Yuqun Zhang, Rui Meng, and Ming Tian. 2025. 'CK2 in the Spotlight: Decoding Its Role in Hematological Malignancies and Therapeutic Applications'. *Discover Oncology* 16 (May): 965. https://doi.org/10.1007/s12672-025-02797-5.

Calvi, L. M., G. B. Adams, K. W. Weibrecht, et al. 2003. 'Osteoblastic Cells Regulate the Haematopoietic Stem Cell Niche'. *Nature* 425 (6960): 841–46. https://doi.org/10.1038/nature02040.

Carrà, Giovanna, Davide Torti, Sabrina Crivellaro, et al. 2016. 'The BCR-ABL/NF-κB Signal Transduction Network: A Long Lasting Relationship in Philadelphia Positive Leukemias'. *Oncotarget* 7 (40): 66287–98. https://doi.org/10.18632/oncotarget.11507.

Castagnetti, Fausto, Gianni Binotto, Isabella Capodanno, et al. 2021. 'Making Treatment-Free Remission (TFR) Easier in Chronic Myeloid Leukemia:

Fact-Checking and Practical Management Tools'. *Targeted Oncology* 16 (6): 823–38. https://doi.org/10.1007/s11523-021-00831-4.

Cayssials, Emilie, Florence Jacomet, Nathalie Piccirilli, et al. 2019. 'Sustained Treatment-Free Remission in Chronic Myeloid Leukaemia Is Associated with an Increased Frequency of Innate CD8(+) T-Cells'. *British Journal of Haematology* 186 (1): 54–59. https://doi.org/10.1111/bjh.15858.

Cayssials, Emilie, Lucie Lefèvre, Amandine Decroos, et al. 2025. 'Innate CD8 T-Cells as a Potential Predictive Biomarker for Deep Molecular Response in Chronic Myeloid Leukemia Patients'. *Cancer Immunology, Immunotherapy* 75 (1): 16. https://doi.org/10.1007/s00262-025-04256-0.

Çelik, Haydar, Katherine E. Lindblad, Bogdan Popescu, et al. 2020. 'Highly Multiplexed Proteomic Assessment of Human Bone Marrow in Acute Myeloid Leukemia'. *Blood Advances* 4 (2): 367–79. https://doi.org/10.1182/bloodadvances.2019001124.

Chan, L. C., K. K. Karhi, S. I. Rayter, et al. 1987. 'A Novel Abl Protein Expressed in Philadelphia Chromosome Positive Acute Lymphoblastic Leukaemia Positive Acute Lymphoblastic Leukaemia'. *Nature* 325 (6105): 635–37. https://doi.org/10.1038/325635a0.

Chan, Lawrence WC, Xihong Lin, Godwin Yung, et al. 2015. 'Novel Structural Co-Expression Analysis Linking the NPM1-Associated Ribosomal Biogenesis Network to Chronic Myelogenous Leukemia'. *Scientific Reports* 5 (1): 10973. https://doi.org/10.1038/srep10973.

Chang, Y. C., S. C. Tien, H. F. Tien, H. Zhang, G. M. Bokoch, and Z. F. Chang. 2009. 'p210Bcr−Abl Desensitizes Cdc42 GTPase Signaling for SDF-1α-Directed Migration in Chronic Myeloid Leukemia Cells'. *Oncogene* 28 (46): 4105–15. https://doi.org/10.1038/onc.2009.260.

Charles A Janeway, Jr, Paul Travers, Mark Walport, and Mark J. Shlomchik. 2001. 'The Humoral Immune Response'. In *Immunobiology: The Immune System in Health and Disease. 5th Edition*. Garland Science. https://www.ncbi.nlm.nih.gov/books/NBK10752/.

Chen, Yong, Baojiang Wang, Yanjuan Chen, et al. 2022. 'HAPLN1 Affects Cell Viability and Promotes the Pro-Inflammatory Phenotype of Fibroblast-Like Synoviocytes'. *Frontiers in Immunology* 13 (June): 888612. https://doi.org/10.3389/fimmu.2022.888612.

Cheng, Hui, Zhaofeng Zheng, and Tao Cheng. 2020. 'New Paradigms on Hematopoietic Stem Cell Differentiation'. *Protein & Cell* 11 (1): 34–44. https://doi.org/10.1007/s13238-019-0633-0.

Chi, Xiaowen, Yuening Guo, Lijuan Zhang, et al. 2021. 'Long Non-Coding RNA GAS5 Regulates Th17/Treg Imbalance in Childhood Pneumonia by Targeting miR-217/STAT5'. *Cellular Immunology* 364 (June): 104357. https://doi.org/10.1016/j.cellimm.2021.104357.

Chiaretti, Sabina, Monica Messina, Sara Grammatico, et al. 2018. 'Rapid Identification of BCR/ABL1-like Acute Lymphoblastic Leukaemia Patients

Using a Predictive Statistical Model Based on Quantitative Real Time-Polymerase Chain Reaction: Clinical, Prognostic and Therapeutic Implications'. *British Journal of Haematology* 181 (5): 642–52. https://doi.org/10.1111/bjh.15251.

Chomel, Jean-Claude, and Ali G. Turhan. 2011. 'Chronic Myeloid Leukemia Stem Cells in the Era of Targeted Therapies: Resistance, Persistence and Long-Term Dormancy'. *Oncotarget* 2 (9): 713–27. https://doi.org/10.18632/oncotarget.333.

Chonat, Satheesh, Mary Risinger, Haripriya Sakthivel, et al. 2019. 'The Spectrum of SPTA1-Associated Hereditary Spherocytosis'. *Frontiers in Physiology* 10 (July): 815. https://doi.org/10.3389/fphys.2019.00815.

Christopher, Matthew J., Fulu Liu, Matthew J. Hilton, Fanxin Long, and Daniel C. Link. 2009. 'Suppression of CXCL12 Production by Bone Marrow Osteoblasts Is a Common and Critical Pathway for Cytokine-Induced Mobilization'. *Blood* 114 (7): 1331–39. https://doi.org/10.1182/blood-2008-10-184754.

Chua, Christelle En Lin, and Bor Luen Tang. 2015. 'The Role of the Small GTPase Rab31 in Cancer'. *Journal of Cellular and Molecular Medicine* 19 (1): 1–10. https://doi.org/10.1111/jcmm.12403.

Cilloni, Daniela, and Giuseppe Saglio. 2012. 'Molecular Pathways: BCR-ABL'. *Clinical Cancer Research* 18 (4): 930–37. https://doi.org/10.1158/1078-0432.CCR-10-1613.

Clark, Richard E., Fotios Polydoros, Jane F. Apperley, et al. 2017. 'De-Escalation of Tyrosine Kinase Inhibitor Dose in Patients with Chronic Myeloid Leukaemia with Stable Major Molecular Response (DESTINY): An Interim Analysis of a Non-Randomised, Phase 2 Trial'. *The Lancet. Haematology* 4 (7): e310–16. https://doi.org/10.1016/S2352-3026(17)30066-2.

Clark, Richard E., Fotios Polydoros, Jane F. Apperley, et al. 2019. 'De-Escalation of Tyrosine Kinase Inhibitor Therapy before Complete Treatment Discontinuation in Patients with Chronic Myeloid Leukaemia (DESTINY): A Non-Randomised, Phase 2 Trial'. *The Lancet Haematology* 6 (7): e375–83. https://doi.org/10.1016/S2352-3026(19)30094-8.

Colavita, Irene, Nicola Esposito, Rosanna Martinelli, et al. 2010. 'Gaining Insights into the Bcr-Abl Activity-Independent Mechanisms of Resistance to Imatinib Mesylate in KCL22 Cells: A Comparative Proteomic Approach'. *Biochimica et Biophysica Acta (BBA) - Proteins and Proteomics* 1804 (10): 1974–87. https://doi.org/10.1016/j.bbapap.2010.04.009.

Cömert, Cagla, Lauren Brick, Debbie Ang, et al. 2020. 'A Recurrent de Novo HSPD1 Variant Is Associated with Hypomyelinating Leukodystrophy'. *Cold Spring Harbor Molecular Case Studies* 6 (3): a004879. https://doi.org/10.1101/mcs.a004879.

Copland, Mhairi. 2022. 'Treatment of Blast Phase Chronic Myeloid Leukaemia: A Rare and Challenging Entity'. *British Journal of Haematology* 199 (5): 665–78. https://doi.org/10.1111/bjh.18370.

Çorbacıoğlu, Şeref Kerem, and Gökhan Aksel. 2023. 'Receiver Operating Characteristic Curve Analysis in Diagnostic Accuracy Studies: A Guide to Interpreting the Area under the Curve Value'. *Turkish Journal of Emergency Medicine* 23 (4): 195–98. https://doi.org/10.4103/tjem.tjem_182_23.

Corbin, Amie S., Anupriya Agarwal, Marc Loriaux, Jorge Cortes, Michael W. Deininger, and Brian J. Druker. 2011. 'Human Chronic Myeloid Leukemia Stem Cells Are Insensitive to Imatinib despite Inhibition of BCR-ABL Activity'. *The Journal of Clinical Investigation* 121 (1): 396–409. https://doi.org/10.1172/JCI35721.

Corrado, Chiara, Laura Saieva, Stefania Raimondo, Alessandra Santoro, Giacomo De Leo, and Riccardo Alessandro. 2016. 'Chronic Myelogenous Leukaemia Exosomes Modulate Bone Marrow Microenvironment through Activation of Epidermal Growth Factor Receptor'. *Journal of Cellular and Molecular Medicine* 20 (10): 1829–39. https://doi.org/10.1111/jcmm.12873.

Cortes, Jorge, Alfonso Quintás-Cardama, and Hagop M. Kantarjian. 2011. 'Monitoring Molecular Response in Chronic Myeloid Leukemia'. *Cancer* 117 (6): 1113–22. https://doi.org/10.1002/cncr.25527.

Crisan, Mihaela, Parham Solaimani Kartalaei, Chris S. Vink, et al. 2015. 'BMP Signalling Differentially Regulates Distinct Haematopoietic Stem Cell Types'. *Nature Communications* 6 (1): 8040. https://doi.org/10.1038/ncomms9040.

Cserjesi, Peter, Doris Brown, Keith L. Ligon, et al. 1995. 'Scleraxis: A Basic Helix-Loop-Helix Protein That Prefigures Skeletal Formation during Mouse Embryogenesis'. *Development* 121 (4): 1099–110. https://doi.org/10.1242/dev.121.4.1099.

Dawadi, Prabin, Bivek Pokharel, Anita Shrestha, et al. 2025. 'From Bench to Bytes: A Practical Guide to RNA Sequencing Data Analysis'. *Frontiers in Genetics* 16 (October): 1697922. https://doi.org/10.3389/fgene.2025.1697922.

Deininger, Michael, Stephen G. O'Brien, François Guilhot, et al. 2009. 'International Randomized Study of Interferon Vs STI571 (IRIS) 8-Year Follow up: Sustained Survival and Low Risk for Progression or Events in Patients with Newly Diagnosed Chronic Myeloid Leukemia in Chronic Phase (CML-CP) Treated with Imatinib.' *Blood* 114 (22): 1126. https://doi.org/10.1182/blood.V114.22.1126.1126.

Denu, Ryan A., and Peiman Hematti. 2016. 'Effects of Oxidative Stress on Mesenchymal Stem Cell Biology'. *Oxidative Medicine and Cellular Longevity* 2016: 2989076. https://doi.org/10.1155/2016/2989076.

Di Bonito, Maurizio, Monica Cantile, Francesca Collina, et al. 2012. 'Overexpression of Cell Cycle Progression Inhibitor Geminin Is Associated with Tumor Stem-Like Phenotype of Triple-Negative Breast Cancer'. *Journal of Breast Cancer* 15 (2): 162–71. https://doi.org/10.4048/jbc.2012.15.2.162.

Di Sanzo, Maddalena, Ilenia Aversa, Gianluca Santamaria, et al. 2016. 'FTH1P3, a Novel H-Ferritin Pseudogene Transcriptionally Active, Is Ubiquitously Expressed and Regulated during Cell Differentiation'. *PLoS ONE* 11 (3): e0151359. https://doi.org/10.1371/journal.pone.0151359.

Dierks, Christine, Ronak Beigi, Gui-Rong Guo, et al. 2008. 'Expansion of Bcr-Abl-Positive Leukemic Stem Cells Is Dependent on Hedgehog Pathway Activation'. *Cancer Cell* 14 (3): 238–49. https://doi.org/10.1016/j.ccr.2008.08.003.

Dominici, M., K. Le Blanc, I. Mueller, et al. 2006. 'Minimal Criteria for Defining Multipotent Mesenchymal Stromal Cells. The International Society for Cellular Therapy Position Statement'. *Cytotherapy* 8 (4): 315–17. https://doi.org/10.1080/14653240600855905.

Dong, Rong, Kate Cwynarski, Alan Entwistle, et al. 2003. 'Dendritic Cells from CML Patients Have Altered Actin Organization, Reduced Antigen Processing, and Impaired Migration'. *Blood* 101 (9): 3560–67. https://doi.org/10.1182/blood-2002-06-1841.

Druker, Brian J., François Guilhot, Stephen G. O'Brien, et al. 2006. 'Five-Year Follow-up of Patients Receiving Imatinib for Chronic Myeloid Leukemia'. *The New England Journal of Medicine* 355 (23): 2408–17. https://doi.org/10.1056/NEJMoa062867.

Duffy, Michelle M., Thomas Ritter, Rhodri Ceredig, and Matthew D. Griffin. 2011. 'Mesenchymal Stem Cell Effects on T-Cell Effector Pathways'. *Stem Cell Research & Therapy* 2 (4): 34. https://doi.org/10.1186/scrt75.

Dulmovits, Brian M., Jimmy Hom, Anupama Narla, Narla Mohandas, and Lionel Blanc. 2017. 'Characterization, Regulation and Targeting of Erythroid Progenitors in Normal and Disordered Human Erythropoiesis'. *Current Opinion in Hematology* 24 (3): 159–66. https://doi.org/10.1097/MOH.0000000000000328.

Dulucq, Stéphanie, Franck E. Nicolini, Delphine Rea, et al. 2022. 'Kinetics of Early and Late Molecular Recurrences after First-Line Imatinib Cessation in Chronic Myeloid Leukemia: Updated Results from the STIM2 Trial'. *Haematologica* 107 (12): 2859–69. https://doi.org/10.3324/haematol.2022.280811.

Dunlock, V. E. 2020. 'Tetraspanin CD53: An Overlooked Regulator of Immune Cell Function'. *Medical Microbiology and Immunology* 209 (4): 545–52. https://doi.org/10.1007/s00430-020-00677-z.

Dunphy, Katie, Despina Bazou, Michael Henry, et al. 2023. 'Proteomic and Metabolomic Analysis of Bone Marrow and Plasma from Patients with Extramedullary Multiple Myeloma Identifies Distinct Protein and Metabolite Signatures'. *Cancers* 15 (15): 3764. https://doi.org/10.3390/cancers15153764.

Dybko, Jaroslaw, Ewa Medras, Olga Haus, et al. 2013. 'CD117 (c-Kit) Expression On CD34+ Cells Participates In The Cytogenetic Response To Imatinib In

CML Patients In First Chronic Phase'. *Blood* 122 (21): 3990. https://doi.org/10.1182/blood.V122.21.3990.3990.

Eden, Rina E., and Jean M. Coviello. 2025. 'Chronic Myelogenous Leukemia'. In *StatPearls*. StatPearls Publishing. http://www.ncbi.nlm.nih.gov/books/NBK531459/.

Ernst, Philipp, Cera Lohse, Michael Lauseker, et al. 2026. 'Treatment Expectations and Goals among Patients with Chronic Myeloid Leukemia in Germany: A Patient-Centered Perspective'. *Leukemia* 40 (1): 29–36. https://doi.org/10.1038/s41375-025-02826-w.

Ershov, Pavel, Evgeniy Yablokov, Yuri Mezentsev, and Alexis Ivanov. 2023. 'Uncharacterized Proteins CxORFx: Subinteractome Analysis and Prognostic Significance in Cancers'. *International Journal of Molecular Sciences* 24 (12): 10190. https://doi.org/10.3390/ijms241210190.

Essers, Marieke A. G., Sandra Offner, William E. Blanco-Bose, et al. 2009. 'IFNα Activates Dormant Haematopoietic Stem Cells in Vivo'. *Nature* 458 (7240): 904–8. https://doi.org/10.1038/nature07815.

Etienne, Gabriel, Joëlle Guilhot, Delphine Rea, et al. 2017. 'Long-Term Follow-Up of the French Stop Imatinib (STIM1) Study in Patients With Chronic Myeloid Leukemia'. *Journal of Clinical Oncology* 35 (3): 298–305. https://doi.org/10.1200/JCO.2016.68.2914.

Feng, Xiaoyun, Yufeng Qin, Yulong Feng, and Yingquan Zhuo. 2025. 'Research on the Functions and Potential Mechanisms of STAT3 in Chronic Myelogenous Leukemia'. *Discover Oncology* 16 (1): 739. https://doi.org/10.1007/s12672-025-02492-5.

Feng, XueFeng, Lin Yang, Xiaojun Liu, et al. 2024. 'Long Non-Coding RNA Small Nucleolar RNA Host Gene 29 Drives Chronic Myeloid Leukemia Progression via microRNA-483-3p/Casitas B-Lineage Lymphoma Axis-Mediated Activation of the Phosphoinositide 3-Kinase/Akt Pathway'. *Medical Oncology* 41 (2): 60. https://doi.org/10.1007/s12032-023-02287-0.

Fernandez Rodriguez, Guillermo, Marco Tarullo, and Alessandro Fatica. 2024. 'N6-Methyladenosine (m6A) RNA Modification in Chronic Myeloid Leukemia: Unveiling a Novel Therapeutic Target'. *Cellular and Molecular Life Sciences: CMLS* 81 (1): 326. https://doi.org/10.1007/s00018-024-05379-w.

Flynn, Charlotte M., Yvonne Garbers, Juliane Lokau, et al. 2019. 'Activation of Toll-like Receptor 2 (TLR2) Induces Interleukin-6 Trans-Signaling'. *Scientific Reports* 9 (1): 7306. https://doi.org/10.1038/s41598-019-43617-5.

Galán-Díez, Marta, Álvaro Cuesta-Domínguez, and Stavroula Kousteni. 2018. 'The Bone Marrow Microenvironment in Health and Myeloid Malignancy'. *Cold Spring Harbor Perspectives in Medicine* 8 (7): a031328. https://doi.org/10.1101/cshperspect.a031328.

Gallipoli, Paolo, Amy Cook, Susan Rhodes, et al. 2014. 'JAK2/STAT5 Inhibition by Nilotinib with Ruxolitinib Contributes to the Elimination of CML CD34+ Cells in Vitro and in Vivo'. *Blood* 124 (9): 1492–501. https://doi.org/10.1182/blood-2013-12-545640.

Gao, Jie, Stephanie Graves, Ute Koch, et al. 2009. 'Hedgehog Signaling Is Dispensable for Adult Hematopoietic Stem Cell Function'. *Cell Stem Cell* 4 (6): 548–58. https://doi.org/10.1016/j.stem.2009.03.015.

Gao, Qianmin, Lipeng Wang, Sicheng Wang, Biaotong Huang, Yingying Jing, and Jiacan Su. 2022. 'Bone Marrow Mesenchymal Stromal Cells: Identification, Classification, and Differentiation'. *Frontiers in Cell and Developmental Biology* 9 (January). https://doi.org/10.3389/fcell.2021.787118.

Geng, Ajun, Ting Wu, Cheguo Cai, et al. n.d. 'A Novel Function of R-Spondin1 in Regulating Estrogen Receptor Expression Independent of Wnt/β-Catenin Signaling'. *eLife* 9: e56434. https://doi.org/10.7554/eLife.56434.

Gerber, Jonathan M., Jessica L. Gucwa, David Esopi, et al. 2013. 'Genome-Wide Comparison of the Transcriptomes of Highly Enriched Normal and Chronic Myeloid Leukemia Stem and Progenitor Cell Populations'. *Oncotarget* 4 (5): 715–28. https://doi.org/10.18632/oncotarget.990.

Giallongo, Cesarina, Alessandra Romano, Nunziatina Laura Parrinello, et al. 2016. 'Mesenchymal Stem Cells (MSC) Regulate Activation of Granulocyte-Like Myeloid Derived Suppressor Cells (G-MDSC) in Chronic Myeloid Leukemia Patients'. *PLOS ONE* 11 (7): e0158392. https://doi.org/10.1371/journal.pone.0158392.

Gieseke, Friederike, Judith Böhringer, Rita Bussolari, Massimo Dominici, Rupert Handgretinger, and Ingo Müller. 2010. 'Human Multipotent Mesenchymal Stromal Cells Use Galectin-1 to Inhibit Immune Effector Cells'. *Blood* 116 (19): 3770–79. https://doi.org/10.1182/blood-2010-02-270777.

Giles, Francis J., Tamas Masszi, María Teresa Gómez Casares, et al. 2019. 'Treatment-Free Remission (TFR) Following Frontline (1L) Nilotinib (NIL) in Patients (Pts) with Chronic Myeloid Leukemia in Chronic Phase (CML-CP): 192-Week Data from the ENESTfreedom Study.' *Journal of Clinical Oncology* 37 (15_suppl): 7013–7013. https://doi.org/10.1200/JCO.2019.37.15_suppl.7013.

Gillet, Ludovic C., Pedro Navarro, Stephen Tate, et al. 2012. 'Targeted Data Extraction of the MS/MS Spectra Generated by Data-Independent Acquisition: A New Concept for Consistent and Accurate Proteome Analysis'. *Molecular & Cellular Proteomics : MCP* 11 (6): O111.016717. https://doi.org/10.1074/mcp.O111.016717.

Giustacchini, Alice, Supat Thongjuea, Nikolaos Barkas, et al. 2017. 'Single-Cell Transcriptomics Uncovers Distinct Molecular Signatures of Stem Cells in Chronic Myeloid Leukemia'. *Nature Medicine* 23 (6): 692–702. https://doi.org/10.1038/nm.4336.

Gnani, Daniela, Stefania Crippa, Lucrezia della Volpe, et al. 2019. 'An Early-Senescence State in Aged Mesenchymal Stromal Cells Contributes to

Hematopoietic Stem and Progenitor Cell Clonogenic Impairment through the Activation of a pro-Inflammatory Program'. *Aging Cell* 18 (3): e12933. https://doi.org/10.1111/acel.12933.

Goff, Daniel J., Angela Court Recart, Anil Sadarangani, et al. 2013. 'A Pan-BCL2 Inhibitor Renders Bone-Marrow-Resident Human Leukemia Stem Cells Sensitive to Tyrosine Kinase Inhibition'. *Cell Stem Cell* 12 (3): 316–28. https://doi.org/10.1016/j.stem.2012.12.011.

Golden, Emily, Rabab Rashwan, Eleanor A. Woodward, et al. 2021. 'The Oncogene AAMDC Links PI3K-AKT-mTOR Signaling with Metabolic Reprograming in Estrogen Receptor-Positive Breast Cancer'. *Nature Communications* 12 (1): 1920. https://doi.org/10.1038/s41467-021-22101-7.

Greene, Joseph T., Ben F. Brian, S. Erandika Senevirathne, and Tanya S. Freedman. 2021. 'Regulation of Myeloid-Cell Activation'. *Current Opinion in Immunology*, Special Section on "Signal transduction controlling immune cell function", vol. 73 (December): 34–42. https://doi.org/10.1016/j.coi.2021.09.004.

Grockowiak, Elodie, Bastien Laperrousaz, Sandrine Jeanpierre, et al. 2017. 'Immature CML Cells Implement a BMP Autocrine Loop to Escape TKI Treatment'. *Blood* 130 (26): 2860–71. https://doi.org/10.1182/blood-2017-08-801019.

Gu, Jingyao, Zhenyao Chen, Xin Chen, and Zhaoxia Wang. 2020. 'Heterogeneous Nuclear Ribonucleoprotein (hnRNPL) in Cancer'. *Clinica Chimica Acta; International Journal of Clinical Chemistry* 507 (August): 286–94. https://doi.org/10.1016/j.cca.2020.04.040.

Guo, F., Y. Wang, J. Liu, S. C. Mok, F. Xue, and W. Zhang. 2016. 'CXCL12/CXCR4: A Symbiotic Bridge Linking Cancer Cells and Their Stromal Neighbors in Oncogenic Communication Networks'. *Oncogene* 35 (7): 7. https://doi.org/10.1038/onc.2015.139.

Hamad, Mohammad Al. 2021. 'Contribution of BCR-ABL Molecular Variants and Leukemic Stem Cells in Response and Resistance to Tyrosine Kinase Inhibitors: A Review'. *F1000Research* 10. https://doi.org/10.12688/f1000research.74570.2.

Hamilton, Ashley, G. Vignir Helgason, Mirle Schemionek, et al. 2012. 'Chronic Myeloid Leukemia Stem Cells Are Not Dependent on Bcr-Abl Kinase Activity for Their Survival'. *Blood* 119 (6): 1501–10. https://doi.org/10.1182/blood-2010-12-326843.

Harutyunyan, Lusine, Astghik Voskanyan, Karen Meliksetyan, et al. 2021. 'CML-307: Assessment of 5-Year OS and Treatment Options in Newly Diagnosed Ph + CML Patients in the Republic of Armenia'. *Clinical Lymphoma Myeloma and Leukemia*, Proceedings of the Society of Hematologic Oncology 2021 Annual Meeting, vol. 21 (September): S333. https://doi.org/10.1016/S2152-2650(21)01779-1.

Hassan, H. T., and A. Zander. 1996. ‘Stem Cell Factor as a Survival and Growth Factor in Human Normal and Malignant Hematopoiesis’. *Acta Haematologica* 95 (3–4): 257–62. https://doi.org/10.1159/000203893.

Hayflick, L., and P. S. Moorhead. 1961. ‘The Serial Cultivation of Human Diploid Cell Strains’. *Experimental Cell Research* 25 (3): 585–621. https://doi.org/10.1016/0014-4827(61)90192-6.

Heil, Lilian R., Eugen Damoc, Tabiwang N. Arrey, et al. 2023. ‘Evaluating the Performance of the Astral Mass Analyzer for Quantitative Proteomics Using Data-Independent Acquisition’. *Journal of Proteome Research* 22 (10): 3290–300. https://doi.org/10.1021/acs.jproteome.3c00357.

Heissig, Beate, Koichi Hattori, Sergio Dias, et al. 2002. ‘Recruitment of Stem and Progenitor Cells from the Bone Marrow Niche Requires MMP-9 Mediated Release of Kit-Ligand’. *Cell* 109 (5): 625–37. https://doi.org/10.1016/S0092-8674(02)00754-7.

Hellqvist, Eva, Frida Holm, Cayla N. Mason, et al. 2013. ‘CD44 Monoclonal Antibody-Enhanced Clearance Of Chronic Myeloid Leukemia Stem Cells From The Malignant Niche’. *Blood* 122 (21): 858. https://doi.org/10.1182/blood.V122.21.858.858.

Hennrich, Marco L., Natalie Romanov, Patrick Horn, et al. 2018. ‘Cell-Specific Proteome Analyses of Human Bone Marrow Reveal Molecular Features of Age-Dependent Functional Decline’. *Nature Communications* 9 (1): 4004. https://doi.org/10.1038/s41467-018-06353-4.

Herranz, Nicolás, and Jesús Gil. 2018. ‘Mechanisms and Functions of Cellular Senescence’. *The Journal of Clinical Investigation* 128 (4): 1238–46. https://doi.org/10.1172/JCI95148.

Herrmann, Harald, Irina Sadovnik, Sabine Cerny-Reiterer, et al. 2014. ‘Dipeptidylpeptidase IV (CD26) Defines Leukemic Stem Cells (LSC) in Chronic Myeloid Leukemia’. *Blood* 123 (25): 3951–62. https://doi.org/10.1182/blood-2013-10-536078.

Herrmann, Harald, Irina Sadovnik, Gregor Eisenwort, et al. 2020. ‘Delineation of Target Expression Profiles in CD34+/CD38− and CD34+/CD38+ Stem and Progenitor Cells in AML and CML’. *Blood Advances* 4 (20): 5118–32. https://doi.org/10.1182/bloodadvances.2020001742.

Herrmann, Oliver, Maja Kim Kuepper, Marlena Bütow, et al. 2019. ‘Infliximab Therapy Together with Tyrosine Kinase Inhibition Targets Leukemic Stem Cells in Chronic Myeloid Leukemia’. *BMC Cancer* 19 (1): 658. https://doi.org/10.1186/s12885-019-5871-2.

Hildebrand, Dominic G., Simon Lehle, Andreas Borst, Sebastian Haferkamp, Frank Essmann, and Klaus Schulze-Osthoff. 2013. ‘α-Fucosidase as a Novel Convenient Biomarker for Cellular Senescence’. *Cell Cycle* 12 (12): 1922–27. https://doi.org/10.4161/cc.24944.

Ho, Matthew, Surendra Dasari, Alissa Visram, et al. 2023. ‘An Atlas of the Bone Marrow Bone Proteome in Patients with Dysproteinemias’. *Blood Cancer Journal* 13 (1): 63. https://doi.org/10.1038/s41408-023-00840-8.

Hochhaus, A., M. Baccarani, R. T. Silver, et al. 2020. ‘European LeukemiaNet 2020 Recommendations for Treating Chronic Myeloid Leukemia’. *Leukemia* 34 (4): 966–84. https://doi.org/10.1038/s41375-020-0776-2.

Hoermann, Gregor, Georg Greiner, and Peter Valent. 2015. ‘Cytokine Regulation of Microenvironmental Cells in Myeloproliferative Neoplasms’. *Mediators of Inflammation* 2015: 869242. https://doi.org/10.1155/2015/869242.

Holyoake, Tessa L., Xiaoyan Jiang, Heather G. Jorgensen, et al. 2001. ‘Primitive Quiescent Leukemic Cells from Patients with Chronic Myeloid Leukemia Spontaneously Initiate Factor-Independent Growth in Vitro in Association with up-Regulation of Expression of Interleukin-3’. *Blood* 97 (3): 720–28. https://doi.org/10.1182/blood.V97.3.720.

Hoo, Zhe Hui, Jane Candlish, and Dawn Teare. 2017. ‘What Is an ROC Curve?’ Concepts. *Emergency Medicine Journal* 34 (6): 357–59. https://doi.org/10.1136/emermed-2017-206735.

Hoogduijn, Martin J., Felix Popp, Richard Verbeek, et al. 2010. ‘The Immunomodulatory Properties of Mesenchymal Stem Cells and Their Use for Immunotherapy’. *International Immunopharmacology*, New Trends in Immunosuppression 2010, vol. 10 (12): 1496–500. https://doi.org/10.1016/j.intimp.2010.06.019.

Horne, Gillian A., Heather Morrison, Victoria Campbell, et al. 2016. ‘Notch Pathway Activation Targets Leukemic Stem Cells in Chronic-Phase Chronic Myeloid Leukemia (CP-CML)’. *Blood* 128 (22): 3057. https://doi.org/10.1182/blood.V128.22.3057.3057.

Hossain, Md Faruq, Lisa Hagenau, Lars R. Jensen, et al. 2026. ‘Molecular Background of Philadelphia Chromosome Dependent Enhancement of Cellular Growth and Tyrosine Kinase Inhibitor Sensitivity’. *Experimental Hematology & Oncology* 15 (February): 26. https://doi.org/10.1186/s40164-026-00758-4.

Houshmand, Mohammad, Giorgia Simonetti, Paola Circosta, et al. 2019. ‘Chronic Myeloid Leukemia Stem Cells’. *Leukemia* 33 (7): 7. https://doi.org/10.1038/s41375-019-0490-0.

Hsieh, Ya-Ching, Kristina Kirschner, and Mhairi Copland. 2021. ‘Improving Outcomes in Chronic Myeloid Leukemia through Harnessing the Immunological Landscape’. *Leukemia* 35 (5): 1229–42. https://doi.org/10.1038/s41375-021-01238-w.

Hu, Y., Y. Chen, L. Douglas, and S. Li. 2009. ‘β-Catenin Is Essential for Survival of Leukemic Stem Cells Insensitive to Kinase Inhibition in Mice with BCR-ABL-Induced Chronic Myeloid Leukemia’. *Leukemia* 23 (1): 109–16. https://doi.org/10.1038/leu.2008.262.

Huang, Shih-Yun, Yu-Hsiu Liu, Yi-Ju Chen, Yi-Yen Yeh, and Huei-Mei Huang. 2018. 'CD69 Partially Inhibits Apoptosis and Erythroid Differentiation via CD24, and Their Knockdown Increase Imatinib Sensitivity in BCR-ABL-Positive Cells'. *Journal of Cellular Physiology* 233 (9): 7467–79. https://doi.org/10.1002/jcp.26599.

Huang, Yutong, Qiang Wu, and Paul Kwong Hang Tam. 2022. 'Immunomodulatory Mechanisms of Mesenchymal Stem Cells and Their Potential Clinical Applications'. *International Journal of Molecular Sciences* 23 (17): 10023. https://doi.org/10.3390/ijms231710023.

Hughes, Amy, Jade Clarson, Carine Tang, et al. 2017. 'CML Patients with Deep Molecular Responses to TKI Have Restored Immune Effectors and Decreased PD-1 and Immune Suppressors'. *Blood* 129 (9): 1166–76. https://doi.org/10.1182/blood-2016-10-745992.

Hughes, Amy, and Agnes S. M. Yong. 2017. 'Immune Effector Recovery in Chronic Myeloid Leukemia and Treatment-Free Remission'. *Frontiers in Immunology* 8 (April): 469. https://doi.org/10.3389/fimmu.2017.00469.

Hughes, Tim P., Jaspal Kaeda, Susan Branford, et al. 2003. 'Frequency of Major Molecular Responses to Imatinib or Interferon Alfa plus Cytarabine in Newly Diagnosed Chronic Myeloid Leukemia'. *New England Journal of Medicine* 349 (15): 1423–32. https://doi.org/10.1056/NEJMoa030513.

Hung, Sheng-Yu, Chien-Chin Lin, Chia-Lang Hsu, et al. 2021. 'The Expression Levels of Long Non-Coding RNA KIAA0125 Are Associated with Distinct Clinical and Biological Features in Myelodysplastic Syndromes'. *British Journal of Haematology* 192 (3): 589–98. https://doi.org/10.1111/bjh.17231.

Huntly, Brian J. P., Hirokazu Shigematsu, Kenji Deguchi, et al. 2004. 'MOZ-TIF2, but Not BCR-ABL, Confers Properties of Leukemic Stem Cells to Committed Murine Hematopoietic Progenitors'. *Cancer Cell* 6 (6): 587–96. https://doi.org/10.1016/j.ccr.2004.10.015.

Idelfonso-García, Osiris Germán, Ruth Pacheco-Rivera, Brisa Rodope Alarcón-Sánchez, et al. 2024. 'Protocol to Detect Senescence-Associated ß-Galactosidase and Immunoperoxidase Activity in Fresh-Frozen Murine Tissues'. *STAR Protocols* 5 (2): 103009. https://doi.org/10.1016/j.xpro.2024.103009.

Iqbal, Nida, and Naveed Iqbal. 2014. 'Imatinib: A Breakthrough of Targeted Therapy in Cancer'. *Chemotherapy Research and Practice* 2014 (1): 357027. https://doi.org/10.1155/2014/357027.

Irani, Yazad D., Amy Hughes, Jade Clarson, et al. 2020. 'Successful Treatment-Free Remission in Chronic Myeloid Leukaemia and Its Association with Reduced Immune Suppressors and Increased Natural Killer Cells'. *British Journal of Haematology* 191 (3): 433–41. https://doi.org/10.1111/bjh.16718.

Irgit, Ayca, Reyhan Kamıs, Belgin Sever, et al. 2025. 'Structure and Dynamics of the ABL1 Tyrosine Kinase and Its Important Role in Chronic Myeloid

Leukemia'. *Archiv Der Pharmazie* 358 (5): e70005. https://doi.org/10.1002/ardp.70005.

Isa, Adiba, Jan O. Nehlin, Hardee J. Sabir, et al. 2010. 'Impaired Cell Surface Expression of HLA-B Antigens on Mesenchymal Stem Cells and Muscle Cell Progenitors'. *PLoS ONE* 5 (5): e10900. https://doi.org/10.1371/journal.pone.0010900.

Jajula, Saikiran, Venkateshwarlu Naik, Bhargab Kalita, et al. 2024. 'Integrative Proteome Analysis of Bone Marrow Interstitial Fluid and Serum Reveals Candidate Signature for Acute Myeloid Leukemia'. *Journal of Proteomics* 303 (July): 105224. https://doi.org/10.1016/j.jprot.2024.105224.

Jamieson, Catriona H. M., Laurie E. Ailles, Scott J. Dylla, et al. 2004. 'Granulocyte–Macrophage Progenitors as Candidate Leukemic Stem Cells in Blast-Crisis CML'. *New England Journal of Medicine* 351 (7): 657–67. https://doi.org/10.1056/NEJMoa040258.

Jang, Yoon-Young, and Saul J. Sharkis. 2007. 'A Low Level of Reactive Oxygen Species Selects for Primitive Hematopoietic Stem Cells That May Reside in the Low-Oxygenic Niche'. *Blood* 110 (8): 3056–63. https://doi.org/10.1182/blood-2007-05-087759.

Järås, Marcus, Petra Johnels, Nils Hansen, et al. 2010. 'Isolation and Killing of Candidate Chronic Myeloid Leukemia Stem Cells by Antibody Targeting of IL-1 Receptor Accessory Protein'. *Proceedings of the National Academy of Sciences* 107 (37): 16280–85. https://doi.org/10.1073/pnas.1004408107.

Jeong, Sin-Gu, and Goang-Won Cho. 2015. 'Endogenous ROS Levels Are Increased in Replicative Senescence in Human Bone Marrow Mesenchymal Stromal Cells'. *Biochemical and Biophysical Research Communications* 460 (4): 971–76. https://doi.org/10.1016/j.bbrc.2015.03.136.

Jiang, X., Y. Zhao, C. Smith, et al. 2007. 'Chronic Myeloid Leukemia Stem Cells Possess Multiple Unique Features of Resistance to BCR-ABL Targeted Therapies'. *Leukemia* 21 (5): 926–35. https://doi.org/10.1038/sj.leu.2404609.

Jin, Linhua, Yoko Tabe, Sergej Konoplev, et al. 2008. 'CXCR4 Up-Regulation by Imatinib Induces Chronic Myelogenous Leukemia (CML) Cell Migration to Bone Marrow Stroma and Promotes Survival of Quiescent CML Cells'. *Molecular Cancer Therapeutics* 7 (1): 48–58. https://doi.org/10.1158/1535-7163.MCT-07-0042.

Jin, Tian, Xuehua Xu, and Dale Hereld. 2008. 'Chemotaxis, Chemokine Receptors and Human Disease'. *Cytokine* 44 (1): 1–8. https://doi.org/10.1016/j.cyto.2008.06.017.

Kaleta, Konrad, Klaudia Janik, Leszek Rydz, Maria Wróbel, and Halina Jurkowska. 2024. 'Bridging the Gap in Cancer Research: Sulfur Metabolism of Leukemic Cells with a Focus on L-Cysteine Metabolism and Hydrogen Sulfide-Producing Enzymes'. *Biomolecules* 14 (7): 7. https://doi.org/10.3390/biom14070746.

Kamath, Amrita V., Jian Wang, Francis Y. Lee, and Punit H. Marathe. 2008. 'Preclinical Pharmacokinetics and in Vitro Metabolism of Dasatinib (BMS-354825): A Potent Oral Multi-Targeted Kinase Inhibitor against SRC and BCR-ABL'. *Cancer Chemotherapy and Pharmacology* 61 (3): 365–76. https://doi.org/10.1007/s00280-007-0478-8.

Kang, Sujin, Toshio Tanaka, Masashi Narazaki, and Tadamitsu Kishimoto. 2019. 'Targeting Interleukin-6 Signaling in Clinic'. *Immunity* 50 (4): 1007–23. https://doi.org/10.1016/j.immuni.2019.03.026.

Kang, Yoon-A., Eric M. Pietras, and Emmanuelle Passegué. 2019. 'Deregulated Notch and Wnt Signaling Activates Early-Stage Myeloid Regeneration Pathways in Leukemia'. *Journal of Experimental Medicine* 217 (3): e20190787. https://doi.org/10.1084/jem.20190787.

Kantarjian, Hagop M., Francis Giles, Norbert Gattermann, et al. 2007. 'Nilotinib (Formerly AMN107), a Highly Selective BCR-ABL Tyrosine Kinase Inhibitor, Is Effective in Patients with Philadelphia Chromosome–Positive Chronic Myelogenous Leukemia in Chronic Phase Following Imatinib Resistance and Intolerance'. *Blood* 110 (10): 3540–46. https://doi.org/10.1182/blood-2007-03-080689.

Kantarjian, Hagop, Neil P. Shah, Andreas Hochhaus, et al. 2010. 'Dasatinib versus Imatinib in Newly Diagnosed Chronic-Phase Chronic Myeloid Leukemia'. *The New England Journal of Medicine* 362 (24): 2260–70. https://doi.org/10.1056/NEJMoa1002315.

Karnik, Sonali J., Connor Gulbronson, Paige C. Jordan, et al. 2025. 'Multiplex Imaging of Murine Bone Marrow Using Phenocycler 2.0™'. *Leukemia* 39 (6): 1476–89. https://doi.org/10.1038/s41375-025-02596-5.

Karpievitch, Yuliya V., Ashoka D. Polpitiya, Gordon A. Anderson, Richard D. Smith, and Alan R. Dabney. 2010. 'Liquid Chromatography Mass Spectrometry-Based Proteomics: Biological and Technological Aspects'. *The Annals of Applied Statistics* 4 (4): 1797–823. https://doi.org/10.1214/10-AOAS341.

Kawasaki, Takumi, and Taro Kawai. 2014. 'Toll-Like Receptor Signaling Pathways'. *Frontiers in Immunology* 5 (September): 461. https://doi.org/10.3389/fimmu.2014.00461.

Kesarwani, Meenu, Zachary Kincaid, Ahmed Gomaa, et al. 2017. 'Targeting C-FOS and DUSP1 Abrogates Intrinsic Resistance to Tyrosine-Kinase Inhibitor Therapy in BCR-ABL-Induced Leukemia'. *Nature Medicine* 23 (4): 472–82. https://doi.org/10.1038/nm.4310.

Kim, Jeong H., Stephanie C. Chu, Jessica L. Gramlich, et al. 2005. 'Activation of the PI3K/mTOR Pathway by BCR-ABL Contributes to Increased Production of Reactive Oxygen Species'. *Blood* 105 (4): 1717–23. https://doi.org/10.1182/blood-2004-03-0849.

Kinstrie, Ross, Gillian A. Horne, Heather Morrison, et al. 2020. 'CD93 Is Expressed on Chronic Myeloid Leukemia Stem Cells and Identifies a Quiescent Population Which Persists after Tyrosine Kinase Inhibitor

Therapy'. *Leukemia* 34 (6): 1613–25. https://doi.org/10.1038/s41375-019-0684-5.

Kolba, Marta D., Wioleta Dudka, Monika Zaręba-Kozioł, et al. 2019. 'Tunneling Nanotube-Mediated Intercellular Vesicle and Protein Transfer in the Stroma-Provided Imatinib Resistance in Chronic Myeloid Leukemia Cells'. *Cell Death & Disease* 10 (11): 817. https://doi.org/10.1038/s41419-019-2045-8.

Krasny, Lukas, and Paul H. Huang. 2021. 'Data-Independent Acquisition Mass Spectrometry (DIA-MS) for Proteomic Applications in Oncology'. *Molecular Omics* 17 (1): 29–42. https://doi.org/10.1039/D0MO00072H.

Krause, Daniela S., Katherine Lazarides, Ulrich H. von Andrian, and Richard A. Van Etten. 2006. 'Requirement for CD44 in Homing and Engraftment of BCR-ABL–Expressing Leukemic Stem Cells'. *Nature Medicine* 12 (10): 1175–80. https://doi.org/10.1038/nm1489.

Krause, Daniela S., David T. Scadden, and Frederic I. Preffer. 2013. 'The Hematopoietic Stem Cell Niche—Home for Friend and Foe?' *Cytometry. Part B, Clinical Cytometry* 84 (1): 10.1002/cyto.b.21066. https://doi.org/10.1002/cyto.b.21066.

Kremlitzka, Mariann, Anna Polgár, Lívia Fülöp, Emese Kiss, Gyula Poór, and Anna Erdei. 2013. 'Complement Receptor Type 1 (CR1, CD35) Is a Potent Inhibitor of B-Cell Functions in Rheumatoid Arthritis Patients'. *International Immunology* 25 (1): 25–33. https://doi.org/10.1093/intimm/dxs090.

Krishnan, Vaidehi, Florian Schmidt, Zahid Nawaz, et al. 2023. 'A Single-Cell Atlas Identifies Pretreatment Features of Primary Imatinib Resistance in Chronic Myeloid Leukemia'. *Blood* 141 (22): 2738–55. https://doi.org/10.1182/blood.2022017295.

Kujawski, Lisa A., and Moshe Talpaz. 2007. 'The Role of Interferon-Alpha in the Treatment of Chronic Myeloid Leukemia'. *Cytokine & Growth Factor Reviews*, Honoring the Milstein Family Support of Interferon Research, vol. 18 (5): 459–71. https://doi.org/10.1016/j.cytogfr.2007.06.015.

Kulkarni, Rohan, and Vaijayanti Kale. 2020. 'Physiological Cues Involved in the Regulation of Adhesion Mechanisms in Hematopoietic Stem Cell Fate Decision'. *Frontiers in Cell and Developmental Biology* 8 (July). https://doi.org/10.3389/fcell.2020.00611.

Kuntz, Elodie M., Pablo Baquero, Alison M. Michie, et al. 2017. 'Targeting Mitochondrial Oxidative Phosphorylation Eradicates Therapy-Resistant Chronic Myeloid Leukemia Stem Cells'. *Nature Medicine* 23 (10): 1234–40. https://doi.org/10.1038/nm.4399.

Kwak, Jae-Yong, Sung-Hyun Kim, Suk Joong Oh, et al. 2017. 'Phase III Clinical Trial (RERISE Study) Results of Efficacy and Safety of Radotinib Compared with Imatinib in Newly Diagnosed Chronic Phase Chronic Myeloid Leukemia'. *Clinical Cancer Research* 23 (23): 7180–88. https://doi.org/10.1158/1078-0432.CCR-17-0957.

Kwon, Munju, Byoung Soo Kim, Sik Yoon, Sae-Ock Oh, and Dongjun Lee. 2024. 'Hematopoietic Stem Cells and Their Niche in Bone Marrow'. *International Journal of Molecular Sciences* 25 (13): 6837. https://doi.org/10.3390/ijms25136837.

Landberg, Niklas, Sofia von Palffy, Maria Askmyr, et al. 2018. 'CD36 Defines Primitive Chronic Myeloid Leukemia Cells Less Responsive to Imatinib but Vulnerable to Antibody-Based Therapeutic Targeting'. *Haematologica* 103 (3): 3. https://doi.org/10.3324/haematol.2017.169946.

Landspersky, Theresa, Merle Stein, Mehmet Saçma, et al. 2024. 'Targeting CDC42 Reduces Skeletal Degeneration after Hematopoietic Stem Cell Transplantation'. *Blood Advances* 8 (20): 5400–5414. https://doi.org/10.1182/bloodadvances.2024012879.

Laperrousaz, Bastien, Sandrine Jeanpierre, Karen Sagorny, et al. 2013. 'Primitive CML Cell Expansion Relies on Abnormal Levels of BMPs Provided by the Niche and on BMPRIb Overexpression'. *Blood* 122 (23): 3767–77. https://doi.org/10.1182/blood-2013-05-501460.

Laurenti, Elisa, and Berthold Göttgens. 2018. 'From Haematopoietic Stem Cells to Complex Differentiation Landscapes'. *Nature* 553 (7689): 418–26. https://doi.org/10.1038/nature25022.

Le, Qiumin, Wenqing Yao, Yuejun Chen, et al. 2016. 'GRK6 Regulates ROS Response and Maintains Hematopoietic Stem Cell Self-Renewal'. *Cell Death & Disease* 7 (11): e2478–e2478. https://doi.org/10.1038/cddis.2016.377.

Lee, Bo Yun, Jung A. Han, Jun Sub Im, et al. 2006. 'Senescence-Associated ß-Galactosidase Is Lysosomal ß-Galactosidase'. *Aging Cell* 5 (2): 187–95. https://doi.org/10.1111/j.1474-9726.2006.00199.x.

Lee, Dabin, Dong Wook Kim, and Je-Yoel Cho. 2020. 'Role of Growth Factors in Hematopoietic Stem Cell Niche'. *Cell Biology and Toxicology* 36 (2): 131–44. https://doi.org/10.1007/s10565-019-09510-7.

Lee, Jaehyeon, Dal Sik Kim, Hye Soo Lee, Sam Im Choi, and Yong Gon Cho. 2017. 'Concurrence of E1a2 and E19a2 BCR-ABL1 Fusion Transcripts in a Typical Case of Chronic Myeloid Leukemia'. *Annals of Laboratory Medicine* 37 (1): 74–76. https://doi.org/10.3343/alm.2017.37.1.74.

Lee, Jin-Gu, Sun-Hye Lee, Dae-Weon Park, et al. 2008. 'Toll-like Receptor 9-Stimulated Monocyte Chemoattractant Protein-1 Is Mediated via JNK-Cytosolic Phospholipase A2-ROS Signaling'. *Cellular Signalling* 20 (1): 105–11. https://doi.org/10.1016/j.cellsig.2007.09.003.

Lee, Jong-Bin, Ji-Youn Hong, Hyeeun Shim, et al. 2025. 'Bone Morphogenetic Protein-2-Derived Osteogenic Peptide Promotes Bone Regeneration via Osteoblastogenesis'. *Regenerative Therapy* 30 (October): 911–19. https://doi.org/10.1016/j.reth.2025.09.006.

Lei, Hu, Hanzhang Xu, Yingying Wang, and Yingli Wu. 2025. 'CHK1-S, a Splicing Variant of CHK1, Suppresses Chronic Myeloid Leukemia'. *Leukemia*

Research 156 (September): 107922. https://doi.org/10.1016/j.leukres.2025.107922.

Lester, Daniel K., Chase Burton, Alycia Gardner, et al. 2023. 'Fucosylation of HLA-DRB1 Regulates CD4+ T Cell-Mediated Anti-Melanoma Immunity and Enhances Immunotherapy Efficacy'. *Nature Cancer* 4 (2): 222–39. https://doi.org/10.1038/s43018-022-00506-7.

Lévesque, J. P., F. M. Helwani, and I. G. Winkler. 2010. 'The Endosteal "Osteoblastic" Niche and Its Role in Hematopoietic Stem Cell Homing and Mobilization'. *Leukemia* 24 (12): 1979–92. https://doi.org/10.1038/leu.2010.214.

Li, Anzhou, Junbao Zhang, Liangping Zhan, et al. 2024. 'TOX2 Nuclear-Cytosol Translocation Is Linked to Leukemogenesis of Acute T-Cell Leukemia by Repressing TIM3 Transcription'. *Cell Death & Differentiation* 31 (11): 1506–18. https://doi.org/10.1038/s41418-024-01352-z.

Li, Haohan, Yuan Wang, Xinghe Tong, et al. 2025. 'The Dual Role of PCDH9 in Tumors, Neurological and Developmental Diseases'. *Medical Oncology* 42 (11): 489. https://doi.org/10.1007/s12032-025-03056-x.

Li, Haopeng, Xin'an Wang, Menghe Zhai, Chengdang Xu, and Xi Chen. 2024. 'Exploration of the Influence of GOLGA8B on Prostate Cancer Progression and the Resistance of Castration-Resistant Prostate Cancer to Cabazitaxel'. *Discover Oncology* 15 (May): 152. https://doi.org/10.1007/s12672-024-00973-7.

Li, Jiapeng, Logan Smith, and Hao-Jie Zhu. 2021. 'Data-Independent Acquisition (DIA): An Emerging Proteomics Technology for Analysis of Drug-Metabolizing Enzymes and Transporters'. *Drug Discovery Today. Technologies* 39 (December): 49–56. https://doi.org/10.1016/j.ddtec.2021.06.006.

Li, Ruo Qi, Lei Yan, Ling Zhang, Yanli Zhao, and Jing Lian. 2024. 'CD74 as a Prognostic and M1 Macrophage Infiltration Marker in a Comprehensive Pan-Cancer Analysis'. *Scientific Reports* 14 (1): 8125. https://doi.org/10.1038/s41598-024-58899-7.

Li, Shaoguang, Robert L. Ilaria, Ryan P. Million, George Q. Daley, and Richard A. Van Etten. 1999. 'The P190, P210, and P230 Forms of the BCR/ABL Oncogene Induce a Similar Chronic Myeloid Leukemia–like Syndrome in Mice but Have Different Lymphoid Leukemogenic Activity'. *The Journal of Experimental Medicine* 189 (9): 1399–412. https://doi.org/10.1084/jem.189.9.1399.

Li, Wei, Min Ji, Fei Lu, et al. 2018. 'Novel AF1q/MLLT11 Favorably Affects Imatinib Resistance and Cell Survival in Chronic Myeloid Leukemia'. *Cell Death & Disease* 9 (9): 855. https://doi.org/10.1038/s41419-018-0900-7.

Li, Zhanzhan, Yanyan Li, Na Li, Liangfang Shen, and Aibin Liu. 2022. 'Silencing GOLGA8B Inhibits Cell Invasion and Metastasis by Suppressing STAT3 Signaling Pathway in Lung Squamous Cell Carcinoma'. *Clinical Science* 136 (11): 895–909. https://doi.org/10.1042/CS20220128.

Li, Zhigang, Jiankun Fan, Yalan Xiao, et al. 2024. ‘Essential Role of Dhx16-Mediated Ribosome Assembly in Maintenance of Hematopoietic Stem Cells’. *Leukemia* 38 (12): 2699–708. https://doi.org/10.1038/s41375-024-02423-3.

Liberti, Maria V., and Jason W. Locasale. 2016. ‘The Warburg Effect: How Does It Benefit Cancer Cells?’ *Trends in Biochemical Sciences* 41 (3): 211–18. https://doi.org/10.1016/j.tibs.2015.12.001.

Liebl, Magdalena C., Jutta Moehlenbrink, Huong Becker, et al. 2021. ‘DAZAP2 Acts as Specifier of the P53 Response to DNA Damage’. *Nucleic Acids Research* 49 (5): 2759–76. https://doi.org/10.1093/nar/gkab084.

Liggett, L. Alexander, and Vijay G. Sankaran. 2020. ‘Unraveling Hematopoiesis through the Lens of Genomics’. *Cell* 182 (6): 1384–400. https://doi.org/10.1016/j.cell.2020.08.030.

Lima, Keli, Diego Antonio Pereira-Martins, Lívia Bassani Lins de Miranda, et al. 2022. ‘The PIP4K2 Inhibitor THZ-P1-2 Exhibits Antileukemia Activity by Disruption of Mitochondrial Homeostasis and Autophagy’. *Blood Cancer Journal* 12 (11): 151. https://doi.org/10.1038/s41408-022-00747-w.

Lin, Chien-Chin, Yueh-Chwen Hsu, Yi-Hung Li, et al. 2017. ‘Higher HOPX Expression Is Associated with Distinct Clinical and Biological Features and Predicts Poor Prognosis in de Novo Acute Myeloid Leukemia’. *Haematologica* 102 (6): 1044–53. https://doi.org/10.3324/haematol.2016.161257.

Liu, Chunyan, Yanfei Ma, Ruihuan Wang, and Guohong Su. 2022. ‘LINC00987 Knockdown Inhibits the Progression of Acute Myeloid Leukemia by Suppressing IGF2BP2-Mediated PA2G4 Expression’. *Anti-Cancer Drugs* 33 (1): e207. https://doi.org/10.1097/CAD.0000000000001188.

Liu, D. D., C. Y. Zhang, Y. Liu, J. Li, Y. X. Wang, and S. G. Zheng. 2022. ‘RUNX2 Regulates Osteoblast Differentiation via the BMP4 Signaling Pathway’. *Journal of Dental Research* 101 (10): 1227–37. https://doi.org/10.1177/00220345221093518.

Liu, Feng, Haibo Qiu, Ming Xue, et al. 2019. ‘MSC-Secreted TGF-β Regulates Lipopolysaccharide-Stimulated Macrophage M2-like Polarization via the Akt/FoxO1 Pathway’. *Stem Cell Research & Therapy* 10 (1): 345. https://doi.org/10.1186/s13287-019-1447-y.

Liu, Feng, Mingzheng Wu, Xixia Wu, Dan Chen, Ming Xie, and Hao Pan. 2023. ‘TGM2 Accelerates Migration and Differentiation of BMSCs by Activating Wnt/β-Catenin Signaling’. *Journal of Orthopaedic Surgery and Research* 18 (1): 168. https://doi.org/10.1186/s13018-023-03656-1.

Liu, Jiaxi, Jinfang Gao, Zixie Liang, et al. 2022. ‘Mesenchymal Stem Cells and Their Microenvironment’. *Stem Cell Research & Therapy* 13 (1): 429. https://doi.org/10.1186/s13287-022-02985-y.

Liu, Menghan, Lin Yang, Xiaojun Liu, et al. 2021. ‘HNRNPH1 Is a Novel Regulator Of Cellular Proliferation and Disease Progression in Chronic Myeloid

Leukemia'. *Frontiers in Oncology* 11 (July): 682859. https://doi.org/10.3389/fonc.2021.682859.

Liu, Shan-Shan, Xiang Fang, Xin Wen, et al. 2024. 'How Mesenchymal Stem Cells Transform into Adipocytes: Overview of the Current Understanding of Adipogenic Differentiation'. *World Journal of Stem Cells* 16 (3): 245–56. https://doi.org/10.4252/wjsc.v16.i3.245.

Liu, Xia, Xiaomei Li, Hui Li, et al. 2024. 'Annexin A1: A Key Regulator of T Cell Function and Bone Marrow Adiposity in Aplastic Anaemia'. *The Journal of Physiology* 602 (22): 6125–52. https://doi.org/10.1113/JP286148.

Liu, Xunhua, Jianxiong Chen, Xiaoli Long, et al. 2022. 'RSL1D1 Promotes the Progression of Colorectal Cancer through RAN-Mediated Autophagy Suppression'. *Cell Death & Disease* 13 (1): 43. https://doi.org/10.1038/s41419-021-04492-z.

Liu, Yonggang, Jiyun Liang, Xi Li, Junyong Huang, Jiangyuan Huang, and Jiale Wang. 2024. 'Interferon-Induced Transmembrane Protein 2 Is a Prognostic Marker in Colorectal Cancer and Promotes Its Progression by Activating the PI3K/AKT Pathway'. *Discover Oncology* 15 (1): 191. https://doi.org/10.1007/s12672-024-01040-x.

Liu, Yu'e, Linjun Weng, Yanjin Wang, et al. 2023. 'Deciphering the Role of CD47 in Cancer Immunotherapy'. *Journal of Advanced Research* 63 (October): 129–58. https://doi.org/10.1016/j.jare.2023.10.009.

Liu, Zhenyou, Yuye Shi, Zhiling Yan, et al. 2020. 'Impact of Anemia on the Outcomes of Chronic Phase Chronic Myeloid Leukemia in TKI Era'. *Hematology* 25 (1): 181–85. https://doi.org/10.1080/16078454.2020.1765563.

Lowery, Jonathan W., and Vicki Rosen. 2018. 'The BMP Pathway and Its Inhibitors in the Skeleton'. *Physiological Reviews* 98 (4): 2431–52. https://doi.org/10.1152/physrev.00028.2017.

Lu, Jielun, Shuyi Chen, Huo Tan, et al. 2021. 'Eukaryotic Initiation Factor-2, Gamma Subunit, Suppresses Proliferation and Regulates the Cell Cycle via the MAPK/ERK Signaling Pathway in Acute Myeloid Leukemia'. *Journal of Cancer Research and Clinical Oncology* 147 (11): 3157–68. https://doi.org/10.1007/s00432-021-03712-5.

Ludwig, Christina, Ludovic Gillet, George Rosenberger, Sabine Amon, Ben C. Collins, and Ruedi Aebersold. 2018. 'Data-independent Acquisition-based SWATH-MS for Quantitative Proteomics: A Tutorial'. *Molecular Systems Biology* 14 (8): e8126. https://doi.org/10.15252/msb.20178126.

Lundberg, Pontus, Axel Karow, Ronny Nienhold, et al. 2014. 'Clonal Evolution and Clinical Correlates of Somatic Mutations in Myeloproliferative Neoplasms'. *Blood* 123 (14): 2220–28. https://doi.org/10.1182/blood-2013-11-537167.

Luo, Wu, Li Song, Xi-Lei Chen, et al. 2016. 'Identification of Galectin-1 as a Novel Mediator for Chemoresistance in Chronic Myeloid Leukemia Cells'. *Oncotarget* 7 (18): 26709–23. https://doi.org/10.18632/oncotarget.8489.

Luong-Gardiol, Noemie, Imran Siddiqui, Irene Pizzitola, et al. 2019. 'γ-Catenin-Dependent Signals Maintain BCR-ABL1+ B Cell Acute Lymphoblastic Leukemia'. *Cancer Cell* 35 (4): 649-663.e10. https://doi.org/10.1016/j.ccell.2019.03.005.

Luz-Crawford, Patricia, Farida Djouad, Karine Toupet, et al. 2016. 'Mesenchymal Stem Cell-Derived Interleukin 1 Receptor Antagonist Promotes Macrophage Polarization and Inhibits B Cell Differentiation'. *Stem Cells* 34 (2): 483–92. https://doi.org/10.1002/stem.2254.

Ma, Jialu, Nathan Pettit, John Talburt, Shanzhi Wang, Sherman M. Weissman, and Mary Qu Yang. 2022. 'Integrating Single-Cell Transcriptome and Network Analysis to Characterize the Therapeutic Response of Chronic Myeloid Leukemia'. *International Journal of Molecular Sciences* 23 (22): 14335. https://doi.org/10.3390/ijms232214335.

Maas, Carolien C. H. M., David van Klaveren, Geneviève I. C. G. Ector, et al. 2022. 'The Evolution of the Loss of Life Expectancy in Patients with Chronic Myeloid Leukaemia: A Population-Based Study in the Netherlands, 1989–2018'. *British Journal of Haematology* 196 (5): 1219–24. https://doi.org/10.1111/bjh.17989.

Maeda, Kazuhiro, Yasuhiro Kobayashi, Nobuyuki Udagawa, et al. 2012. 'Wnt5a-Ror2 Signaling between Osteoblast-Lineage Cells and Osteoclast Precursors Enhances Osteoclastogenesis'. *Nature Medicine* 18 (3): 405–12. https://doi.org/10.1038/nm.2653.

Mahapatra, Kewal Kumar, Soumya Ranjan Mishra, Rohan Dhiman, and Sujit Kumar Bhutia. 2023. 'Stonin 2 Activates Lysosomal-mTOR Axis for Cell Survival in Oral Cancer'. *Toxicology in Vitro* 88 (April): 105561. https://doi.org/10.1016/j.tiv.2023.105561.

Mahon, Francois-Xavier, Markus Pfirrmann, Stéphanie Dulucq, et al. 2024. 'European Stop Tyrosine Kinase Inhibitor Trial (EURO-SKI) in Chronic Myeloid Leukemia: Final Analysis and Novel Prognostic Factors for Treatment-Free Remission'. *Journal of Clinical Oncology: Official Journal of the American Society of Clinical Oncology* 42 (16): 1875–80. https://doi.org/10.1200/JCO.23.01647.

Mahon, François-Xavier, Delphine Réa, Joëlle Guilhot, et al. 2010. 'Discontinuation of Imatinib in Patients with Chronic Myeloid Leukaemia Who Have Maintained Complete Molecular Remission for at Least 2 Years: The Prospective, Multicentre Stop Imatinib (STIM) Trial'. *The Lancet Oncology* 11 (11): 1029–35. https://doi.org/10.1016/S1470-2045(10)70233-3.

Manferdini, C., F. Paolella, E. Gabusi, et al. 2017. 'Adipose Stromal Cells Mediated Switching of the Pro-Inflammatory Profile of M1-like Macrophages Is Facilitated by PGE2: In Vitro Evaluation'. *Osteoarthritis*

and Cartilage 25 (7): 1161–71. https://doi.org/10.1016/j.joca.2017.01.011.

Manley, Paul, Josef Bruggen, Doriano Fabbro, Georg Martiny-Baron, and Thomas Meyer. 2007. 'Extended Kinase Profiling of the Bcr-Abl Inhibitor Nilotinib'. *Cancer Research* 67 (9_Supplement): 3249.

Mansour, Anna, Grazia Abou-Ezzi, Ewa Sitnicka, Sten Eirik W. Jacobsen, Abdelilah Wakkach, and Claudine Blin-Wakkach. 2012. 'Osteoclasts Promote the Formation of Hematopoietic Stem Cell Niches in the Bone Marrow'. *The Journal of Experimental Medicine* 209 (3): 537–49. https://doi.org/10.1084/jem.20110994.

Marlein, Christopher R., Lyubov Zaitseva, Rachel E. Piddock, et al. 2017. 'NADPH Oxidase-2 Derived Superoxide Drives Mitochondrial Transfer from Bone Marrow Stromal Cells to Leukemic Blasts'. *Blood* 130 (14): 1649–60. https://doi.org/10.1182/blood-2017-03-772939.

Martínez-Castillo, Macario, Laura Gómez-Romero, Hugo Tovar, et al. 2023. 'Genetic Alterations in the BCR-ABL1 Fusion Gene Related to Imatinib Resistance in Chronic Myeloid Leukemia'. *Leukemia Research* 131 (August): 107325. https://doi.org/10.1016/j.leukres.2023.107325.

Mauro, Michael J., Brian J. Druker, and Richard T. Maziarz. 2004. 'Divergent Clinical Outcome in Two CML Patients Who Discontinued Imatinib Therapy after Achieving a Molecular Remission'. *Leukemia Research*, The New Era of Imatinib Mesylate, vol. 28 (May): 71–73. https://doi.org/10.1016/j.leukres.2003.10.017.

McHugh, Domhnall, and Jesús Gil. 2018. 'Senescence and Aging: Causes, Consequences, and Therapeutic Avenues'. *The Journal of Cell Biology* 217 (1): 65–77. https://doi.org/10.1083/jcb.201708092.

Meng, Fanbiao, Yunfeng Rui, Liangliang Xu, Chao Wan, Xiaohua Jiang, and Gang Li. 2014. 'Aqp1 Enhances Migration of Bone Marrow Mesenchymal Stem Cells Through Regulation of FAK and ß-Catenin'. *Stem Cells and Development* 23 (1): 66–75. https://doi.org/10.1089/scd.2013.0185.

Miao, Zhechen, Qiang WANG, and Qifa Liu. 2025. 'The BCR/ABL Tyrosine Kinase Induces Production of Reactive Oxygen Species in Hematopoietic Cell'. *Blood* 146 (Supplement 1): 6758. https://doi.org/10.1182/blood-2025-6758.

Minciacchi, Valentina R., Jimena Bravo, Christina Karantanou, et al. 2024. 'Exploitation of the Fibrinolytic System by B-Cell Acute Lymphoblastic Leukemia and Its Therapeutic Targeting'. *Nature Communications* 15 (1): 10059. https://doi.org/10.1038/s41467-024-54361-4.

Miyamoto, Kana, Shigeyuki Yoshida, Miyuri Kawasumi, et al. 2011. 'Osteoclasts Are Dispensable for Hematopoietic Stem Cell Maintenance and Mobilization'. *Journal of Experimental Medicine* 208 (11): 2175–81. https://doi.org/10.1084/jem.20101890.

Morrison, Sean J., and David T. Scadden. 2014. 'The Bone Marrow Niche for Haematopoietic Stem Cells'. *Nature* 505 (7483): 327–34. https://doi.org/10.1038/nature12984.

Moschoi, Ruxanda, Véronique Imbert, Marielle Nebout, et al. 2016. 'Protective Mitochondrial Transfer from Bone Marrow Stromal Cells to Acute Myeloid Leukemic Cells during Chemotherapy'. *Blood* 128 (2): 253–64. https://doi.org/10.1182/blood-2015-07-655860.

Mossie, K., B. Jallal, F. Alves, I. Sures, G. D. Plowman, and A. Ullrich. 1995. 'Colon Carcinoma Kinase-4 Defines a New Subclass of the Receptor Tyrosine Kinase Family'. *Oncogene* 11 (10): 2179–84.

Mou, Rong, Junkai Ma, Xuan Ju, et al. 2024. 'Vasopressin Drives Aberrant Myeloid Differentiation of Hematopoietic Stem Cells, Contributing to Depression in Mice'. *Cell Stem Cell* 31 (12): 1794-1812.e10. https://doi.org/10.1016/j.stem.2024.09.018.

Moura, Arlindo A., Maria Julia B. Bezerra, Aline M. A. Martins, et al. 2022. 'Global Proteomics Analysis of Bone Marrow: Establishing Talin-1 and Centrosomal Protein of 55 kDa as Potential Molecular Signatures for Myelodysplastic Syndromes'. *Frontiers in Oncology* 12 (June): 833068. https://doi.org/10.3389/fonc.2022.833068.

Mu, Hui, Xiaojian Zhu, Hui Jia, Lu Zhou, and Hong Liu. 2021. 'Combination Therapies in Chronic Myeloid Leukemia for Potential Treatment-Free Remission: Focus on Leukemia Stem Cells and Immune Modulation'. *Frontiers in Oncology* 11 (May): 643382. https://doi.org/10.3389/fonc.2021.643382.

Mukaida, Naofumi, Yamato Tanabe, and Tomohisa Baba. 2017. 'Chemokines as a Conductor of Bone Marrow Microenvironment in Chronic Myeloid Leukemia'. *International Journal of Molecular Sciences* 18 (8): 8. https://doi.org/10.3390/ijms18081824.

Najar, Mehdi, Gordana Raicevic, Hicham Id Boufker, et al. 2010. 'Mesenchymal Stromal Cells Use PGE2 to Modulate Activation and Proliferation of Lymphocyte Subsets: Combined Comparison of Adipose Tissue, Wharton's Jelly and Bone Marrow Sources'. *Cellular Immunology* 264 (2): 171–79. https://doi.org/10.1016/j.cellimm.2010.06.006.

Naka, Kazuhito, Takayuki Hoshii, Teruyuki Muraguchi, et al. 2010. 'TGF-β–FOXO Signalling Maintains Leukaemia-Initiating Cells in Chronic Myeloid Leukaemia'. *Nature* 463 (7281): 676–80. https://doi.org/10.1038/nature08734.

Nakajima, Hikaru, Robert Zhao, Troy C. Lund, et al. 2002. 'The BCR/ABL Transgene Causes Abnormal NK Cell Differentiation and Can Be Found in Circulating NK Cells of Advanced Phase Chronic Myelogenous Leukemia Patients1'. *The Journal of Immunology* 168 (2): 643–50. https://doi.org/10.4049/jimmunol.168.2.643.

Nakamura-Ishizu, Ayako, Keiyo Takubo, Masato Fujioka, and Toshio Suda. 2014. 'Megakaryocytes Are Essential for HSC Quiescence through the Production

of Thrombopoietin'. *Biochemical and Biophysical Research Communications* 454 (2): 353–57. https://doi.org/10.1016/j.bbrc.2014.10.095.

Naughton, R., C. Quiney, S. D. Turner, and T. G. Cotter. 2009. 'Bcr-Abl-Mediated Redox Regulation of the PI3K/AKT Pathway'. *Leukemia* 23 (8): 1432–40. https://doi.org/10.1038/leu.2009.49.

Naveiras, Olaia, Valentina Nardi, Pamela L. Wenzel, Frederic Fahey, and George Q. Daley. 2009. 'Bone Marrow Adipocytes as Negative Regulators of the Hematopoietic Microenvironment'. *Nature* 460 (7252): 259–63. https://doi.org/10.1038/nature08099.

Nemeth, Michael J., Lilia Topol, Stacie M. Anderson, Yingzi Yang, and David M. Bodine. 2007. 'Wnt5a Inhibits Canonical Wnt Signaling in Hematopoietic Stem Cells and Enhances Repopulation'. *Proceedings of the National Academy of Sciences* 104 (39): 15436–41. https://doi.org/10.1073/pnas.0704747104.

Nilsson, Susan K., Hayley M. Johnston, Genevieve A. Whitty, et al. 2005. 'Osteopontin, a Key Component of the Hematopoietic Stem Cell Niche and Regulator of Primitive Hematopoietic Progenitor Cells'. *Blood* 106 (4): 1232–39. https://doi.org/10.1182/blood-2004-11-4422.

Nishida, Hiroko, Hiroshi Suzuki, Hiroko Madokoro, et al. 2014. 'Blockade of CD26 Signaling Inhibits Human Osteoclast Development'. *Journal of Bone and Mineral Research* 29 (11): 2439–55. https://doi.org/10.1002/jbmr.2277.

Noel, Brett M., Steven B. Ouellette, Laura Marholz, et al. 2019. 'Multi-Omic Profiling of Tyrosine Kinase Inhibitor-Resistant K562 Cells Suggests Metabolic Reprogramming to Promote Cell Survival'. *Journal of Proteome Research* 18 (4): 1842–56. https://doi.org/10.1021/acs.jproteome.9b00028.

Nowell, Peter C., and David A. Hungerford. 1960. 'Chromosome Studies on Normal and Leukemic Human Leukocytes'. *JNCI: Journal of the National Cancer Institute* 25 (1): 85–109. https://doi.org/10.1093/jnci/25.1.85.

Ntoufa, Stavroula, Marina Gerousi, Stamatia Laidou, et al. 2021. 'RPS15 Mutations Rewire RNA Translation in Chronic Lymphocytic Leukemia'. *Blood Advances* 5 (13): 2788–92. https://doi.org/10.1182/bloodadvances.2020001717.

Nwajei, Felix, and Marina Konopleva. 2013. 'The Bone Marrow Microenvironment as Niche Retreats for Hematopoietic and Leukemic Stem Cells'. *Advances in Hematology* 2013 (January): e953982. https://doi.org/10.1155/2013/953982.

OCK, Sun-A., Yeon-Mi LEE, Ji-Sung PARK, et al. 2016. 'Evaluation of Phenotypic, Functional and Molecular Characteristics of Porcine Mesenchymal Stromal/Stem Cells Depending on Donor Age, Gender and Tissue Source'. *The Journal of Veterinary Medical Science* 78 (6): 987–95. https://doi.org/10.1292/jvms.15-0596.

Ortiz, Luis A., Frederica Gambelli, Christine McBride, et al. 2003. ‘Mesenchymal Stem Cell Engraftment in Lung Is Enhanced in Response to Bleomycin Exposure and Ameliorates Its Fibrotic Effects’. *Proceedings of the National Academy of Sciences of the United States of America* 100 (14): 8407–11. https://doi.org/10.1073/pnas.1432929100.

Pagani, Ilaria S., Naranie Shanmuganathan, Phuong Dang, et al. 2023. ‘Lineage-Specific Detection of Residual Disease Predicts Relapse in Patients with Chronic Myeloid Leukemia Stopping Therapy’. *Blood* 142 (25): 2192–97. https://doi.org/10.1182/blood.2023021119.

Papa, S., I. Vismara, A. Mariani, et al. 2018. ‘Mesenchymal Stem Cells Encapsulated into Biomimetic Hydrogel Scaffold Gradually Release CCL2 Chemokine *in Situ* Preserving Cytoarchitecture and Promoting Functional Recovery in Spinal Cord Injury’. *Journal of Controlled Release* 278 (May): 49–56. https://doi.org/10.1016/j.jconrel.2018.03.034.

Patel, Ami B., Thomas O’Hare, and Michael W. Deininger. 2017. ‘Mechanisms of Resistance to ABL Kinase Inhibition in CML and the Development of next Generation ABL Kinase Inhibitors’. *Hematology/Oncology Clinics of North America* 31 (4): 589–612. https://doi.org/10.1016/j.hoc.2017.04.007.

Pathak, Gopal P., Rashmi Shah, Barry E. Kennedy, et al. 2018. ‘RTN4 Knockdown Dysregulates the AKT Pathway, Destabilizes the Cytoskeleton, and Enhances Paclitaxel-Induced Cytotoxicity in Cancers’. *Molecular Therapy* 26 (8): 2019–33. https://doi.org/10.1016/j.ymthe.2018.05.026.

Patterson, Shaun D., Isla Nosratzadeh, Robin Young, et al. 2024. ‘Common Lymphoid Progenitors and B Cell Subpopulations in the Bone Marrow Are Predictive of Treatment-Free Remission in Chronic Myeloid Leukemia’. *Blood*, 66th ASH Annual Meeting Abstracts, vol. 144 (November): 994. https://doi.org/10.1182/blood-2024-204864.

Pavlovsky, Carolina, Ana Ines Varela, Isolda I. Fernandez, et al. 2020. ‘High Level of Successful TKI Discontinuation in Chronic Myeloid Leukemia (CML) Patients: Preliminary Results of AST-Argentina Stop Trial’. *Blood* 136 (Supplement 1): 3–5. https://doi.org/10.1182/blood-2020-142416.

Pavlovsky, Carolina, Bianca Vasconcelos Cordoba, Maria Sanchez, et al. 2025. ‘Integrating Cytokine Profiles with Clinical and Molecular Biomarkers to Predict Molecular Relapse after TKI Discontinuation in CML Patients’. *Blood*, 67th ASH Annual Meeting Abstracts, vol. 146 (November): 3785. https://doi.org/10.1182/blood-2025-3785.

Peled, Amnon, Shiri Klein, Katia Beider, Jan A. Burger, and Michal Abraham. 2018. ‘Role of CXCL12 and CXCR4 in the Pathogenesis of Hematological Malignancies’. *Cytokine*, Special issue: Chemokines - beyond chemotaxis, vol. 109 (September): 11–16. https://doi.org/10.1016/j.cyto.2018.02.020.

Peled, Amnon, Isabelle Petit, Orit Kollet, et al. 1999. ‘Dependence of Human Stem Cell Engraftment and Repopulation of NOD/SCID Mice on CXCR4’. *Science* 283 (5403): 845–48. https://doi.org/10.1126/science.283.5403.845.

Petit, Isabelle, Martine Szyper-Kravitz, Arnon Nagler, et al. 2002. ‘G-CSF Induces Stem Cell Mobilization by Decreasing Bone Marrow SDF-1 and up-Regulating CXCR4’. *Nature Immunology* 3 (7): 687–94. https://doi.org/10.1038/ni813.

Pierro, Federico, Stefania Stella, Manlio Fazio, et al. 2025. ‘Chronic Myeloid Leukemia and the T315I BCR::ABL1 Mutation’. *International Journal of Molecular Sciences* 26 (23): 11285. https://doi.org/10.3390/ijms262311285.

Pietras, Eric M., Damien Reynaud, Yoon-A. Kang, et al. 2015. ‘Functionally Distinct Subsets of Lineage-Biased Multipotent Progenitors Control Blood Production in Normal and Regenerative Conditions’. *Cell Stem Cell* 17 (1): 35–46. https://doi.org/10.1016/j.stem.2015.05.003.

Pitts, Herbert Augustus, Chi-Keung Cheng, Joyce Sin Cheung, et al. 2023. ‘SPINK2 Protein Expression Is an Independent Adverse Prognostic Marker in AML and Is Potentially Implicated in the Regulation of Ferroptosis and Immune Response’. *International Journal of Molecular Sciences* 24 (11). https://doi.org/10.3390/ijms24119696.

Pizzatti, Luciana, Lílian Ayres Sá, Jamison Menezes de Souza, Paulo Mascarello Bisch, and Eliana Abdelhay. 2006. ‘Altered Protein Profile in Chronic Myeloid Leukemia Chronic Phase Identified by a Comparative Proteomic Study’. *Biochimica et Biophysica Acta (BBA) - Proteins and Proteomics* 1764 (5): 929–42. https://doi.org/10.1016/j.bbapap.2006.02.004.

Plumas, J., L. Chaperot, M. J. Richard, J. P. Molens, J. C. Bensa, and M. C. Favrot. 2005. ‘Mesenchymal Stem Cells Induce Apoptosis of Activated T Cells’. *Leukemia* 19 (9): 1597–604. https://doi.org/10.1038/sj.leu.2403871.

Poulos, Michael G., Peipei Guo, Natalie M. Kofler, et al. 2013. ‘Endothelial Jagged-1 Is Necessary for Homeostatic and Regenerative Hematopoiesis’. *Cell Reports* 4 (5): 1022–34. https://doi.org/10.1016/j.celrep.2013.07.048.

Prieto-Bermejo, Rodrigo, Marta Romo-González, Alejandro Pérez-Fernández, Carla Ijurko, and Ángel Hernández-Hernández. 2018. ‘Reactive Oxygen Species in Haematopoiesis: Leukaemic Cells Take a Walk on the Wild Side’. *Journal of Experimental & Clinical Cancer Research* 37 (1): 125. https://doi.org/10.1186/s13046-018-0797-0.

Qian, Hong, Natalija Buza-Vidas, Craig D. Hyland, et al. 2007. ‘Critical Role of Thrombopoietin in Maintaining Adult Quiescent Hematopoietic Stem Cells’. *Cell Stem Cell* 1 (6): 671–84. https://doi.org/10.1016/j.stem.2007.10.008.

Qin, Pengfei, Yakun Pang, Wenhong Hou, et al. 2021. ‘Integrated Decoding Hematopoiesis and Leukemogenesis Using Single-Cell Sequencing and Its Medical Implication’. *Cell Discovery* 7 (1): 2. https://doi.org/10.1038/s41421-020-00223-4.

Radich, Jerald P., Andreas Hochhaus, Tamás Masszi, et al. 2021. 'Treatment-Free Remission Following Frontline Nilotinib in Patients with Chronic Phase Chronic Myeloid Leukemia: 5-Year Update of the ENESTfreedom Trial'. *Leukemia* 35 (5): 1344–55. https://doi.org/10.1038/s41375-021-01205-5.

Radtke, Daniel, and David Voehringer. 2023. 'Granulocyte Development, Tissue Recruitment, and Function during Allergic Inflammation'. *European Journal of Immunology* 53 (8): 2249977. https://doi.org/10.1002/eji.202249977.

Ratajczak, Mariusz Z., Mateusz Adamiak, Monika Plonka, Ahmed Abdel-Latif, and Janina Ratajczak. 2018. 'Mobilization of Hematopoietic Stem Cells as a Result of Innate Immunity-Mediated Sterile Inflammation in the Bone Marrow Microenvironment—the Involvement of Extracellular Nucleotides and Purinergic Signaling'. *Leukemia* 32 (5): 1116–23. https://doi.org/10.1038/s41375-018-0087-z.

Rea, Delphine, Nicolas Dulphy, Guylaine Henry, et al. 2013. 'Low Natural Killer (NK) Cell Counts and Functionality Are Associated With Molecular Relapse After Imatinib Discontinuation In Patients (Pts) With Chronic Phase (CP)-Chronic Myeloid Leukemia (CML) With Undetectable BCR-ABL Transcripts For At Least 2 Years: Preliminary Results From Immunostim, On Behalf Of STIM Investigators'. *Blood* 122 (21): 856. https://doi.org/10.1182/blood.V122.21.856.856.

Rea, Delphine, Franck E. Nicolini, Michel Tulliez, et al. 2017. 'Discontinuation of Dasatinib or Nilotinib in Chronic Myeloid Leukemia: Interim Analysis of the STOP 2G-TKI Study'. *Blood* 129 (7): 846–54. https://doi.org/10.1182/blood-2016-09-742205.

Recchia, Anna Grazia, Nadia Caruso, Sabrina Bossio, et al. 2015. 'Flow Cytometric Immunobead Assay for Detection of BCR-ABL1 Fusion Proteins in Chronic Myeloid Leukemia: Comparison with FISH and PCR Techniques'. *PLoS ONE* 10 (6): e0130360. https://doi.org/10.1371/journal.pone.0130360.

Reya, Tannishtha, Andrew W. Duncan, Laurie Ailles, et al. 2003. 'A Role for Wnt Signalling in Self-Renewal of Haematopoietic Stem Cells'. *Nature* 423 (6938): 409–14. https://doi.org/10.1038/nature01593.

Reynaud, Damien, Eric Pietras, Keegan Barry-Holson, et al. 2011. 'IL-6 Controls Leukemic Multipotent Progenitor Cell Fate and Contributes to Chronic Myelogenous Leukemia Development'. *Cancer Cell* 20 (5): 661–73. https://doi.org/10.1016/j.ccr.2011.10.012.

Riether, Carsten, Ramin Radpour, Nils M. Kallen, et al. 2021. 'Metoclopramide Treatment Blocks CD93-Signaling-Mediated Self-Renewal of Chronic Myeloid Leukemia Stem Cells'. *Cell Reports* 34 (4). https://doi.org/10.1016/j.celrep.2020.108663.

Ringdén, Olle, Mehmet Uzunel, Ida Rasmusson, et al. 2006. 'Mesenchymal Stem Cells for Treatment of Therapy-Resistant Graft-versus-Host Disease'.

Transplantation 81 (10): 1390. https://doi.org/10.1097/01.tp.0000214462.63943.14.

Ross, David M., Susan Branford, John F. Seymour, et al. 2013. 'Safety and Efficacy of Imatinib Cessation for CML Patients with Stable Undetectable Minimal Residual Disease: Results from the TWISTER Study'. *Blood* 122 (4): 515–22. https://doi.org/10.1182/blood-2013-02-483750.

Rossari, Federico, Filippo Minutolo, and Enrico Orciuolo. 2018. 'Past, Present, and Future of Bcr-Abl Inhibitors: From Chemical Development to Clinical Efficacy'. *Journal of Hematology & Oncology* 11 (1): 84. https://doi.org/10.1186/s13045-018-0624-2.

Rousselot, Philippe, Francoise Huguet, Delphine Rea, et al. 2006. 'Imatinib Mesylate Discontinuation in Patients with Chronic Myelogenous Leukemia in Complete Molecular Remission for More than 2 Years'. *Blood* 109 (1): 58–60. https://doi.org/10.1182/blood-2006-03-011239.

Rowley, Janet D. 1973. 'A New Consistent Chromosomal Abnormality in Chronic Myelogenous Leukaemia Identified by Quinacrine Fluorescence and Giemsa Staining'. *Nature* 243 (5405): 290–93. https://doi.org/10.1038/243290a0.

Ruggero, Davide, and Akiko Shimamura. 2014. 'Marrow Failure: A Window into Ribosome Biology'. *Blood* 124 (18): 2784–92. https://doi.org/10.1182/blood-2014-04-526301.

Saal, Talia M., Christine Pellegrino, Tauseef Ahmed, Karen Seiter, Delong Liu, and Amir Steinberg. 2023. 'Calr+ Myelofibrosis/BCR-ABL Chronic Myeloid Leukemia Overlap Syndrome Treated with Asciminib'. *Blood* 142 (Supplement 1): 6423. https://doi.org/10.1182/blood-2023-184820.

Sadovnik, Irina, Harald Herrmann, Gregor Eisenwort, et al. 2017. 'Expression of CD25 on Leukemic Stem Cells in BCR-ABL1+ CML: Potential Diagnostic Value and Functional Implications'. *Experimental Hematology* 51 (July): 17–24. https://doi.org/10.1016/j.exphem.2017.04.003.

Sadovnik, Irina, Andrea Hoelbl-Kovacic, Harald Herrmann, et al. 2016. 'Identification of CD25 as STAT5-Dependent Growth Regulator of Leukemic Stem Cells in Ph+ CML'. *Clinical Cancer Research* 22 (8): 2051–61. https://doi.org/10.1158/1078-0432.CCR-15-0767.

Sætersmoen, Michelle, Ivan S. Kotchetkov, Lamberto Torralba-Raga, et al. 2025. 'Targeting HLA-E-Overexpressing Cancers with a NKG2A/C Switch Receptor'. *Med* 6 (2): 100521. https://doi.org/10.1016/j.medj.2024.09.010.

Saifullah, Hilbeen Hisham, and Claire Marie Lucas. 2021. 'Treatment-Free Remission in Chronic Myeloid Leukemia: Can We Identify Prognostic Factors?' *Cancers* 13 (16): 16. https://doi.org/10.3390/cancers13164175.

Sands, William A., Mhairi Copland, and Helen Wheadon. 2013. 'Targeting Self-Renewal Pathways in Myeloid Malignancies'. *Cell Communication and Signaling* 11 (1): 33. https://doi.org/10.1186/1478-811X-11-33.

Sattler, Martin, Shalini Verma, Gautam Shrikhande, et al. 2000. 'The BCR/ABL Tyrosine Kinase Induces Production of Reactive Oxygen Species in Hematopoietic Cells *'. *Journal of Biological Chemistry* 275 (32): 24273–78. https://doi.org/10.1074/jbc.M002094200.

Saussele, Susanne, Johan Richter, Joelle Guilhot, et al. 2018. 'Discontinuation of Tyrosine Kinase Inhibitor Therapy in Chronic Myeloid Leukaemia (EURO-SKI): A Prespecified Interim Analysis of a Prospective, Multicentre, Non-Randomised, Trial'. *The Lancet Oncology* 19 (6): 747–57. https://doi.org/10.1016/S1470-2045(18)30192-X.

Sayın, Selim, Murat Yıldırım, Batuhan Erdoğdu, et al. 2025. 'Metabolomic Profiling and Bioanalysis of Chronic Myeloid Leukemia: Identifying Biomarkers for Treatment Response and Disease Monitoring'. *Metabolites* 15 (6): 376. https://doi.org/10.3390/metabo15060376.

Schepers, Koen, Eric M. Pietras, Damien Reynaud, et al. 2013. 'Myeloproliferative Neoplasia Remodels the Endosteal Bone Marrow Niche into a Self-Reinforcing Leukemic Niche'. *Cell Stem Cell* 13 (3): 285–99. https://doi.org/10.1016/j.stem.2013.06.009.

Schroeder, Jan-Hendrik, Gordon Beattie, Jonathan W. Lo, et al. 2023. 'CD90 Is Not Constitutively Expressed in Functional Innate Lymphoid Cells'. *Frontiers in Immunology* 14 (April). https://doi.org/10.3389/fimmu.2023.1113735.

Schultheis, Beate, Melina Carapeti-Marootian, Andreas Hochhaus, Andreas Weißer, John M. Goldman, and Junia V. Melo. 2002. 'Overexpression of SOCS-2 in Advanced Stages of Chronic Myeloid Leukemia: Possible Inadequacy of a Negative Feedback Mechanism'. *Blood* 99 (5): 1766–75. https://doi.org/10.1182/blood.V99.5.1766.

Schütz, C., S. Inselmann, S. Sausslele, et al. 2017. 'Expression of the CTLA-4 Ligand CD86 on Plasmacytoid Dendritic Cells (pDC) Predicts Risk of Disease Recurrence after Treatment Discontinuation in CML'. *Leukemia* 31 (4): 4. https://doi.org/10.1038/leu.2017.9.

Schwarz, Annemarie, Ingo Roeder, and Michael Seifert. 2022. 'Comparative Gene Expression Analysis Reveals Similarities and Differences of Chronic Myeloid Leukemia Phases'. *Cancers* 14 (1): 256. https://doi.org/10.3390/cancers14010256.

Sengupta, A., D. Banerjee, S. Chandra, et al. 2007. 'Deregulation and Cross Talk among Sonic Hedgehog, Wnt, Hox and Notch Signaling in Chronic Myeloid Leukemia Progression'. *Leukemia* 21 (5): 5. https://doi.org/10.1038/sj.leu.2404657.

Shaban, Dania, Nay Najm, Lucie Droin, and Anastasia Nijnik. 2025. 'Hematopoietic Stem Cell Fates and the Cellular Hierarchy of Mammalian Hematopoiesis: From Transplantation Models to New Insights from in Situ Analyses'. *Stem Cell Reviews and Reports* 21 (1): 28–44. https://doi.org/10.1007/s12015-024-10782-8.

Shah, Neil P., Ravi Bhatia, Jessica K. Altman, et al. 2024. ‘Chronic Myeloid Leukemia, Version 2.2024, NCCN Clinical Practice Guidelines in Oncology’. Journal of the National Comprehensive Cancer Network. *Journal of the National Comprehensive Cancer Network* 22 (1): 43–69. https://doi.org/10.6004/jnccn.2024.0007.

Shah, Neil P., Valentín García-Gutiérrez, Antonio Jiménez-Velasco, et al. 2020. ‘Dasatinib Discontinuation in Patients with Chronic-Phase Chronic Myeloid Leukemia and Stable Deep Molecular Response: The DASFREE Study’. *Leukemia & Lymphoma* 61 (3): 650–59. https://doi.org/10.1080/10428194.2019.1675879.

Shah, Neil P., Valentín García-Gutiérrez, Antonio Jiménez-Velasco, et al. 2023. ‘Treatment-Free Remission after Dasatinib in Patients with Chronic Myeloid Leukaemia in Chronic Phase with Deep Molecular Response: Final 5-Year Analysis of DASFREE’. *British Journal of Haematology* 202 (5): 942–52. https://doi.org/10.1111/bjh.18883.

Shah, Neil P., Chris Tran, Francis Y. Lee, Ping Chen, Derek Norris, and Charles L. Sawyers. 2004. ‘Overriding Imatinib Resistance with a Novel ABL Kinase Inhibitor’. *Science* 305 (5682): 399–401. https://doi.org/10.1126/science.1099480.

Shahrin, Nur Hezrin, Daniel Thomson, Carol Wadham, Andreas Schreiber, and Susan Branford. 2019. ‘IMATINIB INDUCES MARKED UPREGULATION OF RECOMBINATION ACTIVATING GENE (RAG) EXPRESSION IN BCR-ABL1 POSITIVE LYMPHOID CELLS’. *Experimental Hematology* 76 (August): S85. https://doi.org/10.1016/j.exphem.2019.06.433.

Shammas, Tara, Malalage N. Peiris, April N. Meyer, and Daniel J. Donoghue. 2025. ‘BCR-ABL: The Molecular Mastermind behind Chronic Myeloid Leukemia’. *Cytokine & Growth Factor Reviews* 83 (June): 45–58. https://doi.org/10.1016/j.cytogfr.2025.05.001.

Shi, Wenning, Cong Xu, Ping Lei, et al. 2024. ‘A Correlation Study of Adhesion G Protein-Coupled Receptors as Potential Therapeutic Targets for Breast Cancer’. *Breast Cancer Research and Treatment* 207 (2): 417–34. https://doi.org/10.1007/s10549-024-07373-z.

Shimomura, Yutaka, Dritan Agalliu, Alin Vonica, et al. 2010. ‘APCDD1 Is a Novel Wnt Inhibitor Mutated in Hereditary Hypotrichosis Simplex’. *Nature* 464 (7291): 1043–47. https://doi.org/10.1038/nature08875.

Shioda, Tatsuo, Hiroyuki Kato, Yukano Ohnishi, et al. 1998. ‘Anti-HIV-1 and Chemotactic Activities of Human Stromal Cell-Derived Factor 1α (SDF-1α) and SDF-1ß Are Abolished by CD26/Dipeptidyl Peptidase IV-Mediated Cleavage’. *Proceedings of the National Academy of Sciences* 95 (11): 6331–36. https://doi.org/10.1073/pnas.95.11.6331.

Siegel, Georg, Torsten Kluba, Ursula Hermanutz-Klein, Karen Bieback, Hinnak Northoff, and Richard Schäfer. 2013. ‘Phenotype, Donor Age and Gender Affect Function of Human Bone Marrow-Derived Mesenchymal Stromal Cells’. *BMC Medicine* 11 (1): 146. https://doi.org/10.1186/1741-7015-11-146.

Silver, I. A., R. J. Murrills, and D. J. Etherington. 1988. 'Microelectrode Studies on the Acid Microenvironment beneath Adherent Macrophages and Osteoclasts'. *Experimental Cell Research* 175 (2): 266–76. https://doi.org/10.1016/0014-4827(88)90191-7.

Sim, Edmund Ui Hang, Chow Hiang Ang, Ching Ching Ng, Choon Weng Lee, and Kumaran Narayanan. 2010. 'Differential Expression of a Subset of Ribosomal Protein Genes in Cell Lines Derived from Human Nasopharyngeal Epithelium'. *Journal of Human Genetics* 55 (2): 118–20. https://doi.org/10.1038/jhg.2009.124.

Singh, Sanjiv, D. Anshita, and V. Ravichandiran. 2021. 'MCP-1: Function, Regulation, and Involvement in Disease'. *International Immunopharmacology* 101 (December): 107598. https://doi.org/10.1016/j.intimp.2021.107598.

Singh, Vivek, Ranjana Singh, and Rashmi Kushwaha. 2024. 'Exploring Novel Protein Biomarkers for Early-Stage Diagnosis and Prognosis of T-Acute Lymphoblastic Leukemia (T-ALL)'. *Hematology, Transfusion and Cell Therapy* 46 (December): S93–111. https://doi.org/10.1016/j.htct.2024.02.016.

Sinha, Ankit, and Matthias Mann. 2020. 'A Beginner's Guide to Mass Spectrometry–Based Proteomics'. *The Biochemist* 42 (5): 64–69. https://doi.org/10.1042/BIO20200057.

Song, Na, Martijn Scholtemeijer, and Khalid Shah. 2020. 'Mesenchymal Stem Cell Immunomodulation: Mechanisms and Therapeutic Potential'. *Trends in Pharmacological Sciences* 41 (9): 653–64. https://doi.org/10.1016/j.tips.2020.06.009.

Sopper, Sieghart, Satu Mustjoki, Deborah White, et al. 2017. 'Reduced CD62L Expression on T Cells and Increased Soluble CD62L Levels Predict Molecular Response to Tyrosine Kinase Inhibitor Therapy in Early Chronic-Phase Chronic Myelogenous Leukemia'. *Journal of Clinical Oncology* 35 (2): 175–84. https://doi.org/10.1200/JCO.2016.67.0893.

Staversky, Rhonda J., Daniel K. Byun, Mary A. Georger, et al. 2018. 'The Chemokine CCL3 Regulates Myeloid Differentiation and Hematopoietic Stem Cell Numbers'. *Scientific Reports* 8 (1): 1. https://doi.org/10.1038/s41598-018-32978-y.

Steinbach, Alison, Stephen M. Clark, and Amber B. Clemmons. 2013. 'Bosutinib: A Novel Src/Abl Kinase Inhibitor for Chronic Myelogenous Leukemia'. *Journal of the Advanced Practitioner in Oncology* 4 (6): 451–55. https://doi.org/10.6004/jadpro.2013.4.6.8.

Stolzing, A., E. Jones, D. McGonagle, and A. Scutt. 2008. 'Age-Related Changes in Human Bone Marrow-Derived Mesenchymal Stem Cells: Consequences for Cell Therapies'. *Mechanisms of Ageing and Development* 129 (3): 163–73. https://doi.org/10.1016/j.mad.2007.12.002.

Strife, A., C. Lambek, D. Wisniewski, M. Wachter, S. C. Gulati, and B. D. Clarkson. 1988. 'Discordant Maturation as the Primary Biological Defect in Chronic Myelogenous Leukemia'. *Cancer Research* 48 (4): 1035–41.

Sugiyama, Tatsuki, Hiroshi Kohara, Mamiko Noda, and Takashi Nagasawa. 2006. 'Maintenance of the Hematopoietic Stem Cell Pool by CXCL12-CXCR4 Chemokine Signaling in Bone Marrow Stromal Cell Niches'. *Immunity* 25 (6): 977–88. https://doi.org/10.1016/j.immuni.2006.10.016.

Suresh, Sevanthy, Vigneshwaran Venkatesan, Saravanabhavan Thangavel, and Srujan Marepally. 2025. 'Exploring MSC and HSPC Interactions: New Frontiers in Hematopoiesis and Transplant Medicine'. *Stem Cell Research & Therapy* 16 (November): 640. https://doi.org/10.1186/s13287-025-04753-0.

Tabera, Soraya, José A. Pérez-Simón, María Díez-Campelo, et al. 2008. 'The Effect of Mesenchymal Stem Cells on the Viability, Proliferation and Differentiation of B-Lymphocytes'. *Haematologica* 93 (9): 1301–9. https://doi.org/10.3324/haematol.12857.

Taichman, Russell S., Marcelle J. Reilly, and Stephen G. Emerson. 1996. 'Human Osteoblasts Support Human Hematopoietic Progenitor Cells in In Vitro Bone Marrow Cultures'. *Blood* 87 (2): 518–24. https://doi.org/10.1182/blood.V87.2.518.bloodjournal872518.

Takubo, Keiyo, Nobuhito Goda, Wakako Yamada, et al. 2010. 'Regulation of the HIF-1α Level Is Essential for Hematopoietic Stem Cells'. *Cell Stem Cell* 7 (3): 391–402. https://doi.org/10.1016/j.stem.2010.06.020.

Tanneeru, Karunakar, and Lalitha Guruprasad. 2013. 'Ponatinib Is a Pan-BCR-ABL Kinase Inhibitor: MD Simulations and SIE Study'. *PLOS ONE* 8 (11): e78556. https://doi.org/10.1371/journal.pone.0078556.

Terashima, Asuka, Kazuo Okamoto, Tomoki Nakashima, Shizuo Akira, Koichi Ikuta, and Hiroshi Takayanagi. 2016. 'Sepsis-Induced Osteoblast Ablation Causes Immunodeficiency'. *Immunity* 44 (6): 1434–43. https://doi.org/10.1016/j.immuni.2016.05.012.

Testa, Ugo, Catherine Labbaye, Germana Castelli, and Elvira Pelosi. 2016. 'Oxidative Stress and Hypoxia in Normal and Leukemic Stem Cells'. *Experimental Hematology* 44 (7): 540–60. https://doi.org/10.1016/j.exphem.2016.04.012.

Thottappillil, Neelima, Mario A. Gomez-Salazar, Mingxin Xu, et al. 2023. 'ZIC1 Dictates Osteogenesis Versus Adipogenesis in Human Mesenchymal Progenitor Cells Via a Hedgehog Dependent Mechanism'. *Stem Cells* 41 (9): 862–76. https://doi.org/10.1093/stmcls/sxad047.

Tirichen, Hasna, Hasnaa Yaigoub, Weiwei Xu, Changxin Wu, Rongshan Li, and Yafeng Li. 2021. 'Mitochondrial Reactive Oxygen Species and Their Contribution in Chronic Kidney Disease Progression Through Oxidative Stress'. *Frontiers in Physiology* 12 (April). https://doi.org/10.3389/fphys.2021.627837.

Toofan, Parto, Caroline Busch, Heather Morrison, et al. 2018. ‘Chronic Myeloid Leukaemia Cells Require the Bone Morphogenic Protein Pathway for Cell Cycle Progression and Self-Renewal’. *Cell Death & Disease* 9 (9): 9. https://doi.org/10.1038/s41419-018-0905-2.

Toofan, Parto, David Irvine, Lisa Hopcroft, Mhairi Copland, and Helen Wheadon. 2014. ‘The Role of the Bone Morphogenetic Proteins in Leukaemic Stem Cell Persistence’. *Biochemical Society Transactions* 42 (4): 809–15. https://doi.org/10.1042/BST20140037.

Toofan, Parto, and Helen Wheadon. 2016. ‘Role of the Bone Morphogenic Protein Pathway in Developmental Haemopoiesis and Leukaemogenesis’. *Biochemical Society Transactions* 44 (5): 1455–63. https://doi.org/10.1042/BST20160104.

Varnum-Finney, Barbara, Louise E. Purton, Monica Yu, et al. 1998. ‘The Notch Ligand, Jagged-1, Influences the Development of Primitive Hematopoietic Precursor Cells’. *Blood* 91 (11): 4084–91. https://doi.org/10.1182/blood.V91.11.4084.

Velten, Lars, Simon F. Haas, Simon Raffel, et al. 2017. ‘Human Haematopoietic Stem Cell Lineage Commitment Is a Continuous Process’. *Nature Cell Biology* 19 (4): 271–81. https://doi.org/10.1038/ncb3493.

Vigón, Lorena, Alejandro Luna, Miguel Galán, et al. 2020. ‘Identification of Immunological Parameters as Predictive Biomarkers of Relapse in Patients with Chronic Myeloid Leukemia on Treatment-Free Remission’. *Journal of Clinical Medicine* 10 (1). https://doi.org/10.3390/jcm10010042.

Vijay, Vindhya, Regan Miller, Gau Shoua Vue, et al. 2019. ‘Interleukin-8 Blockade Prevents Activated Endothelial Cell Mediated Proliferation and Chemoresistance of Acute Myeloid Leukemia’. *Leukemia Research* 84 (September): 106180. https://doi.org/10.1016/j.leukres.2019.106180.

Visnjic, Dora, Zana Kalajzic, David W. Rowe, Vedran Katavic, Joseph Lorenzo, and Hector L. Aguila. 2004. ‘Hematopoiesis Is Severely Altered in Mice with an Induced Osteoblast Deficiency’. *Blood* 103 (9): 3258–64. https://doi.org/10.1182/blood-2003-11-4011.

Vogler, Meike, Yannick Braun, Victoria M. Smith, et al. 2025. ‘The BCL2 Family: From Apoptosis Mechanisms to New Advances in Targeted Therapy’. *Signal Transduction and Targeted Therapy* 10 (1): 91. https://doi.org/10.1038/s41392-025-02176-0.

Vong, Queenie P., Wai-Hang Leung, Jim Houston, et al. 2014. ‘TOX2 Regulates Human Natural Killer Cell Development by Controlling T-BET Expression’. *Blood* 124 (26): 3905–13. https://doi.org/10.1182/blood-2014-06-582965.

Vonica, Alin, Neha Bhat, Keith Phan, et al. 2020. ‘Apcdd1 Is a Dual BMP/Wnt Inhibitor in the Developing Nervous System and Skin’. *Developmental Biology* 464 (1): 71–87. https://doi.org/10.1016/j.ydbio.2020.03.015.

Wang, Bin, Difang Sun, Haifeng Li, and Jinli Chen. 2024. 'A Bird's Eye View of the Potential Role of NFKBIA in Pan-Cancer'. *Heliyon* 10 (10): e31204. https://doi.org/10.1016/j.heliyon.2024.e31204.

Wang, Bingwei, Zhenwei Wang, Tao Zhang, and Guosheng Yang. 2019. 'Overexpression of Thymosin B10 Correlates with Disease Progression and Poor Prognosis in Bladder Cancer'. *Experimental and Therapeutic Medicine* 18 (5): 3759–66. https://doi.org/10.3892/etm.2019.8006.

Wang, Jiaqi, Xinting Ouyang, Weijian Zhu, Qiang Yi, and Jinghua Zhong. 2024. 'The Role of CXCL11 and Its Receptors in Cancer: Prospective but Challenging Clinical Targets'. *Cancer Control : Journal of the Moffitt Cancer Center* 31 (March): 10732748241241162. https://doi.org/10.1177/10732748241241162.

Wang, Li, Lili Wang, Hui Zhang, et al. 2020. 'AREG Mediates the Epithelial-Mesenchymal Transition in Pancreatic Cancer Cells via the EGFR/ERK/NF-κB Signalling Pathway'. *Oncology Reports* 43 (5): 1558–68. https://doi.org/10.3892/or.2020.7523.

Warfvinge, Rebecca, Linda Geironson, Mikael N. E. Sommarin, et al. 2017. 'Single-Cell Molecular Analysis Defines Therapy Response and Immunophenotype of Stem Cell Subpopulations in CML'. *Blood* 129 (17): 2384–94. https://doi.org/10.1182/blood-2016-07-728873.

Warfvinge, Rebecca, Linda Geironson Ulfsson, Parashar Dhapola, et al. 2024. 'Single Cell Multi-Omics Analysis of Chronic Myeloid Leukemia Links Cellular Heterogeneity to Therapy Response'. *eLife* 12 (April). https://doi.org/10.7554/eLife.92074.2.

Weisberg, Ellen, Abdel Kareem Azab, Paul W. Manley, et al. 2012. 'Inhibition of CXCR4 in CML Cells Disrupts Their Interaction with the Bone Marrow Microenvironment and Sensitizes Them to Nilotinib'. *Leukemia* 26 (5): 985–90. https://doi.org/10.1038/leu.2011.360.

Weisberg, Ellen, Paul W. Manley, Werner Breitenstein, et al. 2005. 'Characterization of AMN107, a Selective Inhibitor of Native and Mutant Bcr-Abl'. *Cancer Cell* 7 (2): 129–41. https://doi.org/10.1016/j.ccr.2005.01.007.

Weiss, Frank U. 2014. 'Pancreatic Cancer Risk in Hereditary Pancreatitis'. *Frontiers in Physiology* 5 (February): 70. https://doi.org/10.3389/fphys.2014.00070.

Weng, Zhijie, Yigan Wang, Takehito Ouchi, et al. 2022. 'Mesenchymal Stem/Stromal Cell Senescence: Hallmarks, Mechanisms, and Combating Strategies'. *Stem Cells Translational Medicine* 11 (4): 356–71. https://doi.org/10.1093/stcltm/szac004.

Wilson, Anne, Elisa Laurenti, Gabriela Oser, et al. 2008. 'Hematopoietic Stem Cells Reversibly Switch from Dormancy to Self-Renewal during Homeostasis and Repair'. *Cell* 135 (6): 1118–29. https://doi.org/10.1016/j.cell.2008.10.048.

Wirth, Franziska, Alexander Lubosch, Stefan Hamelmann, and Inaam A. Nakchbandi. 2020. 'Fibronectin and Its Receptors in Hematopoiesis'. *Cells* 9 (12): 2717. https://doi.org/10.3390/cells9122717.

Wolock, Samuel L., Indira Krishnan, Danielle E. Tenen, et al. 2019. 'Mapping Distinct Bone Marrow Niche Populations and Their Differentiation Paths'. *Cell Reports* 28 (2): 302-311.e5. https://doi.org/10.1016/j.celrep.2019.06.031.

Wu, Andrew, Xiaohu Liu, Clark Fruhstorfer, and Xiaoyan Jiang. 2024. 'Clinical Insights into Structure, Regulation, and Targeting of ABL Kinases in Human Leukemia'. *International Journal of Molecular Sciences* 25 (6): 3307. https://doi.org/10.3390/ijms25063307.

Wu, Cheng-Hsien, Te-Fu Weng, Ju-Pi Li, and Kang-Hsi Wu. 2024. 'Biology and Therapeutic Properties of Mesenchymal Stem Cells in Leukemia'. *International Journal of Molecular Sciences* 25 (5): 5. https://doi.org/10.3390/ijms25052527.

Wu, Huiyi, Xiaowei Zhu, Huilin Zhou, Min Sha, Jun Ye, and Hong Yu. 2025. 'Mitochondrial Ribosomal Proteins and Cancer'. *Medicina* 61 (1): 96. https://doi.org/10.3390/medicina61010096.

Wu, Yu-Yao, Gao-Qi Wu, Na-Li Cai, Yan-Ming Xu, and Andy T. Y. Lau. 2023. 'Comparison of Human Eukaryotic Translation Initiation Factors 5A1 and 5AL1: Identification of Amino Acid Residues Important for EIF5A1 Lysine 50 Hypusination and Its Protein Stability'. *International Journal of Molecular Sciences* 24 (7): 6067. https://doi.org/10.3390/ijms24076067.

Xu, XiaoQiang, Rui Sun, YuanZhang Li, et al. 2023. 'Comprehensive Bioinformatic Analysis of the Expression and Prognostic Significance of TSC22D Domain Family Genes in Adult Acute Myeloid Leukemia'. *BMC Medical Genomics* 16 (1): 117. https://doi.org/10.1186/s12920-023-01550-7.

Yamamoto, Ryo, Yohei Morita, Jun Ooehara, et al. 2013. 'Clonal Analysis Unveils Self-Renewing Lineage-Restricted Progenitors Generated Directly from Hematopoietic Stem Cells'. *Cell* 154 (5): 1112–26. https://doi.org/10.1016/j.cell.2013.08.007.

Yamazaki, Satoshi, Atsushi Iwama, Shin-ichiro Takayanagi, Koji Eto, Hideo Ema, and Hiromitsu Nakauchi. 2009. 'TGF-β as a Candidate Bone Marrow Niche Signal to Induce Hematopoietic Stem Cell Hibernation'. *Blood* 113 (6): 1250–56. https://doi.org/10.1182/blood-2008-04-146480.

Yan, Wanhao, Shu Diao, and Zhipeng Fan. 2021. 'The Role and Mechanism of Mitochondrial Functions and Energy Metabolism in the Function Regulation of the Mesenchymal Stem Cells'. *Stem Cell Research & Therapy* 12 (1): 140. https://doi.org/10.1186/s13287-021-02194-z.

Yang, Liping, David Bryder, Jörgen Adolfsson, et al. 2005. 'Identification of Lin– Sca1+kit+CD34+Flt3– Short-Term Hematopoietic Stem Cells Capable of Rapidly Reconstituting and Rescuing Myeloablated Transplant Recipients'. *Blood* 105 (7): 2717–23. https://doi.org/10.1182/blood-2004-06-2159.

Yang, Nae-Cherng, and Miao-Lin Hu. 2005. ‘The Limitations and Validities of Senescence Associated-β-Galactosidase Activity as an Aging Marker for Human Foreskin Fibroblast Hs68 Cells’. *Experimental Gerontology* 40 (10): 813–19. https://doi.org/10.1016/j.exger.2005.07.011.

Yang, Xue, Ying Wang, Valentina Rovella, et al. 2023. ‘Aged Mesenchymal Stem Cells and Inflammation: From Pathology to Potential Therapeutic Strategies’. *Biology Direct* 18 (1): 40. https://doi.org/10.1186/s13062-023-00394-6.

Yang, Yang, Saradhi Mallampati, Baohua Sun, et al. 2013. ‘Wnt Pathway Contributes to the Protection by Bone Marrow Stromal Cells of Acute Lymphoblastic Leukemia Cells and Is a Potential Therapeutic Target’. *Cancer Letters* 333 (1): 9–17. https://doi.org/10.1016/j.canlet.2012.11.056.

Yang, Zhenlin, He Tian, Fenglong Bie, et al. 2021. ‘ERAP2 Is Associated With Immune Infiltration and Predicts Favorable Prognosis in SqCLC’. *Frontiers in Immunology* 12 (December): 788985. https://doi.org/10.3389/fimmu.2021.788985.

Yeasen - Leading Innovation in Molecular Enzymes and Reagents. n.d. ‘Signature Assays for Early Apoptosis: JC-1, JC-10’. Accessed 26 March 2026. https://www.yeasenbio.com/blogs/cell/signature-assays-for-early-apoptosis-jc-1-jc-10.

Yokota, Takafumi. 2019. ‘“Hierarchy” and “Holacracy”; A Paradigm of the Hematopoietic System’. *Cells* 8 (10): 1138. https://doi.org/10.3390/cells8101138.

Yoo, Wonbeak, Hyunji Choi, Jieun Lee, Yeeun Lee, Kyung Chan Park, and Kyunghee Noh. 2024. ‘CRHBP, a Novel Multiple Cancer Biomarker Connected with Better Prognosis and Anti-Tumorigenicity’. *Cancer Cell International* 24 (November): 391. https://doi.org/10.1186/s12935-024-03562-4.

Yun, Jina, Simon Hansen, Otto Morris, et al. 2023. ‘Senescent Cells Perturb Intestinal Stem Cell Differentiation through Ptk7 Induced Noncanonical Wnt and YAP Signaling’. *Nature Communications* 14 (1): 156. https://doi.org/10.1038/s41467-022-35487-9.

Zhang, Bin, Yin Wei Ho, Qin Huang, et al. 2012. ‘Altered Microenvironmental Regulation of Leukemic and Normal Stem Cells in Chronic Myelogenous Leukemia’. *Cancer Cell* 21 (4): 577–92. https://doi.org/10.1016/j.ccr.2012.02.018.

Zhang, Bin, Min Li, Tinisha McDonald, et al. 2013. ‘Microenvironmental Protection of CML Stem and Progenitor Cells from Tyrosine Kinase Inhibitors through N-Cadherin and Wnt–β-Catenin Signaling’. *Blood* 121 (10): 1824–38. https://doi.org/10.1182/blood-2012-02-412890.

Zhang, Haojian, Huawei Li, Hualin S. Xi, and Shaoguang Li. 2012. ‘HIF1α Is Required for Survival Maintenance of Chronic Myeloid Leukemia Stem

Cells'. *Blood* 119 (11): 2595–607. https://doi.org/10.1182/blood-2011-10-387381.

Zhang, Pan, Xiang Li, Chengwei Pan, et al. 2022. 'Single-Cell RNA Sequencing to Track Novel Perspectives in HSC Heterogeneity'. *Stem Cell Research & Therapy* 13 (1): 39. https://doi.org/10.1186/s13287-022-02718-1.

Zhang, Xiao-Guang, Tong Zhang, Chang-Ying Li, Ming-Hao Zhang, and Fang-Min Chen. 2018. 'CD164 Promotes Tumor Progression and Predicts the Poor Prognosis of Bladder Cancer'. *Cancer Medicine* 7 (8): 3763–72. https://doi.org/10.1002/cam4.1607.

Zhang, Xiaoyan, Huaijun Tu, Yazhi Yang, et al. 2016. 'High IL-7 Levels in the Bone Marrow Microenvironment Mediate Imatinib Resistance and Predict Disease Progression in Chronic Myeloid Leukemia'. *International Journal of Hematology* 104 (3): 358–67. https://doi.org/10.1007/s12185-016-2028-9.

Zhang, Yanna, Ting Du, and Xiancheng Chen. 2022. 'ANXA2P2: A Potential Immunological and Prognostic Signature in Ovarian Serous Cystadenocarcinoma via Pan-Carcinoma Synthesis'. *Frontiers in Oncology* 12 (February). https://doi.org/10.3389/fonc.2022.818977.

Zhang, Yifan, Shuai Gao, Jun Xia, and Feng Liu. 2018. 'Hematopoietic Hierarchy – An Updated Roadmap'. *Trends in Cell Biology* 28 (12): 976–86. https://doi.org/10.1016/j.tcb.2018.06.001.

Zhang, Yiming, Ruilin Pan, Kun Li, et al. 2024. 'HSPD1 Supports Osteosarcoma Progression through Stabilizing ATP5A1 and Thus Activation of AKT/mTOR Signaling'. *International Journal of Biological Sciences* 20 (13): 5162–90. https://doi.org/10.7150/ijbs.100015.

Zhao, Chen, Alan Chen, Catriona H. Jamieson, et al. 2009. 'Hedgehog Signalling Is Essential for Maintenance of Cancer Stem Cells in Myeloid Leukaemia'. *Nature* 458 (7239): 776–79. https://doi.org/10.1038/nature07737.

Zhao, Kai, Ling-Ling Yin, Dong-Mei Zhao, et al. 2014. 'IL1RAP as a Surface Marker for Leukemia Stem Cells Is Related to Clinical Phase of Chronic Myeloid Leukemia Patients'. *International Journal of Clinical and Experimental Medicine* 7 (12): 4787–98.

Zhao, Meng, John M. Perry, Heather Marshall, et al. 2014. 'Megakaryocytes Maintain Homeostatic Quiescence and Promote Post-Injury Regeneration of Hematopoietic Stem Cells'. *Nature Medicine* 20 (11): 1321–26. https://doi.org/10.1038/nm.3706.

Zhao, Peiwei, Xiankai Zhang, Zhengrong Duan, et al. 2024. 'Identification of Two Novel Variants in ALG11 Causing Congenital Disorder of Glycosylation'. *Seizure: European Journal of Epilepsy* 121 (October): 235–42. https://doi.org/10.1016/j.seizure.2024.07.020.

Zhao, Zhi-Gang, Wen Xu, Li Sun, Wei-Ming Li, Qiu-Bai Li, and Ping Zou. 2012. 'The Characteristics and Immunoregulatory Functions of Regulatory Dendritic Cells Induced by Mesenchymal Stem Cells Derived from Bone

Marrow of Patient with Chronic Myeloid Leukaemia'. *European Journal of Cancer* 48 (12): 1884–95. https://doi.org/10.1016/j.ejca.2011.11.003.

Zhou, Guohui, Xinmin Yan, Zhenfei Chen, Xing Zeng, and Fangqian Wu. 2023. 'ASPN Synergizes with HAPLN1 to Inhibit the Osteogenic Differentiation of Bone Marrow Mesenchymal Stromal Cells and Extracellular Matrix Mineralization of Osteoblasts'. *Orthopaedic Surgery* 15 (9): 2423–34. https://doi.org/10.1111/os.13803.

Zhou, Haixia, Yue Ge, Lili Sun, et al. 2014. 'Growth Arrest Specific 2 Is Up-Regulated in Chronic Myeloid Leukemia Cells and Required for Their Growth'. *PLOS ONE* 9 (1): e86195. https://doi.org/10.1371/journal.pone.0086195.

Zhou, Junjie, Guangrong Yu, Chengfu Cao, Jinhui Pang, and Xianqi Chen. 2011. 'Bone Morphogenetic Protein-7 Promotes Chondrogenesis in Human Amniotic Epithelial Cells'. *International Orthopaedics* 35 (6): 941–48. https://doi.org/10.1007/s00264-010-1116-3.

Zhou, Yi-Qing, Jean-Pierre Levesque, Antoinette Hatzfeld, et al. 1993. 'Fibrinogen Potentiates the Effect of Interleukin-3 on Early Human Hematopoietic Progenitors'. *Blood* 82 (3): 800–806. https://doi.org/10.1182/blood.V82.3.800.800.